SEP 22 1948

PROCEEDINGS

American Society of Civil Engineers

SEPTEMBER

1948

VOLUME 74 NO. 7

AMERICAN SOCIETY OF CIVIL ENGINEERS

OFFICERS FOR 1948

PRESIDENT

R. E. DOUGHERTY

VICE-PRESIDENTS

Term expires January, 1949:

RALPH B. WILEY
GAIL A. HATHAWAY

Term expires January, 1950:

JOHN W. CUNNINGHAM
CARLTON S. PROCTOR

DIRECTORS

Term expires January, 1949:

SHORTRIDGE HARDESTY
IRVING V. A. HUIE
ALBERT HAERTLEIN
WILLIAM ROY GLIDDEN
WILLIAM M. PIATT
FREDERICK W. PANHORST

Term expires January, 1950:

HARLAND C. WOODS
ROY W. CRUM
LEWIS M. GRAM
SAMUEL A. GREELEY
DANIEL V. TERRELL
WALDEN L. MALONY
DAVID L. ERICKSON

Term expires January, 1951:

WILLIAM M. GRIFFIN
EDMUND A. PRENTIS
JOEL D. JUSTIN
JULIAN HINDS
WEBSTER L. BENHAM
C. GLENN CAPPEL

PAST-PRESIDENTS

Members of the Board

W. W. HORNER
E. M. HASTINGS

TREASURER

CHARLES E. TROUT

EXECUTIVE SECRETARY

WILLIAM N. CAREY

ASSISTANT TREASURER

GEORGE W. BURPEE

ASSISTANT SECRETARY

E. L. CHANDLER

PROCEEDINGS OF THE SOCIETY

SYDNEY WILMOT
Manager of Technical Publications

HAROLD T. LARSEN
Editor of Technical Publications

HERBERT P. ORLAND
Assistant Editor of Technical Publications

COMMITTEE ON PUBLICATIONS

SHORTRIDGE HARDESTY, *Chairman*

ROY W. CRUM
JOEL D. JUSTIN
WILLIAM M. PIATT
EDMUND A. PRENTIS
DANIEL V. TERRELL

PROCEEDINGS

OF THE

AMERICAN SOCIETY OF CIVIL ENGINEERS

VOL. 74 SEPTEMBER, 1948 NO. 7

TECHNICAL PAPERS

AND

DISCUSSIONS

A list of "Current Papers and Discussions" may be found on the page preceding the table of contents

The Society is not responsible for any statement made or opinion expressed in its publications.

Published monthly, except July and August, at Prince and Lemon Streets, Lancaster, Pa., by the American Society of Civil Engineers. Editorial and General Offices at 33 West Thirty-ninth Street, New York 18, N. Y. Reprints from this publication may be made on condition that the full title of paper, name of author, page reference, and date of publication by the Society are given.

Entered as Second-Class Matter, September 23, 1937, at the Post Office at Lancaster, Pa., under the Act of March 3, 1879. Acceptance for mailing at special rate of postage provided for in Section 1103, Act of October 3, 1917, authorized on July 5, 1918.

Subscription (if entered before January 1) $8.00 per annum Price $1.00 per copy

Copyright, 1948, *by the* AMERICAN SOCIETY OF CIVIL ENGINEERS
Printed in the United States of America

	Published	Discussion closes
Bergendorff, R. N., and Sorkin, Josef. Mississippi River Bridge at Dubuque, Iowa	June, 1947	
Discussion in Sept., Oct., 1947, May, 1948		Closed*
Symposium: Problems and Control of Decentralization in Urban Areas	Nov., 1947	
Discussion in Mar., June, 1948		Closed*
Moore, William W. Experiences with Predetermining Pile Lengths	Nov., 1947	
Discussion in Mar., June, 1948		Closed*
Turner, Robert E. Operation of the Conowingo Hydroelectric Plant	Nov., 1947	
Discussion in June, Sept., 1948		Closed*
Hickerson, T. F. Determination of Position and Azimuth by Simple and Accurate Methods	Nov., 1947	
Discussion in June, 1948		Closed*
Bell, S. J. A Centroidal Method of Rigid-Frame Analysis	Nov., 1947	
Discussion in June, Sept., 1948		Closed*
Loring, Samuel J. Experimental Determination of Vibration Characteristics of Structures	Dec., 1947	
Discussion in Mar., June, Sept., 1948		Closed*
Chen Pei-ping. Matrix Analysis of Pin-Connected Structures	Dec., 1947	
Discussion in June, 1948		Closed*
Andrew, Charles E. Unusual Design Problems—Second Tacoma Narrows Bridge	Dec., 1947	
Discussion in June, 1948		Closed*
Stewart, Ralph W. Analysis of Frames with Elastic Joints	Dec., 1947	
Discussion in May, June, Sept., 1948		Closed*
Harza, L. F. The Significance of Pore Pressure in Hydraulic Structures	Dec., 1947	
Discussion in June, Sept., 1948		Oct. 1, 1948
Levinton, Zusse. Elastic Foundations Analyzed by the Method of Redundant Reactions	Dec., 1947	
Discussion in Sept., 1948		Oct. 1, 1948
Symposium: Lateral Earth Pressures on Flexible Retaining Walls	Jan., 1948	
Discussion in June, Sept., 1948		Oct. 1, 1948
Neiman, A. S. Shearing Stress Distribution in Box Girders with Multiple Webs	Feb., 1948	
Discussion in June, Sept., 1948		Oct. 1, 1948
Symposium: Highway Bridge Floors	Mar., 1948	
Discussion in Sept., 1948		Nov. 1, 1948
DuVal, Miles P. The Marine Operating Problems, Panama Canal, and The Solution	Feb., 1947	Nov. 1, 1948
Claybourn, J. G. Sea Level Plan for Panama Canal	Feb., 1947	
Discussion in Feb., June, 1948		Nov. 1, 1948
Symposium: Panama Canal—The Sea-Level Project	Apr., 1948	
Discussion in June, Sept., 1948		Nov. 1, 1948
Chellis, Robert D. The Relationship Between Pile Formulas and Load Tests	May, 1948	
Discussion in Sept., 1948		Nov. 1, 1948
Wimer, H. Dudley, Jr. Stability of Thin-Walled Compression Members	May, 1948	Nov. 1, 1948
Scharff, Maurice R. Valuation and Depreciation of Public Utility Property	June, 1948	Nov. 1, 1948
Report. Review of Slope Protection Methods: Report of the Subcommittee on Slope Protection of the Committee on Earth Dams of the Soil Mechanics and Foundations Division	June, 1948	Nov. 1, 1948

NOTE.—The closing dates herein published are final except when names of prospective discussers are registered for special extension of time.

* Publication of closing discussion pending.

CONTENTS FOR SEPTEMBER, 1948

PAPERS

PAGE

Industrial Wastes: A Symposium.
By Don E. Bloodgood, and F. W. Mohlman 1047

Adjustment of the "Shoran" Triangulation.
By Chung-jui Chu 1063

Unusual Design Problems, Harlan County Dam.
By Louis G. Feil 1071

Expansion Joint Practice in Highway Construction.
By A. A. Anderson 1083

A Simplified Method of Analyzing Suspension Bridges.
By Ling-hi Tsien 1093

Flexural Constants of Haunched Beams by Area Computation.
By Fang-Yin Tsai 1129

DISCUSSIONS

Operation of the Conowingo Hydroelectric Plant.
By John S. Cotton 1161

A Centroidal Method of Rigid-Frame Analysis.
By Leroy A. Beaufoy, and William A. Conwell 1166

Elastic Foundations Analyzed by the Method of Redundant Reactions.
By L. J. Mensch, E. P. Popov, Yi-Mai Yao, Jacob Feld, and Victor R. Bergman 1173

The Significance of Pore Pressure in Hydraulic Structures.
By John S. Cotton, Serge Leliavsky Bey, A. H. Davison, R. E. Ballester, John S. McNown, and V. T. Boughton 1185

Shearing Stress Distribution in Box Girders with Multiple Webs.
By J. G. Clark and W. E. Hanson 1210

Experimental Determination of Vibration Characteristics of Structures.
By F. B. Farquharson, and J. J. Slade, Jr 1219

Analysis of Frames with Elastic Joints.
By George W. Lamb, A. A. Eremin, and J. Charles Rathbun 1223

Panama Canal—The Sea-Level Project: A Symposium.
By George B. Pillsbury, Kenneth S. M. Davidson, Joel D. Justin, W. H. McAlpine, W. E. R. Covell, William Herbert Hobbs, Hibbert Hill, Kenneth C. Reynolds, Gregory P. Tschebotarioff, Charles W. Dohn, and Donald F. Horton 1228

CONTENTS FOR SEPTEMBER, 1948 (*Continued*)

PAGE

Lateral Earth Pressures on Flexible Retaining Walls: A Symposium.
By E. De Beer 1257

The Relationship between Pile Formulas and Load Tests.
By Donovan H. Lee 1261

Highway Bridge Floors: A Symposium.
By Searcy B. Slack 1263

GUIDEPOST FOR TECHNICAL READERS
SEPTEMBER, 1948, *PROCEEDINGS*

Items of value or significance to readers in various fields are here listed. For convenience the distribution is given in terms of the Society's Technical Divisions

Technical Division	*Pages*
Air Transport	1173, 1261
City Planning	1048, 1063
Construction	1071, 1083, 1161, 1219, 1228, 1237, 1257, 1261, 1263
Engineering Economics	1055, 1242
Highway	1080, 1093, 1173, 1257, 1263
Hydraulics	1076, 1083, 1185, 1231
Irrigation	1071
Power	1071, 1161
Sanitary Engineering	1048
Soil Mechanics and Foundations	1071, 1173, 1185, 1235, 1237, 1251, 1257, 1261
Structural	1071, 1083, 1093, 1129, 1166, 1173, 1185, 1210, 1219, 1223, 1257, 1261, 1263
Surveying and Mapping	1063
Waterways	1228

(A constant effort is made to supply technical material to Society members, over the entire range of possible interest. In so far as your specialty may be covered inadequately in the foregoing list, this fact is a gage of the need for your help toward improvement.—Ed.)

HINTS TO AUTHORS

Those who are planning papers for submission to PROCEEDINGS *will expedite Committee action measurably by first studying the standard instructions as to style, content, and format. For reprints, address the Manager, Technical Publications, 33 W. 39th St., New York 18, N. Y.*

AMERICAN SOCIETY OF CIVIL ENGINEERS

Founded November 5, 1852

PAPERS

INDUSTRIAL WASTES
A SYMPOSIUM

PAGE

Effect of Stream Pollution Legislation and Control.
By DON E. BLOODGOOD, Assoc. M. ASCE 1048

Possibilities of Recovery and Utilization.
By F. W. MOHLMAN, ESQ. 1052

NOTE.—Written comments are invited for immediate publication; to insure publication the last discussion should be submitted by **February 1, 1949.**

EFFECT ON STREAM POLLUTION LEGISLATION AND CONTROL

By Don E. Bloodgood,[1] Assoc. M. ASCE

When attempting to show the effect of one thing on another, it is sometimes possible to correlate completely unrelated items so as to make it appear that one is directly the result of the other. Such an unjustified conclusion may be drawn if it is attempted to show the individual effect that industrial wastes have had on bringing about legislation for the control of stream pollution.

Historical Notes

In reviewing the past history of stream pollution it must be recalled that the early complaints resulted from nuisances caused by discharge of sewage and other wastes into streams. People downstream objected to the obnoxious odors which changed their pure country air into the "foul depressing atmosphere" described in many court cases. Whether the elimination of a nuisance is more important than the removal of a positive health hazard is not a difficult question for the sanitary engineer, but to the lay public the more obvious a situation is, the more attention it is given. Whether industrial wastes have been more responsible for the passage of stream pollution control legislation is largely a matter of conjecture. R. Hollowell, Jr.,[2] uses, as an illustration of the earliest objection to this nuisance, in Indiana, the case in 1856 when one Sloan was convicted of causing a nuisance by pouring the slops from the Bates House in Indianapolis into the street, where it made offensive pools along the west side of Illinois Street. Mr. Hollowell also states that the first case of stream pollution in Indiana to come to the attention of the courts occurred in 1868, when a Mr. Taylor was indicted for depositing domestic waste in a spring from which travelers on a near-by highway were accustomed to drink. This indicates that the first recorded difficulties involving wastes were not those of an industrial type, unless for the sake of argument, someone contends that the slops from the Bates House were those from an industrial establishment.

One of the earliest records of complaint of discharge of industrial waste into a watercourse is found in 1886 when a Mr. Mergentheim was indicted, under the nuisance statute of Indiana, "for discharging the water from his woolen mills into the canal at Peru, Indiana, to the discomfiture of those in the vicinity, particularly when the water in the canal was low." In 1893 the Indianapolis Water Company obtained an injunction against the American Strawboard Company which at least registered that the waste from the mill was causing sufficient difficulty to warrant action in the courts. It can be seen from these instances that there were court cases involving industrial stream

[1] Associate Prof., San. Eng., Purdue Univ., West Lafayette, Ind.

[2] "History and Legal Background of Stream Pollution Control in Indiana," by Robert Hollowell, Jr. *Proceedings*, First Industrial Waste Utilization Conference, Purdue Univ., West Lafayette, Ind., 1944 pp. 31–42.

pollution as early as the 1880's. It is presumed, however, that there were about as many complaints over domestic sewage as there were over industrial wastes. In many cities where stream pollution is or has been a problem it is very difficult to state definitely whether the municipal or industrial wastes caused the stream pollution and which of the two brought about the legislation curbing the pollution.

Amount of Industrial Wastes

Industrial wastes discharged into streams in the United States amount to an equivalent population of 60,000,000 and the domestic sewage discharged into these same streams is contributed by from 55,000,000 to 60,000,000, according to one authority.[3] Another states that, roughly, the raw sewage of 47,000,000 persons is emptied into the receiving streams of the United States and that there is an additional equivalent of from 55,000,000 to 60,000,000 persons added by untreated and uncontrolled industrial wastes.[4] These data substantiate each other and indicate that industrial wastes are responsible for at least half of the contamination of the streams today.

In another report[5] it is stated that industrial wastes have a pollutional effect on the streams of Tennessee equivalent to a domestic sewage population of about 1,268,000, which is approximately 1.35 times the population discharging domestic sewage into the streams. The equivalent population does not take into account some of the objectional inorganic compounds from industry that are deterimental to the streams and make some of them unsuitable as sources of domestic water supplies or as habitats for desirable aquatic life. The report of the Ohio River Pollution Survey[6] shows that wastes from 1,800 industrial plants were investigated and that the wastes from these plants represented an estimated equivalent population of 10,000,000. This certainly represents a sizable problem, which must be solved by hard work spurred on by fair and just legislation.

It is not always the magnitude of the industrial waste problem that calls it to the attention of the public. In past years Indianapolis packing plants were cited as the cause of pollution of the White River. In the 1934 report of a survey,[7] it is shown that industrial wastes in Indianapolis contributed only an equivalent population load of 267,728 as against a total equivalent population for the whole city of 600,728. In many cities it may be the additional load brought on by industry which makes it impossible for the receiving stream to purify itself naturally. It is usually true, however, that where there is an industrial waste load there is usually a domestic sewage load of some proportion, and separation of the two may be all but impossible. In some cities industries have contributed quantities of wastes which far exceeded the domestic wastes. In Decatur and Peoria, in Illinois, discharges of industrial wastes

[3] "Industrial Wastes Equivalent to 60 Million Population," by J. K. Hoskins, *Sewage Works Engineering*, October, 1945, p. 493.

[4] "Responsibility for Industrial and Municipal Wastes," by Abel Wolman, *Journal*, A.W.W.A., July, 1946, p. 883.

[5] "Stream Pollution in Tennessee," *ibid.*, April, 1945, p. 350.

[6] "The Ohio River Pollution Survey, 1942," Final Rept. the Ohio River Committee, "Industrial Waste Guides," Supplement D, Federal Security Agency, U. S. Public Health Service, Cincinnati, Ohio.

[7] "The Population Equivalent of Certain Industrial Wastes," by C. K. Calvert and Elliott H. Parks, *Sewage Works Journal*, November, 1934, p. 1159.

have been so great, in comparison with the domestic sewage load, that they have been used as outstanding examples in other states to show the need for strict and strong legislation for industrial waste control. Concentration of some industries, such as the pulp mills in Maine, has brought about difficulties that have attracted legislative attention. These examples indicate that every effort must be made to see that future legislation is adequate to cover all situations involving industrial wastes.

It is of interest to note that some laws must be changed by acts of legislature because they are too specific. In 1945, the Pennsylvania Legislature amended its act of 1937, particularly with respect to industrial wastes, because the 1937 act specifically exempted acid mine drainage and coal mine silt from its provisions until practical methods for treating these wastes became known. The 1945 act removed the exemption from silt, and anthracite operators prepared plans and instituted work on a large scale to comply with the law. These changes indicate the trend in legislation and show that even the difficult tasks are being undertaken on a cooperative basis.

Federal Legislation

No federal stream pollution control law exists, although almost one hundred bills have been submitted to Congress since November, 1897. It is believed that the main reason for this lack is that most of the bills extended federal control.[8] It is interesting to note the indication[8,9] that the failure to pass a federal law governing stream pollution control cannot be blamed on industry. In general, industry has shown a decided interest in assisting the stream pollution abatement program with certain groups sponsoring research projects in their particular fields. On the other hand, industry cannot be expected to show progress in stream pollution abatement when disagreement exists as to which type of federal law is needed.

State Legislation

Legislation provided by the states was strengthened during 1945 and 1946, and is a trend that may be expected to continue. Many of the states have found that their legislation is far from being effective in the proper control of stream pollution because the laws do not permit control measures to be enforced until damage has been done. In preparing added or modified legislation there is danger in making the law too long and cumbersome. Because law is no better than its administrators, however, there is but little danger when administrative power is vested in a board of control.

Indiana legislation requires that pollution of a stream or body of water must be stopped, but does not specify the degree of waste treatment required. This is as it should be, and yet it becomes necessary, sooner or later, to establish permissible standards. Establishment of these standards, which must be founded on scientific investigation, can certainly be helped by the federal services. A question such as, "What quantity of dissolved zinc can be permitted in a stream?" bothers industry more than do federal and state laws.

[8] Report of the Committee on Sewage Disposal, Am. Public Health Assn., Public Health Eng. Section, presented in Cleveland, Ohio, November 12, 1946.

[9] "The Pollution Parade Passes," by Morris M. Cohn, *Sewage Works Engineering*, October, 1946, p. 513.

Some industries have tried to assist in gathering information that is or will be helpful in establishing the needed standards. Progress has been made in determining the toxicity of some of the wastes of the canning industry.[10] W. B. Hart has also contributed data on toxicity studies for the petroleum industry.[11]

Establishment of standards and development of new processes for industrial wastes treatment require study and research. It seems entirely reasonable that this work be carried out by federal and state agencies with funds appropriated for the specific purpose.

Conclusions

(1) Federal legislation can serve the citizens of the United States to the greatest extent by coordinating the activities of state stream pollution control units.

(2) State legislation should authorize a board of control having broad powers so that the board can establish the necessary rules and regulations, which must change with the development of the times.

(3) Industry has no objection to well-written, reasonable laws on stream pollution control.

(4) Development of suitable and improved industrial wastes disposal methods can be brought about by legislation providing for the necessary studies.

[10] "Lethal Effect of Chemicals on Fresh Water Fish," by N. H. Sanborn, *Food Packer*, July, 1945, pp. 40–44.

[11] "The Evaluation of Industrial Wastes, Chemicals and Other Substances to Fresh-Water Fishes," by W. B. Hart, P. Doudoroff, and J. Greenbank, Atlantic Refining Co., 1945.

POSSIBILITIES OF RECOVERY AND UTILIZATION

BY F. W. MOHLMAN,[12] ESQ.

INTRODUCTION

The course of industrial practice is characterized by the progressive recovery, as salvage, of products once discharged to sewers as worthless wastes. The line of distinction between salvage and wastes is steadily moving toward recovery of products within the factory, thus relieving the pollution load in most industries. How this is planned and accomplished is the subject of this paper, which is based largely on data accumulated in Chicago, Ill., during a twelve-year study of industrial wastes, in which more than three hundred plants were inspected, wastes measured, sampled, and analyzed over at least a two-week period, and results computed in pounds of losses per day. During this survey, unit losses were computed, specific processes investigated, excessive losses noted and called to the attention of the plant managers, new salvage processes studied, and the general principles of loss prevention noted. Studies made for industries not in Chicago have also led to knowledge of waste problems of the various chemical, pharmaceutical, metallurgical, and packinghouse industries.

The practice in Chicago has been to measure flow and collect samples every fifteen minutes, to spend at least two weeks at each plant, and to compute data for a number of plants to obtain basic units for each type of industry. Such basic data are needed as the criterion of what is good or bad practice in each industry, but obviously the basic records must not be too limited to permit establishment of norms significant of good practice in operations.

Such norms have been established for packinghouses, breweries, and laundries, as well as for the corn products, by-products, coke, paper, and some types of canning industries. Information is available on salvage practices in the paper pulp, chemical, alcohol, petroleum refining, pickling, plating, and metallurgical industries. Although these results can be mentioned only briefly, data are presented for each industry and discussed as to practices which recover specific substances of value for sale or re-use.

PACKINGHOUSE

Wastes in the packinghouse industry originate in the various departments—stockyards, killing floor, carcass washing, washing and cleaning entrails, paunch manure, blood drainage, tankage, evaporators, hide drainage, hog hair removal, pickling, cooking, rendering, and general cleanup. The larger and more complex the packinghouse, the more effort is made to recover by-products.

In order to show the unit losses, survey data from fourteen Chicago packinghouses are given in Table 1. These results include hog, cattle, and mixed kills, and tonnages varying from 51 to 680 per day. Although individual houses vary rather widely from the average shown, and several surveys have been excluded because losses were known to be excessive and were in process of being

[12] Director of Laboratories, Eng. Dept., San. Dist., Chicago, Ill.

reduced, the data are considered to be representative of average practice in the industry. If losses are greater than these averages, search should be made for the causes which usually can be found.

Separation of the losses per ton of cattle as against the losses per ton of hogs was considered of interest, with data from four surveys of each type available.

TABLE 1.—UNIT PACKINGHOUSE LOSSES, CHICAGO, ILL.

Plant No.	Kill		Liquid loss (gal per ton)	Pollutional Losses (Lb per Ton)			
	Type	Tons per day		B.O.D.	Suspended solids	Nitrogen	Grease
(1)	(2)	(3)	(4)	(5)	(6)	(7)	(8)
1	Hogs.....	51	5,500	36.0	24.0	5.34	1.80
2	Hogs.....	114	2,200	30.1	18.2	2.58	4.61
3	Mixed.....	127	2,600	25.4	9.1	4.05	2.88
4	Hogs.....	139	4,900	26.2	19.6	2.50	5.66
5	Cattle.....	148	1,900	41.5	29.6	4.47	1.35
6	Cattle.....	165	2,800	31.4	29.5	4.02	3.58
7	Cattle.....	168	2,000	21.0	19.9	2.04	2.01
8	Mixed.....	185	2,800	39.4	18.8	5.18	1.20
9	Hogs.....	190	4,500	19.5	14.3	2.93	0.54
10	Mixed.....	303	4,600	33.4	29.9	4.37	4.00
11	Cattle.....	397	6,200	20.0	22.0	2.16	1.10
12	Mixed.....	429	6,500	29.4	26.5	3.41	3.00
13	Mixed.....	661	2,600	13.0	12.5	1.58	1.00
14	Mixed.....	680	8,700	38.5	44.3	4.20	4.20
Average	....	....	4,130	28.9	22.7	3.49	2.64

Such averages did not show very significant differences except, as shown in Table 2, wherein the hog kill shows relatively more biochemical oxygen demand (B.O.D.) and grease per ton. Losses are reduced by efficient skimming to recover grease, increased evaporation to recover tankage, screening to recover paunch manure, and dry rendering to recover grease and tankage.

Skimming can be made more efficient if interplant grease basins are from 2 ft to 4 ft deep, are not too wide, provide from $\frac{1}{2}$-hr detention to 1-hr detention, maintain a velocity of from 1 ft to 2 ft per min, and have arrangements for easy removal of greases by hand skimming. Mechanical rakes or flights, and

TABLE 2.—COMPARISON OF AVERAGE UNIT LOSSES IN CATTLE AND HOG KILLING OPERATIONS

Type of kill	Liquid loss (gal per ton)	Pollutional Losses (Lb per Ton)			
		B.O.D.	Suspended solids	Nitrogen	Grease
Cattle.....	3,225	28.5	25.3	3.17	2.01
Hogs.....	4,300	31.4	20.9	3.15	3.29

possibly vacuators or "pressurators," may be helpful, but are not essential. E. N. Mortenson[13] states that efficient operation should remove enough floating grease so that the effluent contains not more than 0.2 lb per ton kill, as determined by an ingenious procedure originated by him.

[13] "Grease Recovery in the Meat Packing Industry," by E. N. Mortenson, *Bulletin No. 60*, 2d Industrial Waste Conference, Purdue Univ., Lafayette, Ind., January, 1946, p. 28.

A rather crude method of hand skimming has been used for several years at the combined packinghouse flow at the Racine Avenue pumping station of the Sanitary District of Chicago. During the first nine months, from January to September, 1944, the income was $24,730 for 1,124 tons of inedible grease. Since then the income has fallen off, in part, because of the difficult conditions of removal. Because the grease must be mixed in low percentage with other grease or distilled in order to be salable, the limited number of processors who can handle it reduces its field of sale.

One of the most troublesome features of packinghouse wastes is their high nitrogen content. This is largely due to the discharge of tank water, entrainment of foaming in hard-pressed evaporators, and actual loss of blood. Evaporators should be of ample capacity, say, 3,000 gal per hr for a 600-ton house, and so operated that no feed water must be dumped, each day's production is handled immediately, and no tankage is held over. The recovered tankage is valuable and one of the best salvage products in the industry. Screens recover a good proportion of paunch manure, but are not particularly attractive from the standpoint of salvage. Dry rendering is one of the most helpful advances in packinghouse operation for prevention of losses, but the demand for "prime steam lard" hampers its extension in existing packinghouses. However, this helpful procedure is one of the most important advances in the industry.

TABLE 3.—TOTAL UNITED STATES PACKINGHOUSE KILL, DAILY TONNAGES, AND POPULATION EQUIVALENT OF WASTES

Year	Annual kill (million lb)	Average kill (tons per day)	Waste population equivalent (millions)
1930	30,164	50,300	8.70
1935	27,358	45,600	7.89
1940	35,669	59,500	10.29
1941	36,775	61,300	10.60
1942	40,676	67,800	11.73
1943	45,632	76,100	13.16
1944	47,395	79,000	13.67
1945	43,618	72,700	12.58

An over-all estimate of the B.O.D. (computed to population equivalent) of the total United States kill is shown in Table 3. This estimate indicates a maximum loss of 13,670,000 population equivalent in 1944 for the total animal kill. The kill under government inspection was only about 65% of this.

WOOL SCOURING

A recovery worth noting in a field allied to packinghouse practice is the recovery of grease from wool scouring at Bradford, England. It is estimated that about one half of the world's wool supply is cleaned at Bradford and that half the sewage volume is wool scouring liquors. The grease content of the sewage is 890 ppm and the alkalinity 815 ppm. By adding sulfuric acid to an acidity of 100 ppm, wool grease is precipitated with the sludge, which is again acidified and the grease separated through filter presses and drawn off from the water. More than $800,000 worth of products have been sold in one year. This is rather good salvage for a city of 263,000 population.

BREWERY

Brewing is not often recognized as the source of a great deal of industrial waste, although many cities of 20,000 have local breweries, whereas the Chicago

survey, for example, included twenty-eight breweries with production of from 120 bbl to 1,280 bbl of 31 gal each per day, averaging 400 bbl. Most breweries do not include a malting plant and none of those in Chicago produced their own malt. In brewing, malt and rice mashes are boiled separately, mixed, and the wort drawn off to large copper kettles of 450-bbl capacity. The residual grain is usually recovered by pressing in expellers, followed by steam drying. Dried grains amount to about 25% of the original grain used in the process, or about 10 lb per bbl of beer. More recovery would be possible if a more efficient dewatering process were used. In the Chicago studies, the rather large losses from the expellers constituted only 7.5% of the total flow of wastes, but accounted for 37% of the B.O.D. and 31% of the suspended solids. Hops are added to the strained wort and the mixture is boiled, after which the hops are strained out and sometimes burned or dried with the grains. They are not a large proportion of wastes, amounting only to from 0.3 lb to 0.5 lb dry solids per bbl. Their salvage value is low.

After the boiled wort is cooled, yeast is added and fermentation proceeds for about ten days. The beer then is filtered, stored for three months or more, clarified, and bottled. Yeast increases 4 to 1 during fermentation, thus giving a surplus of 3 lb wet yeast, or 0.5 lb dry yeast, per bbl. Formerly, this yeast was wasted, but it is realized that the wastage is a valuable food source, and more and more effort is made to recover the yeast. For example, one Chicago company handles 500,000 lb of yeast (dry basis) per yr, collecting wet yeast from practically all Chicago breweries and refrigerating the wet yeast until ready for processing. The yeast is washed and "de-bittered," then digested with enzymes, filtered, and the filtrate dried and sold at fancy prices as a very rich source of vitamin B complex. The filter cake is dried and used as feed. Other extraction products are also made.

TABLE 4.—COMPARATIVE COST OF TYPICAL PROTEIN FOODS

Food			Protein (%)	Required weight[a] (g)	Cost per day
Type	Unit	Unit cost			
(1)	(2)	(3)	(4)	(5)	(6)
Dried yeast..	Lb	$0.50	45	155	$0.17
Meat.....	Lb	0.50	17.5	400	0.44
Beef liver....	Lb	0.50	19.7	355	0.39
Whole milk...	Qt	0.15	3.5	2,000	0.33
Eggs.....	Dozen	0.50	11.4	614	0.51

[a] To yield 70 g of protein.

Some large brewers dry their entire surplus yeast. The protein value is higher than most foods, as indicated in Table 4. In addition, the vitamin content is especially rich, and the dried yeast can be added to other food products to augment protein or vitamin B deficiencies. Growing realization of the food value of dried brewers' yeast has induced many brewers to keep this product out of the sewer. In Indiana eight of thirteen breweries are equipped to dry their yeast.

The Chicago brewery tests, made in 1937 when only some of the grains were recovered and practically none of the yeast, resulted in unit losses, per barrel, as follows: Gallons of waste, 320; B.O.D., 3.1 lb per day; suspended solids, 1.68 lb per day; and nitrogen, 0.134 lb per day. Based on annual production

and with no recoveries, the unit B.O.D. loss of 18.6 population equivalent per bbl would result, throughout the United States, in the losses shown in Table 5. These data indicate a maximum brewery waste population equivalent of 5,430,000, as compared with 13,670,000, for packinghouse and slaughterhouse waste. However, the brewing industry is aware of the salvage possibilities of grains and yeast and will undoubtedly reduce the over-all losses materially, inasmuch as the potential recovery of brewers' yeast is 43,000,000 lb per yr, a sizable item. During World War II, the Siebel Institute of Chicago, a leading brewers' organization, circulated a 68-page brochure containing data on the value of brewers' yeast as a "victory food." Postwar recoveries confirm the claims of this report on basic research.

TABLE 5.—TOTAL LOSSES FROM UNITED STATES BREWERIES

Year	Quantity (million bbl)	Population equivalent (millions)
1936	56.055	3.47
1938	53.513	3.31
1940	53.675	3.33
1941	59.990	3.72
1942	67.700	4.20
1943	75.042	4.65
1944	85.469	5.30
1945	87.662	5.43

DISTILLERY AND ALCOHOL

Still residues from alcohol manufacture were probably the largest source of pollution of any industrial waste during World War II because of the tremendous program of alcohol manufacture for use in the synthetic rubber industry. It was estimated that without any recovery of still "slop" the population equivalent of such wastes might reach 27,000,000 in 1944, but a substantial proportion was recovered by dewatering and drying in multiple-effect evaporators. At one distillery in Peoria, Ill., the stillage is screened and the effluent centrifuged and finally dried in triple-effect vacuum pans to produce a feed worth from $30 to $35 per ton (in 1943). There appear to be several ways to increase the degree to which vacuum pans will function, among them the preliminary centrifugal treatment. However, all such methods reduce the cost of drying and lead to recovery by production of dried feed. It was estimated[14] that some 1,000,000 tons would be dried in the United States in 1945. This recovery was probably the largest salvage problem undertaken by industry.

CORN PRODUCTS

The story of recoveries of feeds in the corn products industry is rather well known. Losses dropped from a population equivalent of 5.6 persons per bu, before any recoveries were made, to 4.0 by settling of gluten wastes, then to 1.0 when solubles were concentrated by recirculation and dried, and finally to a minimum of 0.45 in 1936. Since then the losses have leveled off at an approximate population equivalent of from 0.6 to 0.8 persons per bu, except for a period of a few months in 1945 when wheat was ground and losses increased again to 1.5 population equivalent per bu (Table 6). During this time the recovered solids were mixed with gluten and hulls and dried, to be sold as feed at $35 or $40 per ton.

[14] "Feed By-Products from Grain Alcohol and Whiskey Stillage," by C. S. Baruff and L. P. Weiner, *Proceedings*, 1st Industrial Waste Conference, Purdue Univ., Lafayette, Ind., November, 1944, p. 87.

Pulp and Paper

Pulping processes include sulfate, soda, and sulfite, of which the first two are, almost completely, "bottled up" by recovery of chemicals. The sulfite process is the concern of all sanitary officials, however, because of its well-known polluting character. Half of the wood goes into the waste liquor, largely

TABLE 6.—Unit Losses in Corn Products Wastes

Year	Grind (bu per day)	Total Population Equivalent (Thousands)			Loss reduction (%)	Unit population equivalent (persons per bu)
		No recovery[a]	Measured loss	Recovery		
(1)	(2)	(3)	(4)	(5)	(6)	(7)
1922	65,500	367	367	0	0	5.6
1923	62,400	348	270	78	22.4	4.3
1924	63,100	352	282	70	19.9	4.5
1925	65,700	368	257	111	30.2	3.9
1926	66,200	371	156	215	58.0	2.4
1927	72,700	407	77	330	81.0	1.05
1928	74,200	416	56	360	86.5	0.75
1929	77,200	432	71	361	83.6	0.9
1930	75,500	422	56	366	86.7	0.75
1931	67,400	378	78	300	79.5	1.15
1932	68,000	382	64	318	83.3	0.95
1933	69,100	388	59	329	85.0	0.85
1934	68,400	383	91	292	76.2	1.3
1935	68,000	382	60	322	84.3	0.9
1936	69,250	389	30	359	92.3	0.45
1937	71,800	404	41	363	89.8	0.55
1938	73,100	411	40	371	90.2	0.55
1939	69,700	391	49	342	87.5	0.7
1940	71,200	400	51	349	87.3	0.7
1941	85,500	480	56	424	88.0	0.65
1942	88,400	496	82	414	83.5	0.95
1943	88,800	498	71	427	85.7	0.8
1944	86,600	495	72	423	85.5	0.85
1945	82,000	467	125	342	73.3	1.5

[a] Proportional to grind.

made up of calcium salts of lignin, sulfonates, sulfites, wood sugars, and lime. The calcium salts are not recoverable as they reappear as calcium sulfate if calcined. Nevertheless, it is possible to use magnesium hydroxide as the basic chemical, add sulfur dioxide, and recover the hydroxide as the same salt by burning off the organic matter and calcining the magnesium sulfite to oxide. This process appears feasible, but is too costly for reconversion of existing plants using the calcium salt. However, new plants can probably use the magnesium salt and thus solve the waste problem just as it has been solved in the sulfate and soda processes.

About all that can be done with sulfite wastes of the calcium type is to investigate the possibilities of fermenting the wood sugars (about 12% of the solids) to alcohol, or recovering fodder yeast by similar processes. Alcohol recovery has been operated at Thorold, Ont., Canada, and Bellingham, Wash., on a large scale, with investment of more than a million dollars. It appears possible to produce alcohol at a price somewhat more than that of alcohol made by chemical synthesis. Prior to World War II about 80% of German sulfite mills recovered alcohol by the fermentation process.

Yeast has been produced from pulp wastes in Europe for some years and the processes are under investigation in Oregon. A committee of the industry in late 1946 studied data available at that time. It appears possible to produce 70,000 tons of high-protein feed per yr in the northwest at less than $0.08 per lb. The economics of this procedure are under investigation, including feeding experiments. Yeast plants are operating at Bellingham and Sumner, Wash. Research is also being directed by the Sulfite Paper Manufacturers' Committee on Waste Disposal in Madison, Wis., in cooperation with the Institute of Paper Chemistry at Appleton, Wis.

The alcohol and yeast processes, however, use only the wood sugars, leaving the lignin and inorganic salts. One process recovers these as calcium sulfolignate, which can be burned or used for making various chemicals. This type of lignin disposal has not had development outside a paper mill at Rothschild, Wis., and hence a more attractive process for disposal of lignin appears desirable.

For paper mill wastes, various degrees of recovery of fiber appear possible, depending on the type of "save-all" adopted. Losses should not exceed 1% of the product. Recirculation of liquor, using chlorine or some other germicide to prevent slimes, appears essential. The National Council for Stream Improvement (of the Pulp, Paper, and Paperboard Industry) is actively studying these and other salvage procedures, as well as final treatment of unrecoverable solids, and may be expected to point the way toward solution of the pulp and paper waste problem.

By-Products Coke

Salvage of phenol from ammonia liquor produced in by-products coke plants has been accomplished for many years by the solvent extraction process or the steaming-out process. Of the four by-products coke plants in Chicago, three have no phenol recovery, whereas the fourth includes a light-oil extraction plant. The data for surveys of these plants are shown in Table 7. These results show that about 1,500 lb of phenol can be recovered daily by a 1,750-ton plant, with a phenol recovery efficiency of 98%. However, the reduction of

TABLE 7.—Unit Losses in By-Products Coke Wastes

Plant No.	Coal use (tons per day)	Polluting Wastes (Lb per Ton of Coal)		Remarks
		Phenol	5-day B.O.D.	
(1)	(2)	(3)	(4)	
1	816	7.62	2.85	No phenol recovery
2	1,526	0.73	1.52	....
3	1,526	0.41	2.09	....
4	1,549	0.77	1.72	....
5	2,075	0.68	1.25	....
6	2,915	1.25	1.97	....
Average	1,735	0.91	1.90	....
7	1,788	0.023[a]	0.44[b]	Phenol recovered

[a] Phenol reduction 97.5%. [b] 5-day B.O.D. reduction 76.8%.

B.O.D. is only 77% by such removal, leaving a population equivalent of 4,600 for a 1,750-ton plant. This residue should be handled in a sewage treatment works, if possible. In Germany the phenol recovered in the Ruhr Valley supplied the needs for phenol-formaldehyde resins and it can be used for such purposes in the United States. Other solvents are possible, especially a war-time product consisting of a mixture of esters of aliphatic alcohols.

Chemicals, Plating, and Pickling

Recovery of products in a chemical plant is usually unattractive financially, as acids or alkalies may be too dilute to warrant concentration, and organic residues may be too dilute or unstable to be recovered. Some chemicals are being recovered, however, notably from 5 tons to 10 tons per day of sulfur from dye wastes containing sodium thiosulfate. Other recoveries include anilin, phthalic acid, and solvents.

Plating solutions are not dumped deliberately, but the metals are usually recovered and the cyanides destroyed. Tin, nickel, chromium, silver, and gold are usually recovered, but not always zinc, lead, or aluminum.

Pickling of copper and brass produces cuprous solutions which may be treated with iron filings or turnings for "cementation" of the copper and discharge of ferrous sulfate. This method of recovery usually is not very expensive and is sometimes profitable. In some cases, base exchange by means of resins may be used for complete recovery of the copper, but the expense is likely to be greater than the return.

Pickling of iron and steel still remains a source of industrial wastes for which no process that will operate profitably has been discovered. Fortunately, pickle liquors are not highly objectionable as stream pollutants, as the acidity is usually neutralized and the iron precipitated, in the stream, with some absorption of dissolved oxygen to oxidize the iron. In some cases the black ferrous sulfide is objectionable in streams, but does not produce odors or menace health. However, there are numerous methods of recovery of ferrous sulfate proposed in patents and with government subsidies, some of which were operated in Germany. Also, one or two plants are operating in England, recovery of sintered iron has been operated in the United States, and the search for a process with more attractive possibilities of return goes on—led by the work of the American Iron and Steel Institute at Mellon Institute in Pittsburgh, Pa. Richard D. Hoak, who is in charge of this work, states:

> "The steel industry has no expectation of making a profit from pickle liquor treatment; but, in accordance with sound business principles, it has adopted temporary disposal expedients to serve in a partially satisfactory manner until research and technology provide the most practical and economical processes for permanent installation."

This is a frank and honest statement of the position of iron and steel manufacturers.

Oil Refineries

Oil-skimming basins of adequate (American Petroleum Institute) design are essential in modern refinery practice and they usually recover enough oil to

pay for their operation. Skimming basins in large refineries near Chicago, of inadequate capacity, still collect several thousand barrels of oil daily. Acid sludge can be handled by various procedures. Alkaline wash waters are still mainly a problem of disposal rather than of salvage.

Tannery, Rubber, and Textiles

Tannery operation does not lend itself to salvage operations, although there are many patents on recovery of chromium salts. Leather scrap, hair, and fleshings may be saved and treated with acid to produce fertilizer, seldom, however, is the procedure profitable. Rubber regeneration is practiced as a salvage operation at a number of plants in the United States, but the liquid wastes from the process are purely a waste treatment problem of considerably increased magnitude, and no salvage appears possible. Textile wastes also offer little opportunity for salvage.

Laundries and Dairies

Laundries and dairies offer little opportunity for salvage. In the former, heat may be conserved by countercurrent flow of hot and cold water. Laundry wastes surveys in Chicago disclosed the unit losses shown in Table 8. When unit losses were applied to all the laundries in the Chicago Sanitary District, the laundry wastes amounted to 7 tons suspended solids per day and a population equivalent of 294,000, based on B.O.D.

TABLE 8.—Unit Losses in Laundry Wastes

Plant No.	Service volume (tons per day)	Waste volume (gal per ton)	Polluting Wastes (Lb per Ton)			
			5-day B.O.D.	Suspended solids	Total nitrogen	Grease
(1)	(2)	(3)	(4)	(5)	(6)	(7)
1	3.2	15,000	95	26	2.0	....
2	3.5	13,000	75	91	1.3	32
3	5.0	14,000	101	39	2.3	30
4	5.3	17,000	168	47	1.6	....
5	7.0	21,000	110	52	2.0	....
6	7.0	13,000	56	35	0.8	28
7	7.5	13,000	80	58	1.1	37
8	9.0	15,000	94	61	2.4	41
9	9.5	17,000	116	53	2.2	42
10	10.0	24,000	129	58	2.4	....
11	13.0	12,000	67	44	0.7	31
12	18.5	22,000	141	34	2.2	....
13	22.0	13,000	75	91	1.3	32
Average	9.3	16,000	100	53	1.7	34

In dairies, drippings and whey may be recovered, but the low value does not appear to pay for the cost of recovery. Milk bottling wastes in Chicago surveys totaled 6 tons suspended solids and a population equivalent of 145,000.

Canning, Beet Sugar, and Candy

The drying of leaky residues from various canneries is under investigation and may lead to recovery and sale of such residues at a profit. Cannery wastes

are unsuitable for recovery and must be treated at the least possible cost. Beet sugar plants produce a waste that is a source of betain and other salvage products. Food processing offers little opportunity for salvage. Candy plants can lose considerable quantities of sugar if not operated carefully.

Summary

This rather brief review of possibilities of recovery and utilization of products from industrial wastes indicates that there are good prospects of salvage in numerous industries and that many former wastes are now recovered and sold at a profit. Even though no profit is realized the procedures discussed are those which recover salable materials and thus reduce the cost of final treatment. A recapitulation of average losses per ton of raw material or product, in selected types of industires, is shown in Table 9.

TABLE 9.—Losses per Ton of Raw Material or Product

Type of industry	Raw material or product	Losses per Ton	
		B.O.D. (lb)	Population equivalent
(1)	(2)	(3)	(4)
Packinghouse.....	Live weight	28.9	173
Brewery.....	Beer	23.6	142
Corn products.....	Corn	4.8	29
By-products coke....	Coal	1.9	11
Laundry.....	Dirty clothes	100	600

No illusions should be held as to the possibilities of profitable recovery. A newcomer envisions great prospects for industry by rather obvious methods of recovery, but by the time all costs are included the process usually works out at a loss. The loss, however, is not so great as the cost of final disposal of the materials by sewage treatment methods, and hence is preferable.

Many recoveries are profitable, such as grease and tankage from packinghouse wastes, wool grease from wool scouring, grains and yeast from breweries, feed and possibly yeast from distilleries, feed from corn products, possibly alcohol or yeast from sulfite liquors, phenol from by-products coke, sulfur from chemical wastes, copper from pickling wastes, oil from refineries, and whey from cheese plants. All these recoveries are in use. However, manufacturers in time come to regard salvage as part of factory operations, and one-time losses such as gluten, feed, grease, yeast, and other products are no longer classed as by-products or wastes, but as primary products of plant operation and profits. This is not a discouraging attitude, but makes the future prospect for profitable recoveries more bleak, although still an attractive field for the conservationist.

AMERICAN SOCIETY OF CIVIL ENGINEERS

Founded November 5, 1852

PAPERS

ADJUSTMENT OF THE "SHORAN" TRIANGULATION

BY CHUNG-JUI CHU,[1] ESQ.

SYNOPSIS

Application of "shoran," a variation of radar, to triangulation necessitates a new method of adjustment. In this paper the various phases of the problem and the several alternatives as to the actual steps to be taken in making the adjustment are discussed. The method employed is first to determine the approximate position of the triangulation stations, and then to find the corrections by the method of least squares. The formulas employed in this method have been simplified by use of the chord distance.

INTRODUCTION

In addition to many other peacetime uses, shoran has found a possible application in triangulation. Instead of measuring the horizontal angles, the distances between the triangulation stations are measured by shoran equipment. This new method will solve the problem of projecting triangulation across fairly wide waters and over high mountains, upon which depends the project of reducing geodetic work throughout the world to the same geodetic datum. A word of caution might be added that at this stage in its development the shoran method cannot completely replace the old method since the new method of measuring short distances does not give the required accuracy.

The chief advantages of the shoran method are:

1. Field operations are simpler than those of the conventional method and can be completed more rapidly. Weather has no great effect on the field work.
2. Rugged terrain presents no problem in the choice of strong triangulation figures.
3. As compared with the old method, formation of the observation and condition equations is much easier, as will be shown hereinafter.
4. An entire country, for example, China, can be covered with no more than fifty pentagons, each with sides about 500 miles in length. Simultaneous

NOTE.—Written comments are invited for immediate publication; to insure publication the last discussion should be submitted by **February 1, 1949.**

[1] Prof. of Surveying, National Tsing Hua Univ., Peiping, China.

adjustment of the whole work is possible without too much labor. The solid network of triangulation thus adjusted should be much stronger than the ordinary arc triangulation of the same order of accuracy.

In general, there are fewer extra equations for the shoran method than for the old method. The number of extra observation equations for a polygon with n sides and a central station, wherein the distances between all the stations except the two fixed ones are measured, is

$$O_e = ({}_{n+1}C_2 - 1) - 2(n-1) = {}_{n+1}C_2 - (2n-1) \quad \ldots\ldots\ldots (1a)$$

in which

$${}_{n+1}C_2 = \frac{\lfloor n+1}{\lfloor (n+1)-2 \, \lfloor 2} = \frac{(n+1)\,n}{2} \quad \ldots\ldots\ldots\ldots (1b)$$

For example, for the pentagon in Fig. 1(a) in which A and B are fixed stations, $O_e = {}_6C_2 - 9 = 15 - 9 = 6$.

Fig. 1(b) is a similar pentagon showing only the directions usually observed by the old method. In this case there are six condition equations, consisting of five angle equations and one side equation. In making this comparison it must be remembered that in Fig. 1(b) the directions, A′ D′, A′ C′, B′ E′, B′ D′, C′ A′, and C′ E′, are not observed. The comparison is not made, therefore, on the same basis, and is intended only to show how a net can be strengthened by measuring all distances between stations. Hereinafter is developed a method of adjusting a solid network of triangulation starting from two fixed stations.

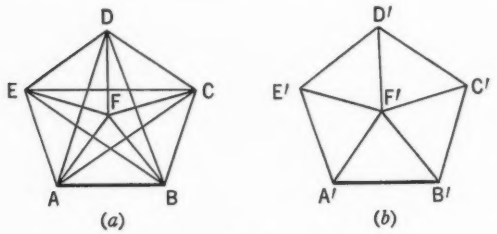

FIG. 1

DETERMINATION OF THE APPROXIMATE POSITIONS

In determining the approximate positions of the triangulation stations the earth is considered to be a sphere. Methods suitable for this determination include: (a) Solution of the spherical triangles; (b) solution of the auxiliary plane triangles; and (c) graphical solution of the spherical triangles by a map projection. The first two methods are too well known to require comment, but it is deemed desirable to explain briefly the graphical method (see "Appendix I").

Stereographic projection is particularly suited to the graphical solution because it has the useful property that all circles on a sphere, great or small, are represented by circles on the projection if the straight lines are considered to be circles of infinite radius. In connection with the methods of determining the preliminary positions, it has been suggested that the astronomic positions might be used instead, for which the zenith camera developed by the United States Army will serve very well indeed.

Corrections to the Approximate Positions

In deriving the formulas for corrections to the approximate positions, the chord distance is used, and the mathematical surface taken to represent the earth is the ellipsoid of revolution. The chord distance, c_{12}, between two stations, S_1 (x_1, y_1, z_1) and S_2 (x_2, y_2, z_2), is given by

$$c_{12} = \sqrt{(x_1 - x_2)^2 + (y_1 - y_2)^2 + (z_1 - z_2)^2} \quad \ldots\ldots (2)$$

Differentiating Eq. 2,

$$dc_{12} = X_{12}\,(dx_1 - dx_2) + Y_{12}\,(dy_1 - dy_2) + Z_{12}\,(dz_1 - dz_2) \quad \ldots\ldots (3a)$$

in which

$$X_{12} = \frac{x_1 - x_2}{c_{12}} \quad \ldots\ldots (3b)$$

$$Y_{12} = \frac{y_1 - y_2}{c_{12}} \quad \ldots\ldots (3c)$$

and

$$Z_{12} = \frac{z_1 - z_2}{c_{12}} \quad \ldots\ldots (3d)$$

If the increments Δx_1, Δy_1, Δz_1, Δx_2, Δy_2, Δz_2, and Δc_{12} are small enough, Eq. 3*a* may be written

$$\Delta c_{12} = X_{12}\,(\Delta x_1 - \Delta x_2) + Y_{12}\,(\Delta y_1 - \Delta y_2) + Z_{12}\,(\Delta z_1 - \Delta z_2) \quad \ldots\ldots (3e)$$

If either station is fixed, Δx, Δy, and Δz are, of course, equal to zero. From the geometric relationships involved,

$$x_1 = N_1 \cos\phi \cos\lambda_1 \quad \ldots\ldots (4a)$$

$$y_1 = N_1 \cos\phi_1 \sin\lambda_1 \quad \ldots\ldots (4b)$$

$$z_1 = N_1 (1 - e^2) \sin\phi_1 \quad \ldots\ldots (4c)$$

$$x_2 = N_2 \cos\phi_2 \cos\lambda_2 \quad \ldots\ldots (4d)$$

$$y_2 = N_2 \cos\phi_2 \sin\lambda_2 \quad \ldots\ldots (4e)$$

and

$$z_2 = N_2 (1 - e^2) \sin\phi_2 \quad \ldots\ldots (4f)$$

in which N_1 and N_2 are the normals to the meridians through the two stations and terminating at the axis of revolution; e is the eccentricity of the ellipsoid of revolution; and λ and ϕ are the longitude and geodetic latitude, respectively, of the station designated by the subscript. Hence,

$$\Delta x_1 = -N_1 \sin\phi_1 \cos\lambda_1 \Delta\phi_1 - N_1 \cos\phi_1 \sin\lambda_1 \Delta\lambda_1 \quad \ldots\ldots (5a)$$

$$\Delta y_1 = -N_1 \sin\phi_1 \sin\lambda_1 \Delta\phi_1 + N_1 \cos\phi_1 \cos\lambda_1 \Delta\lambda_1 \quad \ldots\ldots (5b)$$

$$\Delta z_1 = N_1 (1 - e^2) \cos\phi_1 \Delta\phi_1 \quad \ldots\ldots (5c)$$

$$\Delta x_2 = -N_2 \sin\phi_2 \cos\lambda_2 \Delta\phi_2 - N_2 \cos\phi_2 \sin\lambda_2 \Delta\lambda_2 \quad \ldots\ldots (5d)$$

$$\Delta y_2 = -N_2 \sin\phi_2 \sin\lambda_2 \Delta\phi_2 + N_2 \cos\phi_2 \cos\lambda_2 \Delta\lambda_2 \quad \ldots\ldots (5e)$$

and

$$\Delta z_2 = N_2 (1 - e^2) \cos \phi_2 \Delta \phi_2 \ldots\ldots\ldots\ldots\ldots\ldots\ldots\ldots\ldots\ldots (5f)$$

in which N_1 and N_2 may be regarded as the constants. Substitution of Eqs. 5 in Eq. 3*e* gives

$$\begin{aligned}\Delta c_{12} = {} & N_1 [- X_{12} \sin \phi_1 \cos \lambda_1 - Y_{12} \sin \phi_1 \sin \lambda_1 + Z_{12} (1 - e^2) \cos \phi_1] \Delta \phi_1 \\ & + N_2 [X_{12} \sin \phi_2 \cos \lambda_2 + Y_{12} \sin \phi_2 \sin \lambda_2 - Z_{12} (1 - e^2) \cos \phi_2] \Delta \phi_2 \\ & + N_1 (- X_{12} \cos \phi_1 \sin \lambda_1 + Y_{12} \cos \phi_1 \cos \lambda_1) \Delta \lambda_1 + N_2 (X_{12} \cos \phi_2 \\ & \sin \lambda_2 - Y_{12} \cos \phi_2 \cos \lambda_2) \Delta \lambda_2 \ldots\ldots\ldots\ldots\ldots\ldots\ldots\ldots\ldots\ldots (6)\end{aligned}$$

With the approximate station positions known, the coefficients in Eq. 6 can be computed, and Δc_{12}, the difference between the measured and computed chord distances, determined. The computed chord distance is

$$c_c = \sqrt{(x_1 - x_2)^2 + (y_1 - y_2)^2 + (z_1 - z_2)^2} \ldots\ldots\ldots\ldots (7)$$

There are as many relationships of the type of Eq. 6 as there are measured chord distances. Solution of these observation equations, together with any condition equations, by the method of least squares gives the corrections to the approximate positions.

A slightly different approach to this problem first obtains the corrections to the approximate Cartesian coordinates and then converts them to the corresponding corrections for the approximate geographical coordinates. A variation of this method determines the geographical coordinates directly from the corrected Cartesian coordinates. In addition to the equations, similar to Eq. 3*e*, there should also be included the condition equations like

$$x (1 - e^2) \Delta x + y (1 - e^2) \Delta y + z \Delta z = 0 \ldots\ldots\ldots\ldots (8)$$

in order to have the adjusted points also on the ellipsoid of revolution.

A question naturally arises as to how accurate the preliminary positions should be. The error introduced by use of expressions like Eq. 3*e* should be smaller than Δm, the error in the measured distance, in miles. On this basis the longitude should be accurate to within $\frac{1}{\cos \phi \sin (1 \text{ sec})} \sqrt{\frac{\Delta m}{2 c_a}}$ sec and the latitude to within $\frac{1}{\sin (1 \text{ sec})} \sqrt{\frac{\Delta m}{2 c_a}}$ sec. In these criteria, ϕ is the approximate latitude of the station in question, and c_a is the approximate chord distance between the two stations. Derivations of these criteria are given in "Appendix II."

Conclusion

On an ellipsoid of revolution the chord between two points is unique, but the arc is not. The complicated expression for the change in length of a particular arc due to small variations of the end points is too difficult to solve readily without making approximations. The chord triangle is, therefore, superior to the spheroidal triangle as far as the simplicity of the formulas is concerned.

Judgment must be exercised as to the actual steps to be followed when dealing with a particular problem. It has been suggested that in some regions the vertical deflections of the plumb lines might be so great as to make the astronomic positions unsuitable for the prupose of this method. In this case, or under other circumstances when the preliminary positions, computed or otherwise, are not accurate enough, the individual polygons must be adjusted before adjusting the whole network. Should it be proved necessary to introduce the azimuth equations to strengthen the net, they may be treated as the condition equations.

Appendix I. Approximate Positions by Polar Stereographic Projection

Because of the ease with which it can be constructed and also because the projected circle representing all points equidistant from a station on a sphere is symmetrical with respect to the projected meridian through that station, the polar stereographic projection is preferred to any other projection. In

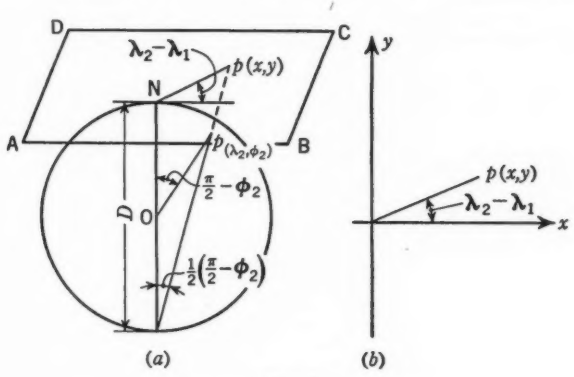

Fig. 2

Fig. 2(*a*) ABCD represents the projection plane tangent to the sphere at the north pole, N, and the circle is the meridian of longitude λ_1, whose projection is taken as the x-axis of the coordinate system shown in Fig. 2(*b*). With the origin at the projection of the north pole the coordinates of the projection of any point P (λ_2, ϕ_2) are

$$x = D \tan \frac{1}{2}\left(\frac{\pi}{2} - \phi_2\right) \cos (\lambda_2 - \lambda_1) \quad \ldots\ldots\ldots\ldots (9a)$$

and

$$y = D \tan \frac{1}{2}\left(\frac{\pi}{2} - \phi_2\right) \sin (\lambda_2 - \lambda_1) \quad \ldots\ldots\ldots\ldots (9b)$$

in which D represents the diameter of the earth and the sign of the longitude is plus or minus depending if it is east or west.

If σ_1 and σ_2 denote, respectively, the angles subtended at the center of the earth by the arcs from an unknown station, S_x (λ_x, ϕ_x), to two known stations, S_1 (λ_1, ϕ_1) and S_2 (λ_2, ϕ_2), the plane coordinates of two points on the meridian of longitude λ_2 and at angular distance σ_2 from S_1 are

$$x_1 = D \tan \frac{1}{2}\left[\frac{\pi}{2} - (\phi_2 + \sigma_2)\right] \cos(\lambda_2 - \lambda_1) \quad \ldots\ldots\ldots (10a)$$

$$y_1 = D \tan \frac{1}{2}\left[\frac{\phi}{2} - (\phi_2 + \sigma_2)\right] \sin(\lambda_2 - \lambda_1) \quad \ldots\ldots\ldots (10b)$$

$$x_2 = D \tan \frac{1}{2}\left[\frac{\pi}{2} - (\phi_2 - \sigma_2)\right] \cos(\lambda_2 - \lambda_1) \quad \ldots\ldots\ldots (10c)$$

and

$$y_2 = D \tan \frac{1}{2}\left[\frac{\phi}{2} - (\phi_2 - \sigma_2)\right] \sin(\lambda_2 - \lambda_1) \quad \ldots\ldots\ldots (10d)$$

The projected locus of a point at angular distance σ_2 from station S_2 is the circle which passes through the coordinates given by Eqs. 10 and has its center at the midpoint of the line joining them. There is a corresponding circle for S_1. One of the intersections of the two circles gives the position of the unknown station. If a projection showing the meridians and the parallels of latitude has been constructed, the position will be given directly in geographical coordinates (λ_x, ϕ_x). If the projection does not include meridians and parallels, the geographical coordinates can be computed from the scaled plane coordinates from the expressions,

$$\tan^2 \frac{1}{2}\left(\frac{\pi}{2} - \phi_x\right) = \frac{x^2 + y^2}{D^2} \quad \ldots\ldots\ldots\ldots\ldots\ldots (11a)$$

and

$$\sin^2(\lambda_x - \lambda_1) = \frac{y^2}{x^2 + y^2} \quad \ldots\ldots\ldots\ldots\ldots\ldots (11b)$$

Appendix II. Derivation of the Criteria of Error

To obtain an expression for the residual discrepancy between the recomputed and the measured chord distances the errors introduced in translating Eq. 3*e* into Eq. 6 by use of Eqs. 4 and 5 are neglected. Since these errors are small as compared with Δx, Δy, and Δz, this omission is justified.

If Δx_1, Δy_1, and Δz_1 denote the required increments of the coordinates of one point so that the computed chord distance between the new point and the fixed one equals the measured chord distance c_1, then,

$$(x_1 + \Delta x_1 - a)^2 + (y_1 + \Delta y_1 - b)^2 + (z_1 + \Delta z_1 - c)^2 = c_1^2 \quad \ldots\ldots (12)$$

in which (x_1, y_1, z_1) are the coordinates of the unknown point, and (a, b, c) are those of the fixed point. Substituting

$$c_a^2 = (x_1 - a)^2 + (y_1 - b)^2 + (z_1 - c)^2 \quad \ldots\ldots\ldots\ldots (13a)$$

and

$$\Delta c_1 = c_1 - c_a \quad \ldots\ldots\ldots\ldots\ldots\ldots\ldots\ldots (13b)$$

in Eq. 12 gives

$$2\,(x_1 - a)\,\Delta x_1 + 2\,(y_1 - b)\,\Delta y_1 + 2\,(z - c)\,\Delta z_1 = c^2{}_a + 2\,c_a\,\Delta c_1 + (\Delta c_1)^2 - [(x_1 - a)^2 + (y_1 - b)^2 + (z_1 - c)^2] - [(\Delta x_1)^2 + (\Delta y_1)^2 + (\Delta z_1)^2] \quad \ldots (14a)$$

or

$$\frac{x_1 - a}{c_a}\,\Delta x_1 + \frac{y_1 - b}{c_a}\,\Delta y_1 + \frac{z_1 - c}{c_a}\,\Delta z_1 = \Delta c_1 + \frac{(\Delta c_1)^2 - [(\Delta x_1)^2 + (\Delta y_1)^2 + (\Delta z_1)^2]}{2\,c_a} \quad \ldots\ldots\ldots (14b)$$

Since the last term on the right side of Eq. 14*b* has been omitted in writing Eq. 3*e*, the recomputed distance would fail to equal c_1 by an amount equal to $\dfrac{(\Delta c_1)^2 - [(\Delta x_1)^2 + (\Delta y_1)^2 + (\Delta z_1)^2]}{2\,c_a}$.

In the following discussion the earth is considered to be a sphere. It is also assumed that chords AB and A′B′ (Fig. 3(*a*)) lie in the same plane, Fig. 3(*a*) shows a cross section of the earth.

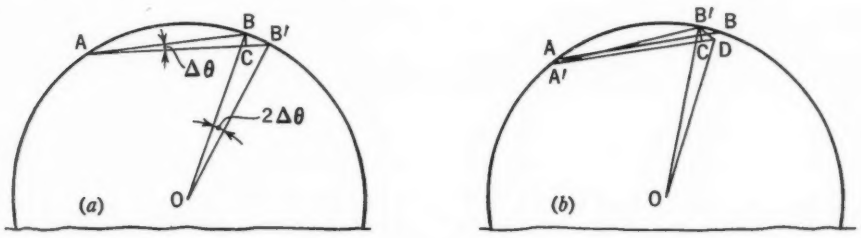

FIG. 3

It is evident that

$$[(\Delta x_1)^2 + (\Delta y_1)^2 + (\Delta z_1)^2] - (\Delta c_1)^2 \doteq (\overline{BB'})^2 - (\overline{CB'})^2 = (\overline{BC})^2 \quad \ldots (15)$$

However,

$$4{,}000 \times 2\,\Delta\theta = \overline{BB'} \doteq \overline{CB'} \doteq \Delta c_1 \quad \ldots\ldots\ldots\ldots\ldots (16)$$

and

$$\overline{AB}\,\Delta\theta \doteq \overline{BC} \quad \ldots\ldots\ldots\ldots\ldots\ldots\ldots\ldots (17)$$

thus,

$$\overline{BC} = \overline{AB}\,\frac{\Delta c_1}{8{,}000} = \Delta c_1\,\frac{c_a}{8{,}000} \quad \ldots\ldots\ldots\ldots\ldots\ldots (18)$$

It is required that the error introduced be smaller than Δm, the error in the measured distance in miles. Therefore,

$$\frac{\left(\Delta c_1\,\dfrac{c_a}{8{,}000}\right)^2}{2\,c_a} < \Delta m \quad \ldots\ldots\ldots\ldots\ldots\ldots (19a)$$

or

$$\Delta c_1 < 8{,}000 \sqrt{\frac{2\,\Delta m}{c_a}} \quad \ldots\ldots\ldots\ldots\ldots\ldots\ldots (19b)$$

If both points are allowed to vary as shown in Fig. 3(*b*), in which $\overline{AB}$ and $\overline{A'D}$ are drawn to be equal and parallel, the error is

$$\frac{(\Delta c_1)^2 - [(\Delta x_1 - \Delta x_2)^2 + (\Delta y_1 - \Delta y_2)^2 + (\Delta z_1 - \Delta z_2)^2]}{2\,c_a}$$

$$\doteq \frac{(\overline{CD})^2 - (\overline{B'D})^2}{2\,c_a} = -\frac{(\overline{B'C})^2}{2\,c_a} \doteq -\frac{\left(\Delta c_1 \frac{c_a}{8{,}000}\right)^2}{2\,c_a} \quad \ldots\ldots\ldots (20)$$

Hence, the limit of Δc_1 is the same; that is, Eq. 19*b* still governs. It is safe to allow a limit $\frac{\Delta c_1}{2}$ at each point as the error falls within the set limit, provided that neither the difference along the meridian, in miles, between the approximate position and the final position, nor that along the parallel of latitude, is greater than $2{,}000\sqrt{\frac{2\,\Delta m}{c_a}}\left(= \frac{1}{2} \times \frac{1}{2}\, 8{,}000 \sqrt{\frac{2\,\Delta m}{c_a}}\right)$. The limits of the difference in longitude and in latitude are given by

$$\Delta\lambda \text{ (in seconds)} < \frac{1}{\cos\phi \sin (1 \text{ sec})} \sqrt{\frac{\Delta m}{2\,c_a}} \quad \ldots\ldots\ldots (21a)$$

and

$$\Delta\phi \text{ (in seconds)} < \frac{1}{\sin (1 \text{ sec})} \sqrt{\frac{\Delta m}{2\,c_a}} \quad \ldots\ldots\ldots\ldots (21b)$$

AMERICAN SOCIETY OF CIVIL ENGINEERS

Founded November 5, 1852

PAPERS

UNUSUAL DESIGN PROBLEMS, HARLAN COUNTY DAM

BY LOUIS G. FEIL,[1] ESQ.

SYNOPSIS

Details and results of extensive analyses of stilling basin, spillway, and embankment designs for a major unit in the proposed flood control plan for a major tributary of the Missouri River are presented in this paper. Among the difficulties overcome in the final design are such foundation conditions as weak shaly chalk, badly faulted and fractured, and interbedded with numerous near-horizontal seams of bentonitic clay, together with almost certain differential settlement of an overlying loess and loess-silt mantle.

LOCATION AND STRUCTURES

The Harlan County Dam and its multipurpose reservoir, scheduled for completion in 1951, is one of the major units proposed by the so-called "Pick-Sloan Plan" (the comprehensive plan for flood control and other purposes in the Missouri River Basin, contained in House Document No. 475, and Senate Document No. 247, Seventy-eighth Congress 2d Session, approved by the Flood Control Act, December 22, 1944) for the control of floods in the Kansas River Basin, at Kansas City (in both Missouri and Kansas), and along the Missouri River downstream from Kansas City. It was designed by the Kansas City District, Corps of Engineers, Department of the Army, which is cooperating with the Bureau of Reclamation, the Fish and Wildlife Service, the National Park Service—all of the United States Department of Interior—the State of Nebraska, and other agencies to assure that optimum use will be made of this project for flood control, irrigation, fish and wildlife conservation, recreation development, and other public services.

The dam site is located on the Republican River in south central Nebraska, approximately 236 miles above the point at which the Republican and Smoky Hill rivers join to form the Kansas River. The reservoir impounded by the dam has a gross capacity of 850,000 acre-ft, of which 500,000 acre-ft are allo-

NOTE.—Written comments are invited for immediate publication; to insure publication the last discussion should be submitted by **February 1, 1949.**

[1] Chf., Design Branch, Kansas City Dist., Corps of Engrs., Dept. of the Army, Kansas City, Mo.

cated to flood control, 150,000 acre-ft to irrigation, and 200,000 acre-ft to conservation and silting. The reservoir controls the runoff from 20,750 sq miles, or about 83% of the total area of the Republican River Basin. Storage, sufficient to permit control of all floods of record in the Republican River, affords direct protection to 138,000 acres along the Republican River and, in addition, lessens the flood hazards for 150,000 acres and 583,000 acres along the Kansas and Missouri rivers, respectively. Storage allocated to irrigation provides water to irrigate approximately 86,700 acres downstream from the dam. At maximum operating pool level the reservoir has a 22,800-acre area, a 15-mile length, and a 118-mile shore line. The conservation pool, extending upstream slightly less than 12 miles, has a 58-mile shore line and a 13,700-acre surface area.

The Republican River Valley at the project site is about 2 miles wide; the river channel, located near the middle of the valley, is approximately 250 ft wide. The flood plain (from El. 1885 to El. 1900) occupies the south half of the valley, lying mostly on the right bank of the river. The left or north side of the valley is occupied by a broad terrace, generally from 35 ft to 60 ft above the flood plain. Bedrock beneath the left terrace is approximately at stream bed elevation (El. 1877), affording a favorable site for an overflow type of spillway structure with relatively short approach and outlet channels. Preliminary studies indicated conclusively that the most economical plan of development would consist of rolled fill embankment sections on the flood plain, the terrace, and the river channel, a concrete overflow spillway section and stilling basin located on the terrace adjacent to the river channel, and adjoining concrete bulkheads tying to the rolled fill embankment sections.

Embankment.—The embankment has a total length of approximately 10,600 ft, a maximum height of approximately 110 ft in the channel section, and average heights in the terrace and flood plain sections of 85 ft and 100 ft, respectively. On the 30-ft wide top of the embankment, at El. 1982, a 22-ft paved roadway is provided. Embankment side slopes vary from 1 on $2\frac{1}{2}$ to 1 on 4. Berms constructed of waste material (principally from the spillway excavation) have been added at the toes of the upstream and downstream slopes on the right bank and channel sections. A section of pervious fill is incorporated in the upstream slope immediately beneath the riprap to minimize sloughing during drawdown.

Concrete Structure.—The concrete structure, including the overflow spillway and bulkhead sections, is approximately 1,400 ft long with a maximum height of 147 ft from bottom of concrete to top of dam. The spillway (Fig. 1) is an ogee type overflow structure controlled by eighteen Tainter gates, 40 ft wide by 30 ft high, which will pass the spillway design flood of 457,000 cu ft per sec with a corresponding head of 31.1 ft above the spillway crest. Inspection, operation, and grouting galleries are provided in the spillway. A highway bridge with a 22-ft roadway and a sidewalk on each side is supported on the gate piers. Although the bridge serves solely as an access roadway during the initial development of the project, it was designed in accordance with highway standards to allow future incorporation in the highway system.

Flood control storage will be released through nine sluices, 5 ft wide by 8 ft high, and uniformly sloped so that their discharge inverts are tangent to the bucket at the toe of the spillway. To minimize cavitation the height of the sluices is reduced 15% at the bucket. Each sluice is controlled by one service gate and one emergency, hydraulically operated slide gate with vented frames. Total sluice capacity varies from 19,500 cu ft per sec with full flood control pool to 14,300 cu ft per sec with depleted irrigation pool.

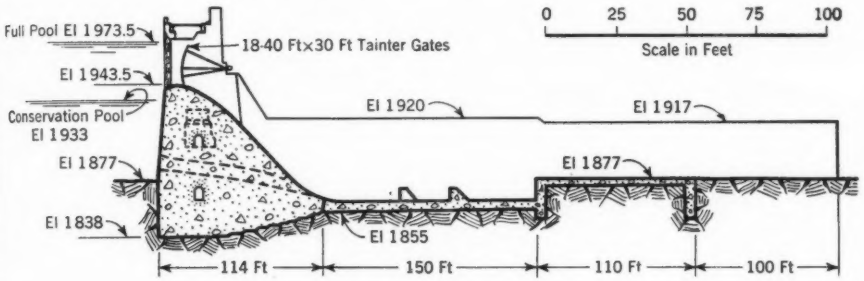

FIG. 1.—ADOPTED DESIGN OF SPILLWAY AND STILLING BASIN

Irrigation releases of approximately 2,000 cu ft per sec will be made through a combination consisting of the flood control slucies, one circular sluice 2.5 ft in diameter in the right bulkhead section, and one circular sluice 5 ft in diameter in the left bulkhead section. The energy of the water discharged by the spillway is dissipated by a 150-ft-long, concrete-lined stilling basin with two rows of 8-ft-high baffle piers, and a control sill 15 ft high and 110 ft wide.

Construction of the embankment requires approximately 12,000,000 cu yd of fill and 260,000 cu yd of riprap and spalls for slope protection. Concrete structures require approximately 3,200,000 cu yd of excavation and 435,000 cu yd of concrete. Total cost of the Harlan County Dam and reservoir is estimated to be more than $25,000,000.

POOR FOUNDATION CONDITIONS

Construction of dams in the Missouri River Basin continually presents unusual problems of interest to the designer. The foundation conditions, varying from dolomite and limestone in the lower sections of the basin to the soft clay shales in the upper reaches of the basin, dictate radically different designs. In the lower areas sites may usually be selected that lend themselves to economical development of all concrete structures; however, the poorer foundations, together with the scarcity of local sources for the production of satisfactory concrete aggregates and the broader river valleys, generally require long, earth fill dams in the upper reaches of the basin, with the concrete structures limited to spillways and outlet works. Although the Harlan County site is of the latter type, local foundation conditions materially affected the designs of both the spillway and embankment structures. Generally the top of the bedrock underlying the site has the same configuration as the existing ground surface. Bedrock formations are chiefly Niobrara shaly chalk and Pierre

shale, but in the right bluffs approximately 40 ft of semiconsolidated Ogallala sand rests unconformably on the Pierre shale. Unconsolidated formations, chiefly loess-silts and sand, cover the bedrock to depths of from 40 ft to 70 ft, or more, in both abutments and in the broad terrace.

The Niobrara shaly chalk is the principal bedrock formation, underlying the entire dam site and the surrounding country for a distance of many miles. It is composed chiefly of minute calcareous shells and, as a rock, is relatively soft. The Niobrara, which is uniform, relatively impervious, and a firm, fairly heavily bedded formation where it is unweathered, is the most competent foundation material present. There are faults and many fracture planes, generally at angles of 45° or larger with the horizontal, as well as numerous near-horizontal seams of impure bentonitic clay varying from a small fraction of an inch to more than 3 in. in thickness.

The Pierre shale is a dark gray, compact clay shale, which disintegrates into a mass of small flakes or crumblike fragments when exposed to weathering. Numerous faults of small displacement cut the Pierre formation, dividing it into blocks of variable dips. It is present in the right abutment and also in an area under the left terrace upstream from the dam.

The Ogallala formation consists of semiconsolidated sands and silts, considerable amounts of volcanic ash, and local lenses of hard indurated quartzite.

Formations covering the bedrock in both abutment ridges consist of a sequence of gravelly sands at the base, overlain by compact and clayey silt of apparent alluvial origin and a surface mantle of loose loess-silt. An alluvial sequence of about 15 ft of gravelly sand overlain by about 10 ft of sandy silt occurs over the bedrock of the terrace. This sequence was subsequently covered by about 25 ft of loess-silt, probably reworked but not readily distinguishable from the loess of the abutments. The alluvium of the flood plain consists of from 5 ft to 10 ft of sandy silt overlying from 5 ft to 35 ft of sand and gravelly sand.

Foundation explorations in the spillway area revealed differences in elevation of the thicker bentonitic seams suggesting vertical displacements approximating 25 ft, attributed to faults in the foundation. One of these faults passes under the spillway structure slightly to the right of the center; the other two pass close to the right and left sides of the main spillway structure. The aggregate thickness of the bentonitic seams in this area is about 1.5 ft in the 100-ft depth of chalk explored. Compression tests of cylinders of sound chalk indicated that the chalk, if free from fracture planes or bentonitic seams, is an adequate foundation. However, the faults and attendant fractures, together with the closely spaced interbeds of bentonitic material, are all indications of the low resistance of the foundation to horizontal forces. Design of an adequate concrete section 147 ft high on such a foundation necessitated thorough investigation.

Special Sampling Procedure

In addition to the usual core drill samples, the presence of the faults and bentonitic seams made it highly desirable to inspect the foundation "in situ" and to obtain relatively large undisturbed samples of the bentonitic material

for laboratory testing. Results of shear and consolidation tests were required in order to evaluate properly the resistance of the foundation to vertical and horizontal forces. Two 36-in. calyx holes drilled for "in situ" inspection were carefully logged and continuous photographic records prepared. Bentonitic seams encountered in one of these holes are shown in Fig. 2. A procedure was devised which allowed recovery of cylindrical samples 33 in. in diameter and of varying heights, containing a bentonitic seam —undisturbed except for the rebound due to the removal of superimposed load.

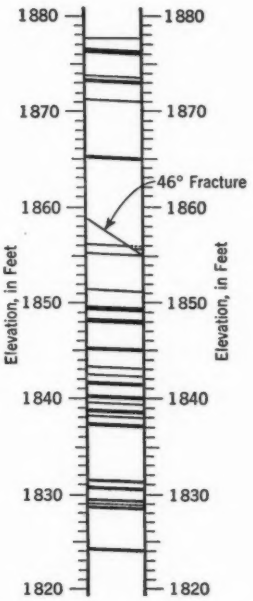

FIG. 2.—TYPICAL LOG OF 36-IN. CALYX HOLE SHOWING BENTONITIC SEAMS

To facilitate removal of the cylinder it was necessary to utilize other bentonitic seams as cleavage planes, which resulted in the use of three seams to recover one for testing. The seams desired for testing were carefully selected from the logs of the two calyx holes, and additional calyx holes were drilled immediately adjacent to those holes. In obtaining the sample every precaution was taken to eliminate rotation or jarring of the sample. Drilling was stopped at the seam at the top of the desired sample, and the following procedure was utilized:

Seven $1\frac{1}{2}$-in. holes were drilled to the approximate depth of the sample. Hardwood pins 1 in. in diameter were "grouted" in six of the seven holes with plaster of Paris, the center hole being utilized to pick up the sample. The calyx hole was then drilled to the seam below the desired sample, as shown by the dotted lines in Fig. 3, and the sample was lifted free by a rod and wedge pickup without barring or blasting. The cylinders were trimmed to approximately 12 in. in height and were cut into 3 equal segments to facilitate handling in the laboratory. Use of hardwood dowels and plaster of Paris allowed all cutting and trimming to be done with a crosscut saw. This method of sampling permitted the laboratory to test the complete segment with the exception of the small corners lost by removal of the dowels. The three samples obtained from each seam permitted testing of each seam under three different vertical loads. The size of the sample required construction of a large shear box and the improvisation of loading and recording devices.

Results of laboratory tests on the chalk varied over a wide range, the compressive breaking strength of sound samples without bentonitic seams averaging approximately 1,000 lb per sq in. Shear tests of the bentonitic seams gave fairly uniform results averaging approximately 0.20 for the coefficient of internal friction, and 0.25 tons per sq ft for cohesion. The consolidation tests indicated that the bentonitic material would consolidate approximately 15% of its original thickness under loads comparable to those imposed by the concrete structure. Design values adopted for the Niobrara shaly chalk were: Bearing, 200 lb per sq in.; shear, 100 lb per sq in.; and modulus of elasticity, 110,000 lb per sq

in. For the bentonite, assuming a safety factor of 1.5, the coefficient of internal friction was chosen as $\frac{0.20}{1.5} = 0.13$, and the cohesion as $\frac{0.25}{1.5} = 0.17$ tons per sq ft. Test values for the bentonitic material conclusively indicate the inherent weakness of the foundation to resist horizontal forces and that the design of any structure could not be considered adequate until the possibility of foundation failure by sliding along a bentonitic seam had been thoroughly investigated. Other important design considerations are: The probability of differential settlement due to the varying thicknesses of bentonite underlying monoliths having identical loadings; the probability of progressive shearing failure due to local overstressing of the laminated foundation and consolidation of the bentonitic material; and the faulted zones in the foundation indicating the probable existence of numerous joint planes in the vicinity of these zones that would affect the ability of the chalk to resist horizontal movement of the structure.

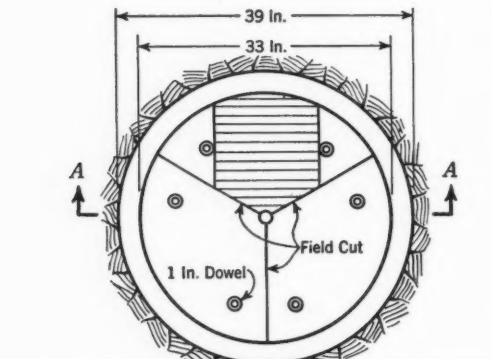

FIG. 3.—METHOD OF RECOVERING UNDISTURBED SAMPLES FROM 36-IN. CALYX HOLE

STILLING BASIN DESIGN STUDIES

In the design of projects of this type one condition in nature is usually of paramount importance and materially affects the design of any major structure. At the Harlan County Dam site this one condition was the low resistance of the foundation to horizontal forces. The problem then was to devise an economical section that would transmit all forces to the foundation in such a manner as to mobilize the greatest possible resistance to sliding, differential settlement, and progressive failure. The low resistance of the foundation to horizontal forces precludes the possibility of the bottom of the stilling basin slab being at a lower elevation than the base of the overflow spillway section; therefore, the over-all height and cost of the overflow section is directly dependent on the design of the stilling basin. To arrive at an economical design for the spillway and stilling basin, designs of five stilling basins were thoroughly tested in 1-to-80 scale models by the United States Waterways Experiment Station at Vicksburg, Miss. In all these tests the efficiency of energy dissipation, the bottom

velocities of the basin and outlet channel, the scour in the outlet channel, and the water surface profiles were carefully analyzed.

The first design consisted of a sloping apron approximately 365 ft long divided into primary and secondary basins by a subdam 40 ft high located 180 ft downstream from the toe of the spillway. The bottom of the apron was set at El. 1856.5. Two rows of 10-ft-high baffle piers and a 2-ft-high stepped end sill were included in the secondary basin. The performance of this design was very satisfactory in the dissipation of the spillway flow before it entered the outlet channel. The model studies indicated that the subdam height could be reduced 5 ft without impairing the efficiency of the basin.

In order to reduce the length of the concrete apron and that of the massive training walls flanking the stilling basin, a second design, consisting of a horizontal apron 122.5 ft long having two rows of 8-ft-high baffle piers and a 10-ft-high stepped end sill, was tested. The bottom of the apron was set at El. 1848. In this design it was assumed that the tailwater depth could be reduced 15%, approximately 7 ft, because of the baffles. The performance of this design was not satisfactory. Excessive impact on the baffle piers indicated that the piers should be moved farther downstream and the apron lengthened and lowered approximately 5 ft.

The modifications indicated by the tests of the second type of basin were incorporated in a third design; they consisted of a sloping apron 186 ft long with two rows of 11-ft-high baffle piers and a 3-ft-high stepped end sill. The apron bottom was set at El. 1840. Performance of this design was generally satisfactory; however, estimated cost of the spillway and stilling basin for this design was approximately $800,000 more than the first design. Also, this third design definitely indicated that deeper tailwater should be obtained by raising the end sill, rather than by lowering the apron.

A fourth design, which consisted of a horizontal apron 136 ft long with two rows of 8-ft-high baffle piers, a 10-ft-high stepped end sill, and a control sill 5 ft above the top of the end sill extending downstream 105 ft and terminating in a cutoff wall, was tested. The apron bottom was set at El. 1855. Performance of this design was not as satisfactory as that of the first and third types in that the piers were subjected to severe impact and the erosion of the outlet channel would cause a secondary jump to form immediately downstream from the control sill. Elimination of the baffle piers resulted in the jump being swept from the apron.

A fifth design, similar to the fourth type except that the stilling basin was lengthened to 150 ft and the stepped end sill was replaced with a 15-ft-high vertical end sill, was also tested. Performance of this design, whereas still not quite as efficient as that for the first and third types for maximum discharge conditions, satisfactorily overcame the difficulties of the fourth design. It was found that the training walls flanking the spillway could be reduced from a total length of 460 ft for the first design to 360 ft for the fifth design without an appreciable effect on erosion downstream from the control sill.

The fifth type of stilling basin design was adopted, thus establishing El. 1855 as the top of the key for any spillway structure. It is estimated that the

adoption of this design in lieu of the first design reduced the cost of the spillway and stilling basin by approximately $500,000, showing conclusively the value of the hydraulic laboratory as a tool for the designer.

Spillway Design Studies

Four concrete overflow sections were studied in considerable detail. The main features of each were essentially the same, varying only in the details required to adapt them to the differing design requirements of the individual structures. The first of the four gravity type spillway structures studied mobilized horizontal resistance to sliding by a conventional tension key at the heel. In the analysis of this section it was considered that failure would occur by sliding along a bentonite seam at the bottom of the key and by shear of the chalk at the downstream toe along a plane inclined at 45° to the horizontal and extending from the bentonite seam to the bottom of the stilling basin slab. The vertical base pressures followed the normal pattern for a gravity section with the typical fluctuation from low to high toe pressure in conformity with the change from empty to full reservoir conditions. Vertical pressures and the magnitude of the pressure fluctuation could be somewhat reduced by sloping the upstream face of the section, and the horizontal pressures could be reduced by deepening the key. Heavy reinforcement would be required, however, to withstand the horizontal shear at the top of the key and the tension in the concrete downstream from the key.

In order to eliminate the tension in the concrete and the necessity of heavy shear reinforcement, a second gravity type structure was studied. In this design the base was sloped and the horizontal forces were transmitted to the foundation by the toe, which was at a lower elevation than the bottom of the stilling basin slab—thus placing the concrete in compression. In the analysis of this section it was assumed that failure would occur by shear of the chalk along a plane inclined at 45° to the horizontal and running from the lowest point of the toe to the bottom of the stilling basin slab. The distribution of foundation pressures would be essentially the same as for the section having the tension heel. The compression toe does not, however, mobilize the weight of the material immediately below the spillway structure, nor does it tend to distribute any of the horizontal forces to the foundation upstream from the toe. Although computations indicated that this structure would be stable, it would aggravate any tendency of progressive failure; in cross section, it has the appearance of attempting to chisel out the material immediatley downstream from the toe and slide into the stilling basin.

The third structure studied was of the round-head buttress type in which horizontal resistance to sliding was mobilized by a bulb at the toe of each monolith. Some of the advantages normally attributed to the buttress type of structure include: (1) The flexibility attained by articulation of the upstream and the downstream slabs, thus minimizing the detrimental effects of differential settlement (in the round-head design, however, a great deal of the flexibility is lost due to the mass of the round heads); (2) the more even distribution

of base pressures than for a gravity section (the unit pressures, however, are usually somewhat larger than for a gravity section of the same height); (3) the minimized uplift pressures due to the smaller base areas; (4) the ease of periodically inspecting and grouting the foundation remaining exposed between buttresses; and (5) the reduction in concrete quantities, which in some instances would be sufficient to offset the increased costs due to the increase in reinforcement and formed areas. The last item would hold particularly in localities where labor is cheap and material costs are high.

The round-head type of structure, although not common, has been successfully utilized for several important projects, among them the Don Martin Dam in Mexico and the Rio Negro Dam in Uruguay. However, in these instances special provisions were not required to transfer horizontal forces to the foundation. The round head, which is the upstream water supporting member, is, in plan, a segment of a circle flaring from the buttress and thus allowing transmission of stresses induced by the water pressures to the buttress by direct compression. Advantages claimed for this type of water supporting member are:

1. The member is in compression under full load.
2. Reinforcement is minimized, as bending and diagonal tension stresses for all practicable purposes are eliminated.
3. A reduction in costs may be effected due to the mass concrete construction of the round head.

Detailed studies indicated that for the foundation conditions at the Harlan County site the buttress type of structure has the following undesirable characteristics:

(*a*) As no upstream cutoff is provided, full hydrostatic head could develop in joints and seams, possibly resulting in a foundation blowout between the buttresses.
(*b*) The weight of the structure would not assist in mobilization of horizontal resistance.
(*c*) The chalk lying between the buttresses and above the bottom of the bulb cannot be mobilized to resist horizontal forces except by friction along the buttress faces.
(*d*) The concentration of stresses at the bulb would aggravate any tendency toward progressive failure.
(*e*) Lack of continuity of the toe which, under adverse and differing jointing conditions of the foundation at individual monoliths, would result in greatly reducing and varying the resistance to horizontal movement afforded these monoliths.
(*f*) Computed tensions occur in the bottom of the buttresses under certain loading conditions.

With a laminated foundation, such as presented by the chalk with interbeds of bentonitic material, it is difficult to design a buttress dam and a gravity dam

that would have exactly comparable safety factors. Unquestionably the gravity structure will mobilize an area equal to the full depth of the key and the width of the monolith, regardless of the occurrence of fracture planes. Under perfect conditions and in a homogeneous material bulbs could be designed to mobilize horizontal resistance to the same degree and in the same manner as the key of the gravity section. However, the chalk is not homogeneous but is laminated by bentonitic seams and broken by fracture planes, making it very susceptible to progressive failure occasioned by local overstresses. Because the fracture planes in the foundation might be so arranged that overstresses in contact bearing or shear could not follow a normal distribution pattern, it was assumed: Failure would occur along a plane inclined at 45° and limited in width to the width of the bulb, and the width and depth of the bulb would be determined by the allowable contact bearing of 200 lb per sq in.

Consideration of the apparent advantages of the gravity section for this particular site led to the study of a modification of the section having a tension heel. The large step originally included in the heel was eliminated, the bottom of the heel was widened, and the remainder of the base was sloped upward at an angle approximately normal to the resultant of the applied forces. The final design cross section is shown in Fig. 1. The upstream face of the section was battered to assure positive base pressures at the heel for all conditions of loading. With this cross section the weight of the chalk below the structure is mobilized and tension in the concrete is kept within allowable limits. In the analysis it was assumed that failure would occur by sliding along the bentonite seam on a level with the base of the heel and shear along an inclined plane from that level at the toe to the bottom of the stilling basin slab, as outlined for the section with the tension key.

Preliminary estimates indicated that the cost of the gravity section would be somewhat less than that of the round-head buttress. Since there appeared to be very real benefits attributable to the selection of the gravity design for the Harlan County foundation, and since no economy would result from the construction of the round-head buttress, the modified gravity section was adopted for construction.

Embankment Design

Foundation problems are not limited to the concrete structure. Laboratory tests indicate that the loose loess-silts of the terrace and abutments, with an average dry weight in their natural state of 80 lb per cu ft, consolidate in a very erratic manner under varying conditions of loading and saturation. The unpredictable nature of the consolidation of saturated loess and the extreme differential settlement which would occur in an earth structure having an over-all height of 85 ft, and founded partly on chalk and partly on 35 ft of loose loess-silts, led to the adoption of a very conservative treatment in the initial stages of the design (Fig. 4). The design contemplates the removal of the loess under the embankment and the construction of an impervious cutoff through the underlying sand and gravel, having sufficient contact with the chalk to assure

that the amount of underseepage would be negligible. In the left abutment, however, a section of the embankment must of necessity rest on undisturbed loess and is subject to some axial and differential settlements. It is planned to strip the loess to a slope of 1 on 3½ and flare the embankment slopes so as to limit the estimated differential settlement of the embankment to a maximum of 1 ft in 100 ft along the axis. This solution is not economical for the main sections of the embankment because the very flat side slopes require an excessive yardage of compacted fill.

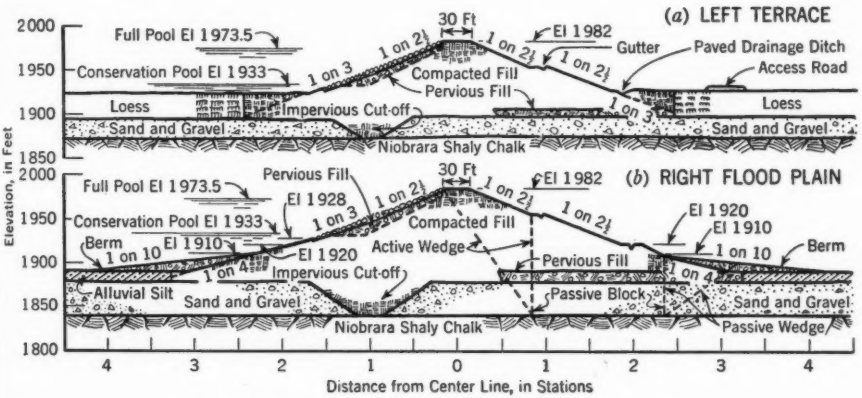

FIG. 4.—TYPICAL VALLEY EMBANKMENT CROSS SECTIONS

The possibility of reducing the removal of loess was a subject of laboratory investigation. It was thought probable that suitable provisions could be made to extend the period of time required for the loess downstream from the cutoff to become saturated, or that positive methods could be devised to prevent this loess from becoming saturated. This, accompanied by partial removal of the loess, would tend to minimize any differential settlement. If such settlement could be limited so as to present only a minor maintenance problem, a material reduction in excavation on the terrace could be safely effected. Such reduced excavation lines in the terrace section approximate a line from the top of the gravelly sand at the downstream side of the impervious cutoff to the ground surface at the downstream toe.

Particular attention was required for the stability of the embankment and foundation as a whole, because of the numerous bentonitic seams which form approximately horizontal shear planes in the chalk. Based on the assumption of sliding on such a seam immediately below the surface of the chalk a wedge type analysis, in which the thrust of the active wedge was equated to the resistance of the passive block and passive wedge, indicated the need for berms in the river channel and flood plain sections. The loess in the right abutment underlain by the faulted Pierre shale required treatment similar to that for the left abutment. In addition, the sand and Ogallala formations require blanketing upstream and drainage downstream from the dam.

ACKNOWLEDGMENTS

Acknowledgment is gratefully made to Col. W. E. Potter, M. ASCE, District Engineer, Kansas City District, Corps of Engineers, and to Messrs. D. H. McCoskey and C. R. Van Orman, Assoc. Members, ASCE, and to E. B. Cohn and H. L. Lowe—all members of his staff—for their helpful suggestions during the preparation of this paper. Thanks are due also to the board of consultants for this project, composed of Messrs. C. P. Berkey, Hon. M. ASCE; W. H. McAlpine, Leroy F. Harza, Arthur Casagrande, S. O. Harper, and Joel D. Justin, Members, ASCE; and Roy W. Carlson, Assoc. M. ASCE, for their material assistance in formulating the design adopted for construction.

AMERICAN SOCIETY OF CIVIL ENGINEERS

Founded November 5, 1852

PAPERS

EXPANSION JOINT PRACTICE IN HIGHWAY CONSTRUCTION

By A. A. Anderson,[1] Assoc. M. ASCE

Synopsis

This paper points out that in concrete highway pavement construction the trend is toward the elimination of expansion joints. It explains why properly maintained modern pavements do not "blow up" even though little or no provision for expansion has been made.

Information taken from the reports on Michigan and Minnesota experimental jointing projects is cited to show typical slab end movements at expansion and contraction joints and how these are affected by different jointing arrangements. Using actual strain gage readings and other data from a 20-ft section of the Minnesota experimental project where the expansion joints were 5,260 ft apart, the compressive stress that developed due to an 83° F rise in the temperature of the concrete is shown to be only 628 lb per sq in. Based on this and the other data presented, it is concluded that in pavements built with properly spaced and maintained contraction joints, expansion joints may be eliminated, except for unusual conditions of construction.

Introduction

In the early days the amount of concrete pavement that could be placed in one day was small, so that even in pavements constructed without intermediate jointing the construction joints were at relatively short intervals. As these early pavements aged, they developed transverse cracking at irregular intervals. Early expansion joints were mastic-filled openings placed at relatively short intervals, ranging from 30 ft to about 150 ft, but these joints did not prevent the formation of cracks at random intervals between the expansion joints. Therefore, some engineers decided that it was unnecessary and uneconomical to install joints except at the end of each day's run. They would allow the pavement to form its own joints by cracking as needed.

Note.—Written comments are invited for immediate publication; to insure publication the last discussion should be submitted by **February 1, 1949.**

[1] Mgr., Highways and Municipal Bureau, Portland Cement Assn., Chicago, Ill.

Many thousands of miles of pavement were built without transverse joints, other than the construction joints at the end of each day's run. These pavements were simple to construct, lower in first cost, and have given good service. Their major difficulty, which did not develop until after the pavement had been in service for five years or more, was a type of expansion failure commonly known as a "blowup."

These blowups were considered evidence that concrete pavements needed expansion joints to protect them from compressive stresses. Therefore, the use of expansion joints was generally resumed, with considerable variation in joint spacing adopted by the various state highway departments. In 1934 the United States Bureau of Public Roads (predecessor of the Public Roads Administration (PRA)) issued regulations which required $\frac{3}{4}$-in. expansion joints at intervals not to exceed 100 ft in concrete pavement on all federal aid roads. A further requirement was that contraction joints be used at intervals not exceeding 30 ft, unless the pavement was adequately reinforced for greater slab length.

For several years jointing practices were in general conformance with this ruling. Later experience indicated the desirability of modification in jointing requirements. Accordingly, the PRA invited a number of state highway departments to cooperate in the construction of experimental projects in which different jointing arrangements would be tested. Six states—California, Kentucky, Michigan, Minnesota, Missouri, and Oregon—joined in the cooperative studies. Progress reports on the experimental projects have been published.[2,3,4,5,6,7,8,9,10,11,12] The results from these experimental projects and the data obtained from surveys of other pavements in service have led to some modification in jointing regulations governing federal aid projects. Considerable freedom in jointing of concrete pavement is permitted—provided that the states are able to support their proposed jointing scheme by sound data from condition surveys or other sources.

Recent changes in state highway department practices in expansion joint spacings reflect the change in regulation. At least six state highway departments now construct their rural pavements without expansion joints, or use such joints only where the pavements join structures—that is, at bridges or at intersections with other pavements. Six state highway departments place their expansion joints at intervals ranging from 300 ft to 600 ft, twelve states use an interval ranging from 100 ft to 120 ft, and the remainder of the state highway departments from which data were available place their expansion

[2] "Investigational Concrete Pavement in Kentucky," by F. P. Anderson, *Proceedings*, Highway Research Board, National Research Council, Washington, D. C., Vol. 20, 1940, p. 337.

[3] "Investigational Concrete Pavement in Michigan," by J. W. Kushing, *ibid.*, p. 339.

[4] "Investigational Concrete Pavement in Minnesota," by F. C. Lang, *ibid.*, p. 348.

[5] "Investigational Concrete Pavement in Oregon," by G. S. Paxson, *ibid.*, Vol. 21, 1941, p. 147.

[6] "Investigational Concrete Pavement in Missouri," by F. V. Reagel, *ibid.*, p. 150.

[7] "Investigational Concrete Pavement in California," by T. E. Stanton, *Research Reports No. 3B*, *ibid.*, Vol. 25, 1945, p. 1.

[8] "Investigational Concrete Pavement in Kentucky," by T. R. Thomas, *ibid.*, p. 28.

[9] "Investigational Concrete Pavement in Michigan," by H. C. Coons, *ibid.*, p. 35.

[10] "Investigational Concrete Pavement in Minnesota," by F. C. Lang, *ibid.*, p. 58.

[11] "Investigational Concrete Pavement in Missouri," by F. V. Reagel, *ibid.*, p. 72.

[12] "Investigational Concrete Pavement in Oregon," by G. S. Paxson, *ibid.*, p. 77.

joints at intervals of less than 100 ft. It is believed that time will eliminate some of the wide variations now in existence, but it is obvious that there still remains considerable difference of opinion on expansion joint spacing. Doubtless many engineers will disagree with the conclusions drawn hereinafter, but their study of the supporting data is respectfully invited.

A discussion of jointing practices in concrete pavement cannot be limited to expansion joints alone. The decision to include or to omit expansion joints in concrete pavement depends, more than any other single factor, on whether contraction joints are installed at intervals that will control cracking. A discussion of expansion joints must include a discussion of contraction joints.

Contraction joint spacing practices of state highway departments are also at variance, but the degree is not as marked as for expansion joint practices. At least thirty-one states place contraction joints at intervals varying from 15 ft to 30 ft. Only one state uses contraction joints spaced less than 15 ft apart, whereas the remainder for which data were available use spacings in excess of 30 ft. Generally speaking, those states, which employ contraction joint spacings in excess of 30 ft, employ a relatively short spacing of expansion joints and place but one or, at most, two contraction joints between successive expansion joints. Of the twelve states which place their expansion joints at intervals of 300 ft or more, all employ a contraction joint spacing ranging from between 15 ft and 30 ft.

Origins of Slab Stresses

Stresses in a concrete highway slab come from two principal sources. Traffic using the pavement causes load stresses which are fairly well understood. Theoretical calculations of load stresses have been checked by actual stress measurements made both in the laboratory and in the field. Load stresses have a bearing on the jointing of concrete pavements. Of greater importance to the joint arrangement, however, are those stresses which are not caused by loads but rather by volume changes that take place within the concrete during and after the hardening period.

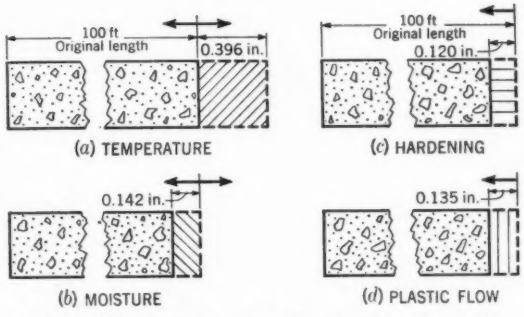

Fig. 1.—Principal Causes of Volume Changes in an Unloaded Concrete Slab

Typical volume changes that may take place in a 100-ft length of concrete pavement are shown graphically in Fig. 1. It is assumed that the pavement is constructed with normal materials and that it is resting on a frictionless subgrade. The greatest volume change is caused by temperature fluctuations. Assuming that the temperature of the concrete at the time of placing was 70° F, and that some time after hardening the temperature of the concrete was raised to 130° F,a 0.396-in. increase in the length of the 100-ft slab could

be expected. This is based on a linear coefficient of thermal expansion of 0.0000055, an average value for normal concrete, and also on the assumption that other factors affecting the volume change have been inactive during the period of temperature rise. If the temperature decreased by 60° F, instead of rising, the pavement would have shortened by an equal amount.

A second factor which will cause change in the length of the slab is a change in the moisture content of the concrete. The concrete tends to expand and contract as its moisture content increases and decreases. The moisture content of pavement concrete changes very slowly, and the effects on volume are not as great as those due to changes in temperature. Nevertheless, in most regions there is a change in average moisture content of pavement concrete from one season to the next and, as would be expected, these seasonal variations will differ from one locality to another. The Minnesota State Highway Department has determined that, for the conditions existing on their experimental project, the unit linear variation in concrete due to seasonal changes in moisture amounts to 0.000118. Using this factor and again assuming that other factors remain inactive, a seasonal change in the length of a 100-ft slab would amount to 0.142 in. Seldom, if ever, will concrete again contain as much moisture as it contained at the time of hardening. Therefore, the over-all effect of moisture changes will always result in a net shortening from the original placement length. Also, in most areas subsequent maximum moisture contents will occur during the season of low temperatures. Thus the volume changes due to moisture and temperature fluctuations tend to offset rather than to augment each other.

It is a well-recognized fact that as concrete hardens shrinkage takes place. Tests reported by various authorities indicate the unit change in length due to shrinkage to be at least 0.0001. Some authorities report considerably higher figures. Using this conservative unit rate, the change in length of the 100-ft slab would be approximately 0.120 in.

When concrete is subjected to a sustained stress, a plastic deformation, commonly called plastic flow, takes place. Data from laboratory and field studies show that the amount of plastic deformation or flow varies with the intensity of the stress and the length of time the stress is maintained. If the 100-ft pavement slab is assumed to be under a compressive stress of 680 lb per sq in. 5 hours per day for a period of 10 days, a plastic flow of about 0.135 in. could be expected. As indicated in Fig. 1, this plastic flow would cause a shortening of the slab.

Each one of the foregoing factors acting alone to cause volume change is fairly easy to apply. For pavements in service, however, these factors do not act singly and any movements which take place in a pavement are due to a combination of two or more of the factors. As temperature causes the greatest and most spectacular changes in the volume of a concrete slab, this factor alone was considered in the past, with little or no consideration being given to other factors. This often led to erroneous conclusions.

If all the factors shown in Fig. 1 acted simultaneously, the slab would be shorter than its 100-ft original length so that even for the assumed high temperature of 130° F there would be no compressive stress. However, all these

changes will not be effective at any one time. If it is assumed that only the change due to temperature and that due to the initial hardening of the concrete have occurred, the slab, at the high temperature of 130° F, would be 0.276 in. longer than the 100-ft initial length. If no space were provided for expansion, the resulting restraint will cause a unit strain of $\frac{0.276}{100 \times 12} = 0.00023$. For concrete of pavement quality and for strains which develop slowly, a suitable value for the modulus of elasticity, E, is 4,000,000 lb per sq in., and the calculated stress corresponding to the strain would be $0.00023 \times 4{,}000{,}000 = 920$ lb per sq in. Plastic flow and the loss of moisture in the slab at the high temperature of 130° F would undoubtedly result in an actual stress below this amount, which may be considered the maximum.

Pavement concrete usually has a compressive strength of more than 4,000 lb per sq in. Even when load stresses are added to the maximum of 920 lb per sq in., the total compressive stress will be less than half the ultimate compressive strength of the concrete. Since studies have shown that stresses up to 50% of the ultimate strength of concrete may be repeated indefinitely without causing fatigue or leading to rupture, it is apparent that compressive stresses which will result from the omission of expansion joints will not be critical in themselves.

What then causes compression failures, commonly known as blowups? Although high stresses undoubtedly do develop at points where blowups occur, they seldom, if ever, develop in newly placed pavements. Rather, they occur after the pavements have been in service for 4 or 5 years. This question has been the subject of much study and all evidence indicates that blowups are caused by a gradual loss of expansion space provided by crack or joint openings because of infiltration of incompressible material. This leads to the conclusion that blowups can be prevented by eliminating infiltration or reducing it to an insignificant amount. Much evidence shows this conclusion to be true.

It is extremely difficult to maintain an effective sealing which will avoid infiltration of foreign material into haphazard cracks. Therefore, an effective method of preventing blowups is to joint the pavement so that intermediate cracking will be controlled. This can be done economically and effectively by installing contraction joints of the "dummy groove" type at a suitable spacing. The short slab lengths required for crack control will reduce joint openings, and dummy groove joints are more readily maintained than cracks. Experience shows that under average maintenance infiltration is practically prevented.

The primary function of contraction joints is to form slab lengths that will reduce tensile stresses and prevent the formation of intermediate cracks. These cracks are caused by a combination of tensile stresses resulting from wheel loads, curling, and differential movement of the subgrade, or by subgrade restraint to contraction during hardening of the concrete, contraction due to drops in temperature, or reduction in moisture content. Some of these stresses decrease as individual slabs become shorter. By reducing slab lengths some of the stresses will be kept small and the combined tensile stresses will not be great enough to cause the formation of intermediate cracks.

Experience from roads in service is the best guide as to spacing of contraction joints which will control cracking. In most instances about 20 ft will be satisfactory. The type of aggregate used in the concrete has a major influence, slag and small size siliceous gravel requiring a spacing of about 15 ft. Some aggregates, such as crushed granite or limestone, may permit satisfactory control of cracking by contraction joints spaced at 25 ft or more, but spacings in excess of 25 ft are generally to be avoided as they will be productive of excessive opening and closing of the joint and thus increase the difficulty of maintaining a satisfactory seal and make the joint less effective for load transference. Experience with pavements in service indicates that these joint spacings will prevent intermediate cracks and will also keep the average joint opening small enough so that it can be kept sealed without difficulty, providing the distance between expansion joints is relatively large or that expansion joints are completely eliminated.

Experimental Results

It is of interest to compare the foregoing discussion on jointing with the data from the experimental projects which were constructed by the six state highway departments in cooperation with the PRA during 1940 and 1941. All six projects were constructed with a series of paving sections in which numerous combinations of expansion and contraction joint spacings were used, thus making it possible to study the effect of different jointing arrangements. The

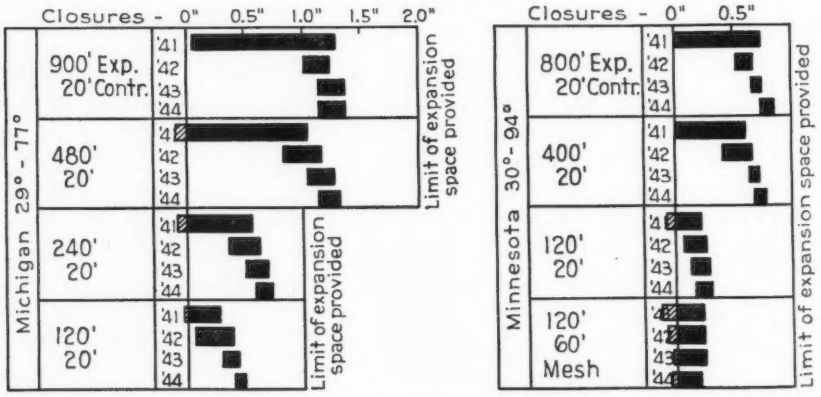

Fig. 2.—Typical Annual and Progressive Changes in Expansion Joint Widths

information presented herein was obtained from the Michigan and Minnesota projects, both constructed in 1940, after 4 years of service. These data were considered typical and were compiled from reports[2,3,4,5,6,7,8,9,10,11,12] published in 1945. Fig. 2 shows the annual and progressive changes in expansion joint openings that have taken place on various sections of these two projects. Referring to the Michigan project during the warmest time of its first year (1941) the joint closed 1.30 in. As the pavement subsequently cooled the joint did not return to its original opening, but there was a residual closure of

about 1 in. During the warm period of the second year the joint closure was about 1.25 in. from the original, but the total movement that took place in that joint during 1942 amounted to only 0.25 in. In 1943 a residual closure of about 1.15 in. remained; the total movement in that year amounted to about 0.17 in. In 1944, when the pavement was in its fourth year, the total amount of joint movement was again less than 0.20 in., indicating that the movement at that particular joint tended to become stabilized.

In following through the joint spacings of 480 ft, 240 ft, and 120 ft, it is seen that the movements taking place at each joint follow the pattern of the one previously outlined—namely, that the greatest movement at any expansion joint takes place the first year and that the amount of recovery is relatively small. After a period of from two to three years, the movement that takes place within any expansion joint has become stabilized and is small. As would be expected, the closer the spacing of the expansion joints, the less is the movement that takes place the first year. However, even an expansion joint spacing of 120 ft does not prevent the gradual closing of the joint.

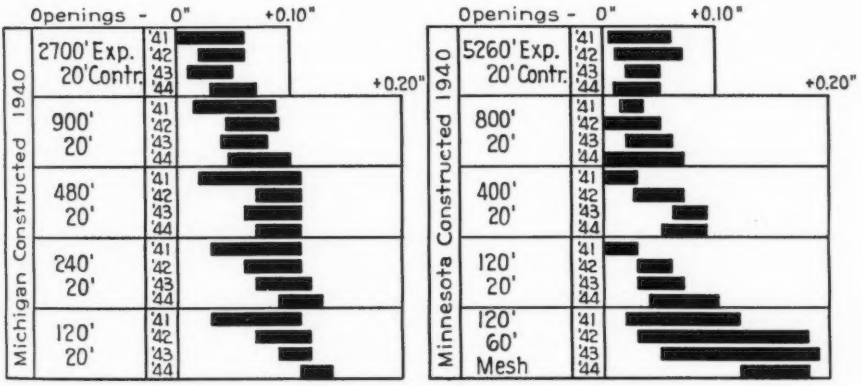

FIG. 3.—TYPICAL ANNUAL AND PROGRESSIVE CHANGES IN CONTRACTION JOINT WIDTHS

By referring to the Minnesota data, it can be seen that they follow the same trend as those from the Michigan project. Results similar to those shown herein have been noted by other observers. It has often been said that due to the rapid closure of expansion joints and the small amount of recovery that takes place, it is but a short time until expansion joints in reality serve only as contraction joints.

Fig. 3 shows the contraction joint movements which accompanied the variations in expansion joint openings shown in Fig. 2 and reveals some interesting facts. The annual average movement that takes place at any contraction joint is relatively small where the pavement is divided into the short panels used on the two projects for which data are given and is not greatly affected by the spacing of the expansion joints. However, as the distance between expansion joints becomes less, the maximum opening of contraction joints which takes place during each successive year becomes greater, and the

annual residual joint opening likewise becomes larger. The extremes of this pattern can be seen in the action of the Minnesota contraction joints for expansion joint spacings of 120 ft and 5,260 ft. In the 120-ft expansion joint spacing, there is a progressive increase in both maximum and residual opening at the contraction joints with no apparent sign of stability even after 4 years. However, in the 5,260-ft section these are more or less constant after the first year. By the third year the maximum joint openings, as well as the residual joint openings, are about half of those occurring where the expansion joints are spaced at 120 ft. After studying Fig. 3 it is apparent that the smaller maximum and residual contraction joint openings are found where the expansion joints are spaced at longer intervals.

Fig. 4 shows the average seasonal changes in contraction joint openings resulting from the use of various combinations of expansion and contraction joint spacings. Almost without exception the average maximum contraction joint opening for any one spacing of contraction joints varies inversely with the

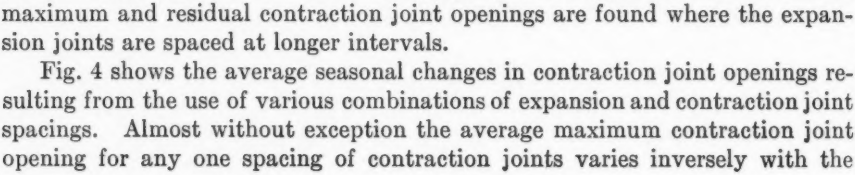

FIG. 4.—AVERAGE SEASONAL CHANGES IN CONTRACTION JOINT WIDTHS AS RELATED TO SPACINGS OF EXPANSION AND CONTRACTION JOINTS

distance between expansion joints. It can also be seen, taking corresponding data from each group, that for any particular expansion joint spacing both the opening and the annual movement at contraction joints materially decrease as the distance between contraction joints becomes shorter. The joint arrangements on the Minnesota project varied somewhat from those used in Michigan; however, the same trends are apparent.

In reading the magnitude of joint opening for any particular section, it must be remembered that the values shown are average for all contraction joints within that section. Within any section, especially one having expansion joints spaced in excess of 1,000 ft, the contraction joints near the center of the section generally have smaller annual movement than those near the expansion joints. Two or three contraction joints on each side of the expansion joints may be expected to open more than indicated herein, and this fact must be given consideration in the design of the slab.

Actual measurements on two contraction joints (adjacent to a 20-ft panel approximately in the center of the section of the Minnesota project where the

expansion joints were spaced 1 mile apart) show the joint openings measured in February, when the concrete had a temperature of 29° F, to be 0.056 in. and 0.052 in., respectively. Similar values obtained in August, when the temperature was 112° F, were 0.004 in. and 0.012., respectively. With this information, and knowing the actual coefficient of expansion and modulus of elasticity, it is possible to make a theoretical determination of the probable stress that existed in the pavement when the temperature was the highest recorded on the project. The temperature rise is 83° F. Were this 20 ft of pavement completely unrestrained, this rise in temperature would have caused a lengthening of the slab equal to 0.109 in. However, the actual increase in slab length was only 0.046 in., the difference between the average joint openings measured in February and August. Between this winter and summer period, data from the project show the moisture content of the pavement decreased and produced a net shortening between winter and summer of 0.028 in. The restrained movement thus amounts to 0.035 in., which represents the amount of elongation which would have occurred in a slab completely free of restraint, but which was prevented from occurring in this restrained slab and was absorbed in the 20-ft length of pavement, producing a unit strain of 0.000146.

Using the actual measured value of 4,300,000 lb per sq in. for the modulus of elasticity, the computed stress developed in this slab amounts to only 628 lb per sq in., which is approximately $\frac{1}{6}$ of the actual 28-day compressive strength of this concrete and cannot be considered critical. Strain measurements made at plugs installed in the immediate vicinity of this slab show that for the same temperature of 112° F, the stress was 684 lb per sq in., only 56 lb per sq in. higher than that obtained in the foregoing computation. This is undoubtedly very close to the maximum stress which has developed on this project. It is of interest to note that strain measurements at quarter points in the mile showed substantially the same compressive stress.

These data from the experimental projects agree with the previously presented analysis of stresses which may develop in pavements built without expansion joints but with contraction joints at short intervals. Both the data and the analysis explain why pavements constructed with little or no provisions for expansion, but with well-constructed and maintained contraction joints at relatively close intervals, do not rupture during periods of high temperature.

Conclusions

Based on the information and data presented, which is substantiated by other experimental projects and studies that have been made on pavements in service, the following conclusions may be drawn:

During the construction of concrete pavement, little or no expansion space need be provided if—

(1) The pavement is constructed of materials that have normal expansion characteristics;

(2) The pavement is constructed during those periods of the year when the temperatures are well above freezing;

(3) The pavement is divided into relatively short panels by satisfactory contraction joints so spaced as to prevent the formation of intermediate cracks; and

(4) The contraction joints are properly maintained to prevent the infiltration of incompressible material.

Thus, with infiltration controlled by the installation and maintenance of properly spaced dummy contraction joints, it appears that concrete pavements do not need expansion joints. Only in concrete pavement built during cold weather does there seem to be any reason for using expansion joints, and even then they are needed only at long spacing, perhaps from 600 ft to 800 ft. In fact, concrete pavement built without excess expansion space may be expected to have increased structural capacity and to give better performance than pavement having expansion joints at short intervals. In addition it is simpler and less expensive to construct, easier to maintain, and has better riding qualities. It can be stated that the current trend in jointing practices on modern American highways is in the directions indicated.

AMERICAN SOCIETY OF CIVIL ENGINEERS

Founded November 5, 1852

PAPERS

A SIMPLIFIED METHOD OF ANALYZING SUSPENSION BRIDGES

BY LING-HI TSIEN,[1] ESQ.

SYNOPSIS

A rational method of analysis for the design of suspension bridges is presented in this paper. The proposed method gives simple and explicit equations of the horizontal tension in a cable and a direct method of determining maximum moments, shears, deflections, and slopes in the stiffening trusses. A slide rule may be used in all computations. The tiresome cut-and-try processes inherent in the existing methods are avoided.

Typical computations for Mount Hope suspension bridge in Rhode Island illustrate the method, proving that the accuracy is high and that the saving in labor is considerable.

INTRODUCTION

1. Description of Method.—Many investigators have shown that the so-called "elastic theory" is not adequate for the exact design of a suspension bridge. The deflection theory is more accurate and is used extensively; but it involves many cut-and-try processes and a computing machine or a table of logarithms must be used to avoid possibilities of serious errors. The "trigonometric series" method developed by S. Timoshenko[2] has distinct advantages over the deflection theory method in several respects; but the expressions are not completely explicit, and the computations are lengthy and involved. Moreover, the location and magnitude of maximum bending moments and shears in a stiffening truss for various loading conditions cannot be determined directly without trial and error.

The method proposed herein eliminates all these inconveniences. It will be presented in three parts: Part I deals with the computation of horizontal tension in the cable; Part II with the moment equations in the stiffening truss;

NOTE.—Written comments are invited for immediate publication; to insure publication the last discussion should be submitted by **February 1, 1949.**

[1] Prof., Civ. Eng., National Univ. of Chekiang, Hangchow, Chekiang, China.

[2] "The Stiffness of Suspension Bridges," by S. Timoshenko, *Transactions*, ASCE, Vol. 94, 1930, p. 377.

and Part III with the design of the stiffening truss (determination of maximum moments, shears, deflections, and slopes).

Two important conclusions are reached as follows:

(*a*) When the live load moves on the bridge, the horizontal tension in a cable varies very closely according to certain circular functions irrespective of both the ratio between the dead load and the live load, and the degree of stiffness of the truss; and

(*b*) The equations of moments and shears can be reduced to explicit and simple forms in hyperbolic functions which are suitable for the direct determination of maxima by mathematics, with certain acceptable approximations.

In Parts I and III, some minor approximations are introduced in the derivation, but the maximum possible error is within a few percentage points and the calculated result is probably more accurate than that obtained by the cut-and-try method. The approximations are certainly justified by the considerable saving in labor and the mistakes that are avoided because the formulas are clear and explicit. Because of its simplicity and accuracy, the method can be used for preliminary design purposes as well as for the final analysis of a suspension bridge. To illustrate the design procedure, the paper includes a complete analysis of Mount Hope suspension bridge between Bristol and Portsmouth, R. I.

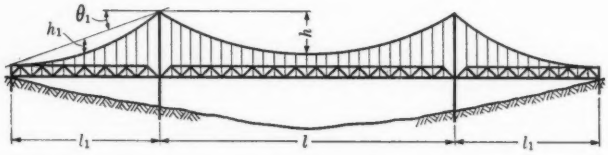

FIG. 1

Fig. 1 is a line diagram of a two-hinged suspension bridge of the type discussed in this paper. The theory applies equally well to the bridge with straight backstays.

2. Notation.—The letter symbols in this paper are defined where they first appear, in the text or by illustrations. They conform essentially to American Standard Letter Symbols for Structural Analysis, prepared by a Committee of the American Standards Association, with Society participation.

PART I. VARIATION OF THE HORIZONTAL COMPONENT OF CABLE TENSION

LIVE LOAD MOVING SYMMETRICALLY BOTH WAYS FROM THE CENTER LINE OF THE SPAN

3. Extreme Types of Suspension Bridge.—First, it is the writer's purpose to study the variation of H (the horizontal component of the tension in the cable due to live load) by analyzing two extreme cases applied to suspension bridges, namely:

Case *a*. The cable is not stiffened (moment of inertia of stiffening truss $I = 0$), and the ratio of live load to dead load, $q = p/w$, ranges from 0 to 1. (In other words, p varies from 0 to w.)

Case *b*. The cable is perfectly stiffened ($I \rightarrow \infty$), and q also ranges from 0 to 1.

It will be assumed first that the span length and cable length do not change. The effects of side span interaction, cable stretch, and temperature effect are discussed in sections 14 to 20.

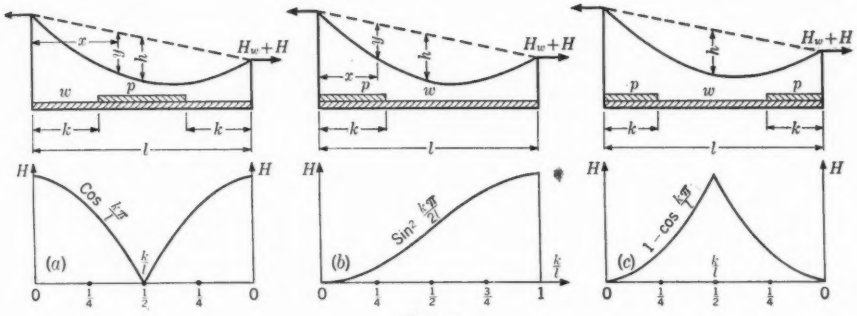

FIG. 2

4. Case a: $I = 0$.—Consider the inclined parabolic cable as shown in Fig. 2(*a*). The original ordinate of the cable[3] is

$$y = \frac{4f}{l^2}(l\,x - x^2) \qquad (1)$$

When a center partial live load is applied, the cable will assume the shape of three parabolas with common tangents at their junctions, which occur at the two ends of the live load (see Fig. 2(*a*)). The new ordinates of the cable can be obtained as follows: When $x < k$, considering $\Sigma M = 0$ at section x,

$$(H_w + H)\,y_1 = \frac{w}{2}(l\,x - x^2) + \frac{p\,(l - 2\,k)}{2}\,x \qquad (2a)$$

or

$$y_1 = \frac{w\,(l\,x - x^2) + p\,(l - 2\,k)\,x}{2\,(H_w + H)} \qquad (2b)$$

When $l - k > x > k$,

$$(H_w + H)\,y_2 = \frac{w}{2}(l\,x - x^2) + \frac{p\,(l - 2\,k)}{2}\,x - \frac{p\,(x - k)^2}{2} \qquad (3a)$$

or

$$y_2 = \frac{w\,(l\,x - x^2) + p\,(l\,x - k^2 - x^2)}{2\,(H_w + H)} \qquad (3b)$$

If the cable length does not change, the external work performed in deflecting the cable must be equal to zero; hence,

$$\int_0^k w\,(y_1 - y)\,dx + \int_k^{l/2}\left(w + \frac{p}{2}\right)(y_2 - y)\,dx = 0 \qquad (4)$$

[3] "Preliminary Design of Suspension Bridges," by Shortridge Hardesty and Harold E. Wessman, *Transactions*, ASCE, Vol. 104, 1939, p. 582, Eq. 2.

Substituting Eqs. 1, 2*b*, and 3*b* in Eq. 4, performing the integrations and combining terms,

$$H = \frac{p\,l^2}{8\,f}\left[\frac{2 - 4\,\frac{k^2}{l^2}\left(3 - 2\,\frac{k}{l}\right) + q\left(1 - 2\,\frac{k}{l}\right)^2\left(1 + 4\,\frac{k}{l}\right)}{2 + q - 2\,q\,\frac{k^2}{l^2}\left(3 - 2\,\frac{k}{l}\right)}\right]$$

$$= \frac{p\,l^2}{8\,f}\,F_1(k, q)\,..(5)$$

in which q is the ratio p/w.

Therefore, when the live load, p, moves symmetrically both ways from the center of the span, k varies from 0.5 to 0. The horizontal component of cable tension H due to live load will be a function of k and q, as defined by Eq. 5.

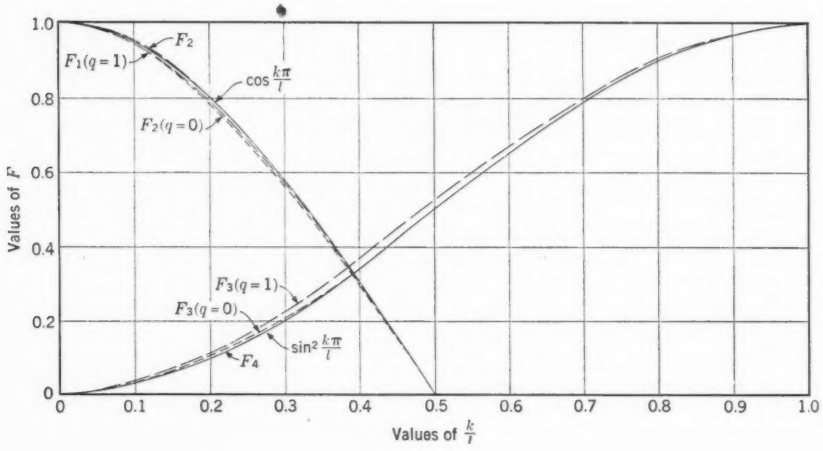

FIG. 3

5. *Case b: $I \rightarrow \infty$.*—When the stiffness of bridge increases to a certain extent, the cable will remain practically undistorted, so that the so-called "elastic theory" becomes almost true and will give exact solution. When a central partial live load is applied, the "elastic theory" gives the equation for H as follows:[4]

$$H = \frac{\frac{1}{15}\,p\,f\,l^3\,[1 - k^2\,(5 - 5\,k^2 + 2\,k^3)]}{\frac{8}{15}\,f^2\,l + \frac{I\,L_s}{A}} \quad \ldots\ldots\ldots\ldots (6a)$$

Neglecting the effect of cable stretch, $\frac{I\,L_s}{A}$, it can be reduced to

$$H = \frac{p\,l^2}{8\,f}\,[1 - k^2\,(5 - 5\,k^2 + 2\,k^3)] = \frac{p\,l^2}{8\,f}F_2(k) \quad \ldots\ldots\ldots (6b)$$

[4] "Modern Framed Structures," by J. B. Johnson, C. W. Bryan, and F. E. Turneaure, John Wiley & Sons, Inc., New York, N. Y., 9th Ed., 1916, Pt. II, p. 219, Eq. 15.

Fig. 3 shows that the two functions F_1 and F_2 are practically the same when q varies from 0 to 1, and it can be very closely represented by the trigonometric function $\cos \frac{k\pi}{l}$ for $\frac{k}{l}$ from 0.5 to 0. The difference between $\cos \frac{k\pi}{l}$ with F_2 is practically indistinguishable. Thus, it may be concluded that:

Theorem 1.—

When live load moves symmetrically from each side of the center of the span of a suspension bridge (with parabolic cable and a horizontal or inclined chord), the horizontal component of the induced cable tension, H, increases (very closely) in proportion to the function $\cos \frac{k\pi}{l}$ irrespective of both the degree of truss stiffness and the ratio of live load to dead load, within limits $q = 0$ to $q = 1$.

This may be expressed by

$$H = \frac{p\,l^2}{8\,f\,D} \cos \frac{k\pi}{l} \ldots\ldots\ldots\ldots\ldots\ldots\ldots\ldots (7)$$

in which k varies from $\frac{1}{2}\,l$ to 0; and D is a correction factor for cable stretch and side span effects, being unity in the present case. To estimate these effects, one needs only to consider the particular case when the span is fully covered by a uniform live load ($k = 0$). Factor D is a function of the physical properties of the bridge and will remain nearly constant for other cases of loading.

Live Load Advancing from One End of Span

6. Case a: $I = 0$.—As in the case of symmetrical live loading, the original ordinates of the cable are determined by Eq. 1. When $x < k$, the equation $\Sigma M = 0$ gives (Fig. 2(*b*))

$$(H_w + H)\,y_1 = \frac{w}{2}\,(l\,x - x^2) + \frac{pk\left(l - \frac{k}{2}\right)}{l}\,x - \frac{p\,x^2}{2} \ldots\ldots (8a)$$

or

$$y_1 = \frac{w\,(l\,x - x^2) + p\left(2\,k\,x - \frac{k^2\,x}{l} - x^2\right)}{2\,(H_w + H)} \ldots\ldots\ldots\ldots (8b)$$

When $x > k$,

$$(H_w + H)\,y_2 = \frac{w}{2}\,(l\,x - x^2) + \frac{p\,k\left(l - \frac{k}{2}\right)}{l}\,x - p\,k\left(x - \frac{k}{2}\right) \ldots (9a)$$

or

$$y_2 = \frac{w\,(l\,x - x^2) + p\left(-\frac{k^2\,x}{l} + k^2\right)}{2\,(H_w + H)} \ldots\ldots\ldots\ldots (9b)$$

Substituting the values of y_1 and y_2 in Eqs. 8 and 9 in the work equation,

$$\int_0^k \left(w + \frac{p}{2}\right)(y_1 - y)\,dx + \int_k^l w\,(y_2 - y)\,dx = 0 \ldots\ldots\ldots (10)$$

and performing integrations,

$$H = \frac{p\,l^2}{8\,f}\left[\frac{2\,\frac{k^2}{l^2}\left(3 - 2\,\frac{k}{l}\right) + q\,\frac{k^3}{l^3}\left(4 - 3\,\frac{k}{l}\right)}{2 + q\,\frac{k^2}{l^2}\left(3 - 2\,\frac{k}{l}\right)}\right] \quad \ldots\ldots\ldots (11)$$

7. *Case b: $I \rightarrow \infty$.*—For the reason stated in section 6, the "elastic theory" gives, for this case of loading, the equation of H as follows:[5]

$$H = \frac{\frac{1}{30}\,p\,f\,l^3\,[k^2\,(2\,k^3 - 5\,k^2 + 5)]}{\frac{8}{15}\,f^2\,l + \frac{I\,L_s}{A}} \quad \ldots\ldots\ldots\ldots (12)$$

Again neglecting the effect of cable stretch, $\frac{I\,L_s}{A}$, Eq. 12 becomes

$$H = \frac{p\,l^2}{8\,f}\,[k^2\,(2\,k^3 - 5\,k^2 + 5)] = \frac{p\,l^2}{8\,f}\,F_4(k) \quad \ldots\ldots\ldots\ldots (13)$$

Fig. 3 shows that the two functions F_3 and F_4 are practically the same when q varies from 0 to 1 and that they both vary very closely according to the trigonometric function $\sin^2 \frac{k\,\pi}{2\,l}$ for $\frac{k}{l}$ from 0 to 1. The curve of $\sin^2 \frac{k\,\pi}{2\,l}$ almost coincides with F_4 and F_3 ($q = 0$). A conclusion can then be made:

Theorem 2.—

When the live load advances from one end of the span of a suspension bridge (with a horizontal or inclined chord), the horizontal component of induced cable tension varies (very closely) in proportion to the function $\sin^2 \frac{k\,\pi}{2\,l}$, irrespective of both the degree of truss stiffness and the ratio of live load to dead load (from $q = 0$ to $q = 1$).

Theorem 2 may be expressed algebraically as follows:

$$H = \frac{p\,l^2}{8\,f\,D}\sin^2 \frac{k\,\pi}{2\,l} \quad \ldots\ldots\ldots\ldots\ldots\ldots (14)$$

in which k varies from 0 to l. Factor D is the same as in Eq. 7. Eq. 14 also can be written as follows:

$$H = \frac{p\,l^2}{8\,f\,D}\,\frac{1}{2}\left(1 - \cos \frac{k\,\pi}{l}\right) \quad \ldots\ldots\ldots\ldots\ldots (15)$$

In other words, the horizontal tension H due to a partial loading from one end (Fig. 2(*b*)) is equal to the half of the difference between H due to full loading and H due to a corresponding center loading (Fig. 2(*a*)). Consequently, one may write Theorem 3, as follows:

Theorem 3.—

[5] "Modern Framed Structures," by J. B. Johnson, C. W. Bryan, and F. E. Turneaure, John Wiley & Sons, Inc., New York, N. Y., 9th Ed., 1916, Pt. II, p. 218, Eq. 13.

In suspension bridges, for different loading conditions, the cable tension can be computed by superposition, with sufficient accuracy for all practical purposes.

Live Load Advancing from Both Ends of Span

8. Horizontal Tension H for a Live Load Advancing from Both Ends.—When the live load advances symmetrically from both ends of the span (Fig. 2(*c*)), superposition yields

$$H = \frac{p\,l^2}{8\,f\,D}\left(1 - \cos\frac{k\,\pi}{l}\right) \ldots\ldots\ldots\ldots\ldots\ldots (16)$$

in which k varies from 0 to $\frac{1}{2}\,l$. Factor D is the same as in Eq. 7.

A Moving Concentrated Load

9. Horizontal Tension H for a Moving Concentrated Load.—A concentrated load P can be considered analogous to a uniform load covering an infinitesimal length—that is, $p \times dk$. Therefore,

$$H = \frac{p\,l^2}{8\,f\,D}\left[\sin^2\frac{\pi}{2\,l}\,(k + dk) - \sin^2\frac{\pi\,k}{2\,l}\right] = \frac{p\,dk\,l^2}{8\,f\,D}\frac{d}{dk}\sin^2\frac{k\,\pi}{2\,l} \ldots (17a)$$

or

$$H = \frac{P\,l\,\pi}{16\,f\,D}\sin\frac{k\,\pi}{l} \ldots\ldots\ldots\ldots\ldots\ldots (17b)$$

General Expression for H When the Main Span Is Loaded

10. Sag Changes.—When a live load moves on a bridge, or when a temperature change occurs, stress is induced in the cable and in the truss. Any change of cable tension or temperature causes a change in the length of the cable and affects the shape of the curve, increasing or decreasing the center sag. A change in cable stress also causes a change in the side span sag. This in turn causes a movement of the tower tops, which affects the main span length and its sag.

11. Moment in Stiffening Truss When the Sag Changes.—Whenever the center sag changes by an amount Δf, the stiffening truss is raised or lowered by the same amount at the center. If the suspender forces (s) are uniformly distributed, the center deflection of the truss will be given by

$$\Delta f = \frac{5}{384}\frac{s\,l^4}{E\,I} \ldots\ldots\ldots\ldots\ldots\ldots (18a)$$

and the center moment by

$$M = \frac{s\,l^2}{8} = \frac{9.6\,E\,I}{l^2}\,\Delta f \ldots\ldots\ldots\ldots\ldots\ldots (18b)$$

In other words, a change in center sag, Δf, will produce a positive or negative moment at the center of the stiffening truss as determined by Eq. 18*b*. A positive Δf (downward) produces a positive moment (compression in the top chord).

12. Span Fully Loaded and Subjected to a Temperature Change.—At mean temperature and when there is no live load on the bridge, the lengths of the

suspender rods are so adjusted that the stiffening truss is relieved of all stresses and the dead load is uniformly supported by the cable, so that

$$H_w = \frac{w\,l^2}{8\,f} \quad \ldots\ldots (19)$$

The loading conditions and the temperature are now changed as follows:

Description	Condition
Total uniform load per unit length	$w + p$
Temperature change	$\pm\,\Delta t$
Horizontal component of cable tension	$H_w + H$
Cable sag in main span	$f + \Delta f_p \pm \Delta f_t$

Considering the static equation, $\Sigma M = 0$, the formula for the center section of the main span can be written as follows:

$$(H_w + H)\,(f + \Delta f_p \pm \Delta f_t) + \frac{9.6\,E\,I}{l^2}\,(\Delta f_p \pm \Delta f_t) = \frac{(w+p)\,l^2}{8} \quad \ldots (20a)$$

or

$$H\left\{1 + \frac{\Delta f_p}{f}\left[1 + \frac{H_w}{H}\left(1 + \frac{9.6\,E\,I}{H_w\,l^2}\right)\right] \pm \frac{\Delta f_t}{f}\right\} = \frac{p\,l^2}{8\,f} \mp H_w\left(1 + \frac{9.6\,E\,I}{H_w\,l^2}\right)\frac{\Delta f_t}{f} \quad \ldots (20b)$$

Let $q = \frac{p}{w}$; $c^2{}_0 = \frac{H_w}{E\,I}$; $B = 1 + \frac{9.6\,E\,I}{H_w\,l^2} = 1 + \frac{9.6}{c^2{}_0\,l^2}$. Then

$$H = \frac{p\,l^2}{8\,f}\,\frac{1 \mp T}{1 + N \pm N_t} = \frac{p\,l^2}{8\,f\,D_{\pm t}}\,(1 \mp T) \quad \ldots\ldots (21)$$

This is the expression of H for the case of a full span live load, in which

$$T = \frac{B}{q}\,\frac{\Delta f_t}{f} \quad \ldots\ldots (22a)$$

$$N = \frac{\Delta f_p}{f}\left(1 + \frac{H_w}{H}\,B\right) \quad \ldots\ldots (22b)$$

$$N_t = \frac{\Delta f_t}{f} \quad \ldots\ldots (22c)$$

and

$$D_{\pm t} = 1 + N \pm N_t \quad \ldots\ldots (22d)$$

13. Span Arbitrarily Loaded.—For the case of partial loading (see sections 5, 7, and 8), the general expression of the horizontal component of cable tension is as follows (see subsequently in Table 1):

$$H = \frac{p\,l^2}{8\,f\,D_{\pm t}}\left[F\left(\frac{k}{l}\right) \mp T\right] \quad \ldots\ldots (23)$$

in which $F\left(\frac{k}{l}\right)$ represents certain trigonometrical functions that vary according to the loading distribution (see sections 5 to 8), and B, N, N_t, T, and $D_{\pm t}$ are the constants defined in section 12. The upper signs of T, N_t, and $D_{\pm t}$ correspond to a rise of temperature, and the lower ones to a drop of temperature.

Determination of Design Constants

14. Sag Changes Δf_t and Δf_p.—In Eqs. 22*a*, 22*b*, and 22*c*, Δf_t is the sag change due to change in temperature, and the sag change Δf_p is partly due to the effect of side span and partly due to the stretch of the cable. These two factors, respectively, give the two components N_s and N_c of the constant N.

15. Factor N_s to Reflect the Effect of Side Spans.—An increase of H in cable produces a change in sag, Δf_1, in the side span which can be evaluated as follows: Apply the static equation, $\Sigma M = 0$, at the center of the side span:

$$(H_w + H)(f_1 + \Delta f_1) + \frac{9.6\,E\,I_1}{l^2_1}\Delta f_1 = \frac{w_1 l^2_1}{8} = H_w f_1 \ldots\ldots (24a)$$

from which

$$\Delta f_1 = \frac{-1}{1 + \frac{H_w}{H} B_1} f_1 \ldots\ldots (24b)$$

In Eq. 24*b*,

$$B_1 = 1 + \frac{9.6\,E\,I_1}{H_w\,l^2_1} = 1 + \frac{9.6}{c^2_{01}\,l^2_1} \ldots\ldots (25a)$$

and, in Eq. 25*a*,

$$c^2_{01} = \frac{H_w}{E\,I_1} \ldots\ldots (25b)$$

Because of Δf_1, the length of cable in the side span will change by an amount equal to[6]

$$\Delta l_1 = -\frac{16\,n_1}{3\sec^2\alpha_1}\Delta f_1 \ldots\ldots (26a)$$

in which $n_1 = f_1/l_1$ is the sag ratio of the side span, and α_1 is the inclination of the chord of side span cable. When the saddle moves on the tower tops, a change occurs in the length of the main span, equal to

$$\Delta l = -2\,\Delta l_1 \ldots\ldots (26b)$$

This, in turn, affects the sag of main span by an amount Δf equal to[6]

$$\Delta f = -\frac{15 - 40\,n^2 + 288\,n^4}{16\,n\,(5 - 24\,n^2)}\Delta l \doteqdot -\frac{3\,\Delta l}{16\,n(1 - 2.35\,n^2)} \ldots\ldots (27)$$

Substituting the values from Eqs. 24*b* and 26 in Eq. 27,

$$\frac{\Delta f}{f} = \frac{2\,r\,n^2_1}{\sec^2\alpha_1\,n^2\,(1 - 2.35\,n^2)} \times \frac{1}{1 + \frac{H_w}{H} B_1} \ldots\ldots (28)$$

[6] "A Practical Treatise on Suspension Bridges," by D. B. Steinman, John Wiley & Sons, Inc., New York, N. Y., 2d Ed., 1929, p. 11, Eq. (52).

in which $n = f/l$, the sag ratio of the main span, and $r = l_1/l$. Then the value of N due to side span effect will be

$$N_s = \frac{2\,r\,n^2{}_1}{\sec^2 \alpha_1\, n^2\,(1 - 2.35\,n^2)} \times \frac{1 + \frac{H_w}{H} B}{1 + \frac{H_w}{H} B_1} \quad \ldots\ldots\ldots (29a)$$

Neglecting temperature change, $H = \frac{p\,l^2}{8\,f\,(1 + N)}$ and $\frac{H_w}{H} = \frac{1 + N}{q}$, which may be assumed to be $\frac{1.2}{q}$ as a first approximation. In a suspension bridge, with the center span fully loaded, the value of $(1 + N)$ usually varies between 1.10 to 1.30. As $\frac{\Delta f}{f}$ is small compared to unity, an error of 10% in the value of $\frac{\Delta f}{f}$ will involve an error of only 1% or 2% in the final value of H. Moreover, the error more or less compensates for itself since, in Eq. 29*a*, it appears both in the numerator and in the denominator. Therefore, the value of N_s can be written with sufficient accuracy as follows:

$$N_s = \frac{2\,r}{\sec^2 \alpha_1\,(1 - 2.35\,n^2)} \frac{n^2{}_1}{n^2} \frac{q + 1.2\,B}{q + 1.2\,B_1} \quad \ldots\ldots\ldots (29b)$$

16. Factor N_c to Reflect Cable Stretch.—The total virtual work (W_1) due to the vertical displacement η of the suspender forces (s) plus the cable weight (g) must be equal to the total work (W_2) done by the cable tension ($H_w + H$) in stretching the cable. These work quantities W_1 and W_2 are expressed, approximately,[7] as the integrated products of the forces and their respective displacements, as follows:

$$W_1 = \int_l \left(g + \frac{s}{2}\right) \eta\, dx = \frac{8\,f}{l^2} \left(H_w + \frac{H}{2}\right) \int_l \eta\, dx \quad \ldots\ldots\ldots (30a)$$

and

$$W_2 = \sum \left(H_w + \frac{H}{2}\right) \left(\frac{H}{E_c\,A_0} \int_l \frac{A_0}{A} \frac{ds^3}{dx^2}\right) \quad \ldots\ldots\ldots (30b)$$

The symbol $\sum$ (in Eq. 30*b*) denotes the summation of work done in stretching the cable in all spans and segments of cable. Eq. 30*a* deals only with the main span, since the side span effect is considered separately. In Eq. 30*b*, A denotes the cable section at any point, and A_0 denotes the cable section at midspan.

When the main span is fully loaded, the cable deforms from the initial parabola (sag = f) to another parabola with a bigger sag equal to $f + \Delta f$; therefore, the deflection η may be expressed by

$$\eta = \frac{4\,\Delta f}{l^2}\,(l\,x - x^2) \quad \ldots\ldots\ldots\ldots\ldots\ldots (31)$$

[7] "A Practical Treatise on Suspension Bridges," by D. B. Steinman, John Wiley & Sons, Inc., New York, N. Y., 2d Ed., 1929, p. 250.

Substituting in Eq. 30*a* and integrating,

$$W_1 = \frac{8\,f}{l^2}\left(H_w + \frac{H}{2}\right)\frac{2}{3}\,\Delta f\,l \ldots\ldots\ldots\ldots\ldots\ldots (32a)$$

Let $L_s = \sum \int_l \frac{A_0}{A}\,\frac{ds^3}{dx^2}$, then Eq. 30*b* becomes

$$W_2 = \left(H_w + \frac{H}{2}\right)\frac{H}{E_c\,A_0}\,L_s \ldots\ldots\ldots\ldots\ldots\ldots (32b)$$

For a wire cable having a uniform section A, one may write, with sufficient accuracy[8]

$$L_s = \sum l\,(\sec^3\alpha + 8\,n^2) \ldots\ldots\ldots\ldots\ldots\ldots (33a)$$

For an eyebar cable with variable A proportional to the slope secant $\frac{ds}{dx}$, one may write, with sufficient accuracy,[8]

$$L_s = \sum l\,(\sec^2\alpha + \frac{16}{3}\,n^2) \ldots\ldots\ldots\ldots\ldots\ldots (33b)$$

in which $n = f/l$ and α is the inclination of chord in any span and segment of cable. The symbol $\sum$ denotes the summation of similar expressions for all spans, and segments of cable. Equating W_1 and W_2,

$$\frac{\Delta f}{f} = \frac{3}{16}\,\frac{H}{E_c\,A_0}\,\frac{L_s}{n^2\,l} \ldots\ldots\ldots\ldots\ldots\ldots (34)$$

The value of N due to cable stretch will be

$$N_c = \frac{3}{16}\,\frac{H}{E_c\,A_0}\,\frac{L_s}{n^2\,l}\left(1 + \frac{H_w}{H}\,B\right) \ldots\ldots\ldots\ldots\ldots\ldots (35a)$$

or, using $\frac{H_w}{H} = \frac{1.2}{q}$ as before,

$$N_c = \frac{0.187}{n^2}\,\frac{H_w}{E_c\,A_0}\,\frac{L_s}{l}\left(\frac{q}{1.2} + B\right) \ldots\ldots\ldots\ldots\ldots\ldots (35b)$$

17. Factors N_t and T in Relation to Temperature Change.—When the temperature changes, the cable lengthens or shortens by a distance which changes the sag, f, an amount Δf_t. The extent of the deformation can be evaluated in a manner similar to that for determining the effect of cable stretch due to live load. The virtual work, W_1, done in the vertical displacement is equal to

$$W_1 = \frac{8\,f}{l^2}\left(H_w + \frac{H}{2}\right)\frac{2}{3}\,\Delta f_t\,l \ldots\ldots\ldots\ldots\ldots\ldots (36a)$$

The work, W_2, done by the cable tension $H_w + H$ is equal to

$$W_2 = \left(H_w + \frac{H}{2}\right)\epsilon\,\Delta_t\,L_t \ldots\ldots\ldots\ldots\ldots\ldots (36b)$$

[8] "A Practical Treatise on Suspension Bridges," by D. B. Steinman, John Wiley & Sons, Inc., New York, N. Y., 2d Ed., 1929, p. 251.

in which ϵ is the temperature coefficient of expansion of cable; Δ_t is the temperature change; and[8]

$$L_t = \sum \int \frac{ds^2}{dx} = \sum l \left(\sec^2 \alpha + \frac{16}{3} n^2 \right) \ldots\ldots\ldots\ldots (37)$$

Equating W_1 and W_2,

$$\frac{\Delta f_t}{f} = \frac{3}{16} \frac{\epsilon \Delta_t L_t}{n^2 l} \ldots\ldots\ldots\ldots\ldots\ldots\ldots\ldots (38a)$$

Then

$$N_t = \frac{0.187 \epsilon \Delta_t L_t}{n^2 l} \ldots\ldots\ldots\ldots\ldots\ldots\ldots\ldots (38b)$$

and

$$T = \frac{B}{q} N_t = \frac{0.187 \epsilon \Delta t L_t B}{n^2 l q} \ldots\ldots\ldots\ldots\ldots\ldots\ldots\ldots (38c)$$

General Expression of H When the Side Span Is Loaded

18. Both Side Spans Fully Loaded.—Let H be the horizontal component of cable tension induced by a live load, p, which fully covers both side spans. The sag of the main span will be changed by an amount $\Delta f'$.

Applying the condition $\sum M = 0$ at the center of the main span,

$$(H_w + H)(f + \Delta f') + \frac{9.6 E I}{l^2} \Delta f' = \frac{w l^2}{8} = H_w f \ldots\ldots\ldots\ldots (39a)$$

Hence,

$$H = \frac{p l^2}{8 f} \frac{B}{q} \frac{-\frac{\Delta f'}{f}}{1 + \frac{\Delta f'}{f}} \ldots\ldots\ldots\ldots\ldots\ldots\ldots\ldots (39b)$$

As $\frac{\Delta f'}{f}$ is very small compared to unity, the value of H due to side span loads is small as compared to that when the main span is fully loaded. Considering the cable stretch and side span effects, the equation for H may be written, with sufficient accuracy, as follows:

$$H = \frac{p l^2}{8 f D_{st}} (2 S) \ldots\ldots\ldots\ldots\ldots\ldots\ldots\ldots (40a)$$

in which

$$S = -\tfrac{1}{2} \frac{B}{q} \frac{\Delta f'}{f} \ldots\ldots\ldots\ldots\ldots\ldots\ldots\ldots (40b)$$

19. One Side Span Arbitrarily Loaded.—According to the conclusions of sections 5, 7, and 8 and the results given in section 18, when a side span is subject to partial loading, the general expression for H will be

$$H = \frac{p l^2}{8 f D} \left[S F \left(\frac{k}{l_1} \right) \right] \ldots\ldots\ldots\ldots\ldots\ldots\ldots\ldots (41)$$

in which $F\left(\frac{k}{l_1}\right)$ is a certain trigonometrical function according to the loading distribution (see subsequently in Table 1).

20. Computation of Factor S.—According to Eq. 40*b*,

$$2S = -\frac{B}{q}\frac{\Delta f'}{f} \ldots\ldots\ldots\ldots\ldots\ldots\ldots\ldots (42)$$

in Eq. 42, $\Delta f'$ is the change of center span sag due to full loading of both side spans. Both $\frac{\Delta f'}{f}$ and H are relatively small in this case. The cable stretch, which depends only upon the magnitude of H, is also practically negligible. Only the value of $\Delta f'$ due to side span effect need be considered.

By a similar process as given in section 15,

$$\frac{\Delta f'}{f} = \frac{-2}{\sec^2 \alpha_1 (1 - 2.35\, n^2)} \frac{n_1}{n} \frac{f_1}{f} \frac{q_1}{B_1} \ldots\ldots\ldots\ldots\ldots (43)$$

in which $q_1 = \frac{p}{w_1}$. Since, by Eq. 19, $H_w = \frac{w\, l^2}{8\, f} = \frac{w_1\, l^2_1}{8\, f_1}$, the same intensity of live load (p) yields $\frac{q_1}{q} = \frac{w}{w_1} = \frac{l^2_1}{l^2}\frac{f}{f_1}$ and, using $r = l_1/l$,

$$S = -\tfrac{1}{2}\frac{B}{q}\frac{\Delta f'}{f} = \frac{r^2}{\sec^2 \alpha_1 (1 - 2.35\, n^2)} \frac{n_1}{n} \frac{B}{B_1} \ldots\ldots\ldots\ldots (44)$$

Computation of H for a Moving Concentrated Load

21. H-Equation for a Moving Concentrated Load.—Section 9 permits writing the following general expression for H due to a moving concentrated load P, applied at a distance k from the left support:

$$H = \frac{P\, l\, \pi}{16\, f\, D_{\pm t}} \left(\sin \frac{k\, \pi}{l} \mp T \right) \ldots\ldots\ldots\ldots\ldots (45)$$

By reasoning similar to that in sections 10 to 17, the constants $D_{\pm t}$ and the factors T are the same as in the case of uniform live load, except that the live load ratio, q, must be replaced by $q' = \frac{P\, \pi}{2\, w\, l}$ in the formulas.

Summary, Part I

22. Design Formulas of H.—The equations of H for various loading conditions useful in design are presented in Table 1. They are exceedingly simple in form and are as accurate as the results computed by the deflection theory. These values are used to compute the force H for several existing bridges (such as the Mount Hope Bridge, in Rhode Island, Manhattan Bridge in New York, N. Y., and in a numerical example solved[9] by J. I. Parcel and the late G. A. Maney, Members, ASCE), and the results for different loading conditions check very closely with those calculated by the more exact equations of the deflection theory.

[9] "An Elementary Treatise on Statically Indeterminate Stresses," by J. I. Parcel and G. A. Maney, John Wiley & Sons, Inc., New York, N. Y., 2d Ed., 1936.

TABLE 1.—Equations of H for Various Loading Conditions

Constants

$$D_{\pm t} = 1 + N_s + N_c \pm N_t$$

$$T = \frac{B}{q} N_t$$

$$S = \frac{r^2}{\sec^2 \alpha_1 \, (1 - 2.35\, n^2)} \frac{n_1}{n} \frac{B}{B_1}$$

$$B = 1 + \frac{9.6}{c^2{}_0 \, l^2}$$

$$B_1 = 1 + \frac{9.6}{c^2{}_{01} \, l^2{}_1}$$

$$N_s = \frac{2\, r}{\sec^2 \alpha_1 \, (1 - 2.35\, n^2)} \frac{n^2{}_1}{n^2} \frac{q + 1.2\, B}{q + 1.2\, B_1}$$

$$N_c = \frac{0.187}{A_0 \, E_c} \frac{H_w}{n^2} \frac{L_s}{l} \left(\frac{q}{1.2} + B \right)$$

$$N_t = \frac{0.187 \, \epsilon \, \Delta t \, L_t}{n^2 \, l}$$

$$r = \frac{l_1}{l}\,; n = \frac{f}{l}\,; n_1 = \frac{f_1}{l_1}$$

$$c^2{}_0 = \frac{H_w}{E\, I}\,; c^2{}_{01} = \frac{H_w}{E\, I_1}$$

$q = \frac{p}{w}$, for uniform live load

$q = \frac{P\, \pi}{2\, w\, l}$, for a concentrated load

Case	Loading condition	Temperature	Equation
I	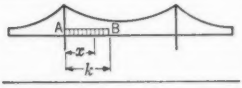	Highest	$H_{\mathrm{I}} = \frac{p\, l^2}{8\, f\, D_{+t}} \left(\sin^2 \frac{k\, \pi}{2\, l} - T \right)$
II	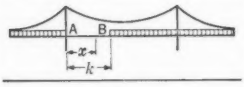	Lowest	$H_{\mathrm{II}} = \frac{p\, l^2}{8\, f\, D_{-t}} \left(\cos^2 \frac{k\, \pi}{2\, l} + 2\, S + T \right)$
III	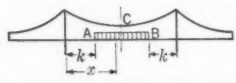	Highest	$H_{\mathrm{III}} = \frac{p\, l^2}{8\, f\, D_{+t}} \left(\cos \frac{k\, \pi}{l} - T \right)$
IV	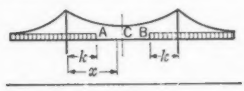	Lowest	$H_{\mathrm{IV}} = \frac{p\, l^2}{8\, f\, D_{-t}} \left(1 - \cos \frac{k\, \pi}{l} + 2\, S + T \right)$
V		Highest	$H_{\mathrm{V}} = \frac{p\, l^2}{8\, f\, D_{+t}} (S - T)$
VI	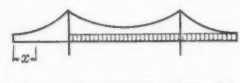	Lowest	$H_{\mathrm{VI}} = \frac{p\, l^2}{8\, f\, D_{-t}} (1 + S + T)$
VII	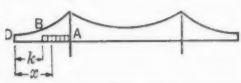	Highest	$H_{\mathrm{VII}} = \frac{p\, l^2}{8\, f\, D_{+t}} \left(S \cos^2 \frac{k\, \pi}{2\, l_1} - T \right)$
VIII		Lowest	$H_{\mathrm{VIII}} = \frac{p\, l^2}{8\, f\, D_{-t}} \left(1 + S + S \sin^2 \frac{k\, \pi}{2\, l_1} + T \right)$
IX		Lowest	$H = \frac{p\, l^2}{8\, f\, D_{-t}} (1 + 2\, S + T)$
X	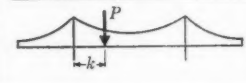	Highest or lowest	$H = \frac{P\, l\, \pi}{16\, f\, D_{\pm t}} \left(\sin \frac{k\, \pi}{l} \pm T \right)$

PART II. EQUATIONS FOR MOMENTS M IN A STIFFENING TRUSS

Introduction

23. Assumptions.—The following derivation of the moment equations involves the same assumptions as are used in the deflection theory. The equations are the same as those obtained by the deflection theory, but they are condensed in forms more suitable for further mathematical treatments. The equations of shear, slope, and deflection, of the stiffening truss, can be obtained easily by differentiating or integrating the M-equations.

A symbol Q is introduced in these equations; thus:

$$Q = H \frac{8\,f}{p\,l^2} \qquad (46)$$

It will be shown that the major and direct effect of H on the truss appears in this term.

The Stiffening Truss Under Various Loading Conditions

24. Derivation of M-Equations.—When the bridge is subject only to dead load (w), and at mean temperature, the suspender force is intended to be equal to w, and the differential equation of the cable curve is

$$\frac{d^2y}{dx^2} = \frac{-\,w}{H_w} \qquad (47)$$

When an additional suspender force, s, due to live load or temperature change, acts upon the cable, the cable ordinates become $y + \eta$, and the differential equation becomes

$$\frac{d^2(y+\eta)}{dx^2} = -\,\frac{w+s}{H_w + H} \qquad (48a)$$

or

$$-\,w - \frac{H}{H_w}\,w + (H_w + H)\,\frac{d^2\eta}{dx^2} = -\,w - s \qquad (48b)$$

Since the differential equation of curvature for the stiffening truss is

$$\frac{d^2\eta}{dx^2} = -\,\frac{M}{E\,I} \qquad (49)$$

therefore Eq. 48*b* gives

$$s = p\,Q + c^2\,M \qquad (50)$$

in which

$$Q = H \frac{8\,f}{p\,l^2} \qquad (51a)$$

and

$$p\,Q = \frac{H}{H_w}\,w \qquad (51b)$$

and

$$c^2 = \frac{H_w + H}{E\,I} \qquad (51c)$$

For the loaded and unloaded segments of truss, respectively,

$$\frac{d^2M}{dx^2} = s - p \quad \ldots\ldots (52a)$$

and

$$\frac{d^2M}{dx^2} = s \quad \ldots\ldots (52b)$$

Substituting Eqs. 52 in Eq. 50,

$$\frac{d^2M}{dx^2} - c^2 M = -p(1 - Q) \quad \ldots\ldots (53a)$$

and

$$\frac{d^2M}{dx^2} - c^2 M = p\,Q \quad \ldots\ldots (53b)$$

By solving these differential equations, the moment equation for the loaded segment of truss becomes

$$M = C' \cosh (c\,x) + C'' \sinh (c\,x) + \frac{p}{c^2}(1 - Q) \quad \ldots\ldots (54a)$$

and that, for the unloaded segment,

$$M = C' \cosh (c\,x) + C'' \sinh (c\,x) - \frac{p}{c^2} Q \quad \ldots\ldots (54b)$$

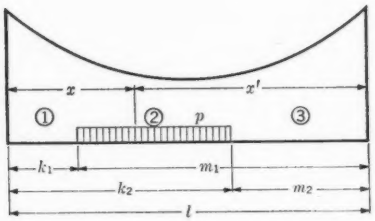

FIG. 4

in which C' and C'' are constants of integration which may be determined when the loading conditions are fixed.

25. Evaluation of C′ and C″.—Consider the case of the loading shown in Fig. 4. It is evident that the M-curve will have three different forms, characterized by three different pairs of constants, corresponding to the segments (1), (2), and (3). The six equations of conditions are:

At $x = 0$—

$$M_1 = 0 \quad \ldots\ldots (55a)$$

at $x = k_1$—

$$M_1 = M_2; \quad \text{and} \quad \frac{dM_1}{dx} = \frac{dM_2}{dx} \quad \ldots\ldots (55b)$$

at $x = k_2$—

$$M_2 = M_3; \quad \text{and} \quad \frac{dM_2}{dx} = \frac{dM_3}{dx} \quad \ldots\ldots (55c)$$

and at $x = l$—

$$M_3 = 0 \quad \ldots\ldots (55d)$$

Substituting the moment M from Eqs. 54 in Eqs. 55 and solving the latter, the resulting three pairs of constants are as follows:

$$\left.\begin{aligned} C'_1 &= \frac{p}{c^2} Q \\ C''_1 &= \frac{p}{c^2}\left[-Q \tanh \frac{c\,l}{2} + \frac{\cosh (c\,m_1) - \cosh (c\,m_2)}{\sinh (c\,l)} \right] \end{aligned}\right\} \quad \ldots\ldots (56a)$$

$$C'_2 = \frac{p}{c^2}\{-(1-Q) - [\cosh(c\,k_1) - 1]\}$$

$$C''_2 = \frac{p}{c^2}\left[(1-Q)\tanh\frac{c\,l}{2} + \frac{\cosh(c\,k_1)-1}{\tanh(c\,l)} - \frac{\cosh(c\,m_2)-1}{\sinh(c\,l)}\right] \quad \ldots(56b)$$

$$C'_3 = \frac{p}{c^2}\{Q - [\cosh(c\,k_1) - \cosh(c\,k_2)]\}$$

$$C''_3 = \frac{p}{c^2}\left[-Q\tanh\frac{c\,l}{2} + \frac{\cosh(c\,k_1) - \cosh(c\,k_2)}{\tanh(c\,l)}\right] \quad \ldots(56c)$$

Let $x' = 1 - x$ and

$$A_x = \frac{\cosh c\left(\frac{l}{2} - x\right)}{\cosh\frac{c\,l}{2}} \quad \ldots(57)$$

Substituting the resulting values of C' and C'' in Eqs. 54, the moment in the three segments of Fig. 4 will be: Segment (1)—

$$M = \frac{p\,l^2}{c^2\,l^2}\left[-Q(1 - A_x) + \frac{\cosh(c\,m_1) - \cosh(c\,m_2)}{\sinh(c\,l)}\sinh(c\,x)\right] \quad \ldots(58a)$$

segment (2)—

$$M = \frac{p\,l^2}{c^2\,l^2}\left[(1-Q)(1-A_x) - \frac{\cosh(c\,k_1)-1}{\sinh(c\,l)}\sinh(c\,x') - \frac{\cosh(c\,m_2)-1}{\sinh(c\,l)}\sinh(c\,x)\right] \quad \ldots(58b)$$

and segment (3)—

$$M = \frac{p\,l^2}{c^2\,l^2}\left[-Q(1 - A_x) + \frac{\cosh(c\,k_2) - \cosh(c\,k_1)}{\sinh(c\,l)}\sinh(c\,x')\right] \quad \ldots(58c)$$

Eqs. 58 will suffice for all conditions of uniform live load ordinarily met in practice. Different formulas for particular cases are condensed in Table 2. In the case of a single concentrated load, P, items 13 and 14, Table 2, the moment equations for the two segments (at the right and at the left of the load) may be derived similarly and will be as follows:

$$M_1 = -\frac{P\,l}{c\,l}\left[Q'(1 - A_x) - \frac{\sinh(c\,m)}{\sinh(c\,l)}\sinh(c\,x)\right] \quad \ldots(59a)$$

and

$$M_2 = -\frac{P\,l}{c\,l}\left[Q'(1 - A_x) - \frac{\sinh(c\,k)}{\sinh(c\,l)}\sinh(c\,x')\right] \quad \ldots(59b)$$

in which

$$Q' = H\frac{8\,f}{P\,c\,l^2} \quad \ldots(60)$$

TABLE 2.—Moment Formulas for Typical Live Loadings

Variables

$x' = l - x$

$A_x = \dfrac{\cosh c\left(\frac{l}{2} - x\right)}{\cosh \frac{c\,l}{2}}$

Constants

$Q = H\dfrac{8\,f}{p\,l^2}$; $\quad m = l - k$; $\quad B_m = \dfrac{\cosh (c\,m) - 1}{\sinh (c\,l)}$

$Q' = H\dfrac{8\,f}{P\,c\,l^2}$; $\quad A_k = \dfrac{\sinh c\left(\frac{l}{2} - k\right)}{\cosh \frac{c\,l}{2}}$; $\quad B_k = \dfrac{\cosh (c\,k) - 1}{\sinh (c\,l)}$

Loading condition	Item	Bending moments
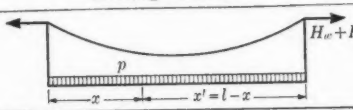	1	$M = \dfrac{p\,l^2}{c^2\,l^2}(1 - Q)(1 - A_x)$
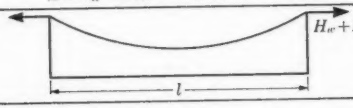	2	$M = \dfrac{-\,p\,l^2}{c^2\,l^2} Q\,(1 - A_x)$; or $M = -\,H\dfrac{8\,f}{c^2\,l^2}(1 - A_x)$
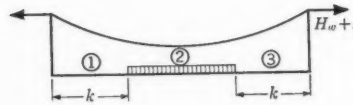	3	$M_1 = \dfrac{-\,p\,l^2}{c^2\,l^2}[Q\,(1 - A_x) - A_k \sinh (c\,x)]$
	4	$M_2 = \dfrac{p\,l^2}{c^2\,l^2}\{(1 - Q)(1 - A_x) - A_x\,[\cosh (c\,k) - 1]\}$
	5	$M_3 = \dfrac{-\,p\,l^2}{c^2\,l^2}[Q\,(1 - A_x) - A_k \sinh (c\,x')]$
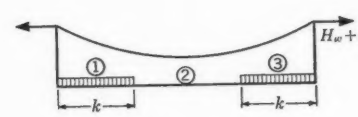	6	$M_1 = \dfrac{p\,l^2}{c^2\,l^2}[(1 - Q)(1 - A_x) - A_k \sinh (c\,x)]$
	7	$M_2 = \dfrac{-\,p\,l^2}{c^2\,l^2}\{Q\,(1 - A_x) - A_x\,[\cosh (c\,k) - 1]\}$
	8	$M_3 = \dfrac{p\,l^2}{c^2\,l^2}[(1 - Q)(1 - A_x) - A_k \sinh (c\,x')]$
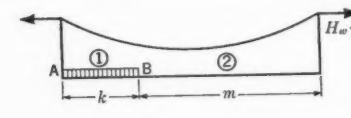	9	$M_1 = \dfrac{p\,l^2}{c^2\,l^2}[(1 - Q)(1 - A_x) - B_m \sinh (c\,x)]$
	10	$M_2 = \dfrac{-\,p\,l^2}{c^2\,l^2}[Q\,(1 - A_x) - B_k \sinh (c\,x')]$
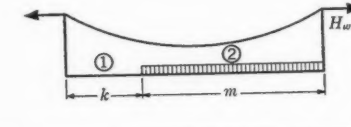	11	$M_1 = \dfrac{-\,p\,l^2}{c^2\,l^2}[Q\,(1 - A_x) - B_m \sinh (c\,x)]$
	12	$M_2 = \dfrac{p\,l^2}{c^2\,l^2}[(1 - Q)(1 - A_x) - B_k \sinh (c\,x')]$
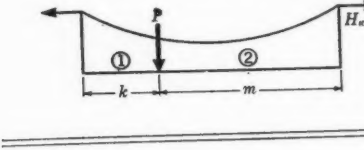	13	$M_1 = \dfrac{-\,P\,l}{c\,l}\left[Q'(1 - A_x) - \dfrac{\sinh (c\,m)}{\sinh (c\,l)} \sinh (c\,x)\right]$
	14	$M_2 = \dfrac{-\,P\,l}{c\,l}\left[Q'(1 - A_x) - \dfrac{\sinh (c\,k)}{\sinh (c\,l)} \sinh (c\,x')\right]$

STIFFENING TRUSS ENTIRELY LOADED

26. Deflection, Slope, Moment, Shear, and Truss Load.—An interesting illustration of the structural behaviors of a stiffening truss is offered by the case in which the span is completely covered by live load (Fig. 5).

Integrating and differentiating the moment equation in Table 2, item 1, the different expressions for truss functions are as follows: For deflection, the expression is

$$\eta = \frac{p\,l^4}{c^4\,l^4\,E\,I}(1-Q)\left[\frac{c^2\,l^2}{2}\left(\frac{x}{l}-\frac{x^2}{l^2}\right) - \left(1-\frac{\cosh c\,l\left(\frac{1}{2}-\frac{x}{l}\right)}{\cosh\frac{c\,l}{2}}\right)\right] \quad ..(61a)$$

which reveals that the deflection diagram is a superposition of a parabola and a (1 − cosh)-curve as shown in Fig. 5(*f*).

For slope, the expression is

$$\theta = \frac{-\,p\,l^3}{c^3\,l^3\,E\,I}(1-Q)\left[c\,l\left(\frac{1}{2}-\frac{x}{l}\right) - \frac{\sinh c\,l\left(\frac{1}{2}-\frac{x}{l}\right)}{\cosh\frac{c\,l}{2}}\right] \quad ..(61b)$$

which reveals that the slope diagram is a superposition of a straight line and a (− sinh)-curve as shown in Fig. 5(*e*).

For moment, the expression is

$$M = \frac{p\,l^2}{c^2\,l^2}(1-Q) \times\left[1-\frac{\cosh c\,l\left(\frac{1}{2}-\frac{x}{l}\right)}{\cosh\frac{c\,l}{2}}\right] \quad ..(61c)$$

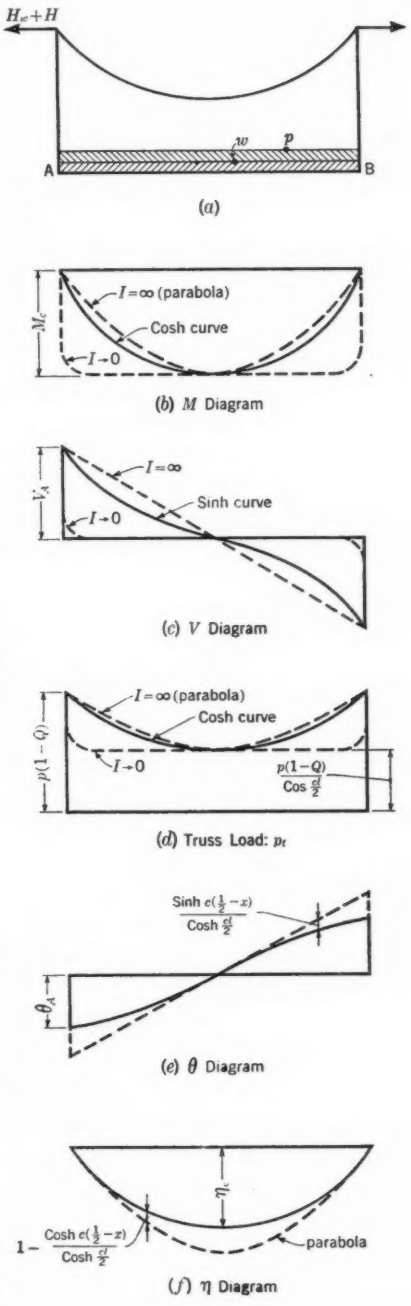

FIG. 5

which reveals that the moment diagram is a hyperbolic cosine curve symmetrical about the center of span as shown in Fig. 5(*b*).

For shear, the expression is

$$V = \frac{p\,l}{c\,l}(1 - Q)\left[\frac{\sinh c\,l\left(\frac{1}{2} - \frac{x}{l}\right)}{\cosh \frac{c\,l}{2}}\right] \ldots\ldots\ldots\ldots (61d)$$

which reveals that the shear diagram is a hyperbolic sine curve as shown in Fig. 5(*c*).

For truss load, the expression is

$$p_t = p\,(1 - Q)\,\frac{\cosh c\,l\left(\frac{1}{2} - \frac{x}{l}\right)}{\cosh \frac{c\,l}{2}} \ldots\ldots\ldots\ldots\ldots (61e)$$

which reveals that the diagram of truss load is a hyperbolic cosine curve, maximum at both ends and minimum at center as shown in Fig. 5(*d*).

27. Limit Case, $c\,l \to 0$.—If the dimensionless number $c\,l$ approaches zero, $I \to \infty$, and Q tends to be zero, since H approaches zero, Eqs. 61 have the following limiting values, respectively,

$$\eta \to \frac{p\,l^4}{24\,E\,I}\left(\frac{x}{l} - 2\,\frac{x^3}{l^3} + \frac{x^4}{l^4}\right) \ldots\ldots\ldots\ldots\ldots (62a)$$

$$\theta \to \frac{p\,l^3}{24\,E\,I}\left(1 - 6\,\frac{x^2}{l^2} + 4\,\frac{x^3}{l^3}\right) \ldots\ldots\ldots\ldots\ldots (62b)$$

$$M \to \frac{p\,l^2}{2}\left(\frac{x}{l} - \frac{x^2}{l^2}\right) \ldots\ldots\ldots\ldots\ldots\ldots\ldots (62c)$$

$$V \to p\,l\left(\frac{1}{2} - \frac{x}{l}\right) \ldots\ldots\ldots\ldots\ldots\ldots\ldots (62d)$$

and

$$p_t \to p \ldots\ldots\ldots\ldots\ldots\ldots\ldots\ldots\ldots\ldots (62e)$$

which correspond to the case of a simply supported beam without suspension.

28. Limit Case, $c\,l \to \infty$.—If $c\,l$ approaches infinity, the limiting values of Eqs. 61 will be

$$\eta \to \frac{p\,l^2}{H_w + H}(1 - Q)\,\frac{1}{2}\left(\frac{x}{l} - \frac{x^2}{l^2}\right) \ldots\ldots\ldots\ldots (63a)$$

$$\theta \to \frac{p\,l}{H_w + H}(1 - Q)\left(\frac{1}{2} - \frac{x}{l}\right) \ldots\ldots\ldots\ldots\ldots (63b)$$

$$M \to 0 \ldots\ldots\ldots\ldots\ldots\ldots\ldots\ldots\ldots\ldots (63c)$$

$$V \to 0 \ldots\ldots\ldots\ldots\ldots\ldots\ldots\ldots\ldots\ldots (63d)$$

$$p_t \to 0 \ldots\ldots\ldots\ldots\ldots\ldots\ldots\ldots\ldots\ldots (63e)$$

—which correspond to the case of an unstiffened cable span.

29. Flexibility Factor, $c\,l$.—Sections 27 and 28 reveal that the dimensionless term $c\,l$ characterizes the flexibility of a suspension bridge: The more flexible

the bridge, the larger the value of $c\,l$. It can be designated as the "flexibility factor" of a suspension bridge.

From an investigation of the existing stiffened suspension bridges, it is found that the usual range of $c\,l$ is between 0 and 10.

30. Maximum Values of η, θ, M, V, and p_t.—The maximum deflection occurs at the center of span; it will be obtained in putting $x = l/2$ in Eq. 61*a* and is equal to

$$\eta_c = \frac{p\,l^4}{c^4\,l^4} \times \frac{1-Q}{E\,I}\left(\frac{c^2\,l^2}{8} - 1 - \frac{1}{\cosh\frac{c\,l}{2}}\right) \doteqdot \frac{5}{384}\frac{p\,l^4}{E\,I}\left[\frac{1-Q}{1+\frac{c^2\,l^2}{9.7}}\right] \quad (64)$$

The maximum slope occurs at both ends of span. In putting $x = 0$ and $x = l$ in Eq. 61*b*, it will be

$$\theta_{A,B} = \mp\frac{p\,l^4}{c^3\,l^3} \times \frac{1-Q}{E\,I}\left(\frac{c\,l}{2} - \tanh\frac{c\,l}{2}\right) \doteqdot \mp\frac{p\,l^3}{24\,E\,I}\left[\frac{1-Q}{1+\frac{c^2\,l^2}{10.5}}\right] \quad (65)$$

The maximum moment occurs at the center of span; it will be obtained in putting $x = \frac{l}{2}$ in Eq. 61*c* and is equal to

$$M_c = \frac{p\,l^2}{8}\left[\frac{8\,(1-Q)}{c^2\,l^2}\tanh\frac{c\,l}{2}\tanh\frac{c\,l}{4}\right] \quad (66)$$

The maximum shear occurs at both ends of span. In putting $x = 0$ and $x = l$ in Eq. 61*d*—

$$V_{A,B} = \pm\frac{p\,l}{2}\left[\frac{2\,(1-Q)}{c\,l}\tanh\frac{c\,l}{2}\right] \quad (67)$$

—and the maximum truss load occurs at both ends of span. In putting $x = 0$ and $x = l$ in Eq. 61*e*,

$$p_t = p\,[1 - Q] \quad (68)$$

The last members of Eqs. 64 and 65 are found empirically; they are simple in form and fairly exact for the usual range of $c\,l$ (from 0 to 10). The values outside the brackets of Eqs. 64 to 68 are those corresponding to the case of a simply supported girder without suspension. It is obvious, then, that the terms within the bracket may be considered as coefficients reflecting the effect of suspension by a cable for different functions.

31. Effect of Variable Suspender Force on Value of H.—As $\eta_c = \Delta f$, Eq. 64 may be transformed into the following form:

$$H\,f + \frac{H_w + H}{1.01}\Delta f + \frac{9.6\,E\,I}{l^2}\Delta f = \frac{p\,l^2}{8} \quad (69)$$

Eq. 69 is the static equation $\Sigma M = 0$, at the center of the span, as used in Part I, with the assumption that the suspender forces are uniformly distributed. The coefficient of the quantity $(H_w + H)$, 1/1.01 rather than unity, is a measure of the error induced by the foregoing assumption that the last quantity in Eq. 64 is a deflection coefficient due to suspension. Its effect on the resulting cable stress is only about 1%, but its effect on moment is much greater.

32. Elastic Theory.—In Eqs. 64 to 68, if $I = \infty$ or $c\,l = 0$, but $Q \neq 0$ (that is, $H \neq 0$), all coefficients due to suspension reduce to $(1 - Q)$, and (since the fundamental assumption in this theory is that the stressed cable curve remains undistorted, when loaded) these equations become equal to those obtained by the so-called "elastic theory." It is shown then that the more flexible the truss (the larger the value of $c\,l$) the greater will be the error of the elastic theory.

PART III. DESIGN PROCEDURE, MAXIMUM MOMENTS, SHEARS, SLOPES, AND DEFLECTIONS IN STIFFENING TRUSS

Introduction

33. Cases of Loading and Temperature.—To determine the maximum bending moment, shear, slope, and deflection for a given section of the stiffening truss, one must refer to the appropriate loading condition. There are eight cases of loading and temperature to be considered in the design computations,[10,11] but, in customary practice, the extent of the live load (k) for maximum values of these variables must be found by trial and error, and the calculation is rather tiresome. Moreover, the location of the maximum positive and negative moments in the truss cannot be determined without drawing the complete maximum N-curve, although it is known to occur approximately at the quarter point of the span.

With the help of the simplified formulas for H and M in this paper, one may undertake a direct analytical determination of the maximum conditions.

The different cases of loading and temperature will be presented in the same order (Cases I to VIII) as is done elsewhere by D. B. Steinman,[11] M. ASCE. The H-formulas corresponding to each of these cases (H_{I} to H_{VIII}) may be found in Table 1, and the corresponding M-formulas in Table 2.

Case I

34. Maximum Positive Moment in Main Span.—In this case (see Table 1) the main span is loaded uniformly a distance x from the left end, the side spans are not loaded, and the highest probable temperature is assumed.

From Table 2, line 9, for segment AB:

$$M = \frac{p\,l^2}{c^2\,l^2}\left\{(1 - Q)\left[1 - \frac{\cosh c\left(\frac{l}{2} - x\right)}{\cosh\frac{c\,l}{2}}\right] - \frac{\cosh c\,(l - k) - 1}{\sinh(c\,l)}\sinh(c\,x)\right\} \quad \ldots (70)$$

[10] "Modern Framed Structures," by J. B. Johnson, C. W. Bryan, and F. E. Turneaure, John Wiley & Sons, Inc., New York, N. Y., Pt. II, 9th Ed., 1916.

[11] "A Practical Treatise on Suspension Bridges," by D. B. Steinman, John Wiley & Sons, Inc., New York, N. Y., 2d Ed., 1929.

in which

$$Q = H_1 \frac{8\,f}{p\,l^2} = \frac{1}{D_{+t}} \left(\sin^2 \frac{k\,\pi}{2\,l} - T \right) \ldots\ldots\ldots\ldots\ldots (71)$$

The moment varies from section to section and also varies at any given section as the live load moves along the span. The maximum value occurs when the conditions $\frac{dM}{dx} = 0$ and $\frac{dM}{dk} = 0$ are satisfied simultaneously. The differentiation with respect to x is easily performed; but, as c and Q both vary with k, the differentiation with respect to k gives a result too involved for exact solution.

For a given load (k, c, and Q all being constant), the condition $\frac{dM}{dx} = 0$ gives the position x_{+m} of the maximum moment, as follows:

$$\tanh (c\,x_{+m}) = \tanh \frac{c\,l}{2} - \frac{\cosh c\,(l - k) - 1}{(1 - Q) \sinh (c\,l)} \ldots\ldots\ldots\ldots (72)$$

and the maximum M becomes

$$(+)\ M\ (\max) = \frac{p\,l^2}{c^2\,l^2} (1 - Q) \tanh (c\,x_{+m}) \tanh \frac{c\,x_{+m}}{2} \ldots\ldots\ldots (73)$$

both of which can be easily calculated.

It is still necessary, however, to determine the load length k_{+m} which will give the highest of all possible maxima. The differentiation will be greatly simplified by the assumption that c is nearly constant as k varies. This is almost true when the live load ratio $q = \frac{p}{w}$ is small, and is only slightly in error for ordinary values of loading. A numerical investigation of the effect of variations in the value of c shows that it can be largely compensated for by using a higher value of the constant c_f in the equation $\frac{dM}{dk} = 0$, which corresponds to assuming full span loading irrespective of the actual length of k; that is,

$$c = c_f = \sqrt{\frac{H_w + H_f}{E\,I}} = (\text{constant}) \ldots\ldots\ldots\ldots\ldots (74)$$

In Eq. 74, H_f is the horizontal force in the cable when the main span is fully loaded and the highest possible temperature is assumed (that is, $H_f = H_1$ at $k = l$). Therefore, the condition $\frac{dM}{dk} = 0$ gives, approximately,

$$\frac{\sinh c_f\,(l - k_{+m})}{\sin \frac{k_{+m}\,\pi}{l}} = \frac{\pi}{2\,c_f\,l\,D_{+t}} \sinh c_f\,l \left(\tanh \frac{c_f\,l}{2} - \tanh \frac{c_f\,x_{+m}}{2} \right) \ldots (75)$$

The simultaneous equations required to solve for x_{+m} and k_{+m} are then Eqs. 72 and 75. The computations involve assuming two or three successive values of k (from $0.35\,l$ to $0.45\,l$), simultaneously, in Eqs. 72 and 75 and ob-

taining two curves of $x = f(k)$, whose intersection gives the final values of k_{+m} and x_{+m} (use $c = c_f$ in both equations).

An extensive numerical investigation of existing bridges shows that it is also possible to proceed more easily as follows: Assume $x_{+m} = 0.22\,l$ in Eq. 75

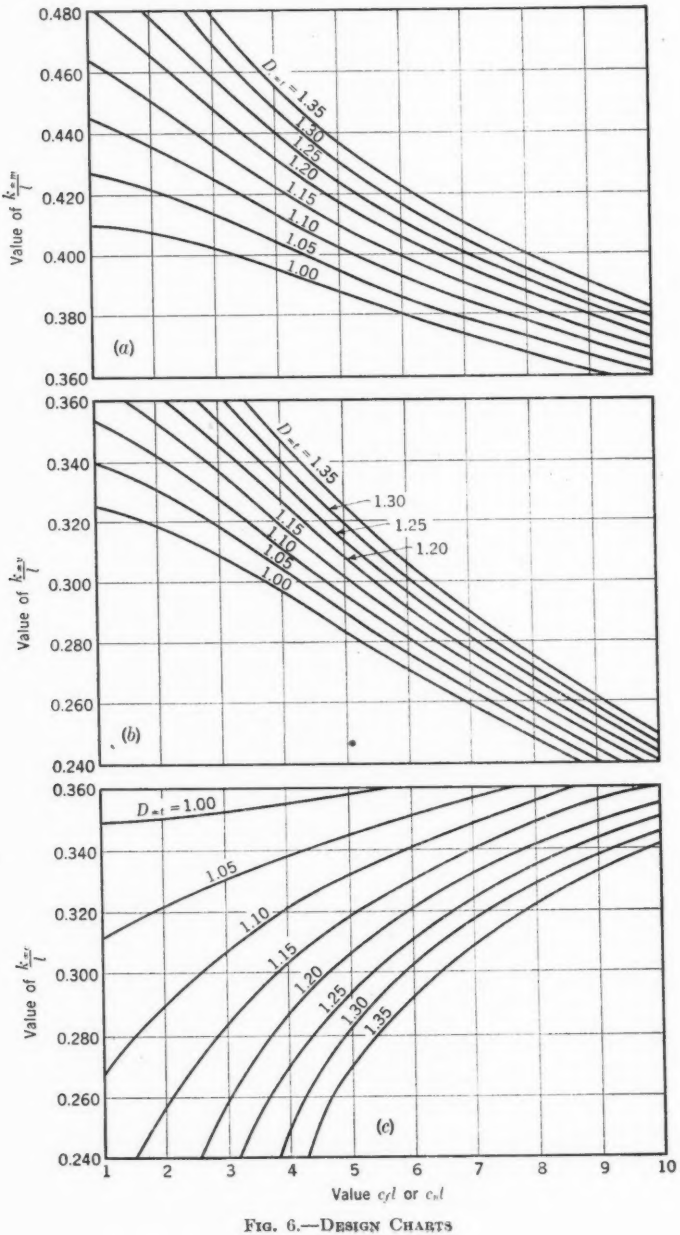

FIG. 6.—DESIGN CHARTS

and solve for k_{+m} which will be very nearly the actual load length k_{+m}. Then compute the corresponding values of H, c, and Q, substitute them into Eqs. 72 and 73, and derive x_{+m} and the maximum value of $+M$ in the truss. If the value of x_{+m} thus found differs too much from the assumed value $0.22\,l$, a second calculation can be made by using the new value of x_{+m} in Eq. 75, and solving again for k_{+m}; but the correction would be small (especially for the magnitude of maximum $+M$) and not worthwhile in usual cases.

To facilitate the solution of Eq. 75 (in which $x_{+m} = 0.22\,l$ is assumed), Fig. 6(*a*) is given to read directly when D_{+t} and $c_f\,l$ are known.

35. Maximum Positive Shear + V at Left End.—The shear equation is as follows:

$$V = \frac{dM}{dx} = \frac{p\,l}{c\,l}\left[(1 - Q)\,\frac{\sinh c\left(\frac{l}{2} - x\right)}{\cosh \frac{c\,l}{2}} - \frac{\cosh c\,(l - k) - 1}{\sinh (c\,l)}\cosh (c\,x)\right] \quad \ldots (76)$$

At the end, $x = 0$, the end shear equation is

$$V_A = \frac{p\,l}{c\,l}\left[(1 - Q)\tanh \frac{c\,l}{2} - \frac{\cosh c\,(l - k) - 1}{\sinh (c\,l)}\right] \quad \ldots\ldots (77)$$

The shear will be maximum when the load length k satisfies the condition $\frac{dV_A}{dk} = 0$. By the same procedure as in section 34, the differentiation is simplified by assuming a constant value of $c = c_f$. Therefore, the condition $\frac{dV_A}{dk} = 0$ gives

$$\frac{\sinh c_f\,(l - k_{+v})}{\sin \frac{k_{+v}\,\pi}{l}} = \frac{\pi}{c_f\,l\,D_{+t}}\sinh^2 \frac{c_f\,l}{2} \quad \ldots\ldots (78)$$

Fig. 6(*b*) contains the curve necessary to read k_{+v} directly when both D_{+t} and $c_f\,l$ are known.

When k_{+v} has been found, c and Q can be computed accordingly. Substituting these values in Eq. 78, the maximum positive shear at the left end can easily be determined.

36. Maximum Positive Shear at Center with Span Reversed (That Is, with the Live Load Starting from the Right End of the Span).—To find the maximum center shear, one end of the live load must be at the center section so that $k = 0.5\,l$, substituting the values of k and $x = 0.5\,l$ in Eq. 77, the maximum positive shear at the center is equal to

$$+ V_c = \frac{p\,l}{2\,c\,l}\tanh \frac{c\,l}{4} \quad \ldots\ldots (79a)$$

in which

$$c = \sqrt{\frac{H_w + H_{I(k=0.5l)}}{E\,I}} \quad \ldots\ldots\ldots\ldots\ldots\ldots\ldots\ldots (79b)$$

CASE II

37. Maximum Negative Moment in Main Span.—In this case (see Table 1) the loading is the reverse of Case I; that is, the side spans are both loaded and the main span is partly loaded from the right-hand tower, a distance $l - k$. The lowest probable temperature is assumed.

From Table 2, item 11, for segment AB,

$$M = -\frac{p\,l^2}{c^2\,l^2}\left\{ Q\left[1 - \frac{\cosh c\left(\frac{l}{2} - x\right)}{\cosh \frac{c\,l}{2}} \right] - \frac{\cosh c\,(l-k) - 1}{\sinh (c\,l)} \sinh (c\,x) \right\} \quad \ldots (80a)$$

in which

$$Q = H_{II}\frac{8\,f}{p\,l^2} = \frac{1}{D_{-t}}\left(\cos^2 \frac{k\,\pi}{2\,l} + 2\,s + T \right) \quad \ldots\ldots\ldots\ldots (80b)$$

The condition $\frac{dM}{dx} = 0$ gives

$$\tanh (c\,x_{-m}) = \tanh \frac{c\,l}{2} - \frac{\cosh c\,(l-k) - 1}{Q \sinh (c\,l)} \quad \ldots\ldots\ldots\ldots (81)$$

and

$$(-)\,M\ (\max) = -\frac{p\,l^2}{c^2\,l^2}\,Q \tanh (c\,x_{-m}) \tanh \frac{c\,x_{-m}}{2} \quad \ldots\ldots\ldots\ldots (82)$$

The assumption, that c remains nearly constant as k varies, is also made here in order to differentiate $\frac{dM}{dk} = 0$; but a smaller value of c, corresponding to no load in the main span, is used to compensate for the effect of variation of c:

$$c = c_n = \sqrt{\frac{H_w + H_n}{E\,I}} = (\text{constant}) \quad \ldots\ldots\ldots\ldots\ldots\ldots (83)$$

in which H_n is the horizontal force in the cable when the live load covers both side spans, when the main span is not loaded, and when the temperature is assumed at its lowest (that is, $H_n = H_{II}$ at $k = l$). Approximately, therefore, the condition $\frac{dM}{dk} = 0$ gives

$$\frac{\sinh c_n\,(l - k_{-m})}{\sin \frac{k_{-m}\,\pi}{l}} = \frac{\pi}{2\,c_n\,l\,D_{-t}}\left(\tanh \frac{c_n\,l}{2} - \tanh \frac{c_n\,x_{-m}}{2} \right) \quad \ldots\ldots (84)$$

The two simultaneous equations necessary to solve for x_{-m} and k_{-m} are then Eqs. 81 and 84. The solution can be determined in a manner similar to that used in Case I, section 34. Fig. 6(*a*) can also be used to read k_{-m} when D_{-t} and $c_n\, l$ are calculated.

38. Maximum Negative Shear at the Left End.—In a manner similar to that used in Case I, section 35, the end shear equation is found to be

$$V_A = -\frac{p\, l}{c\, l}\left[Q \tanh \frac{c\, l}{2} - \frac{\cosh c\,(l-k) - 1}{\sinh (c\, l)} \right] \ldots\ldots\ldots (85a)$$

Assuming also that c is nearly constant and equal to c_n, the condition $\frac{dV_A}{dk} = 0$ gives

$$\frac{\sinh c_n\,(l - k_{-v})}{\sin \frac{k_{-v}\,\pi}{l}} = \frac{\pi}{c_n\, l\, D_{-t}} \sinh^2 \frac{c_n\, l}{2} \ldots\ldots\ldots\ldots (85b)$$

Fig. 6(*b*) can also be used to read k_{-v} directly when D_{-t} and $c_n\, l$ are known.

39. Maximum Negative Shear at Center (with Span Reversed).—Similar to Case I, section 36, the maximum center shear is found by Eq. 79*a*, in which c, in terms of H_{II} is found by Eq. 79*b*.

Case III

40. Maximum Positive Moment at the Center of Main Span.—In this case (see Table 1) the main span is loaded symmetrically at each side of the center, the side spans are not loaded, and the highest probable temperature is assumed.

From Table 2, item 4, for segment AB,

$$M = \frac{p\, l^2}{c^2\, l^2}\left\{ (1-Q)\left[1 - \frac{\cosh c\left(\frac{l}{2} - x\right)}{\cosh \frac{c\, l}{2}} \right] - \frac{\cosh c\left(\frac{l}{2} - x\right)}{\cosh \frac{c\, l}{2}} \left[\cosh (c\, k) - 1\right] \right\} \ldots (86a)$$

in which

$$Q = H_{III}\frac{8\, f}{p\, l^2} = \frac{1}{D_{+t}}\left(\cos \frac{k\,\pi}{l} - T \right) \ldots\ldots\ldots\ldots (86b)$$

At the center, $x = \frac{l}{2}$, and the moment equation (Eq. 86*a*) will be

$$M_c = \frac{p\, l^2}{c^2\, l^2}\left[(1-Q)\left(1 - \frac{1}{\cosh \frac{c\, l}{2}} \right) - \frac{\cosh (c\, k) - 1}{\cosh \frac{c\, l}{2}} \right] \ldots\ldots (86c)$$

It will be maximum when k satisfies the condition $\frac{dM_c}{dk} = 0$. Assuming that

c remains nearly constant and equal to c_f (corresponding to full loading of main span, the same as in Case I), the condition $\frac{dM}{dk} = 0$ gives

$$\frac{\sinh (c_f\, k_{+c})}{\sin \frac{k_{+c}\, \pi}{l}} = \frac{\pi}{c_f\, l\, D_{+t}} \left(\cosh \frac{c_f\, l}{2} - 1 \right) \ldots\ldots\ldots\ldots (87)$$

Fig. 6(*c*) is given to obtain k_{+c} directly as a function of D_{+t} and $c_f\, l$. With k_{+c} found, H_{III}, c, and Q can be calculated, and the maximum positive moment $+M$ at the center will be determined easily from Eq. 86*c*.

Case IV

41. Maximum Negative Moment at the Center of Main Span.—Both side spans are loaded for this case (see Table 1) and the center span is loaded symmetrically from the towers a distance k toward the center. The lowest probable temperature is assumed.

In a manner, similar to that used in Case III, the center moment equation is

$$M_c = -\frac{p\, l^2}{c^2\, l^2} \left[Q \left(1 - \frac{1}{\cosh \frac{c\, l}{2}} \right) - \frac{\cosh (c\, k) - 1}{\cosh \frac{c\, l}{2}} \right] \ldots\ldots (88a)$$

in which

$$Q = H_{IV} \frac{8\, f}{p\, l^2} = \frac{1}{D_{-t}} \left(1 - \cos \frac{k\, \pi}{l} + 2\, S + T \right) \ldots\ldots\ldots (88b)$$

Assuming $c = c_n$ corresponding to a no-load condition on the main span as in Case II, the condition $\frac{dM_c}{dk} = 0$ gives

$$\frac{\sinh (c_n\, k_{-c})}{\sin \frac{k_{-c}\, \pi}{l}} = \frac{\pi}{c_n\, l\, D_{-t}} \left(\cosh \frac{c_n\, l}{2} - 1 \right) \ldots\ldots\ldots\ldots (89)$$

Eq. 89 can also be solved by reference to Fig. 6(*c*), first obtaining k_{-c} as a function of D_{-t} and $c_n\, l$.

Case V

42. Maximum Positive Moment in Side Span.—With only one side span fully loaded and assuming the highest probable temperature, Table 2, item 1, shows that the moment for the loaded side span is equal to

$$M = \frac{p\, l^2_1}{c^2_1\, l^2_1} (1 - Q) \left[1 - \frac{\cosh c_1 \left(\frac{l_1}{2} - x \right)}{\cosh \frac{c_1\, l_1}{2}} \right] \ldots\ldots\ldots (90a)$$

in which

$$Q = H_V \frac{8\, f_1}{p\, l^2_1} \ldots\ldots\ldots\ldots\ldots\ldots\ldots (90b)$$

The moment reaches a maximum simultaneously in every section of the loaded span. The highest maximum positive moment, $+M$, occurs at the center section, since the maximum M-curve is a hyperbolic cosine curve symmetrical about the center of span. It is equal to

$$M_{c1} = \frac{p\,l^2_1}{c^2_1\,l^2_1}(1 - Q)\left(1 - \frac{1}{\cosh\frac{c_1\,l_1}{2}}\right); \text{ or}$$

$$M_{c1} = \frac{p\,l^2_1}{c^2_1\,l^2_1}(1 - Q)\tanh\frac{c_1\,l_1}{2}\tanh\frac{c_1\,l_1}{4} \quad \ldots\ldots\ldots\ldots (91)$$

Case VI

43. Maximum Negative Moment in Side Span.—The loading for this case is the reverse of Case V; that is, the live load covers the entire bridge except one side span. The lowest probable temperature is assumed.

In a manner similar to Case V, section 42, the equation for maximum negative moment in the unloaded side span is

$$M = -\frac{p\,l^2_1}{c^2_1\,l^2_1}Q\left[1 - \frac{\cosh c_1\left(\frac{l_1}{2} - x\right)}{\cosh\frac{c_1\,l_1}{2}}\right] \quad \ldots\ldots\ldots\ldots (92a)$$

in which

$$Q = H_{VI}\frac{8\,f_1}{p\,l^2_1} \quad \ldots\ldots\ldots\ldots\ldots\ldots\ldots\ldots (92b)$$

The maximum negative moment at the center is

$$M_{c1} = -\frac{p\,l^2_1}{c^2_1\,l^2_1}Q\left(1 - \frac{1}{\cosh\frac{c_1\,l_1}{2}}\right); \text{ or}$$

$$M_{c1} = \frac{p\,l^2_1}{c^2_1\,l^2_1}Q\tanh\frac{c_1\,l_1}{2}\tanh\frac{c_1\,l_1}{4} \quad \ldots\ldots\ldots\ldots\ldots (93)$$

Case VII

44. Maximum Positive Shear at Any Section in Side Span.—The left side span is partly loaded, from the tower toward the anchorage, as shown in Table 1. There is no live load on the remainder of the bridge; and the highest probable temperature is assumed. From Table 2, by differentiating the M-equation of line 12,

$$V = \frac{dM}{dx} = \frac{p\,l_1}{c_1\,l_1}\left[(1 - Q)\frac{\sinh c_1\left(\frac{l_1}{2} - x\right)}{\cosh\frac{c_1\,l_1}{2}} + \frac{\cosh(c_1\,k) - 1}{\sinh(c_1\,l_1)}\cosh c_1(l_1 - x)\right] \quad \ldots\ldots (94a)$$

in which

$$Q = H_{\text{VII}} \frac{8 f_1}{p l^2_1} \quad \ldots\ldots (94b)$$

As the one end of partial loading must extend to the given section where the maximum shear is sought, it is possible to substitute $k = x$ to obtain the maximum shear at any section x, so that

$$+ V = \frac{p l_1}{c_1 l_1} \left[(1 - Q) \frac{\sinh c_1 \left(\frac{l_1}{2} - x \right)}{\cosh \frac{c_1 l_1}{2}} + \frac{\cosh (c_1 x) - 1}{\sinh (c_1 l_1)} \cosh c_1 (l_1 - x) \right] \quad \ldots (95)$$

At the center of the span where $x = \frac{l_1}{2} (= k)$, the maximum positive shear will be

$$V_{c1} = \frac{p l_1}{2 c_1 l_1} \tanh \frac{c_1 l_1}{4} \quad \ldots\ldots (96)$$

In Eq. 96,

$$c_1 = \sqrt{\frac{H_w + H_{\text{VII}(k=0.5l1)}}{E I_1}} \quad \ldots\ldots (97)$$

At the left end, $x = 0$, the maximum positive shear will be

$$V = \frac{p l_1}{c_1 l_1} (1 - Q) \tanh \frac{c_1 l_1}{2} \quad \ldots\ldots (98)$$

in which Q and $c_1 l_1$ correspond to full loading condition on this side span.

Case VIII

45. Maximum Negative Shear at Any Section in Side Span.—In Case VIII, the loading is the reverse of that in Case VII; that is, the loaded part of the left side span in Case VII is the only part left unloaded in Case VIII (see Table 1). The lowest probable temperature is assumed.

In a manner similar to that used in Case VII, the equation for maximum negative shear is found to be

$$V = - \frac{p l_1}{c_1 l_1} \left[Q \frac{\sinh c_1 \left(\frac{l_1}{2} - x \right)}{\cosh \frac{c_1 l_1}{2}} + \frac{\cosh c_1 (l_1 - x) - 1}{\sinh (c_1 l_1)} \cosh (c_1 x) \right] \quad \ldots (99a)$$

in which

$$Q = H_{\text{VIII}} \frac{8 f_1}{p l^2_1} \quad \ldots\ldots (99b)$$

At the center of span, $x = \frac{l_1}{2}$, the maximum negative shear will be

$$V_{c1} = - \frac{p l_1}{2 c_1 l_1} \tanh \frac{c_1 l_1}{4} \quad \ldots\ldots (100a)$$

in which

$$c_1 = \sqrt{\frac{H_w + H_{VIII(k=0.5l)}}{E\,I_1}} \quad \ldots\ldots\ldots\ldots\ldots\ldots (100b)$$

At the left end, $x = 0$, the maximum negative shear will be

$$V = -\frac{p\,l_1}{c_1\,l_1} Q \tanh \frac{c_1\,l_1}{2} \quad \ldots\ldots\ldots\ldots\ldots\ldots (100c)$$

in which Q and $c_1\,l_1$ correspond to the condition of no load on this side span.

Curves of Maximum Moment in the Main Span

46. Simplified Method.—To obtain the maximum positive, or maximum negative, moment at each section of the main span, it is necessary to substitute different values of x in Eqs. 75 and 84; and it is also necessary to solve for k, the corresponding load length that will produce maximum positive, or maximum negative, moment at the section x considered. With k determined, substituting in Eq. 70 or 80*a*, the maximum positive, or maximum negative, moment at x can be calculated.

In sections 34 to 41, a procedure has been given for determining: (*a*) The values of x_{+m} and x_{-m}, which are the locations of the points of maximum moments (positive and negative); (*b*) the maximum values of positive moment and negative moment at points x_{+m} and x_{-m}; (*c*) the maximum values of positive moment and negative moment at the center of the main span; and (*d*) the maximum positive and negative shears at the ends of the span (the slopes of the maximum moment curves ($\pm M$) at the ends of the span).

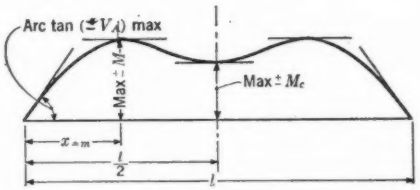

FIG. 7

These four items give five points (two zero points, two maxima points, and one minimum point) and five tangents of each curve of maximum moment (Fig. 7), and the intermediate parts can be sketched in readily by free hand. The most important information about these curves having been determined exactly, the resulting moment curves are sufficiently accurate for practical purposes.

Maximum Center Deflection in the Stiffening Truss

47. Main Span and Side Span.—It is known that the maximum downward deflection at center in any span is produced under the probable highest temperature with full live load on the span alone. Then, the maximum value is expressed by Eq. 66 in which Q and $c\,l$ correspond to the temperature and loading condition previously cited.

Maximum Increase of Grade in the Stiffening Truss

48. Increase in Grade.—Many investigators[12] have suggested the increase of grade as a criterion to define the rigidity of a suspension bridge. For a vehicle

[12] "A Generalized Deflection Theory for Suspension Bridges," by D. B. Steinman, *Transactions*, ASCE, Vol. 100, 1935, pp. 1132–1234.

traveling across a suspension bridge the point at which the maximum grade occurs is near the towers for a hinged truss. As in most suspension bridges, if there is a camber of several feet in the main span, and the side spans have a grade leading upward to the main span, the resultant grade will be maximum when the upward slope is maximum at the end of the main span, or when the downward slope is maximum at the tower end of the side span.

49. End of Main Span.—The maximum upward slope at the left end evidently occurs at the loading and temperature conditions in Case II, Table 1. The equations of slope can be obtained by integrating the M-equation $\left(\theta = \int \frac{M}{E\,I}\,dx\right)$. Making $x = 0$ in the θ-equation of the left (unloaded) segment, the equation of end slope will be

$$\theta_A = \frac{p\,l^3}{E\,I\,c^3\,l^3}\left(\frac{c\,l}{2} - \tanh\frac{c\,l}{2}\right)[Q - f(k)] \quad \ldots\ldots\ldots (101a)$$

or, by Eq. 65,

$$\theta_A = \frac{p\,l^3}{24\,E\,I}\,\frac{Q - f(k)}{1 + \frac{c^2\,l^2}{10.5}} \quad \ldots\ldots\ldots\ldots\ldots\ldots (101b)$$

in which

$$Q = H_{II}\,\frac{8\,f}{p\,l^2} \quad \ldots\ldots\ldots\ldots\ldots\ldots\ldots (102)$$

and

$$f(k) = \frac{c^2\,(l-k)^2 \sinh(c\,l) - 2\,c\,l \tanh\frac{c\,(l-k)}{2}\sinh c\,(l-k)}{c^2\,l^2 \sinh(c\,l) - 2\,c\,l \tanh\frac{c\,l}{2}\sinh(c\,l)} \quad \ldots\ldots (103)$$

It seems necessary to try several values of k in Eq. 101a to find which one will give the maximum value of θ_A. However, a numerical study leads one to believe that

Theorem 4.—

The maximum upward grade change at the end of main span will be produced under the probable lowest temperature with the full live load on both side spans and approximately the far half of the main span.

Thus, with $k = \frac{1}{2}\,l$, Eq. 103 becomes

$$f(k)_{k=0.5l} = \frac{\frac{1}{4}\,c\,l - \tanh\frac{c\,l}{4}\,\frac{1}{\cosh\frac{c\,l}{2}}}{c\,l - 2\tanh\frac{c\,l}{2}} \quad \ldots\ldots\ldots\ldots (104)$$

With H_{II}, Q, and $c\,l$ computed for $k = \frac{l}{2}$, Eq. 104 gives the value of $f(k)$ and Eq. 103 will give the maximum increase of grade at end of main span. The result is approximate, but the error is slight.

50. Tower End of Side Span.—The maximum increase of grade at tower end occurs at the loading and for the assumed temperature condition of Case V,

Table 1. It is equal to

$$\theta_A = \frac{p\,l^3_1}{24\,E\,I_1} \times \frac{1 - Q}{1 + \frac{c^2_1\,l^2_1}{10.5}} \quad \ldots\ldots\ldots\ldots\ldots\ldots\ldots\ldots (105)$$

in which Q and $c_1\,l_1$ correspond to the same values in Case V, Table 1, only one side span is fully loaded and the highest probable temperature is assumed.

Illustrative Example, Mount Hope Bridge

51. Data.—The Mount Hope suspension bridge will be used to illustrate the typical design computations. The results check almost exactly with those obtained by the deflection theory, but a complete analysis requires only from about 6 hours to 8 hours. All numerical values are calculated on a 12-in. slide rule. The following data are used:

Description	Main span	Side span
Length, l, in feet	1,188.33	498.33
Sag, f, in feet	118.795	20.891
Sag ratio $f/l = n$	0.100	0.042
$E\,I$, in (Feet)^2-Kips—		
Main span	123,511,000	
Side span	120,408,000	
Cable section, A, in square inches	75.92	
Sec α_1	1.043	
Live load, p, in kips per foot of bridge	0.750	
Dead load, w, in kips per foot of bridge	2.650	
Coefficient of expansion, ϵ	65×10^{-6}	
Temperature change, Δt, in degrees Centigrade	$\pm 60°$	
Cable Length Functions, in Feet—		
For cable stretch, L_s	3,133	
For temperature change, L_t	2,996	

52. Constants.—By reference to Table 1, design constants are determined as follows:

$r = l_1/l = 0.42$; $\quad n_1/n = 0.42$; $\quad q = p/w = 0.283$;

$N_s = 0.0805$ (Eq. 29*b*); $\quad N_c = 0.1280$ (Eq. 35*b*); $\quad N_t = 0.0185$ (Eq. 38*b*);

$\frac{p\,l^2}{8\,f} = 1{,}113$; $\quad \frac{p\,l^2}{8\,f\,D_{+t}} = 907$; $\quad \frac{p\,l^2}{8\,f\,D_{-t}} = 936$;

$$H_w = \frac{w\,l^2}{8\,f} = \frac{w_1\,l^2_1}{8\,f_1} = 3{,}940 \text{ kips};$$

$$S = 0.0372 \text{ (Eq. 44)};$$

$$T = \frac{B}{q}\,N_t = 0.0795;$$

$c^2_0\,l^2 = \frac{H_w\,l^2}{E\,I} = 45$; $\quad c^2_{01}\,l^2_1 = \frac{H_w\,l^2_1}{E\,I_1} = 8.1$;

$B = 1 + \frac{9.6}{c^2_0\,l^2} = 1.213$; $\quad B_1 = 1 + \frac{9.6}{c^2_{01}\,l^2_1} = 2.182$;

$D_{+t} = 1 + N_s + N_c + N_t = 1.227$; $\quad D_{-t} = 1 + N_s + N_c - N_t = 1.190$.

53. H-Formulas.—Maximum H occurs when all three spans are fully loaded and when the temperature is at its lowest. This is Case IX in Table 1, from which H (max) = 936 (1 + 2 × 0.0372 + 0.0795) = 1,080 kips. The deflection theory, by comparison, yields 1,079 kips. By similar use of Table 1, the force H, in kips, for different loading conditions is, as follows:

Case	Horizontal tension, H, in kips
I	$H_{I} = 907 \left(\sin^2 \frac{k\,\pi}{2\,l} - 0.0795 \right)$
II	$H_{II} = 936 \left(\cos^2 \frac{k\,\pi}{2\,l} + 0.1539 \right)$
III	$H_{III} = 907 \left(\cos \frac{k\,\pi}{l} - 0.0795 \right)$
IV	$H_{IV} = 936 \left(1 - \cos \frac{k\,\pi}{l} + 0.1539 \right)$
V	$H_{V} = -38$
VI	$H_{VI} = 1{,}045$
VII	$H_{VII} = 907 \left(0.0372 \cos^2 \frac{k\,\pi}{2\,l_1} - 0.0795 \right)$
VIII	$H_{VIII} = 936 \left(0.0372 \sin^2 \frac{k\,\pi}{2\,l_1} + 1.1167 \right)$

Fig. 8 shows the curves of H_{I}, H_{II}, H_{III}, and H_{IV} as functions of k/l.

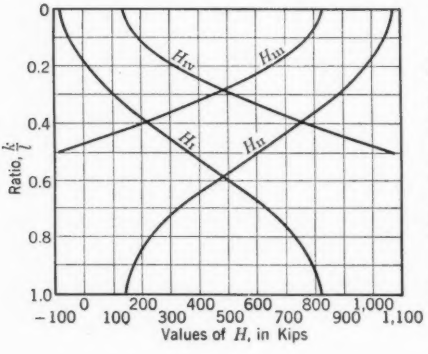

FIG. 8

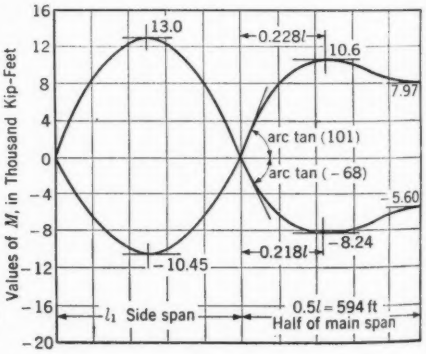

FIG. 9

54. Maximum Deflections.—Case III, Table 1, defines the maximum deflection at the center of the main span. For this case: $k = 0$; $H_{III} = 835$; $Q = \frac{835}{1{,}113} = 0.75$; and $c^2_f\, l^2 = 45 \left(1 + \frac{835}{3{,}940} \right) = 54.6$. By Eq. 64, $\eta_c = \frac{5}{384} \times \frac{0.75 \times 1{,}188.33^4}{123{,}511{,}000} \times \frac{1 - 0.75}{1 + \frac{45}{9.7}} = 5.98$ ft. This value of η_c compares with 6.10 ft determined by the deflection theory.

Case V, Table 1, defines the maximum deflection at the center of the side spans. Again, $H_V = -38$; $Q = -0.034$; $c^2_1 l^2_1 = 8.1\left[1 + \frac{(-38)}{3{,}940}\right] = 8.1$; and, inserting appropriate values in Eq. 64, $\eta_{c1} = \frac{5}{384} \times \frac{0.750 \times 498.33^4}{120{,}408{,}000} \times \frac{1 - (-0.034)}{1 + \frac{8.1}{9.7}} = 2.84$ ft. This value of η_{c1} checks the value computed by the deflection theory.

55. Maximum Increase of Grade.—Case II, Table 1, defines the maximum slope at the end of the main span. For this case, $k = \frac{l}{2}$; $H = 612$; $Q = 0.559$; and $c^2 l^2 = 52.0$. By Eq. 104, $f(k) = 0.336$. By Eq. 101*b*, $\theta_A = \frac{0.750 \times 1{,}188.33^3}{24 \times 123{,}511{,}000} \times \frac{0.55 - 0.336}{1 + \frac{52.0}{10.5}} = 0.0153$, which checks against 0.0152 by the deflection theory.

For the maximum slope at the tower end of the side span $H = -38$; $Q = -0.034$; and $c^2_1 l^2_1 = 8.1$. By Eq. 105, $\theta_A = \frac{0.750 \times 498.33^3}{24 \times 120{,}408{,}000} \times \frac{1 - (-0.034)}{1 + \frac{8.1}{10.5}} = 0.0191$, as against 0.0194 by the deflection theory.

56. Maximum Positive Moment.—Values of H in the problem of determining the location and magnitude of the maximum moment in the main span are given under Case I, Table 1. With $c_f l = \sqrt{54.6} = 7.4$ and $D_{+t} = 1.227$, entering Fig. 6(*a*), $k_{+m} = 0.395\,l$. Therefore, $H_I = 234$; $Q = 0.21$; and $c\,l = 6.90$. By making appropriate substitutions in Eq. 72, solve for $\tanh(c\,x_{+m}) = 0.9175$, from which $c\,x_{+m} + 1.57$ and $x_{+m} = 0.228\,l$. Finally, Eq. 73 yields: $+M$ (max) = 10,600 ft-kips, compared with 10,500 ft-kips by the deflection theory.

The loading conditions of the maximum positive moment at the center of the main span correspond with Case III, Table 1. For this case, $c_f l = 7.4$ and $D_{+t} = 1.227$; entering Fig. 6(*c*) to determine k: $k_{+c} = 0.332\,l$. Therefore, $H_{III} = 380$; $Q = 0.341$; and $c\,l = 7.03$; and, by Eq. 86*c*, $M_c = 7{,}970$ ft-kips, as compared with 7,960 ft-kips by the deflection theory.

Finally, Case V, Table 1, represents the conditions for maximum positive moment in the center of the side span. Referring to section 54, $H_V = -38$; $Q = -0.034$; and $c_1 l_1 = 2.83$. Proper insertion of values in Eq. 91 yields: $M_c = 13{,}000$ ft-kips, as compared with 12,970 ft-kips by the deflection theory.

57. Maximum Negative Moment.—Similar to section 56, the location and magnitude of the maximum negative moment of the main span are represented by Case II, Table 1. With $c_n l = \sqrt{46.7} = 6.84$ and $D_{-t} = 1.19$, Fig. 6(*a*) yields $k_{-m} = 0.396\,l$. Therefore, $H = 760$; $Q = 0.682$; and $c\,l = 7.34$. By Eq. 81 $\tanh(c\,x_{-m}) = 0.9214$; $c\,x_{-m} = 1.6$; and $x_{-m} = 0.218\,l$. Then, by Eq. 82, the maximum negative moment is $-8{,}240$ ft-kips ($-8{,}180$ ft-kips by the deflection theory).

The loading condition of the maximum negative moment at the center of the main span corresponds with Case IV, Table 1. With $c_n l = 6.84$ and $D_{-t} = 1.19$, Fig. 6(*c*) yields $k_{-c} = 0.331 l$. Therefore, $H_{IV} = 610$; $Q = 0.548$; and $c l = 7.21$. With these values in Eq. 88*a*, $M_c = -5{,}600$ ft-kips ($-5{,}580$ ft-kips by the deflection theory).

For the center of the side span (Case VI, Table 1), $H_{VI} = 1{,}045$; $Q = 0.938$; $c_1 l_1 = 3.2$; and, by Eq. 93, $M_c = -10{,}450$ ft-kips ($-10{,}190$ ft-kips by the deflection theory).

58. Maximum Positive Shear.—At the end of the main span, the condition for maximum positive shear is defined by Case I, Table 1, with $c_f l = 7.4$ and $D_{+t} = 1.227$; and Fig. 6(*b*) yields $k_{+v} = 0.375 l$. Therefore, $H_I = 86$; $Q = 0.077$; $c l = 6.78$; and, by substitution in Eq. 77, $V_A = 101$ kips, which checks the deflection theory.

At the center of the main span (Case I, Table 1), $k = 0.5 l$; $H_I = 381$; $c l = 7.03$; and, by Eq. 79*a*, the maximum positive shear, V_c, is 60 kips, which again agrees with the deflection theory.

At the end of the side spans (Case VII, Table 1), $k = 0$; $H_{VII} = -38$; $Q = -0.034$; $c_1 l_1 = 2.83$; and, by substitution in Eq. 98, the maximum positive shear V is 122 kips (121 kips by the deflection theory).

At the center of the side spans (Case VII, Table 1), $k = 0.5 l$; $H = -55$; $c_1 l_1 = 2.83$; and, by Eq. 97, the maximum positive shear V is 40 kips, which agrees with the deflection theory.

59. Maximum Negative Shear.—At the end of the main span the condition for maximum negative shear V is defined by Case II, Table 1, in which, with $c_n l = 6.84$, and $D_{-t} = 1.19$, Fig. 6(*b*) yields $k_{-v} = 0.279 l$. Therefore, $H_{II} = 912$; $Q = 0.819$; $c l = 7.45$; and, by substitutions in Eq. 85*a*, $V = -83$ kips, which is a check on the deflection theory.

At the center of the main span (Case II, Table 1), $k = 0.5 l$; $H_{II} = 612$; $c l = 7.21$; and, in Eq. 79*a*, $V = -59$ kips, which again checks the deflection theory.

At the end of the side span (see Case VIII, Table 1), $k = 0$; $H_{VIII} = 1{,}045$; $Q = 0.938$; $c_1 l_1 = 3.2$; and, by Eq. 100*c*, the maximum negative shear V is -101 (also -101 by the deflection theory).

Finally, for maximum negative shear at the center of a side span (Case VIII, Table 1), $k = 0.5 l$; $H_{VIII} = 1{,}065$; $c_1 l_1 = 3.21$; and, by Eq. 100*a*, $V = -39$ kips (deflection theory -38 kips).

60. Curves of Maximum Moment.—As explained in Part III, section 46, a fairly accurate curve of maximum moment for the main span of a suspension bridge can be drawn free hand between the five points and five tangents obtained by the foregoing computations. The curves of maximum moment for the side spans (see Fig. 9) are hyperbolic cosine curves which are maximum at the center and zero at both ends.

61. Acknowledgments.—The writer is indebted to C. H. Tsien (professor of mechanical engineering, National University of Chekiang, China) for many of his helpful and valuable suggestions during the course of this study.

In view of the extreme scarcity of technical literature in China during World War II, the writer counted himself doubly fortunate in having available the work of Mr. Steinman,[11] as a guide in the preparation of this paper.

AMERICAN SOCIETY OF CIVIL ENGINEERS

Founded November 5, 1852

PAPERS

FLEXURAL CONSTANTS OF HAUNCHED BEAMS BY AREA COMPUTATION

By Fang-Yin Tsai,[1] M. ASCE

Synopsis

A simple and accurate method for computing the flexural constants (shape and load constants) of haunched beams is presented in this paper. For a haunched beam considered as simply supported, the various end "angle changes" are used as the flexural constants, whose values are computed from the various "momental" (moment of area) diagrams of the absolute or relative reciprocal I-diagram, all about one end of the beam. The method differs from existing methods mainly in the following two respects: (1) The various angle changes are computed from the reciprocal I-diagram instead of from the M/I-diagram as in the usual moment-area method for computing beam deflections; and (2) the values of the various moments of the reciprocal I-diagram are computed from the areas of its respective momental diagrams, obtained one from another, simply by multiplying the ordinates of the preceding diagram by their respective moment arms, instead of summing up, always inaccurately, the moments of its many elementary areas of triangular, trapezoidal, or even rectangular shape, as in the usual methods.

The advantages of the method over existing methods are obvious, because, for the various common types of loading, the relations between the angle changes and the momental areas of the reciprocal I-diagram may be expressed by comparatively simple exact formulas, and the area of any diagram, no matter how irregular in character, may be computed with satisfactory accuracy by simple methods.

For those who prefer it, a simple graphical method of constructing the various momental diagrams from the reciprocal I-diagram is presented. Also presented are five theorems of momental areas for further simplifying the

Note.—Written comments are invited for immediate publication; to insure publication the last discussion should be submitted by **February 1, 1949.**

[1] Prof. of Structural Eng. and formerly Dean of College of Eng., National Chung Cheng Univ., Nanchang, Kiangsi, China; Prof. of Structural Eng., The Kiangsi Provincial Polytechnic Inst., Nanchang, Kiangsi, China.

computations of the method. Three typical numerical examples illustrate the application of the method to the computation of the various angle changes, and also the conversion of the angle changes into the various constants used in the method of moment distribution introduced by Hardy Cross, Hon. M. ASCE.

Introduction

Analysis or design of continuous frames having haunched beams by any method necessitates the use of certain flexural constants of the beams. For haunched beams of several common types, there are available many comprehensive tables and charts showing these flexural constants variously expressed, but for haunched beams of uncommon types the predetermination of their flexural constants is always imperative. As the exact determination of such flexural constants by direct integration is usually difficult if not impossible, approximation by either numerical or graphical summation is always necessary. Existing methods for such approximation, under whatever disguise, fall mainly into the categories: (*a*) Replacement of the actual M/I-diagram or the $1/I$-diagram by a number of trapezoidal or triangular elementary areas as represented by the method[2] of G. E. Large and Clyde Morris, Members, ASCE; and (*b*) substitution for the actual reciprocal I-curve of one or two arbitrary curves through only a few points as represented by Walter H. Weiskopf and John W. Pickworth,[3] Members, ASCE. The first method is equivalent to approximating the area under any curve by the so-called "trapezoidal rule," the accuracy of which can scarcely be judged satisfactory unless a fairly large number of segments is used. The second method can scarcely be considered simple, since fitting of the substitute reciprocal I-curve usually requires a few trials. Its accuracy is also questionable, inasmuch as the substitute curve rarely fits the actual one exactly, especially when the actual reciprocal I-curve is irregular or changes direction abruptly.

The object of this paper is to present a simple and accurate method for computing the flexural constants of haunched beams, with all the aforementioned objections of existing methods removed. In this method, all the flexural constants are expressed first in terms of the moments (first, second, third, and fourth as any case requires), about one end of the beam, of the I_o/I-diagram which may be called the "relative reciprocal" I-diagram. In this concept I is the moment of inertia of the cross section at any section of a beam, and I_o is some arbitrary value of I used as a standard in the computation, for which the maximum, the minimum, or some other value may be employed according to the user's preference. The use of the $1/I$-diagram suffices to serve the purpose as well, but the use of the I_o/I-diagram considerably facilitates the numerical work of computation. Values of these moments are then expressed in terms of the areas of the various momental diagrams obtained by multiplying

[2] "The Moment Distribution Method of Structural Analysis Extended to Lateral Loads and Members of Variable Section," by G. E. Large and Clyde Morris, *Bulletin No. 66*, Ohio State Univ., Columbus, Ohio, 1932, p. 14.

[3] "Tapered Structural Members: An Analytical Treatment," by Walter H. Weiskopf and John W. Pickworth, *Transactions*, ASCE, Vol. 102, 1937, p. 1.

the ordinates of the relative reciprocal I-diagram by the various powers of their respective moment arms. Therefore, determination of the flexural constants of haunched beams is reduced to area computations. The advantages of the method presented herein over existing methods are obvious when it is considered that: (1) The relations between the flexural constants and the areas of the various momental diagrams are theoretically as exact as any principle of applied mechanics; (2) the various momental diagrams can be easily obtained, one after another, from the relative reciprocal I-diagram by simple processes of numerical or graphical multiplication with the integers 1, 2, 3, 4, $\cdots$, n as multipliers; and (3) the computation of the area of any diagram, no matter how irregular its character, is simple and may be easily accomplished with satisfactory accuracy by any simple method such as the planimeter or Simpson's rule.

Notation.—The letter symbols used in this paper are defined where they first appear, in text or in illustrations, and are assembled for convenience of reference in the Appendix.

Definition of Flexural Constants

For a beam having asymmetrical haunches and subjected to any loading, there are five and only five flexural constants of independent character. Determination of these constants must precede analysis or design of the beam as a member in a continuous frame. The values of three of such flexural constants, known as "shape constants," depend only on the shape of beam, whereas those of the remaining two, known as "load constants," depend on both the shape of the beam and the type of loading. If the shape of beam is symmetrical with respect to the center line of its span, the number of shape constants is reduced to two; if the loading is also symmetrical, there is only one load constant. Certain methods of analysis for continuous frames, such as the moment distribution method,[4] necessitate use of four shape constants, of which three are of independent character, the fourth being easily derived when any three are determined.

The shape and load constants of haunched beams may be expressed in various systems to suit any particular method of analysis. Elsewhere,[5] the author has already explained those constants in the various prevailing systems with regard to their characteristics and adaptability to certain methods in conjunction with a comprehensive conversion table showing their equivalents.

Among the various systems of expressing the shape and load constants for haunched beams, that of using the end "angle changes" with the beam considered as simply supported, apparently first introduced by German authors and used by Ernst Suter[6] and A. Strassner[7] in developing their methods of analysis, is perhaps the most fundamental and also the most elegant because the end angle changes: (*a*) Possess a clear and definite physical meaning; (*b*) represent, directly, the predominant deformations of continuous frames, on the

[4] "Analysis of Continuous Frames by Distributing Fixed-End Moments," by Hardy Cross, *Transactions*, ASCE, Vol. 96, 1932, p. 1.

[5] *Ibid.*, Vol. 102, 1937, pp. 41–53.

[6] "Die Methode der Festpunkte," by Ernst Suter, Julius Springer, Berlin, 1932.

[7] "Neuere Methoden zur Statik der Rahmenträgwerke und der elastischen Bogenträger," by A. Strassner, Wilhelm Ernst und Sohn, Berlin, Band I, 1925.

basis of which most of the methods of analysis are developed; (*c*) are computed from the condition of a simply-supported beam, the simplest basic determinate structure, to which continuous structures are usually reduced before proceeding with their analysis; (*d*) always first appear, either explicitly or implicitly, in the computation of the flexural constants in any other system and by any method; and (*e*) give exceedingly simple results in certain methods of analysis, as in the case of the theorem of three moments presented previously by the author.[8] In this paper, therefore, the end angle changes are used as the flexural constants for haunched beams.

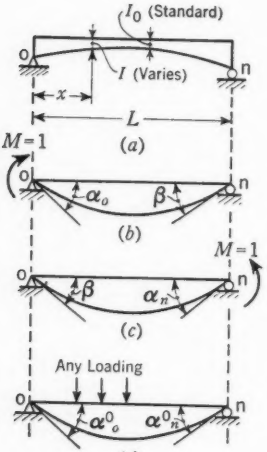

FIG. 1

Considering a haunched beam as simply supported at its two ends (Fig. 1(*a*)) and subjected successively to the loadings shown in Figs. 1(*b*), 1(*c*), and 1(*d*), the following end angle changes occur: α_o or α_n represents the angle change at end o or end n due to a unit moment applied, respectively, at the same end; β represents the angle change at either end due to a unit moment applied at the other end; and α^o_o or α^o_n represents the angle change at the ends o or n, respectively, due to any given loading. It is evident that α_o, α_n, and β are shape constants, whereas α^o_o and α^o_n are load constants. Of course, the flexural constants in terms of those angle changes cannot be used directly in all methods of analysis, but, with their values determined, the constants in any other system needed in any method of analysis may be easily derived according to the previously mentioned conversion table.[5]

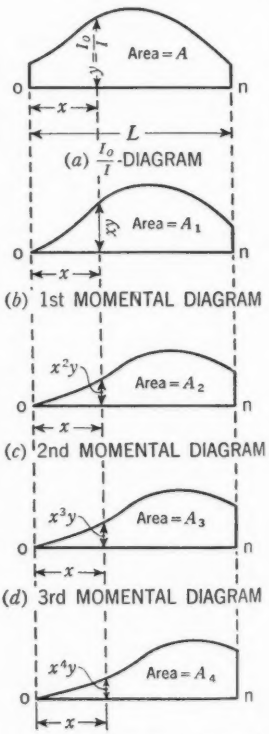

FIG. 2

MOMENTS AND MOMENTAL AREAS OF I_o/I-DIAGRAMS

Fig. 2(*a*) shows the I_o/I-diagram for a haunched beam of length L, the ordinate at any distance x from end o being designated, for the sake of brevity, by y, so that

$$y = \frac{I_o}{I} \qquad (1)$$

[8] *Transactions*, ASCE, Vol. 102, 1937, p. 45.

The area of this relative reciprocal I-diagram is

$$A = \int_o^n y\,dx \ldots\ldots\ldots\ldots\ldots\ldots\ldots\ldots\ldots\ldots (2)$$

and its first moment about point o will be

$$Q = \int_o^n x\,y\,dx \ldots\ldots\ldots\ldots\ldots\ldots\ldots\ldots\ldots\ldots (3)$$

Multiplication of all the ordinates of the relative reciprocal I-diagram by their respective values of x gives the first momental diagram (Q-diagram) about point o (Fig. 2(b)). The area A_1 of this diagram is evidently equal to Q. Thus,

$$A_1 = \int_o^n y\,x\,dx \ldots\ldots\ldots\ldots\ldots\ldots\ldots\ldots\ldots\ldots (4)$$

Similarly, if all the ordinates of the first momental diagram be multiplied, successively and thrice, by their respective values of x, the second, third, and fourth momental diagrams, all about end o, of the relative reciprocal I-diagram will be obtained, one after another, as shown respectively in Figs. 2(c), 2(d), and 2(e). Letting the areas of these momental diagrams be called "momental areas" and designated by A_2, A_3, and A_4, respectively,

$$A_2 = \int_o^n y\,x^2\,dx \ldots\ldots\ldots\ldots\ldots\ldots\ldots\ldots\ldots\ldots (5)$$

$$A_3 = \int_o^n y\,x^3\,dx \ldots\ldots\ldots\ldots\ldots\ldots\ldots\ldots\ldots\ldots (6)$$

and

$$A_4 = \int_o^n y\,x^4\,dx \ldots\ldots\ldots\ldots\ldots\ldots\ldots\ldots\ldots\ldots (7)$$

For beams with symmetrical haunches, the various momental areas about end o are equal, respectively, to those about end n, from which, by the parallel axis theorem, may be obtained

$$L\,A_1 = \tfrac{1}{2}\,L^2\,A \ldots\ldots\ldots\ldots\ldots\ldots\ldots\ldots\ldots\ldots (8)$$

and

$$\frac{A_3}{L} = -\tfrac{1}{2}\,L\,A_1 + \tfrac{3}{2}\,A_2 = -\tfrac{1}{4}\,L^2\,A + \tfrac{3}{2}\,A_2 \ldots\ldots\ldots\ldots\ldots (9)$$

Eqs. 8 and 9 are useful in simplifying the results for symmetrical haunched beams.

If preferred, the various momental diagrams may be obtained from the relative reciprocal I-diagram by simple graphical constructions. For example, in Fig. 3, project the ordinate y at any point m of the relative reciprocal I-diagram to the vertical line through point n. The line joining points a

and o intersects y at point b. It is evident that

$$\frac{b\,m}{x} = \frac{y}{L} \quad \ldots\ldots\ldots\ldots\ldots\ldots\ldots\ldots\ldots\ldots (10a)$$

or

$$b\,m = \frac{x\,y}{L} \quad \ldots\ldots\ldots\ldots\ldots\ldots\ldots\ldots\ldots\ldots (10b)$$

It is obvious that $b\,m$ is the ordinate, divided by the constant L, at point m for the desired first momental diagram about point o. Similarly, projection of $b\,m$ to the vertical line through n gives point f, and the line joining this point with o intersects the ordinate at c. Then,

$$c\,m = \frac{x}{L}\,b\,m = \frac{x^2\,y}{L^2} \ldots (11)$$

which is the ordinate, divided by the constant L^2, at point m, for the desired second momental diagram about point o. Proceeding in the same manner, the ordinates $d\,m$ and $e\,m$, divided, respectively, by the constants L^3 and L^4, at the same point for the desired third and fourth momental diagrams, may be obtained as follows:

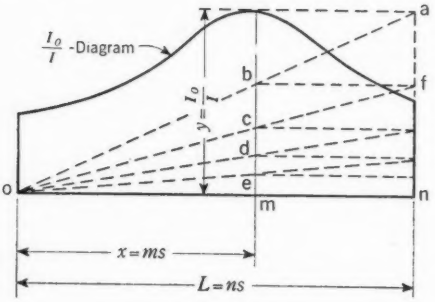

FIG. 3

$$d\,m = \frac{x}{L}\,c\,m = \frac{x^3\,y}{L^3} \quad \ldots\ldots\ldots\ldots\ldots\ldots\ldots\ldots (12)$$

and

$$e\,m = \frac{x}{L}\,d\,m = \frac{x^4\,y}{L^4} \quad \ldots\ldots\ldots\ldots\ldots\ldots\ldots\ldots (13)$$

Hereinafter it will be shown that the three shape constants of a haunched beam, α_o, α_n, and β, may be expressed entirely in terms of the momental diagram areas A, A_1, and A_2, and the two load constants, $\alpha^o{}_o$ and $\alpha^o{}_n$, also may be expressed entirely in terms of the areas. The factors needed for each of the common types of loading are as follows: A, A_1, and A_2 for concentrated loads; A, A_1, A_2, and A_3 for uniform load distributed in any manner along the length of beam; and A_1, A_2, A_3, and A_4 for uniformly varying load. For symmetrical beams or loadings, the items of the areas needed for both shape and load constants may be somewhat modified.

SHAPE CONSTANTS

Referring to Figs. 1(*b*) and 1(*c*) and applying the method of moment area or of virtual work, the three shape constants, α_o, α_n, and β, may be determined

as follows:

$$\alpha_n = \frac{1}{E\,I_o\,L^2}\int_o^n y\,x^2\,dx \quad \ldots\ldots (14)$$

$$\alpha_o = \frac{1}{E\,I_o\,L^2}\int_o^n y\,(L-x)^2\,dx$$

$$= \frac{1}{E\,I_o\,L^2}\left(L^2\int_o^n y\,dx - 2\,L\int_o^n y\,x\,dx + \int_o^n y\,x^2\,dx\right) \quad \ldots (15)$$

$$\beta = \frac{1}{E\,I_o\,L^2}\int_o^n y\,x\,(L-x)\,dx = \frac{1}{E\,I_o\,L^2}\left(L\int_o^n y\,x\,dx - \int_o^n y\,x^2\,dx\right) \quad \ldots (16)$$

in which E is the modulus of elasticity of the beam material. Eqs. 14, 15, and 16 may be rewritten in terms of the various momental areas as follows:

$$E\,I_o\,\alpha_n = \frac{1}{L^2}\,A_2 \quad \ldots\ldots (17)$$

$$E\,I_o\,\alpha_o = A - \frac{2}{L}\,A_1 + \frac{1}{L^2}\,A_2 \quad \ldots\ldots (18)$$

and

$$E\,I_o\,\beta = \frac{1}{L}\,A_1 - \frac{1}{L^2}\,A_2 \quad \ldots\ldots (19)$$

For beams with symmetrical haunches, it is obvious, from the relations in Eqs. 8 and 9, that

$$E\,I_o\,\alpha_n = E\,I_o\,\alpha_o = E\,I_o\,\alpha = \frac{1}{L^2}\,A_2 \quad \ldots\ldots (20)$$

and

$$E\,I_o\,\beta = \tfrac{1}{2}\,A - \frac{1}{L^2}\,A_2 \quad \ldots\ldots (21)$$

For beams with constant I ($y = 1$), it is evident from Eqs. 14 and 16 that

$$E\,I\,\alpha = \frac{L}{3} \quad \ldots\ldots (22)$$

and

$$E\,I\,\beta = \frac{L}{6} \quad \ldots\ldots (23)$$

Load Constants

The load constants, $\alpha^o{}_o$ and $\alpha^o{}_n$, for a haunched beam subjected to any of the common types of loading may be expressed entirely in terms of the various momental areas in the same manner as are their shape constants. They will be determined by the two general equations—

$$\alpha^o{}_o + \alpha^o{}_n = \int_o^n \frac{M}{E\,I}\,dx \quad \ldots\ldots (24)$$

and

$$\alpha^{o}_{n} = \frac{1}{L}\int_{o}^{n} \frac{M\,x}{E\,I}\,dx \ldots\ldots\ldots\ldots\ldots\ldots\ldots\ldots (25)$$

—based on the principle of moment area or virtual work.

For the sake of brevity, Eqs. 24 and 25 may be rewritten

$$E\,I_o\,(\alpha^{o}_{o} + \alpha^{o}_{n}) = \int_{o}^{n} M\,y\,dx \ldots\ldots\ldots\ldots\ldots\ldots\ldots\ldots (26)$$

and

$$E\,I_o\,\alpha^{o}_{n} = \frac{1}{L}\int_{o}^{n} M\,y\,x\,dx \ldots\ldots\ldots\ldots\ldots\ldots\ldots\ldots (27)$$

The difference between Eqs. 26 and 27 obviously will give the value of α^{o}_{o}. Formulas for load constants will be deduced for six common cases of basic loading. Those for several other cases of loading can be easily derived therefrom by superposition or subtraction.

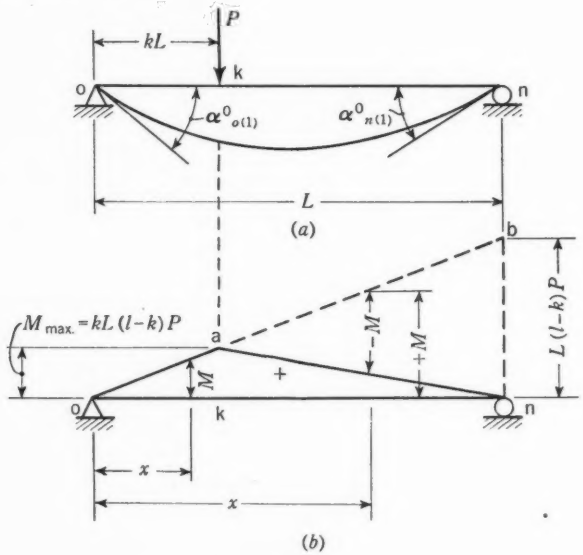

FIG. 4

Case 1. Concentrated Load at Any Point.—Fig. 4(*a*) shows a simply-supported haunched beam subjected to a concentrated load P at any point k at a distance $k\,L$ from end o. As shown in Fig. 4(*b*), the bending moment diagram is the triangle oan, which may be considered as the sum of the positive triangle obn and the negative triangle abn. It may be easily shown that the positive bending moment M, at any section at a distance x from the left end, for the triangle obn covering the length on, will be

$$M = x\,(1 - k)\,P \ldots\ldots\ldots\ldots\ldots\ldots\ldots\ldots (28)$$

The negative bending moment M' for the triangle abn covering the length kn will be,

$$-M' = -(x - k\,L)\,P \ldots\ldots\ldots\ldots\ldots\ldots (29)$$

Substituting the values of M and $-M'$ from Eqs. 28 and 29 in Eqs. 26 and 27, and designating, for the sake of clearness, the two load constants in this case of loading $\alpha^o{}_{o(1)}$ and $\alpha^o{}_{n(1)}$,

$$E\,I_o\,(\alpha^o{}_{o(1)} + \alpha^o{}_{n(1)}) = \left[(1-k) \int_o^n y\,x\,dx - \int_k^n y\,x\,dx + k\,L \int_k^n y\,dx \right] P = [k\,L\,A_{(kn)} - A_{1(kn)} + (1-k)\,A_1]\,P \ldots (30)$$

and

$$E\,I_o\,\alpha^o{}_{n(1)} = \frac{1}{L}\left[\int_o^n y\,x^2\,dx - k \int_o^n y\,x^2\,dx - \int_k^n y\,x^2\,dx + k\,L \int_k^n y\,x\,dx \right] P \ldots (31)$$

Therefore, noting that

$$A_2 - A_2\,(kn) = A_{2(ok)} \ldots\ldots\ldots\ldots\ldots\ldots (32)$$

and, simplifying,

$$E\,I_o\,\alpha^o{}_{n(1)} = \left[k\,A_{1(kn)} + \frac{1}{L}\,A_{2(ok)} - \frac{k}{L}\,A_2 \right] P \ldots\ldots\ldots (33a)$$

and

$$E\,I_o\,\alpha^o{}_{o(1)} = \left[k\,L\,A_{1(kn)} + (1+k)\,A_{1(ok)} - 2\,k\,A_1 - \frac{1}{L}\,A_{2(ok)} + \frac{k}{L}\,A_2 \right] P \ldots (33b)$$

In Eqs. 33, the various areas with the subscript (ok) indicate the areas to be computed from their respective diagrams between the ordinates at points o and k only. A similar situation exists for areas with the subscript (kn). Eqs. 33 may be used conveniently for computing the influence diagrams for the load constants, since any change in the position of the single concentrated load affects only the value of k and the position of point k in those equations.

For a symmetrical haunched beam with a concentrated load at its center,

$$\alpha^o{}_{o(1)} = \alpha^o{}_{n(1)} = \alpha^o{}_{(1)} \ldots\ldots\ldots\ldots\ldots\ldots (34)$$

Noting that $k = 0.5$; $A_{(kn)} = 0.5\,A$; $A_{1(ok)} = A_1 - A_{1(kn)}$ and the relation in Eq. 8, it is obvious from Eq. 30 that

$$E\,I_o\,\alpha^o{}_{(1)} = \tfrac{1}{2}\,A_{1(ok)}\,P \ldots\ldots\ldots\ldots\ldots\ldots (35)$$

in which $A_{1(ok)}$ is the area of the first momental diagram between points o and k.

Case 2. Uniform Load Covering Whole Length of Beam.—The two load constants for this case of loading will be designated $\alpha^o{}_{n(2)}$ and $\alpha^o{}_{o(2)}$. The

bending moment at any section at a distance m from end o is

$$M = \tfrac{1}{2}(L\,x - x^2)\,w \quad \ldots\ldots (36)$$

Substituting Eq. 36 in Eqs. 26 and 27,

$$E\,I_o\,[\alpha^o{}_{o(2)} + \alpha^o{}_{n(2)}] = \frac{1}{2}\left(L \int_o^n y\,x\,dx - \int_o^n y\,x^2\,dx \right) w = \tfrac{1}{2}(L\,A_1 - A_2)w \ldots (37)$$

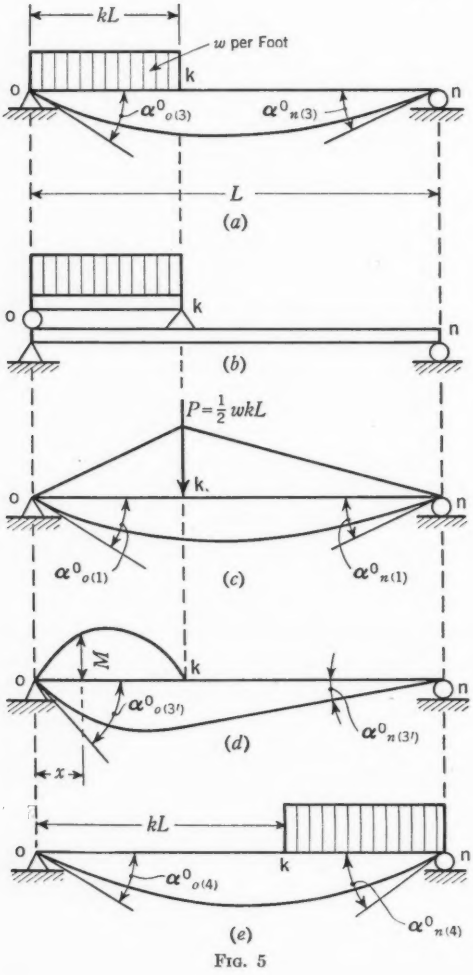

FIG. 5

and

$$E\,I_o\,\alpha^o{}_{n(2)} = \frac{1}{2}\left(\int_o^n y\,x^2\,dx - \frac{1}{L}\int_o^n y\,x^3\,dx \right) w \ldots (38)$$

Therefore,

$$E\,I_o\,\alpha^o{}_{n(2)} = \frac{1}{2}\left(A_2 - \frac{1}{L}A_3 \right) w \ldots (39)$$

and

$$E\,I_o\,\alpha^o{}_{o(2)} = \left[\frac{1}{2}\left(L\,A_1 + \frac{1}{L}A_3 \right) - A_2 \right] w \ldots (40)$$

For a symmetrical haunched beam,

$$\alpha^o{}_{o(2)} = \alpha^o{}_{n(2)} = \alpha^o{}_{(2)} \ldots (41)$$

From Eqs. 37 and 38,

$$E\,I_o\,\alpha^o{}_{(2)} = \tfrac{1}{4}(\tfrac{1}{2}L^2\,A - A_2)w \ldots (42)$$

Comparing Eq. 42 with Eq. 21,

$$\alpha^o{}_{(2)} = \tfrac{1}{4}\,\beta\,w\,L^2 \ldots . (43)$$

Case 3. Uniform Load Covering Partial Length at Left End. —The loading is shown in Fig. 5(*a*). If the load is considered to be applied to the beam on through the stringer ok as shown in Fig. 5(*b*), the bending moment diagram is then resolved into two component parts: A triangle with length on as base, due to a concentrated load of $\frac{1}{2}\,w\,k\,L$ at point k as shown in Fig. 5(*c*); and a

parabola with length ok as base, due to a uniform load on the stringer ok as shown in Fig. 5(*d*). Evidently, the sum of the load constants for the two component parts at either end will be equal to that for the given loading at the same end. The load constants for Fig. 5(*c*) will be the same as those for case 1 when $P = \frac{1}{2} w k L$. Those for Fig. 5(*d*), designated by $\alpha^o{}_{n(3')}$ and $\alpha^o{}_{o(3')}$, may be computed as before by Eqs. 26 and 27:

$$M = (\tfrac{1}{2} k L x - \tfrac{1}{2} x^2) w \ldots\ldots\ldots\ldots\ldots\ldots (44)$$

$$E I_o [\alpha^o{}_{n(3')} + \alpha^o{}_{o(3')}] = \left(\tfrac{1}{2} k L \int_o^k y\, x\, dx - \frac{1}{2} \int_o^k y\, x^2\, dx \right) w$$

$$= \frac{w}{2} [k L A_{1(ok)} - A_{2(ok)}] \ldots (45)$$

$$E I_o \alpha^o{}_{n(3')} = \left(\frac{k}{2} \int_o^k y\, x^2\, dx - \frac{1}{2L} \int_o^k y\, x^3\, dx \right) w$$

$$= \frac{1}{2} \left[k A_{2(ok)} - \frac{1}{L} A_{3(ok)} \right] w \ldots (46)$$

$$E I_o \alpha^o{}_{o(3')} = \frac{1}{2} \left[k L A_{1(ok)} - (1 + k) A_{2(ok)} + \frac{1}{L} A_{3(ok)} \right] w \ldots\ldots (47)$$

Adding Eqs. 46 and 47 to the results obtained (with $P = \frac{1}{2} w k L$) from Eqs. 32 and 33, respectively, and simplifying,

$$E I_o \alpha^o{}_{n(3)} = \frac{1}{2} \left[k^2 L A_{1(kn)} + 2 k A_{2(ok)} - k^2 A_2 - \frac{1}{L} A_{3(ok)} \right] w \ldots . (48)$$

and

$$E I_o \alpha^o{}_{o(3)} = \frac{1}{2} \left[k^2 L^2 A_{(kn)} + (2 + k) k L A_{1(ok)} - 2 k^2 L A_1 \right.$$

$$\left. - (1 + 2 k) A_{2(ok)} + k^2 A_2 + \frac{1}{L} A_{3(ok)} \right] w \ldots (49)$$

When $k = 1$, $A_{(kn)} = A_{1(kn)} = 0$, and all subscripts (ok) are deleted, then Eqs. 48 and 49 become, respectively, identical with Eqs. 39 and 40, as they should be.

Case 4. Uniform Load Covering Partial Length at Right End.—The loading is shown in Fig. 5(*e*), in which the left end of the loading is at a distance $k L$ from the left end of the beam. The two load constants, $\alpha^o{}_{n(4)}$ and $\alpha^o{}_{o(4)}$, may be obtained by taking the differences between those in cases 2 and 3.

$$\alpha^o{}_{(4)} = \alpha^o{}_{(2)} - \alpha^o{}_{(3)} \ldots\ldots\ldots\ldots\ldots\ldots (50)$$

Substituting the proper load constants from cases 2 and 3 in Eq. 50 and simplifying,

$$E I_o \alpha^o{}_{n(4)} = \frac{1}{2} \left[- k^2 L A_{1(kn)} + (1 + k^2) A_2 - 2 k A_{2(ok)} - \frac{I}{L} A_{3(kn)} \right] w \ldots (51)$$

$$E I_o \alpha^o{}_{o(4)} = \frac{1}{2} \left[- k^2 L^2 A_{(kn)} - (2 + k) k L A_{1(ok)} \right.$$

$$\left. + (1 + 2 k^2) L A_1 + (1 + 2 k) A_{2(ok)} - (2 + k^2) A_2 + \frac{I}{L} A_{3(kn)} \right] w \ldots (52)$$

When $k = 0$, Eqs. 51 and 52 will be reduced, respectively, to Eqs. 39 and 40, as they should be.

Case 5. Triangular Load with Maximum Intensity at Right End.—The bending moment at any section a distance x from the left end is

$$M = \frac{1}{6}\left(L\,x - \frac{1}{L}\,x^3 \right) w \ldots\ldots\ldots\ldots\ldots\ldots (53)$$

Letting the load constants for this loading be designated by $\alpha^o{}_{n(5)}$ and $\alpha^o{}_{o(5)}$, and proceeding as before by Eqs. 26 and 27,

$$E\,I_o\,[\alpha^o{}_{o(5)} + \alpha^o{}_{n(5)}] = \frac{1}{6}\left(L\,A_1 - \frac{1}{L}\,A_3 \right) w \ldots\ldots\ldots\ldots (54a)$$

$$E\,I_o\,\alpha^o{}_{n(5)} = \frac{1}{6}\left(A_2 - \frac{1}{L^2}\,A_4 \right) w \ldots\ldots\ldots\ldots\ldots (54b)$$

and

$$E\,I_o\,\alpha^o{}_{o(5)} = \frac{1}{6}\left(L\,A_1 - A_2 - \frac{1}{L}\,A_3 + \frac{1}{L^2}\,A_4 \right) w \ldots\ldots\ldots (55)$$

For a symmetrical haunched beam, Eq. 55 may be simplified by the relation of Eq. 9 so that

$$E\,I_o\,\alpha^o{}_{o(5')} = \frac{1}{6}\left(\frac{3}{4}\,L^2\,A - \frac{5}{2}\,A_2 + \frac{1}{L^2}\,A_4 \right) w \ldots\ldots\ldots\ldots (56)$$

Eq. 54*b* admits no simplification, hence

$$\alpha^o{}_{n(5')} = \alpha^o{}_{n(5)} \ldots\ldots\ldots\ldots\ldots\ldots\ldots\ldots (57)$$

Case 6. Triangular Load with Maximum Intensity at the Left End.—The bending moment at any section a distance x from the left end is

$$M = \frac{1}{6}\left(2\,L\,x - 3\,x^2 + \frac{1}{L}\,x^3 \right) w \ldots\ldots\ldots\ldots\ldots (58)$$

Letting the load constants for this loading be designated by $\alpha^o{}_{n(6)}$ and $\alpha^o{}_{o(6)}$ and proceeding as before by Eqs. 26 and 27,

$$E\,I_o\,[\alpha^o{}_{o(6)} + \alpha^o{}_{n(6)}] = \frac{1}{6}\left(2\,L\,A_1 - 3\,A_2 + \frac{1}{L}\,A_3 \right) w \ldots\ldots\ldots (59)$$

$$E\,I_o\,\alpha^o{}_{n(6)} = \frac{1}{6}\left(2\,A_2 - \frac{3}{L}\,A_3 + \frac{1}{L^2}\,A_4 \right) w \ldots\ldots\ldots\ldots (60)$$

and

$$E\,I_o\,\alpha^o{}_{o(6)} = \frac{1}{6}\left(2\,L\,A_1 - 5\,A_2 + \frac{4}{L}\,A_3 - \frac{1}{L^2}\,A_4 \right) w \ldots\ldots\ldots (61)$$

For a symmetrical haunched beam, Eqs. 60 and 61 may be simplified by the relations of Eqs. 8 and 9 so that

$$E\,I_o\,\alpha^o{}_{n(6')} = \frac{1}{6}\left(\frac{3}{4}\,L^2\,A - \frac{5}{2}\,A_2 + \frac{1}{L^2}\,A_4 \right) w \ldots\ldots\ldots\ldots (62)$$

and

$$E\,I_o\,\alpha^o{}_{o(6')} = \frac{1}{6}\left(A_2 - \frac{1}{L^2}\,A_4\right)w \quad \ldots\ldots (63)$$

It may be noted that the following relations are always valid and may serve as checks:

$$\alpha^o{}_{n(5)} + \alpha^o{}_{n(6)} = \alpha^o{}_{n(2)} \quad \ldots\ldots (64)$$

$$\alpha^o{}_{o(5)} + \alpha^o{}_{o(6)} = \alpha^o{}_{o(2)} \quad \ldots\ldots (65)$$

$$\alpha^o{}_{n(5')} = \alpha^o{}_{o(6')} \quad \ldots\ldots (66)$$

$$\alpha^o{}_{o(5')} = \alpha^o{}_{n(6')} \quad \ldots\ldots (67)$$

and

$$\alpha^o{}_{n(5')} + \alpha^o{}_{o(5')} = \alpha^o{}_{n(6')} + \alpha^o{}_{o(6')} = \alpha^o{}_{(2)} \quad \ldots\ldots (68)$$

The foregoing six cases cover the common types of loading usually encountered in practice. For convenience of reference and application, the

TABLE 1.—SUMMARY OF FORMULAS FOR LOAD CONSTANTS

Case	Loading	Beam	Load Constants	
			$E\,I_o\,(\alpha^o{}_o + \alpha^o{}_n)$	$E\,I_o\,\alpha^o{}_n$
(1)	(2)	(3)	(4)	(5)
1	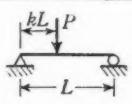	Asymmetrical	$[k\,L\,A_{(kn)} - A_{1(kn)} + (1-k)\,A_1]\,P$	$\left[k\,A_{1(kn)} + \frac{1}{L}\,A_{2(ok)} - \frac{k}{L}\,A_2\right]P$
		Symmetrical	Also $k = \frac{1}{2}$: $P\,A_{1(ok)}$	$\frac{1}{2}\,P\,A_{1(ok)}$
2	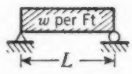	Asymmetrical	$\frac{1}{2}\,[L\,A_1 - A_2]\,w$	$\frac{1}{2}\left[A_2 - \frac{1}{L}\,A_3\right]w$
		Symmetrical	$\frac{1}{2}\,[\frac{1}{2}\,L^2\,A - A_2]\,w$ or $\frac{1}{2}\,E\,I_o\,\beta\,w\,L^2$	$\frac{1}{4}\,[\frac{1}{2}\,L^2\,A - A_2]\,w$ or $\frac{1}{4}\,E\,I_o\,\beta\,w\,L^2$
3	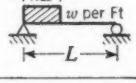	Asymmetrical	$\frac{1}{2}\,[k^2\,L^2\,A_{(kn)} + 2\,k\,L\,A_{1(ok)} - k^2\,L\,A_1 - A_{2(ok)}]\,w$	$\frac{1}{2}\left[k^2\,L\,A_{1(kn)} + 2\,k\,A_{2(ok)} - k^2\,A_2 - \frac{1}{L}\,A_{3(ok)}\right]w$
4	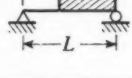	Asymmetrical	$\frac{1}{2}\,[-k^2\,L^2\,A_{(kn)} - 2\,k\,L\,A_{1(ok)} + (1+k^2)\,L\,A_1 - A_{2(kn)}]\,w$	$\frac{1}{2}\left[-k^2\,L\,A_{1(kn)} - 2\,k\,A_{2(ok)} + (1+k^2)\,A_2 - \frac{1}{L}\,A_{3(kn)}\right]w$
5	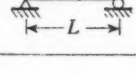	Asymmetrical	$\frac{1}{6}\left[L\,A_1 - \frac{1}{L}\,A_3\right]w$	$\frac{1}{6}\left[A_2 - \frac{1}{L^2}\,A_4\right]w$
		Symmetrical	$\frac{1}{4}\,[\frac{1}{2}\,L^2\,A - A_2]\,w$	
6	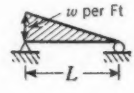	Asymmetrical	$\frac{1}{6}\left[2\,L\,A_1 - 3\,A_2 + \frac{1}{L}\,A_3\right]w$	$\frac{1}{6}\left[A_2 - \frac{3}{L}\,A_3 + \frac{1}{L^2}\,A_4\right]w$
		Symmetrical	$\frac{1}{8}\,[\frac{1}{2}\,L^2\,A - A_2]\,w$	$\frac{1}{6}\left[\frac{3}{4}\,L^2\,A - \frac{5}{2}\,A_2 + \frac{1}{L^2}\,A_4\right]w$

formulas for the load constants for these six cases of loading are tabulated in Table 1, in which Col. 4 gives the formulas for the sum $E\,I_o\,(\alpha^o_o + \alpha^o_n)$ instead of that for $E\,I_o\,\alpha^o_o$ alone, because the former are much shorter and therefore more convenient to apply than the latter. From Table 1 formulas for load constants for several other types of loading not given may be derived. Thus, for a uniform load covering partial length near the middle of a beam (Fig. 6(*a*)), the load constants may be considered as equal to the difference between those for the loadings shown in Figs. 6(*b*) and 6(*c*), and, therefore, may be computed by the formulas given for case 3. For the loading shown in Figs. 6(*d*) and 6(*e*), load constants may be obtained by adding those for case 2 to those for cases 5 and 6, respectively.

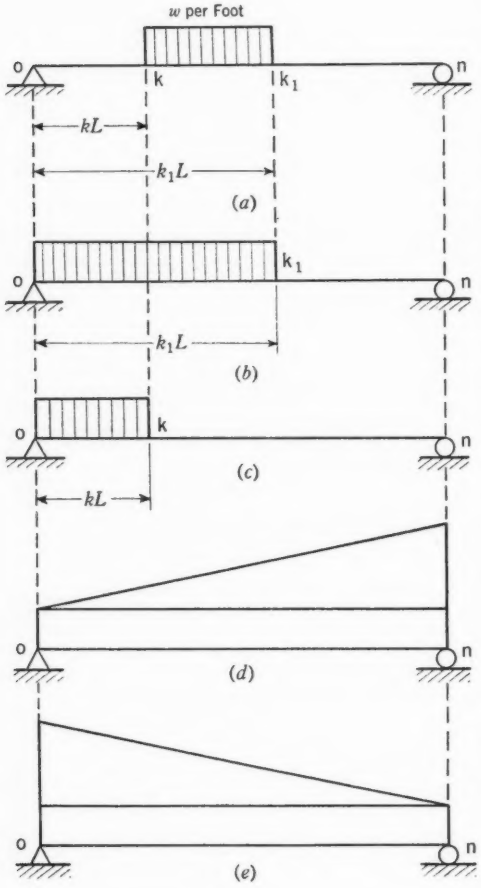

FIG. 6

For nonuniform load distributed in any irregular manner, the M/I-diagram or $M\,I_o/I$-diagram must be used. For computing the ordinates of its bending moment diagram, the simplified numerical procedure presented by N. M. Newmark,[9,10,11] M. ASCE, is recommended. As soon as the $M\,I_o/I$-diagram has been obtained, the load constants may be computed by the following equations, which are evident from Eqs. 26 and 27:

$$E\,I_o\,(\alpha^o_o + \alpha^o_n) = A_{(m)} \quad \ldots\ldots (69)$$

$$E\,I_o\,\alpha^o_n = \frac{1}{L}\,A_{1(m)} \quad \ldots\ldots (70)$$

and

$$E\,I_o\,\alpha^o_o = A_{(m)} - \frac{1}{L}\,A_{1(m)} \quad \ldots\ldots (71)$$

in which $A_{(m)}$ is the area of the $M\,I_o/I$-diagram, and $A_{1(m)}$ is the area of its first momental diagram about the left end.

[9] "Numerical Procedure for Computing Deflections, Moments, and Buckling Loads," by N. M. Newmark, *Transactions*, ASCE, Vol. 108, 1943, p. 1161.

[10] *Ibid.*, p. 1169, Fig. 7.

[11] *Ibid.*, p. 1171, Fig. 10.

Area Computation

The total or partial areas of the various momental diagrams may be easily computed with satisfactory accuracy by Simpson's rule:

$$A = \tfrac{1}{3}\, s\, [(y_o + y_n) + 4\,(y_1 + y_3 + \cdots + y_{n-i}) + 2\,(y_2 + y_4 + \cdots + y_{n-2})] \ldots (72)$$

In applying Simpson's rule, the beam length is divided into n number of equal segments of length s. The ordinates of the various momental diagrams at the points of division o, 1, 2, $\cdots$, n are, respectively, $y_o, y_1, y_2, \cdots, y_n$. Simpson's rule is obtained by assuming that the curve connecting three consecutive ordinates is a quadratic parabola, and therefore is applicable only when n is an even number. When n is an odd number, the area between y_o and y_1, designated by A_{o-1}, may be computed separately and the remaining area between y_1 and y_n, designated by A_{1-n}, may be computed by a modification of Simpson's rule—

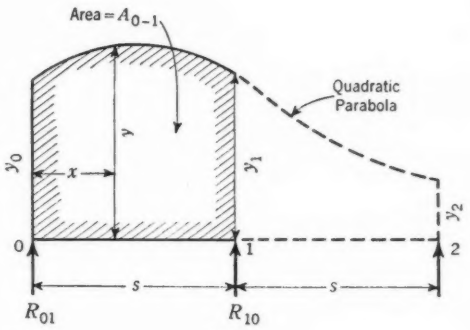

Fig. 7

$$A_{1-n} = \tfrac{1}{3}\, s\, [(y_1 + y_n) + 4\,(y_2 + y_4 + \cdots + y_{n-1}) + 2\,(y_3 + y_5 + \cdots + y_{n-2})] \ldots (73)$$

Fig. 7 shows a quadratic parabola passing the three ordinates y_o, y_1, and y_2. The ordinate at any point will be

$$y = \frac{1}{2}\left(\frac{x}{s} - 1\right)\left(\frac{x}{s} - 2\right) y_0 - \frac{x}{s}\left(\frac{x}{s} - 2\right) y_1 + \frac{x}{2\,s}\left(\frac{x}{s} - 1\right) y_2 \ldots (74)$$

Therefore,

$$A_{o-1} = \int_o^s y\, dx = \frac{s}{3}\left(\frac{5}{4}\, y_o + 2\, y_1 - \tfrac{1}{4}\, y_2\right) \ldots\ldots\ldots\ldots (75)$$

Combining Eqs. 73 and 75 and simplifying, Simpson's rule may be obtained for an odd value of n,

$$A = \frac{s}{3}\left[\frac{5}{4}\, y_o + 3\, y_1 + \frac{15}{4}\, y_2 + y_n + 4\,(y_4 + y_6 + \cdots + y_{n-1}) + 2\,(y_3 + y_5 + \cdots + y_{n-2})\right] \ldots (76)$$

Eq. 76 is not so accurate as Eq. 72, and therefore should not be used unless unavoidable.

Application of Eqs. 72 to 76 is limited to the case where the relative reciprocal I-diagram is a smooth curve without any change throughout the length of

the beam. For the type of haunched beam shown in Fig. 8(*a*), in which the relative reciprocal *I*-diagram has an abrupt change at point k (Fig. 8(*b*)), the diagram should be divided into two sections by the ordinate at point k. The areas of these sections should be computed separately and then added.

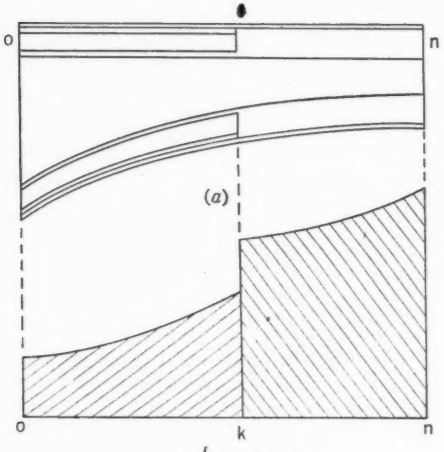

FIG. 8

Let y_m be the ordinate of the relative reciprocal *I*-diagram at any point m which is at a distance $x = m\,s$ from end o. The ordinates of the various momental diagrams A_1, A_2, A_3, and A_4 are, respectively,

$$y'_m = s\,(m\,y_m) \ldots . (77)$$

$$y''_m = s\,(m\,y'_m) = s^2\,(m^2\,y_m) \ldots (78)$$

$$y'''_m = s\,(m\,y''_m) = s^3\,(m^3\,y_m) \ldots (79)$$

and

$$y''''_m = s\,(m\,y'''_m) = s^4\,(m^4\,y_m) \ldots (80)$$

Thus the various momental diagrams may be obtained, one after another, from the relative reciprocal *I*-diagram by multiplying the ordinates of the preceding diagram successively by the integers 0, 1, 2, $\cdots$, n. Of course, the areas computed from these diagrams must be multiplied, respectively, by s, s^2, s^3, and s^4 to obtain their correct values. If the values of y'_m, y''_m, $\cdots$, $y^n{}_m$ in terms of y_m from Eqs. 77 to 80 are substituted in Eq. 72 or Eq. 76, the areas A_2, A_3, $\cdots$, A_n are obtained directly without constructing their diagrams.

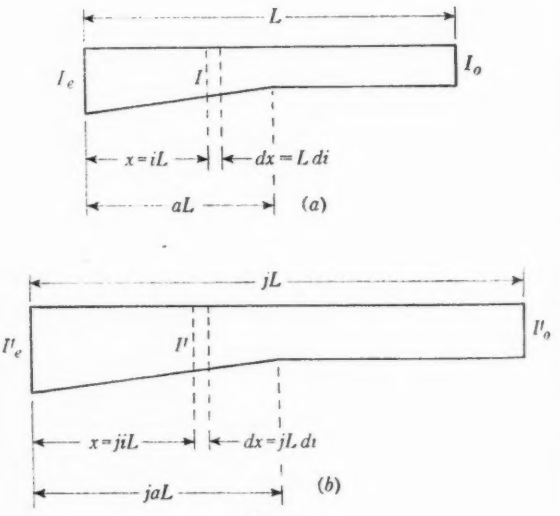

FIG. 9

THEOREMS OF MOMENTAL AREAS

Another distinct advantage of the method is that the computations may be further simplified by application of the theorems of momental areas, which

will reduce to a minimum the work of plotting the various momental diagrams and of computing their areas.

Theorem of Similitude.—When two haunches or haunched beams of the same type (straight, parabolic, or sharply curved) are proportional in length and have the same ratios between their moments of inertia at all the corresponding sections ($I'/I = I'_o/I_o = I'_e/I_e$) as shown in Fig. 9, the areas of their I_o/I-diagrams and their various momental areas about the same end have definite relations of proportionality. Let A, A_1, and A_2 represent elements for the beam shown in Fig. 9(*a*), and let A_j, A_{1j}, and A_{2j} represent elements for the beam shown in Fig. 9(*b*). Also, if $x = i\,L$, and $dx = L\,di$, by Eq. 2,

$$A = \int_0^L \frac{I_o}{I}\,dx = L\int_0^1 y\,di \qquad (81)$$

and

$$A_j = \int_0^{jL} \frac{I'_o}{I'}\,dx = j\,L\int_0^1 y\,di \qquad (82)$$

Therefore,

$$\frac{A_j}{A} = j \qquad (83)$$

Similarly,

$$\frac{A_{1j}}{A_1} = j^2 \qquad (84)$$

$$\frac{A_{2j}}{A_2} = j^3 \qquad (85)$$

$$\frac{A_{3j}}{A_3} = j^4 \qquad (86)$$

and

$$\frac{A_{4j}}{A_4} = j^5 \qquad (87)$$

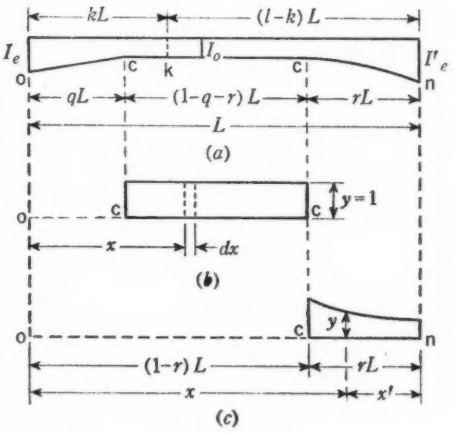

FIG. 10

Theorem of Constant Section.—When a haunched beam contains a section with constant moment of inertia (section cc, Fig. 10(*a*)), the area of the I_o/I-diagram of that section and its various momental areas about the left end, designated by A_c, A_{1c}, A_{2c}, $\cdots$, A_{nc}, may be computed separately without plotting its various momental diagrams. Referring to Fig. 10(*b*),

$$A_c = (1 - q - r)\,L \qquad (88)$$

$$A_{1c} = \int_{qL}^{(1-r)L} x\,dx = \tfrac{1}{2}L^2(1 - q - r)(1 + q - r)$$

$$= \tfrac{1}{2}L\,A_c(1 + q - r) \qquad (89)$$

$$A_{2c} = \int_{qL}^{(1-r)L} x^2\,dx = \tfrac{1}{3}L^3(1 - q - r)\left[(1 - r)^2 + q(1 + q - r)\right]$$

$$= \tfrac{2}{3}q\,L\,A_{1c} + \tfrac{1}{3}(1 - r)^2 L^2 A_c \qquad (90)$$

$$A_{3c} = \int_{qL}^{(1-r)L} x^3\,dx = \tfrac{1}{4}L^4(1-q-r)(1+q-r)[(1-r)^2+q^2]$$
$$= \tfrac{1}{2}L^2 A_{1c}[(1-r)^2+q^2] \quad (91)$$

$$A_{4c} = \int_{qL}^{(1-r)L} x^4\,dx = \tfrac{1}{5}L^5(1-r)(1-q-r)(1+q-r)$$
$$\times[(1-r)^2+q^2] + \tfrac{1}{5}L^5 q^4(1-q-r)$$
$$= \tfrac{4}{5}(1-r)L A_{3c} + \tfrac{1}{5}q^4 L^4 A_c \quad (92)$$

Theorem of Parallel Axes.—When the area of the I_o/I-diagram and its various momental areas of the haunch (or haunched beam) on (Fig. 10(*c*)) about its right end, designated by A'_r, A'_{1r}, A'_{2r}, $\cdots$, A'_{4r}, are known, those of the same haunch (or haunched beam) about the left end, designated by A_r, A_{1r}, A_{2r}, $\cdots$, A_{4r}, may be computed by the following:

$$A_r = A'_r \quad (93)$$

$$A_{1r} = \int_{(1-r)L}^{L} x\,y\,dx = \int_0^{rL}(L-x')\,y\,dx$$
$$= L\int_0^{rL} y\,dx - \int_0^{rL} x'\,y\,dx = L A'_r - A'_{1r} \quad (94)$$

and

$$A_{2r} = \int_{(1-r)L}^{L} x^2\,y\,dx = \int_0^{rL}(L-x')^2\,y\,dx$$
$$= L^2\int_0^{rL} y\,dx - 2L\int_0^{rL} x'\,y\,dx + \int_0^{rL}(x')^2\,y\,dx$$
$$= L^2 A'_r - 2L A'_{1r} + A'_{2r} \quad (95)$$

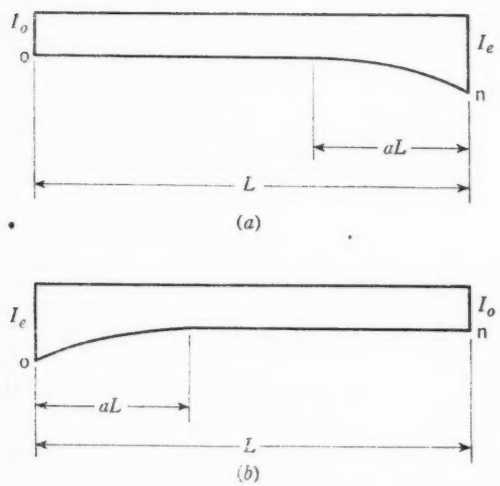

FIG. 11

Similarly,

$$A_{3r} = L^3 A'_r - 3L^2 A'_{1r} + 3L A'_{2r} - A'_{3r} \quad (96)$$

and

$$A_{4r} = L^4 A'_r - 4L^3 A'_{1r} + 6L^2 A'_{2r} - 4L A'_{3r} + A'_{4r} \quad (97)$$

It may be noted that Eqs. 93 to 97 are independent of the value of r and are equally applicable when $r = 1$. Therefore, when the area of the I_o/I-diagram and its various momental areas for the asymmetrical haunched beam (Fig. 11(*a*)) about either end are known and are taken as A'_r, A'_{1r}, A'_{2r}, $\cdots$, A'_{4r}, those about the same end for the same beam placed in the reversed position (Fig. 11(*b*)) will obviously be A_r, A_{1r}, A_{2r}, $\cdots$, A_{4r} which may be computed by Eqs. 93 to 97.

When the right haunch cn of the beam in Fig. 10(*a*) is of the same type (straight, parabolic, or sharply curved) as the left haunch oc, and also $I'_c = I_c$, the values of areas for the right haunch about its right end may be obtained from those for the left haunch about its left end by Eqs. 83 to 87.

Theorem of Combination.—When a haunched beam is composed of several different sections (such as the beam in Fig. 10(*a*)), the area of the I_o/I-diagram and its various momental areas about the left end will be equal to the sum of those of its component sections oc, cc, and cn about the same end. Thus, the value of the momental diagram areas for the whole beam will be

$$A = A_q + A_c + A_r \quad \ldots\ldots (98)$$

$$A_1 = A_{1q} + A_{1c} + A_{1r} \quad \ldots\ldots (99)$$

$$A_2 = A_{2q} + A_{2c} + A_{2r} \quad \ldots\ldots (100)$$

$$A_3 = A_{3q} + A_{3c} + A_{3r} \quad \ldots\ldots (101)$$

and

$$A_4 = A_{4q} + A_{4c} + A_{4r} \quad \ldots\ldots (102)$$

The various partial areas with subscript (*ok*) covering the partial length $k\,L$ from the left end of the beam, which are needed for determining the load constants in cases 1, 3, and 4, may be computed as usual when $k < q$. When $q < k < (1 - r)$ (see Fig. 10(*a*)), they will be equal to the sum of those for the sections oc and ck, the latter being obtained from Eqs. 88 to 92 by substituting $1 - k$ for r. When $(1 - r) < k < 1$, the various partial areas with subscript (*kn*) will be first computed as usual and then subtracted from the various total areas for the entire length of beam to obtain those partial areas with subscript (*ok*).

Theorem of Symmetry.—For symmetrical haunched beams such as those shown in Fig. 12, the areas of the I_o/I-diagram and its various momental areas about the left end may be obtained from those of the left half also about the same end. Since the beams are symmetrical, the area of the I_o/I-diagram and its various momental areas of the right half about the right end are evidently equal to those of the left half about the left end. Thus, when Eqs. 93 to 97 are substituted in Eqs. 98 to 102 with $A_c = A_{1c} = \cdots = 0$, and, with subscripts r transformed to subscripts q, equations are obtained for computing the values of the various momental areas of symmetrical haunched

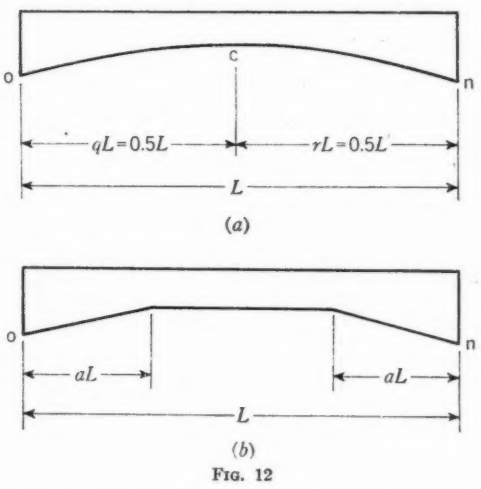

FIG. 12

beams—

$$A = 2\,A_q \ldots\ldots (103)$$

$$A_1 = L\,A_q \ldots\ldots (104)$$

$$A_2 = L^2\,A_q - 2\,L\,A_{1q} + 2\,A_{2q} \ldots\ldots (105)$$

$$A_3 = L^3\,A_q - 3\,L^2\,A_{1q} + 3\,L\,A_{2q} \ldots\ldots (106)$$

and

$$A_4 = L^4\,A_q - 4\,L^3\,A_{1q} + 6\,L^2\,A_{2q} - 4\,L\,A_{3q} + 2\,A_{4q} \ldots\ldots (107)$$

The various partial areas with subscript (ok) covering the partial length $k\,L$ at the left half of the beam, needed for computing the load constants in cases 1, 3, and 4, may be computed as usual when $k < 0.5$. When $k > 0.5$, the symmetrical haunched beam may be reversed in position so that $k < 0.5$.

The previously given five theorems obviously offer simplified procedures for computation. When the area of the I_o/I-diagram and its various momental areas of certain haunch about either end are known, the corresponding elements easily may be computed without plotting the various momental diagrams for:

(*a*) Any other haunch of the same type with the same ratio between the moments of inertia at both ends, but with different lengths; and

(*b*) Any haunched beam, symmetrical or asymmetrical, with or without a section of constant moment of inertia, containing either the same haunch or any other haunch as defined in (*a*).

It is shown subsequently by numerical examples that the application of the foregoing five theorems in many cases will simplify greatly the work of computation.

Numerical Examples

To illustrate the application of the method as well as the five theorems of momental areas, three typical numerical examples are given. In order that the results computed by this method may be checked, the shape of a haunched beam is taken from previously published[12,13] tables. With the I_o/I-diagram and its various momental diagrams plotted, the computations are divided into the following steps:

(1) Computation of the total areas of the various momental diagrams;

(2) Computation of the shape constants in terms of the end angle changes;

(3) Computation of the load constants in terms of the end changes for the desired type of loading; and

(4) Conversion of the shape and load constants in terms of the end angle changes into other systems to suit any method of continuous frame analysis, such as the Cross method of moment distribution.[4]

Example I.—The relative depth and moment of inertia and the I_o/I-diagram of the asymmetrical haunched beam are shown in Figs. 13(*a*), 13(*b*), and 13(*c*).

[12] "Nuere Methoden zur Statik der Rahmenträgwerke und der elastischen Bogenträger," by A. Strassner, Wilhelm Ernst und Sohn, Berlin, Band I, 1925, pp. 101–112.

[13] "Analysis of Continuous Frames," by E. B. Russell, San Francisco, Calif., 1934 (lithographed), pp. 24–29.

Note that, according to the notation used by E. B. Russell,[13] the length of haunch is $a\,L = 0.5\,L$; b, the ratio of the moment of inertia at the small end to that at the large end of the haunch, is equal to 0.2; and L is the length of the beam. The theorems of constant section and of combination will be applied

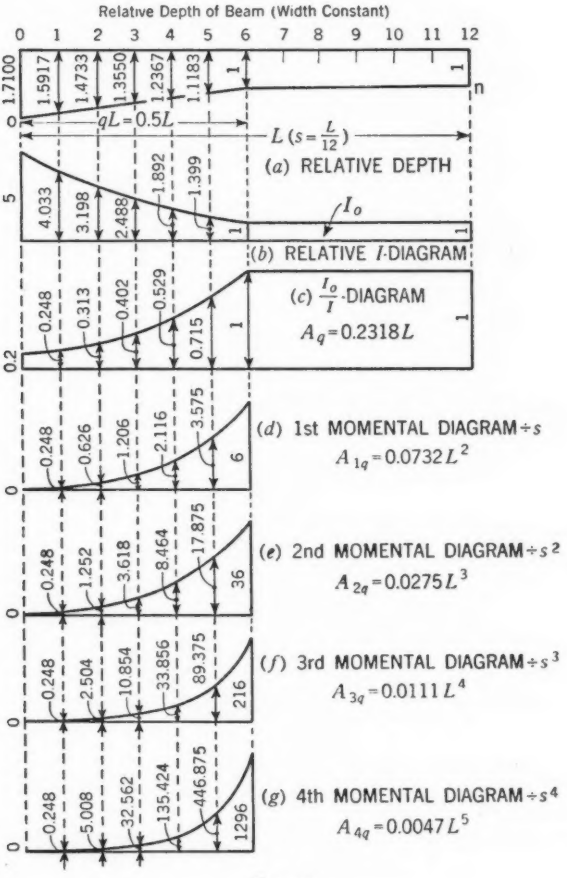

FIG. 13

by first computing the various momental areas for the haunch only, and then adding them to those of the constant section to obtain the values for the whole beam. The momental diagrams for the haunch only are obtained as shown in Figs. 13(d), 13(e), 13(f), and 13(g), from which the areas are

$$A_q = \frac{1}{3}\left(\frac{L}{12}\right)[(0.2 + 1) + 4(0.248 + 0.402 + 0.715) + 2(0.313 + 0.529)] = 0.2318\,L\,. . (108a)$$

$$A_{1q} = \frac{1}{3}\left(\frac{L}{12}\right)^2 [(0 + 6) + 4(0.248 + 1.206 + 3.575) + 2(0.626 + 2.116)] = 0.0732\, L^2 \quad (108b)$$

$$A_{2q} = \frac{1}{3}\left(\frac{L}{12}\right)^3 [(0 + 36) + 4(0.248 + 3.618 + 17.875) + 2(1.252 + 8.464)] = 0.0275\, L^3 \quad (108c)$$

$$A_{3q} = \frac{1}{3}\left(\frac{L}{12}\right)^4 [(0 + 216) + 4(0.248 + 10.854 + 89.375) + 2(2.504 + 33.856)] = 0.0111\, L^4 \quad (108d)$$

and

$$A_{4q} = \frac{1}{3}\left(\frac{L}{12}\right)^5 [(0 + 1{,}296) + 4(0.248 + 32.562 + 446.875) + 2(5.008 + 135.424)] = 0.0047\, L^5 \quad (108e)$$

The momental areas of the constant section are computed by Eqs. 88 to 92 with $q = 0.5$ and $r = 0$:

$$A_c = 0.5000\, L \quad (109a)$$

$$A_{1c} = \tfrac{1}{2}\,(0.5)\,(1 + 0.5)\,L^2 = 0.3750\, L^2 \quad (109b)$$

$$A_{2c} = \tfrac{2}{3}\,(0.5)\,(0.3750)\,L^3 + \tfrac{1}{3}\,(0.5)\,L^3 = 0.2917\, L^3 \quad (109c)$$

$$A_{3c} = \tfrac{1}{2}\,(0.3750)\,(1 + \overline{0.5^2})\,L^4 = 0.2344\, L^4 \quad (109d)$$

and

$$A_{4c} = \tfrac{4}{5}\,(0.2344)\,L^5 + \tfrac{1}{5}\,(0.5)^4\,(0.5000)\,L^5 = 0.1938\, L^5 \quad (109e)$$

The various total momental areas of the beam are, therefore,

$$A = A_q + A_c = 0.2318\, L + 0.5000\, L = 0.7318\, L \quad (110a)$$

$$A_1 = A_{1q} + A_{1c} = 0.0732\, L^2 + 0.3750\, L^2 = 0.4482\, L^2 \quad (110b)$$

$$A_2 = A_{2q} + A_{2c} = 0.0275\, L^3 + 0.2917\, L^3 = 0.3192\, L^3 \quad (110c)$$

$$A_3 = A_{3q} + A_{3c} = 0.0111\, L^4 + 0.2344\, L^4 = 0.2455\, L^4 \quad (110d)$$

and

$$A_4 = A_{4q} + A_{4c} = 0.0047\, L^5 + 0.1938\, L^5 = 0.1985\, L^5 \quad (110e)$$

The coefficients for the angle changes computed from Strassner's tables[12] are given in parentheses immediately following the results obtained by the method herein described:

$$E\, I_o\, \alpha_n = \frac{1}{L^2}\, A_2 = 0.3192\, L \;\; (0.3190) \quad (111a)$$

$$E\, I_o\, \alpha_o = A - \frac{2}{L}\, A_1 + \frac{1}{L^2}\, A_2 = (0.7318 - 2 \times 0.4482 + 0.3192)\, L = 0.1546\, L \;\; (0.1547) \quad (111b)$$

and

$$E\, I_o\, \beta = \frac{1}{L}\, A_1 - \frac{1}{L^2}\, A_2 = (0.4482 - 0.3192)\, L = 0.1290\, L \;\; (0.1290) \quad (111c)$$

Load constants in terms of angle changes are computed for the following four cases of loading. Their coefficients computed from Strassner's tables[12] for cases 1 and 2 of loading (Strassner's tables covering only these two cases) are given in parentheses immediately following the results obtained by the method of this paper.

Case 1. Concentrated Load at Point 8 ($k = \frac{2}{3}$).—The various partial areas with subscript (kn) needed in this case are computed by Eqs. 88 to 90 with $q = \frac{2}{3}$ and $r = 0$, since between point k and point n the beam section is constant:

$$A_{(kn)} = (1 - \tfrac{2}{3})\, L = \tfrac{1}{3}\, L = 0.3333\, L \ldots\ldots\ldots\ldots (112a)$$

$$A_{1(kn)} = \tfrac{1}{2} \times \tfrac{1}{3}\,(1 + \tfrac{2}{3})\, L^2 = \frac{5}{18}\, L^2 = 0.2778\, L^2 \ldots\ldots\ldots (112b)$$

and

$$A_{2(kn)} = (\tfrac{2}{3} \times \tfrac{2}{3} \times \frac{5}{18} + \tfrac{1}{3} \times \tfrac{1}{3})\, L^3 = \frac{19}{81}\, L^3 = 0.2346\, L^3 \ldots\ldots (112c)$$

$$A_{1(ok)} = A_1 - A_{1(kn)} = (0.4482 - 0.2778)\, L^2 = 0.1704\, L^2 \ldots\ldots (113a)$$

and

$$A_{2(ok)} = A_2 - A_{2(kn)} = (0.3192 - 0.2346)\, L^3 = 0.0846\, L^3 \ldots\ldots (113b)$$

$$E\, I_o\, [(\alpha^o{}_{o(1)} + \alpha^o{}_{n(1)}] = [\tfrac{2}{3} \times 0.3333 - 0.2778 + (1 - \tfrac{2}{3})\, 0.4482]\, P\, L^2 = 0.0938\, P\, L^2 \ldots\ldots (114a)$$

$$E\, I_o\, \alpha^o{}_{n(1)} = (\tfrac{2}{3} \times 0.2778 + 0.0846 - \tfrac{2}{3} \times 0.3192)\, P\, L^2 = 0.0570\, P\, L^2 \quad (0.0570) \ldots\ldots (114b)$$

and

$$E\, I_o\, \alpha^o{}_{o(1)} = (0.0938 - 0.0570)\, P\, L^2 = 0.0368\, P\, L^2 \quad (0.0369) \ldots\ldots (114c)$$

Case 2. Uniform Load Covering Whole Length of Beam.—

$$E\, I_o\, \alpha^o{}_{n(2)} = \tfrac{1}{2}\,(0.3192 - 0.2455)\, w\, L^3 = 0.0368\, w\, L^3 \quad (0.0368) \ldots\ldots (115a)$$

and

$$E\, I_o\, \alpha^o{}_{o(2)} = [\tfrac{1}{2}\,(0.4482 + 0.2455) - 0.3192]\, w\, L^3 = 0.0277\, w\, L^3 \quad (0.0277) \ldots\ldots (115b)$$

Case 5. Triangular Load with Maximum Intensity of w per Foot at Right End.—

$$E\, I_o\, [\alpha^o{}_{o(5)} + \alpha^o{}_{n(5)}] = \tfrac{1}{6}\,(0.4482 - 0.2455)\, w\, L^3 = 0.0338\, w\, L^3 \ldots\ldots (116a)$$

$$E\, I_o\, \alpha^o{}_{n(5)} = \tfrac{1}{6}\,(0.3192 - 0.1985) w\, L^3 = 0.0201\, w\, L^3 \ldots\ldots (116b)$$

and

$$E\, I_o\, \alpha^o{}_{o(5)} = (0.0338 - 0.0201) w\, L^3 = 0.0137\, w\, L^3 \ldots\ldots (116c)$$

Case 6. Triangular Load with Maximum Intensity of w per Foot at the Left End.—

$$E\, I_o\, [\alpha^o{}_{o(6)} + \alpha^o{}_{n(6)}] = \tfrac{1}{6}\,(2 \times 0.4482 - 3 \times 0.3192 + 0.2455)\, w\, L^3 = 0.0307\, w\, L^3 \ldots\ldots (117a)$$

$$E\, I_o\, \alpha^o{}_{n(6)} = \tfrac{1}{6}\,(2 \times 0.3192 - 3 \times 0.2455 + 0.1985)\, w\, L^3 = 0.0167\, w\, L^3 \ldots\ldots (117b)$$

and

$$E\,I_o\,\alpha^o{}_{o(6)} = (0.0307 - 0.0167)\,w\,L^3 = 0.0140\,w\,L^3 \ldots\ldots (117c)$$

Note that these results satisfy Eqs. 64 and 65.

Formulas for conversion of angle changes into the constants used in the Cross method are taken from the author's table, previously[5] mentioned with the one exception that the relative stiffness factors (which are equal to the absolute stiffness factors divided by 4 E and correspond to I/L for a beam with constant moment of inertia) are used to check Russell's coefficients, which are given in parentheses immediately following the results obtained by the method of this paper. The carry-over factors are

$$C_{on} = \frac{\beta}{\alpha_n} = \frac{0.1290}{0.3192} = 0.404\ (0.405) \ldots\ldots (118a)$$

and

$$C_{no} = \frac{\beta}{\alpha_o} = \frac{0.1290}{0.1546} = 0.834\ (0.835) \ldots\ldots (118b)$$

The relative stiffness factors are

$$S'_o = \frac{S_o}{4\,E} = \frac{\alpha_n}{4\,E\,(\alpha_o\,\alpha_n - \beta^2)} = \frac{0.3192}{4\,(0.1546 \times 0.3192 - \overline{0.1290^2})} \times \frac{I_o}{L} = \frac{0.3192}{4 \times 0.0327} \times \frac{I_o}{L} = 2.44\,\frac{I_o}{L}\ (2.44) \ldots (119a)$$

and

$$S'_n = \frac{S_n}{4\,E} = \frac{\alpha_o}{4\,E\,(\alpha_o\,\alpha_n - \beta^2)} = \frac{0.1546}{4 \times 0.0327} \times \frac{I_o}{L} = 1.18\,\frac{I_o}{L}\ (1.18) \ldots (119b)$$

Fixed-end moments are computed by

$$M_{fn} = \frac{\alpha_o\,\alpha^o{}_n - \beta\,\alpha^o{}_o}{\alpha_o\,\alpha_n - \beta^2} \ldots\ldots (120a)$$

and

$$M_{fo} = \frac{\alpha_n\,\alpha^o{}_o - \beta\,\alpha^o{}_n}{\alpha_o\,\alpha_n - \beta^2} \ldots\ldots (120b)$$

For cases 1, 2, 5, and 6, Eqs. 120 become, respectively,

$$M_{fn(1)} = \frac{0.1546 \times 0.0570 - 0.1290 \times 0.0368}{0.0327}\,P\,L = \frac{0.004065}{0.0327}\,P\,L = 0.1243\,P\,L\ (0.124) \ldots (121a)$$

and

$$M_{fo(1)} = \frac{0.3192 \times 0.0368 - 0.1290 \times 0.0570}{0.0327}\,P\,L = \frac{0.004394}{0.0327}\,P\,L = 0.1343\,P\,L\ (0.135) \ldots (121b)$$

$$M_{fn(2)} = \frac{0.1546 \times 0.0368 - 0.1290 \times 0.0277}{0.0327}\,w\,L^2 = \frac{0.002116}{0.0327}\,w\,L^2 = 0.0647\,w\,L^2\ (0.065) \ldots (122a)$$

and

$$M_{fo(2)} = \frac{0.3192 \times 0.0277 - 0.1290 \times 0.0368}{0.0327} w L^2$$

$$= \frac{0.004095}{0.0327} w L^2 = 0.1251 w L^2 \quad (0.125) \ldots (122b)$$

$$M_{fn(5)} = \frac{0.1546 \times 0.0201 - 0.1290 \times 0.0137}{0.0327} w L^2$$

$$= \frac{0.001340}{0.0327} w L^2 = 0.0820 \frac{w L^2}{2} \quad (0.082) \ldots (123a)$$

and

$$M_{fo(5)} = \frac{0.3192 \times 0.0137 - 0.1290 \times 0.0201}{0.0327} w L^2$$

$$= \frac{0.001780}{0.0327} w L^2 = 0.1088 \frac{w L^2}{2} \quad (0.108) \ldots (123b)$$

$$M_{fn(6)} = \frac{0.1546 \times 0.0167 - 0.1290 \times 0.0140}{0.0327} w L^2$$

$$= \frac{0.000773}{0.0327} w L^2 = 0.0472 \frac{w L^2}{2} \quad (0.047) \ldots (124a)$$

and

$$M_{fo(6)} = \frac{0.3192 \times 0.0140 - 0.1290 \times 0.0167}{0.0327} w L^2$$

$$= \frac{0.002315}{0.0327} w L^2 = 0.1416 \frac{w L^2}{2} \quad (0.142) \ldots (124b)$$

Example II.—The symmetrical haunched beam shown in Fig. 14 is composed of two asymmetrical beams, each of which has the same shape as that in Example I, except that the length is 0.5 L, hence the values of the momental areas of the beam may be computed by the application of the foregoing theorems from the results obtained in Example I without plotting the various momental diagrams.

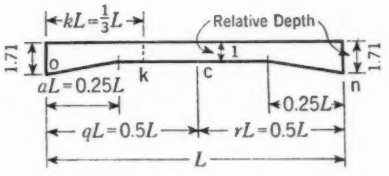

FIG. 14

The load constants are computed for cases 1 and 2 only, hence the values of A_3 and A_4 are not needed. The values of A_q, A_{1q}, and A_{2q} for the left half, oc of the beam may be computed from the values of A, A_1, and A_2 obtained in Example I by Eqs. 83 to 85 with $j = 0.5$:

$$A_q = 0.5 \times 0.7318 L = 0.3659 L \ldots\ldots\ldots\ldots (125a)$$

$$A_{1q} = (0.5)^2 0.4482 L^2 = 0.1121 L^2 \ldots\ldots\ldots\ldots (125b)$$

and

$$A_{2q} = (0.5)^3 0.3192 L^3 = 0.0399 L^3 \ldots\ldots\ldots\ldots (125c)$$

The values of A, A_1, and A_2 for the whole beam may be computed by Eqs. 103 to 105:

$$A = 2\,A_q = 2 \times 0.3659\,L = 0.7318\,L \ldots\ldots\ldots\ldots (126a)$$

$$A_1 = L\,A_q = 0.3659\,L^2 \ldots\ldots\ldots\ldots\ldots\ldots (126b)$$

and

$$A_2 = L^2\,A_q - 2\,L\,A_{1q} + 2\,A_{2q}$$
$$= (0.3659 - 2 \times 0.1121 + 2 \times 0.0399)\,L^3 = 0.2216\,L^3 \ldots (126c)$$

Shape constants, in terms of angle changes, are

$$E\,I_o\,\alpha = \frac{1}{L^2}\,A_2 = 0.2216\,L \;\; (0.2217) \ldots\ldots\ldots\ldots (127a)$$

and

$$E\,I_o\,\beta = \tfrac{1}{2}\,A - \frac{1}{L^2}\,A_2 = (0.5 \times 0.7318 - 0.2216)\,L$$
$$= 0.1443\,L \;\; (0.1443) \ldots (127b)$$

Load constants in terms of angle changes are as follows:

Case 1. Concentrated Load at $k\,L = L/3$.—The various partial areas needed also are computed from those obtained in Example I. In this example $A_{(kc)}$ corresponds to $A_{(kn)}$ in Example I, and the same is true for $A_{1(ok)}$ and $A_{2(ok)}$ in the two examples:

$$A_{(kc)} = 0.5 \times 0.3333\,L = 0.1667\,L \ldots\ldots\ldots\ldots (128a)$$

$$A_{(kn)} = A_{(kc)} + A_{(cn)} = A_{(kc)} + A_q = (0.1667 + 0.3659)\,L = 0.5326\,L \ldots (128b)$$

$$A_{1(ok)} = (0.5)^2\,0.1704\,L^2 = 0.0426\,L^2 \ldots\ldots\ldots\ldots (128c)$$

$$A_{1(kn)} = A_1 - A_{1(ok)} = (0.3659 - 0.0426)L^2 = 0.3233\,L^2 \ldots\ldots (128d)$$

and

$$A_{2(ok)} = (0.5)^3\,0.0846\,L^3 = 0.0106\,L^3 \ldots\ldots\ldots\ldots (128e)$$

Also,

$$E\,I_o\,[\alpha^o{}_{o(1)} + \alpha^o{}_{n(1)}]$$
$$= [\tfrac{1}{3} \times 0.5326 - 0.3233 + (1 - \tfrac{1}{3})\,0.3659]\,P\,L^2 = 0.0982\,P\,L^2 \ldots (129a)$$

$$E\,I_o\,\alpha^o{}_{n(1)} = [\tfrac{1}{3} \times 0.3233 + 0.0106 - \tfrac{1}{3} \times 0.2216]\,P\,L^2$$
$$= 0.0445\,P\,L^2 \;\; (0.0445) \ldots (129b)$$

and

$$E\,I_o\,\alpha^o{}_{o(1)} = (0.0982 - 0.0445)P\,L^2 = 0.0537\,P\,L^2 \;\; (0.0537) \ldots (129c)$$

Case 2. Uniform Load Covering Whole Length of Beam.

$$E\,I_o\,\alpha^o{}_{(2)} = \tfrac{1}{4}\,E\,I_o\,\beta\,w\,L^2 = 0.25 \times 0.1443\,w\,L^3 = 0.0361\,w\,L^3 \;\; (0.0361) \ldots (130)$$

Conversion of angle changes into the constants used in the Cross method[4] is as shown hereafter. The beam is that in Russell's tables[13] with $a = 0.25$

and $b = 0.2$. Russell's coefficients are again given in parentheses immediately following those obtained by this method to serve as a check. The carry-over factor is

$$C_{on} = C_{no} = C = \frac{0.1443}{0.2216} = 0.651\ (0.650) \ldots\ldots\ldots\ldots (131)$$

The relative stiffness factor is

$$S'_o = S'_n = S' = \frac{0.2216}{4\,[(0.2216)^2 - (0.1443)^2]} \times \frac{I_o}{L} = \frac{0.0554}{0.0283} \times \frac{I_o}{L} = 1.96\,\frac{I_o}{L}\ (1.95) \ldots (132)$$

Fixed-end moments for case 1 are

$$M_{fn(1)} = \frac{0.2216 \times 0.0445 - 0.1443 \times 0.0537}{0.0283}\,P\,L = \frac{0.00210}{0.0283}\,P\,L = 0.0746\,P\,L\ (0.075) \ldots (133a)$$

and

$$M_{fo(1)} = \frac{0.2216 \times 0.0537 - 0.1443 \times 0.0445}{0.283}\,P\,L = \frac{0.00548}{0.0283}\,P\,L = 0.1938\,P\,L\ (0.194) \ldots (133b)$$

For case 2, the fixed-end moments are

$$M_{f(2)} = \frac{\alpha^o\,(\alpha - \beta)}{\alpha^2 - \beta^2} = \frac{\beta}{4\,(\alpha + \beta)}\,w\,L^2 = \frac{0.1443}{4\,(0.2216 + 0.1443)}\,w\,L^2 = 0.0987\,w\,L^2\ (0.099) \ldots (133c)$$

Example III.—To demonstrate further the application of the five theorems of momental areas in simplifying the computations of this method, the values of A, A_1, and A_2 for the asymmetrical beam with haunch at both ends (Fig. 15) will be computed from the results obtained in Example I without plotting the various momental diagrams. Two different methods may be used.

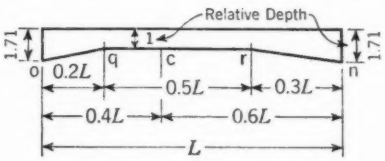

FIG. 15

(*a*) The beam is considered as composed of the three sections oq, qr, and rn, the haunches oq and rn being similar to haunch oc of the beam in Example I. For haunch oq, $j = \frac{0.2}{0.5} = 0.4$,

$$A_q = 0.4 \times 0.2318\,L = 0.092720\,L \ldots\ldots\ldots\ldots (134a)$$

$$A_{1q} = (0.4)^2\,0.0732\,L^2 = 0.011712\,L^2 \ldots\ldots\ldots\ldots (134b)$$

and

$$A_{2q} = (0.4)^3\, 0.0275\, L^3 = 0.001760\, L^3 \quad \ldots\ldots (134c)$$

For haunch rn, $j = \dfrac{0.3}{0.5} = 0.6$,

$$A'_r = 0.6 \times 0.2318\, L = 0.139080\, L \quad \ldots\ldots (135a)$$

$$A'_{1r} = (0.6)^2\, 0.0732\, L^2 = 0.026352\, L^2 \quad \ldots\ldots (135b)$$

$$A'_{2r} = (0.6)^3\, 0.275\, L^3 = 0.005940\, L^3 \quad \ldots\ldots (135c)$$

$$A_r = 0.139080\, L \quad \ldots\ldots (135d)$$

$$A_{1r} = (0.139080 - 0.026352) L^2 = 0.112728\, L^2 \quad \ldots\ldots (135e)$$

and

$$A_{2r} = (0.139080 - 2 \times 0.026352 + 0.005940) L^3 = 0.092316\, L^3 \quad \ldots (135f)$$

For the constant-depth section, qr, $q = 0.2$, $r = 0.3$,

$$A_c = (1 - 0.2 - 0.3)\, L = 0.500000\, L \quad \ldots\ldots (136a)$$

$$A_{1c} = (0.5)\ (0.500000)\ (1 + 0.2 - 0.3) L^2 = 0.225000\, L^2 \quad \ldots (136b)$$

and

$$A_{2c} = \tfrac{2}{3}\ (0.2)\ (0.225000) L^3 + \tfrac{1}{3}\ (0.7)^2\ (0.500000) L^3 = 0.111667\, L^3 \quad \ldots (136c)$$

For the whole beam,

$$A = (0.092720 + 0.500000 + 0.139080) L = 0.731800\, L \quad \ldots (137a)$$

$$A_1 = (0.011712 + 0.225000 + 0.112728) L^2 = 0.349440\, L^2 \quad \ldots (137b)$$

and

$$A_2 = (0.001760 + 0.11667 + 0.092316) L^3 = 0.205743\, L^3 \quad \ldots (137c)$$

(*b*) The beam is considered as composed of the two asymmetrical beams oc and cn, both being similar to the beam in Example I. For asymmetrical beam oc, $j = 0.4$,

$$A_q = 0.4 \times 0.7318\, L = 0.292720\, L \quad \ldots\ldots (138a)$$

$$A_{1q} = (0.4)^2\, 0.4482\, L^2 = 0.071712\, L^2 \quad \ldots\ldots (138b)$$

and

$$A_{2q} = (0.4)^3\, 0.3192\, L^3 = 0.20429\, L^3 \quad \ldots\ldots (138c)$$

For asymmetrical beam cn, $j = 0.6$,

$$A'_r = 0.6 \times 0.7318\, L = 0.439080\, L \quad \ldots\ldots (139a)$$

$$A'_{1r} = (0.6)^2\, 0.4482\, L^2 = 0.161352\, L^2 \quad \ldots\ldots (139b)$$

$$A'_{2r} = (0.6)^3\, 0.3192\, L^3 = 0.068947\, L^3 \quad \ldots\ldots (139c)$$

$$A_r = 0.439080\, L \quad \ldots\ldots (139d)$$

$$A_{1r} = (0.439080 - 0.161352)\, L^2 = 0.277728\, L^2 \quad \ldots\ldots (139e)$$

and

$$A_{2r} = (0.439080 - 2 \times 0.161352 + 0.068947)L^3 = 0.185323\,L^3 \ldots (139f)$$

For the whole beam,

$$A = (0.292720 + 0.439080)L = 0.731800\,L \ldots\ldots\ldots (140a)$$

$$A_1 = (0.071712 + 0.277728)L^2 = 0.349440\,L^2 \ldots\ldots\ldots (140b)$$

and

$$A_2 = (0.020429 + 0.185323)L^3 = 0.205752\,L^3 \ldots\ldots\ldots (140c)$$

These two methods practically check. The values of A_3 and A_4, if desired, may be computed in the same manner.

Conclusion

The foregoing three numerical examples suffice to demonstrate the simplicity as well as the accuracy of the method presented in this paper. With the various momental diagrams for a given haunched beam once constructed, the shape and load constants for any of the common types of loading all can be computed from the areas of those diagrams. No separate M-diagram or M/I-diagram is needed for each loading, as is necessary in any of the existing methods. Since the computation of the flexural constants is reduced at last to that of the area of a plane figure under a curve, the accuracy of the method lies entirely in the area computation. Hence, the method can yield results with any desired accuracy if the length of beam is divided into a sufficient number of equal segments. Ordinarily, the division of the length of beam into ten or twelve equal segments will give satisfactory accuracy for practical purposes.

When the flexural constants of a number of haunched beams containing the same or similar haunches are to be computed, the five theorems of momental areas may be applied in simplifying the necessary computations. These five theorems represent the unique feature of the method, which is unparalleled by other methods within the author's knowledge.

APPENDIX. NOTATION

The following letter symbols, adopted for use in the paper and in its discussions, conform essentially to American Standard Letter Symbols for Mechanics, Structural Engineering and Testing Materials (ASA—Z10a—1932) prepared by a Committee of the American Standards Association, with Society representation, and approved by the Association in 1932.

The dimensions of the letter symbols are indicated in parentheses following each symbol with f representing a force, l representing a length, and p representing a pure number or ratio.

A (l) = area of the I_o/I-diagram for entire length of beam, with the following subscripts for discrimination: (ok) and (kn) for the partial lengths ok and kn, respectively; c for the section of the beam with a constant moment of inertia; q for the left haunch

or part of the beam; r for the right haunch or part of the beam (these rules applying also to the following symbols: A_1, A_2, A_3, and A_4);

A_1 (l^2) = area of first momental diagram of the I_o/I-diagram for the entire length about the left end of the beam;

A'_{1r} = area of first momental diagram of I_o/I-diagram for the right haunch or the part of the beam about the right end of the beam (the same rule applying also to A_2, A_3, and A_4);

A_2 (l^3) = area of the second momental diagram of the I_o/I-diagram for the entire length about the left end of the beam;

A_3 (l^4) = area of the third momental diagram of the I_o/I-diagram for the entire length about the left end of the beam;

A_4 (l^5) = area of the fourth momental diagram of the I_o/I-diagram for the entire length about the left end of the beam;

$A_{(m)}$ ($f\,l^2$) = area of the $M\,I_o/I$-diagram for the entire length of the beam;

$A_{1(m)}$ ($f\,l^3$) = area of the first momental diagram of the $M\,I_o/I$-diagram about the left end of the beam;

a (p) = proportional length of the haunch;

b (p) = ratio of the moment of inertia at the small end to that at the large end of haunch;

C (p) = carry-over factor;

C_{on} = carry-over factor from end o to end n;

C_{no} = carry-over factor from end n to end o;

E ($f\,l^{-2}$) = modulus of elasticity of the material;

I (l^4) = moment of inertia of the cross section at any section of the beam;

I' = moment of inertia of the cross section for another beam;

I_e (l^4) = moment of inertia of cross section at end of beam; I'_e = moment of inertia of cross section for another end or another beam;

I_o (l^4) = an arbitrary value of I used as a standard in computation;

I'_o = an arbitrary value of I used as a standard in computation for another beam;

i (p) = a ratio, x/L;

j (p) = ratio between length of two similar haunches, beams, or parts of beams;

k (p) = ratio of distance of point k measured from left end of the beam to the entire beam length;

L (l) = length of the beam;

M ($f\,l$) = bending moment at any section of the beam;

M_f ($f\,l$) = fixed-end moment due to applied loads, with subscript o or n indicating, respectively, at left end or right end of beam;

m (p) = ratio of distance of point m measured from the left end of the beam to the entire beam length;

n (p) = number of equal segments into which the length of the beam is divided;

P = a concentrated load;

Q (l^2) = first moment of A about left end of beam;

q (p) = proportional length of the left haunch or part of the beam;
r (p) = proportional length of the right haunch or part of the beam;
S $(f\,l)$ = absolute stiffness factor, with subscript o or n indicating left or right end of beam, respectively;
S' (l^3) = relative stiffness factor $= \dfrac{S}{4\,E}$, with subscript o or n indicating left or right end of beam, respectively;
s (l) = length of equal segments into which the length of the beam is divided;
w = uniform load per unit length;
x (l) = abscissa of any point measured from the left end of beam;
x' $(l) = L - x$;
y (p) = the ordinate of the I_o/I-diagram $\left(= \dfrac{I_o}{I}\right)$, with subscripts o, 1, 2, $\cdots$, m, $\cdots$, n indicating its value at points at a distance of os, $1s$, $2s$, $\cdots$, ms, $\cdots$, ns from the left end of the beam;
y'_m (l) = ordinate at any point m of the first momental diagram of the I_o/I-diagram about the left end of the beam;
y''_m (l^2) = ordinate at any point m of the second momental diagram of the I_o/I-diagram about the left end of the beam;
y'''_m (l^3) = ordinate at any point m of the third momental diagram of the I_o/I-diagram about the left end of the beam;
y''''_m (l^4) = ordinate at any point m of the fourth momental diagram of the I_o/I-diagram about the left end of the beam;
α $(f^{-1}\,l^{-1})$ = angle change at either end of a simply-supported beam due to a unit moment applied at the same end, with subscript o or n indicating, respectively, at left or right end;
α^o (p) = angle change at either end of a simply-supported beam due to any applied loads, with subscript o or n indicating, respectively, at left or right end; and
β $(f^{-1}\,l^{-1})$ = angle change at either end of a simply-supported beam due to a unit moment applied at the other end.

AMERICAN SOCIETY OF CIVIL ENGINEERS

Founded November 5, 1852

DISCUSSIONS

OPERATION OF THE CONOWINGO HYDROELECTRIC PLANT

Discussion

BY JOHN S. COTTON

JOHN S. COTTON,[9] M. ASCE.—The highly successful operation of the Conowingo plant in Maryland has been well described by Mr. Turner. Examination of the performance indicates that almost all available water and head are utilized effectively. The secret of this record is sufficient data on rainfall and runoff, and cooperation by all concerned. Because of rising fuel costs, such run-of-river plants are becoming more attractive.

Such a run-of-river hydro project, as exemplified by Conowingo, is highly economical and desirable. This type of project usually operates in conjunction with a large steam generating system, has considerable pondage, and usually has short transmission lines. If fuel is relatively costly, the installed capacity of hydro power is based primarily upon supplying large amounts of energy to the load curve. Such plants have moderate annual capacity factors and operate continuously to utilize the available flows as far as it is economically feasible. If fuel is relatively low priced, the installed capacity of hydro power is based primarily upon the relative capacity and energy demands of the load curve peak. Such plants have low fixed charges and annual capacity factors, and are used to carry system peaks. Usually, a compromise is made in order to obtain the greatest return, and the plant is operated at various positions in the load curve in order to utilize the seasonal water flow efficiently.

This utilization for Conowingo is demonstrated by the integrated load curve (Fig. 11). The integrated load curve shows clearly the relation between kilowatts and kilowatt-hours for each position of the hydro plant on the load curve. Table 4 shows daily capacity factors (line 2) and daily system load factors (line 4) derived from the integrated load curve. The hydro plant also furnished the necessary kilowatt-hours to the load for cases I, II, and III, as shown by lines 5 and 6, Table 4.

NOTE.—This paper by Robert E. Turner was published in November, 1947, *Proceedings*. Discussion on this paper has appeared in *Proceedings*, as follows: June, 1948, by Joel D. Justin, E. T. Schuleen, and Gordon R. Williams.

[9] Cons. Engr., San Anselmo, Calif.

It will be noted that, for cases I, II, and III, the hydro at all times furnishes its full kilowatt rating to the system load thus obviating the necessity of constructing steam plant capacity amounting to 260,000 kw. The annual value of capacity in the form of a steam generating plant, "hot and spinning," is at least from $18 to $20 per kw.

TABLE 4.—FACTORS DERIVED FROM THE INTEGRATED LOAD CURVES, FIG. 11(*c*)

Line	Factors (daily)	Case I	Case II	Case III	Case IV	Case V
1	Flow, in cubic feet per second.....	High	Medium	Low	4,000[a]	2,000[b]
2	Hydro capacity— 260,000 kw	100%	67.2%	24.0%	9.8%	5.2%
3	Steam capacity— 1,070,000 kw	65.3%	72.2%	83.7%	87.0%	89.0%
4	Load factor (system)— 1,330,000 kw	72.0%	72.0%	72.0%	72.0%	72.0%
5	Daily hydro energy output, in thousand kilowatt-hours.....	6,200	4,200	1,500	640	320
6	Dependable hydro capacity, in thousand kilowatts.....	260	260	260	....	...

[a] 90% of the time. [b] 100% of the time.

The hydro energy supplied would cost at least from 3 mills to 4 mills per kw-hr to produce in a steam generating plant. At times of low or moderate energy output from the hydro plant, the steam generating plant must generate more kilowatt-hours, the steam capacity remaining the same. This is indicated by the daily load factors for hydro and steam in lines 2 to 4, Table 4.

Since hydro could not fully supply the energy demands in cases IV and V the full capacity of the plant could not be utilized and the hydro capacity factors shown for cases IV and V (lines 5 and 6, Table 4) could not be realized. Working back in Fig. 11 from the available hydro energy, the dependable hydro capacities for cases IV and V would be:

Basis	Approximate dependable hydro capacity
90% time flow	215,000 kw
100% time flow	155,000 kw

It is obvious that, if hydro with pondage is given the very favorable position at the top of the load curve peak, a large dependable hydro capacity can be made available with very little hydro energy.

Except in very small isolated plants the basis of 100% time flow is not a reasonable criterion for dependable hydro capacity. For larger hydro plants with simple interconnections 90% time flows are commonly used. In systems as large as that in which the Conowingo plant operates, bases, of either 100% time flow or 90% time flow, are rather severe because: (*a*) Power systems are rarely loaded to maximum capacity; (*b*) spare steam equipment is available for use in infrequent emergencies; (*c*) the power construction program is ordinarily ahead of actual need; and (*d*) the systems are interconnected.

A run-of-river hydro plant in a small system usually is capable of generating energy in excess of load requirements. In large systems however, there is a greater amount of energy in the top section of the load curve per kilowatt of

Power in Watts x 10^8
Steam peak
Hydro peak loading
Discharge 10,000 cu ft per sec
Generation 1.5 million kw-hr
Steam peak
Steam base and steam peak loading
Discharge 27,000 cu ft per sec
Generation 4.2 million kw-hr
Hydro base loading
Discharge 45,000 cu ft per sec
Generation 6.2 million kw-hr
Minimum steam base
A.M.
P.M.
Time of Day
(a) LOAD CURVE
Percentage of Time
(b) LOAD DURATION CURVE
Million Kilowatt-Hours
(c) INTEGRATED LOAD CURVE
(Actual peak = 9.3 x 10^8 watts)
Hydro
Steam
13.3
13.1
10.5
9.17
6.7
5.08
2.5
2.6
2.47
2.58
0.2
1.5
4.2
6.2
6.0
12.2
15.65
19.85
21.55
23.05

FIG. 11

peak, and usually all the hydro energy can be utilized. Hydro utilization under the load curve increases roughly as the square root of the system load.

In a large integrated power system, most of the run-of-river hydro capacity, as well as the hydro energy, can be utilized under the load curve. Therefore, hydro capacity and energy should have the same value as steam capacity and energy, and not merely fuel saving (kilowatt-hour) value—provided that, when the hydro capacity is assigned to the peak of the load curve during low flows, hydro can (except on very rare occasions) furnish the corresponding energy called for in this part of the peak. If hydro, as the result of ordinary low flows and insufficient pondage, cannot supply enough energy to satisfy its full capacity at the peak loading, then only that part of the hydro capacity which has sufficient energy for that area of the peak can be regarded as firm. If greater flows exist, then the hydro capacity can be assigned a lower position on the load curve depending upon the available hydro energy.

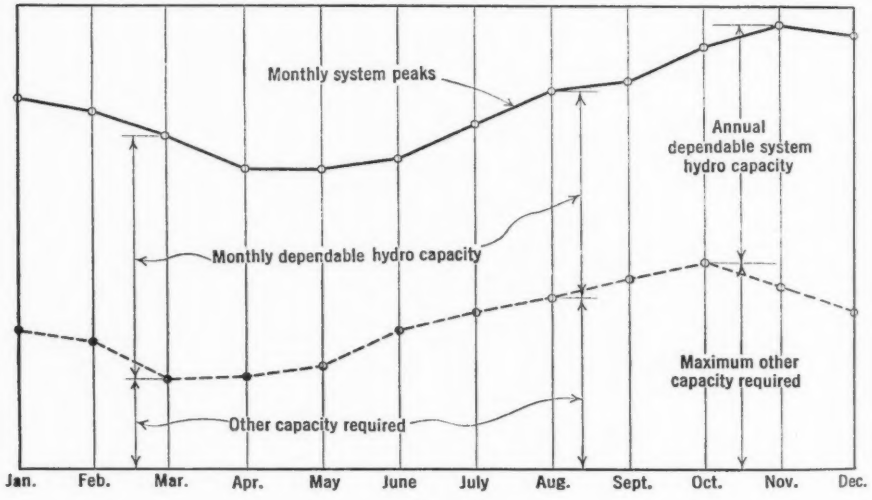

FIG. 12

Hence, it is primarily a matter of system experience in arriving at the practical dependable capacity of a run-of-river hydro project in a large integrated system. It appears then that the dependable capacity of Conowingo is equal to about 215,000 kw provided that hydro always has the most favorable positions in the load curve. This corresponds to about the 94% time flow on an annual basis.

The writer is of the opinion that certain standard power definitions are not applicable for large systems. Firm power is defined as "the power intended to be always available even under emergency conditions." A steam generating plant meets this condition, but a run-of-river hydro project in an integrated power system does not, although it furnishes considerable dependable kilowatt capacity and variable energy to the system load, in an acceptable manner. This definition is satisfactory if it is interpreted that furnishing power at

variable capacity factors is allowable. In an isolated project the hydro capacity factor would be fixed by the total load whereas in an integrated system it need not be. A more logical definition in this case is, as follows:

> "Firm hydro power under system operation is that portion of the total installed capacity of the hydro plant which under existing conditions of load, stream flow, and pondage, is capable of performing the same function in serving the part of the load allocated to it that an alternative steam plant could perform."

On this basis, the firm power of Conowingo would be about 155,000 kw, or more

Probably the fairest criterion in the case of hydro in an integrated system is "dependable hydroelectric capacity," as defined by the Federal Power Commission:

> "Dependable hydroelectric capacity is intended to be the capacity value of the system hydroelectric plants in serving, together with the other available system capacity, the maximum annual system peak load. For any specified period it represents, on the basis of complete utilization of available storage energy over the critical flow periods, the difference between the peak load for that period and the maximum other capacity required. Where a portion of storage energy is scheduled to be held as a reserve for emergency use only, the dependable capacity should also include the reserve capacity value of such energy reserve. The maximum monthly dependable capacity is not necessarily the same as the annual dependable hydroelectric capacity as the annual peak demand may not occur in the same month, requiring the maximum capacity from other than system hydroelectric plants."

This is illustrated in Fig. 12. The writer does not have sufficient data to determine the dependable capacity of Conowingo.

AMERICAN SOCIETY OF CIVIL ENGINEERS

Founded November 5, 1852

DISCUSSIONS

A CENTROIDAL METHOD OF RIGID-FRAME ANALYSIS

Discussion

BY LEROY A. BEAUFOY, AND WILLIAM A. CONWELL

LEROY A. BEAUFOY,[11] ESQ.—It is difficult to follow this paper because of the variability of dimensions in the quantities employed. Thus, whereas in Eq. 3 it will be found that the dimensions of I are L^4, in Eq. 9 both I_z and I_{zo} have the dimensions L^3; yet in Eqs. 21*b* and 21*d* the dimensions of I_z and I_{zo}, respectively, are $1/L$. Similarly, in Eqs. 15*a* and 15*b*, respectively, the dimensions of I_x and I_y are L^3, but in Eq. 18*c* these quantities are given the dimension L. (It may be claimed that, as Eq. 18*c* is the algebraic expression of a graphical construction in which I_x and I_y are represented vectorially, the dimension L is rational; however, in the construction relating to Eq. 19 I_o is given the dimensions L^3 and not L.) Again, in Eq. 5 the quantity L_o is assigned the dimension L, but in Eq. 21*a* the dimensions become $1/L^3$; in Eq. 21*e* I_o has the dimensions $1/L$ and not L^3 (compare Eq. 19). All this makes the interpretation of the equations in the paper anything but a straightforward matter, since the same symbols have different meanings in different places.

Section 6, "Application to Structures with Both Ends Hinged," seems to be based on a fundamental error. It may easily be demonstrated—for example, by virtual work methods—that Eq. 24 applies to a structure with one end fixed and the other end free, and not to a structure with both ends hinged. Thus, referring to Fig. 21, in which any continuous bent AB is fixed at point B and free at point A, it may be shown that the displacements at point A due to a force F_o acting in the direction AB are as given in Fig. 21. The elastic centroid conception enables one to distinguish between displacements due to rotation and those due to translation. The coordinate axes through points A and O, respectively, are (z, y) and (z_o, y_o) as used in the paper. Because of translation without rotation, a rigid arm AO would move to A′O′ and because of rotation without translation, it would move about O′ from O′A′ to O′A″.

NOTE.—This paper by S. J. Bell was published in November, 1947, *Proceedings*. Discussion on this paper has appeared in *Proceedings* as follows: June, 1948, by L. E. Grinter, Alexis L. Gluckmann, Yi-Mai Yao, and Phil M. Ferguson.

[11] Univ. Reader in Civ. Eng., King's College, Univ. of London, London, England.

Then the horizontal projection of AA′ is

$$\Delta_{zAT} = \frac{F_o I_{zo}}{E I} \quad \ldots\ldots\ldots\ldots\ldots\ldots\ldots\ldots (39)$$

and the horizontal projection of A′A″ is

$$\Delta_{zAR} = \frac{F_o Z^2_o L_o}{E I} \quad \ldots\ldots\ldots\ldots\ldots\ldots\ldots\ldots (40)$$

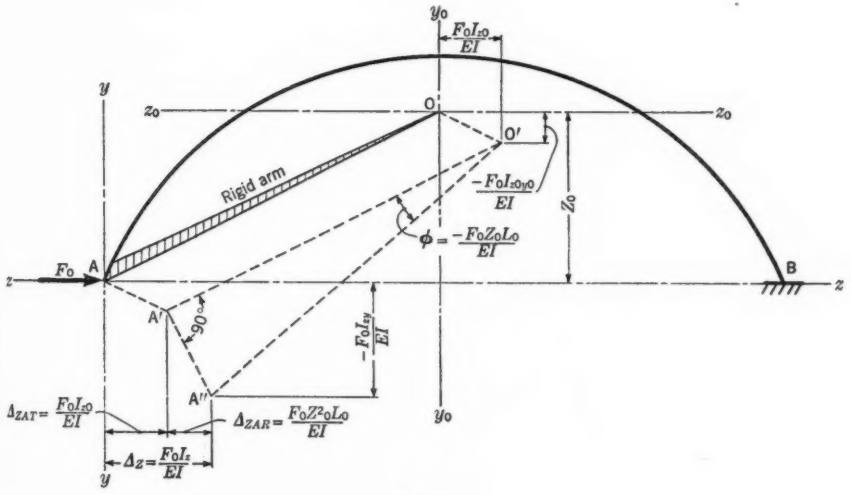

FIG. 21

It will also be noted that the total horizontal displacement of point A is

$$\Delta_z = \frac{F_o I_z}{E I} \quad \ldots\ldots\ldots\ldots\ldots\ldots\ldots\ldots (41a)$$

and the total vertical displacement is

$$\Delta_y = -\frac{F_o I_{zy}}{E I} \quad \ldots\ldots\ldots\ldots\ldots\ldots\ldots\ldots (41b)$$

Fig. 21 also shows values of the rotation ϕ, and of the horizontal and vertical displacements of the elastic centroid.

Thus, Eq. 24 would not appear to be correct for a bent with both ends hinged. Incidentally, it should be noted that Fig. 3 gives the symbols Δ_{zT} and Δ_{zR} different meanings from those used in Eq. 24. In Fig. 3, these movements refer to the centroid end of the rigid arm R_A; in Eq. 24, to the free end of the bent. In Fig. 21, therefore, the writer has used the symbols Δ_{zAT} and Δ_{zAR}.

The numerical examples are not very convincing; rather, they are the reverse. For instance, in Example 6 the author misleads himself into regarding Δ_{oA} as the "actual movement" of point A. In fact, the relative displacement of points A and B requires a force F_o in the line AB and this relative displace-

ment will be achieved by separate movements of points A and B in the line AB, without lateral movement as suggested in Fig. 14, by the displacement Δ_{oA}, which has a component perpendicular to AB. These separate end translations can have any actual values—in Example 6 only the relative value is fixed at 2 in. Thus, for example, points A and B may both move 1 in. (each toward the other), or point A may move $\frac{1}{2}$ in. and point B $1\frac{1}{2}$ in., etc. The end rotations are readily obtained by the conjugate beam method. For $F_o = 1$ lb, the $\frac{M}{EI}$-diagram is as shown in Fig. 22, from which the end reactions on the conjugate beam are determined as presented in Table 2.

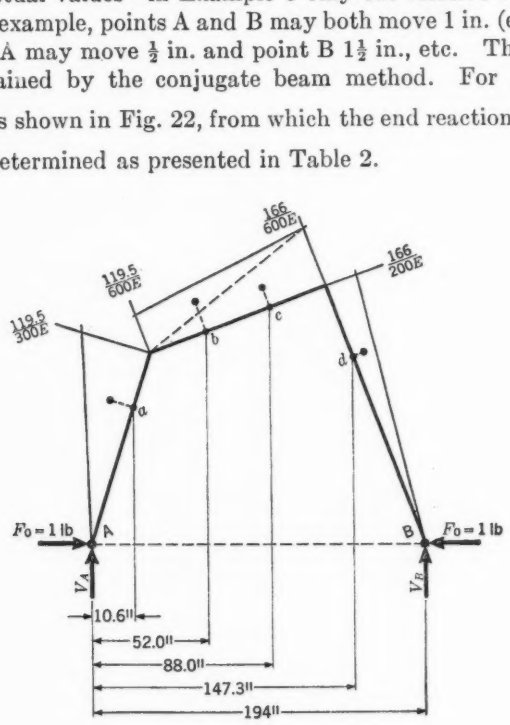

FIG. 22

TABLE 2.—DETERMINATION OF END REACTIONS ON THE CONJUGATE BEAM (FIG. 22)

Elastic weight (1)	Area of $\frac{M}{EI}$-diagram (2)	Lever arm from A (in.) (3)	Col. 2 × Col. 3 × E (4)
a	$60 \times 119.5/300\ E = 23.9/E$	10.6	253.5
b	$60 \times 119.5/600\ E = 11.95/E$	52.0	621.5
c	$60 \times 166\ /600\ E = 16.6/E$	88.0	1,460
d	$90 \times 166\ /900\ E = 16.6/E$	147.3	2,450
Total	$69.1/E$	....	4,785.0

Hence,

$$V_B = \frac{4{,}785}{194\ E} = +\frac{24.6}{E} \quad \ldots\ldots (42a)$$

and

$$V_A = -\frac{(69.1 - 24.6)}{E} = -\frac{44.5}{E} \quad \ldots\ldots (42b)$$

in which V_B and V_A are the reactions at ends B and A of the conjugate beam, respectively.

The end reactions are the slopes of the beam. Using the author's value of 7,630 lb for F_o, $\theta_B = \frac{+ 24.6 \times 7{,}630}{30 \times 10^6} = + 0.00625$ radian; and $\theta_A = \frac{- 44.6 \times 7{,}630}{30 \times 10^6} = - 0.01135$ radian. The total change of slope is, therefore, 0.0176 radian, as obtained by the author, but the actual slopes at the ends are very different from the values in the paper. According to Mr. Bell's solution, this total change of slope is equally divided between the two ends. It will be noticed that in Example 6 the author states: "* * * Assuming this movement [2 in.] equally divided between the two ends, find the rotation* * *." Whether the relative displacement is equally or unequally divided will not affect the end rotations, and in the present case it is not possible for these to have equal values.

The writer is mystified by the author's use of the elastic centroid. If Figs. 11, 13, and 14 are compared, it would appear that the elastic centroid is the same in all cases—that is, irrespective of end-fixing conditions. Evidently, the author does not give the term "elastic centroid" its usual meaning, which would, for example, call for the location of the elastic centroid in the case of Fig. 14 to be at the midpoint of line AB.

In Fig. 10, inasmuch as the total change of slope between points A and B is zero due to the fixity of the ends, a simple check on the continuity of the frame is provided by the fact that the total area of the $\frac{M}{EI}$-diagram must be zero. Applying this check, and omitting E, as it is constant throughout, the total area of the $\frac{M}{EI}$-diagram $= \frac{60}{300}(237{,}220 - 245{,}400) + \frac{60}{600}(253{,}580 - 245{,}400) + \frac{90}{900}(255{,}580 - 282{,}220) = - 3{,}681$—and not zero. It follows that the moments are in error. In fact, it will be found that there are discrepancies of the order of 5%. It would probably be agreed that a check on the self-sufficiency of the results of any graphical construction is always desirable, particularly so when it may easily be applied as in the present instance.

Finally, the procedure described in Section 7 of the paper for determining deflections suffers from the inherent drawback that it involves differences of quantities that are of the same order of magnitude. Thus, very small percentage errors in either of the quantities (the determinate and the indeterminate quantities) may lead to gross errors in the value for the deflection. This point is well illustrated by Example 8, in which an increase of 1% in the value of the determinate deflection combined with a reduction of 1% in the value of the indeterminate deflection leads to an increase of nearly 23% in the value of the total deflection. If the values for rotation are considered, the comparison is even more striking. Thus, changes of 1% in the determinate and indeterminate rotations give rise to a change of more than 125% in the value of the total rotation. As both of these quantities are determined graphically, it becomes

questionable whether the graphical construction permits the attainment of a sufficient degree of accuracy.

Using the moment distribution method, the writer found in the present case that the moments at points A, E, D, and B were +242,080, −243,730, +257,270, and −267,410, respectively, as compared with the values shown in Fig. 10. These moments are readily checked, as ends A and B are fixed, and therefore the total change of slope is zero—that is, the total area of the $\frac{M}{EI}$-diagram is zero. Applying this check, $\frac{300}{60}(+242{,}080 - 243{,}730) + \frac{60}{600}(257{,}270 - 243{,}730) + \frac{90}{900}(+257{,}270 - 267{,}410) = +10$, which indicates a small residual error due to use of the slide rule. Hence, by the moment area method the value of the rotation at point D may at once be obtained as $\frac{1}{30 \times 10^6 \times 900}(257{,}270 \times 90 - 267{,}410 \times 90) = -0.0000338$ radian; and the value of the translation at point D as $\frac{1}{30 \times 10^6 \times 900}(257{,}270 \times 90 \times 60 - 267{,}410 \times 90 \times 120) = -0.05551$ in. These values should be compared with the author's values of −0.000094 radian and −0.062 in., respectively.

Elimination of all such errors in the paper as those mentioned would enable the reader better to appraise the value of this paper.

WILLIAM A. CONWELL,[12] M. ASCE.—The value of this paper is felt by the writer to lie in two characteristics: First, it is of more than academic interest; and, second, it assists in visualizing the action of a structure under loads. The first point is borne out by the fact that the author's method was developed to shorten the time required for solution of such problems in the field. This implies that the method has been successfully used in design offices and, therefore, has proved its worth in competition with other methods. The visualization of structural action obtained from this method is good. When these actions are referred to the centroid, however, there creeps into the method an element which is extraneous to the structure itself and is, therefore, somewhat of a departure. Mr. Bell relies on the methods of Castigliano in developing his thesis. In line with a visualization of a structural action, it might have been advantageous to use simply the geometry of flexure. It should be pointed out that the method is, of course, limited in application to bents of a single aisle or frames of one span.

The writer believes that, since the paper deals with a method of analysis which the author expects to compete successfully with other established methods, it should have contained some comparisons with the older methods and should have listed the advantages and disadvantages of each. He will attempt to make a few such comparisons with the thought that the author may like to comment on them in his closing discussion.

[12] Gen. Engr., Structural Eng. and Design Dept., Duquesne Light Co., Pittsburgh, Pa.

The moment-distribution method,[13] although not generally applicable to the curved structures adopted by the author in demonstrating the theory, is definitely applicable to the numerical examples illustrating his method. Moment distribution has, of course, been proved in the field. Since it relies on geometry, it is always intimately associated with the deformation of the structure and does not require the reference of deformations to any point outside the structure. Furthermore, in its application it is not limited to single spans. The writer was struck by the parallel between Mr. Bell's method and the column analogy[3] in the type of data employed. Inasmuch as all the data required for a solution of the problem by the column analogy are available before the author resorts to his circle of inertia, the point is raised as to whether its application might not be desirable. It is true that the column analogy in its working offers no information on the deformation of the structure; that knowledge must be obtained after the solution by a considerstion of the bending

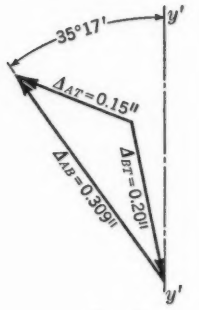

FIG. 23

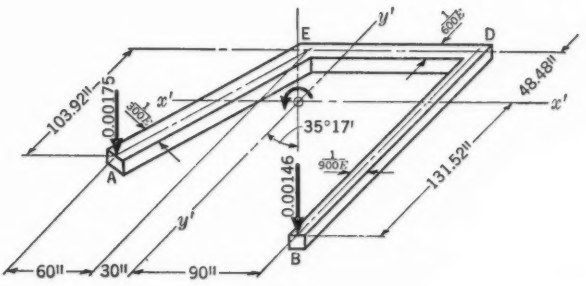

FIG. 24

moments developed. If, however, it is required to obtain quick values of the bending moments, the column analogy, which enables the computer to arrange computations in easily tabulated form, may prove an expeditious method of obtaining such results.

Example 2 is a natural one for the application of the column analogy. Fig. 23 shows the vector triangle required to obtain the relative deflections of ends A and B of the frame. Fig. 24 shows an isometric view of the analogous column for the frame, to which the angular rotations have been applied as loads and the lateral movement has been applied as a moment about the line of the movement. Values for the analogous column shown in Fig. 24 are as follows:

$$A = \frac{0.8}{E} \text{ (lb}^{-1} \text{ in.}^{-1}) \quad \ldots\ldots (43a)$$

$$I'_x = \frac{1{,}720}{E} \text{ (lb}^{-1} \text{ in.}) \quad \ldots\ldots (43b)$$

$$I'_y = \frac{3{,}600}{E} \text{ (lb}^{-1} \text{ in.}) \quad \ldots\ldots (43c)$$

[13] "Analysis of Continuous Frames by Distributing Fixed-End Moments," by Hardy Cross, *Transactions*, ASCE, Vol. 96, 1932, p. 1.

[3] "The Column Analogy," by Hardy Cross, *Bulletin No. 215*, Univ. of Illinois Eng. Experiment Station, Urbana, Ill., 1930.

and

$$I'_{zy} = -\frac{165}{E} \text{ (lb}^{-1} \text{ in.)} \ldots\ldots\ldots\ldots\ldots\ldots\ldots\ldots (43d)$$

Fig. 25 indicates the unit stresses produced in the analogous column by the application of the deflections as loads. It is seen that such stresses in the column correspond to the bending moments in the frame for which the solution

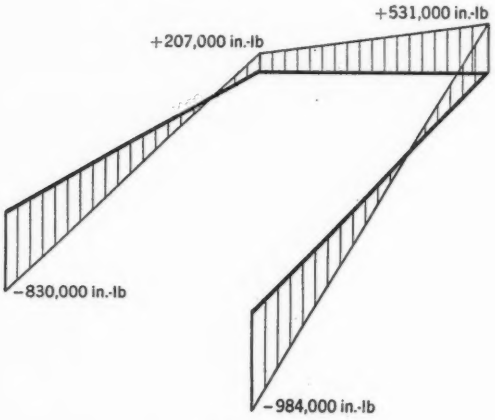

FIG. 25

is sought. Incidentally, the values of the bending moments so obtained indicate the degree of difference which might be expected between the semigraphical solution of the author and the writer's analytical slide rule work.

Mr. Bell's review of a comparison of the centroidal method with the methods treated in this discussion and with others in regular use would, it is believed, form a valuable addition to the paper.

Corrections for *Transactions:* In November, 1947, *Proceedings*, on page 1406, in Eqs. 25, change "Δ_{zT}" to "Δ_{zR}" and change "Δ_{zR}" to "Δ_{zT}." (In June, 1948, *Proceedings*, lines 42 and 43, the right-hand members should be the same as in the original.)

AMERICAN SOCIETY OF CIVIL ENGINEERS

Founded November 5, 1852

DISCUSSIONS

ELASTIC FOUNDATIONS ANALYZED BY THE METHOD OF REDUNDANT REACTIONS

Discussion

BY L. J. MENSCH, E. P. POPOV, YI-MAI YAO, JACOB FELD, AND VICTOR R. BERGMAN

L. J. MENSCH,[2] M. ASCE.—Although this method of analyzing flexible supports is ingenious, it can be improved. For symmetrical loadings, as well as for many unsymmetrical loadings, the assumption of a parabolic line of deformation will simplify the analysis. This is demonstrated for the case in

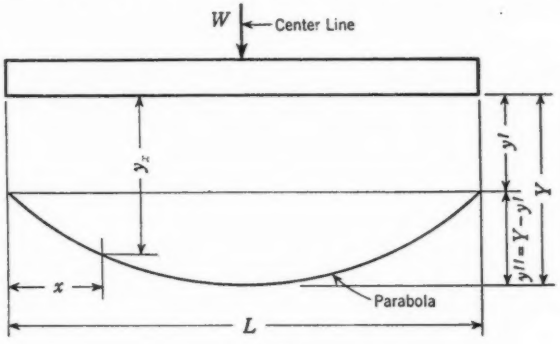

FIG. 9

Fig. 7, as shown in Fig. 9. The following formulas apply:

$$y' = k\,p' \ldots\ldots (14a)$$

$$Y - y' = k\,p'' \ldots\ldots (14b)$$

$$Y = k\,p''' \ldots\ldots (14c)$$

and

$$W = \frac{L\,y'}{k} + \frac{Y - y'}{k}\frac{2}{3}L \ldots\ldots (15)$$

At any distance, x, from one end the ordinate is

$$y_x = \frac{4\,(Y - y')}{L^2}(L\,x - x^2) + y' \ldots\ldots (16)$$

NOTE.—This paper by Zusse Levinton was published in December, 1947, *Proceedings*.

[2] Contractor, Evanston, Ill.

It is not difficult to find the moment at such a point from the parabolic distribution and from the uniform load p', since

$$M_x = \frac{4\,(Y - y')}{k\,L^2}\left(\frac{L\,x^3}{6} - \frac{x^4}{12}\right) + \frac{y'\,x^2}{2\,k} \quad \ldots\ldots\ldots\ldots (17)$$

The deflection due to the parabolic distribution and the uniform load p' is

$$Y' - y' = \int_0^{L/2} \frac{M_x \times dx}{E\,I} = \frac{(Y - y')\,L^4}{303\,E\,I\,k} + \frac{y'\,L^4}{128\,E\,I\,k} \quad \ldots\ldots\ldots (18)$$

For the values, $E = 432{,}000$ kips per sq ft, $I = \frac{27}{12}$, $k = 0.01$, and $L^4 = 810{,}000$, $\frac{L^4}{E\,I\,k} = \frac{1{,}000}{12}$, and Eq. 18 reduces to

$$\frac{12\,(Y - y')}{1{,}000} = \frac{Y - y'}{303} + \frac{y'}{128} \quad \ldots\ldots\ldots\ldots\ldots (19)$$

From Eqs. 15 and 19, it is easily found that $Y = 0.0404$ ft, $y' = 0.0213$ ft, $p''' = 4.04$ kips per sq ft, and $p' = 2.13$ kips per sq ft. In the writer's opinion the value of E should be taken as only 144,000 kips per sq ft when the initial modulus in cylinder tests is 3,000,000 lb per sq in., because of flow of the concrete due to long continued loading. In this case, Eqs. 15 and 19 give values of $p''' = 4.8$ kips per sq ft, and $p' = 0.395$ kips per sq ft. By setting $y' = 0$ in Eq. 18, the length L, at which the reactions at the ends become zero, can be found. For the values $E = 144{,}000$ and $k = 0.01$, L becomes 31.5 ft in a beam 3 ft deep.

E. P. Popov,[3] Assoc. M. ASCE.—An interesting subject—that of beams on elastic foundations—is presented in the paper by Mr. Levinton. Important applications of the theory to practical engineering projects are cited, and the point of view developed in the paper regarding the elastic foundation as equivalent to a series of redundant reactions is interesting. Likewise, the division of the total deflection of an elastic beam into three components, shown graphically in Fig. 1, is worthy of note. This interpretation clarifies the physical concepts involved in the problem, although the definition of y_{s2}, in Fig. 1, is a little ambiguous. The author's treatment of these physical concepts sheds some new light on the subject; but other phases presented in the paper seem open to criticism.

In the "Introduction," the author gives the impression that the beams analyzed were supported by a homogeneous elastic medium of infinite depth. Later, a remark is made to the effect that a solution for such beams of infinite length is available. Neither the author's solution nor the one usually available for an infinite beam is really that of a beam on an elastic continuum. A simplifying assumption, introduced in 1867 by E. Winkler,[4] is normally made—namely, that the reaction forces of the foundation are proportional to the deflection of the beam at that point. This type of an elastic foundation may

[3] Asst. Prof. of Civ. Eng., Dept. of Eng., Univ. of California, Berkeley, Calif.

[4] "Die Lehre von der Elasticität und Festigkeit," by E. Winkler, Dominicus, Prag, 1867, p. 182.

be thought of as one composed of an infinite number of independent springs. Such independence of each "spring" capable of taking a force in either direction is definitely implied in assumptions (1) and (2) in the "Introduction." This cardinal assumption holds quite rigorously in a network of beams, pressure vessels, and shells; but, for soil foundations, it can only be regarded as a practical approximation.

The chief aim of the author is to make available a method of analysis for beams on elastic foundations to the "practical" engineer. The paper avoids references, but, it should be noted, nevertheless, that "theoretical" engineers have studied the problem exhaustively. In one such work by M. Hetenyi[5] ready "exact" formulas are available for a great many cases of simple loading on beams of finite length. For complicated loadings, solutions are possible by merely substituting tabular values into formulas and by superposition. Solutions for an infinite beam on an elastic foundation form only the fundamental cases. All the necessary higher functions, as well as sines and cosines of angles, are tabulated in Professor Hetenyi's work. This information, fully compiled and developed, is now more accessible than formerly.[6,7,8,9,10]

Professor Hetenyi presents a perfectly general method for the solution of almost any conceivable loading.[11] The general method is based on an exact solution for an infinite beam. Such a beam is conditioned by certain moments and shears applied on the infinite beam so as to create zero moment and zero shear at the points corresponding to the ends of the actual beam. In this manner a part of the infinite beam between the points of zero moment and shear corresponds to the actual beam. The writer has applied such computations to Example 1 of the paper to test the merits of Mr. Levinton's method.

In addition to the aforementioned procedures giving exact solutions, a third procedure is discussed by Professor Hetenyi based on the use of trigonometric series.[12] This method appears to be particularly adaptable to practical problems. Substituting values directly into simple formulas gives an equation for the deflection of the beam. As many terms of a series as desired may be used, but in most cases one term suffices. For example, for the beam shown in Fig. 5, the equation[13] for the elastic curve due to moments alone is

$$y = -\frac{M_o \frac{2\pi}{l} \cos\frac{\pi c}{l}}{\frac{\pi^4 E I}{2 l^3} + \frac{l k}{2} - \frac{4 l k}{\pi^2}} \left(\frac{2}{\pi} - \sin\frac{\pi x}{l}\right) \ldots\ldots\ldots (20)$$

[5] "Beams on Elastic Foundation," by M. Hetenyi, Univ. of Michigan Press, Ann Arbor, Mich., 1946.

[6] "Die Berechnung des Eisenbahnoberbaues," by H. Zimmermann, W. Ernst und Sohn, Berlin, 2d Ed., 1930.

[7] "Theorie des Trägers auf elastischer Unterlage und ihre Anwendung auf den Tiefbau," by K. Hayashi, Julius Springer, Berlin, 1921.

[8] "Analysis of Beams on Elastic Foundation," by A. A. Umansky, Central Research Inst. of Auto-Transportation, Leningrad, 1933.

[9] "Analysis of Beams on Elastic Foundations," by A. N. Krylov, Academy of Sciences of U. S. S. R., Leningrad, 2d Ed., 1931.

[10] "Strength of Materials," by S. Timoshenko, Pt. II, D. Van Nostrand Co., Inc., New York, N. Y., 2d Ed., Pt. II, 1941, p. 1.

[11] "Beams on Elastic Foundation," by M. Hetenyi, Univ. of Michigan Press, Ann Arbor, Mich., 1946, p. 47.

[12] *Ibid.*, p. 69.

[13] *Ibid.*, p. 72.

In Example 2 of the paper $M_o = 120$ ft-kips; $c = 8$ ft; k is the reciprocal of Mr. Levinton's foundation constant; x is the distance to a particular point from the end of the beam in feet; and the deflection of the beam due to moments alone becomes

$$y = -0.01055\left(\frac{2}{\pi} - \sin\frac{\pi x}{60}\right) \quad \ldots\ldots\ldots\ldots\ldots\ldots (21)$$

Similar simple expressions are available to express the deflection caused by pairs of symmetrically placed concentrated loads. Adding—that is, superposing—three such equations (one for moments and two for the concentrated loads), the second example of the paper yields

$$p = k\,y + 0.60 = 4.56 + 2.95 \sin\frac{\pi x}{60} \quad \ldots\ldots\ldots\ldots\ldots\ldots (22)$$

A more accurate solution of the same problem may be readily obtained by using two terms of a series, which then yields

$$p = k\,y + 0.60 = 4.53 + 2.99 \sin\frac{\pi x}{60} + 0.051 \sin\frac{\pi x}{20} \quad \ldots\ldots\ldots (23)$$

To obtain this more accurate solution two sets of two simultaneous equations had to be solved. A comparison of values of p (in kips per square feet) computed by Eqs. 22 and 23 is as follows:

x	Eq. 22	Eq. 23
0	4.56	4.53
12	6.30	6.34
24	7.37	7.35

Thus, it must be concluded that even a one-term solution gives results sufficiently accurate for practical purposes.

In examining the method presented by Mr. Levinton and in comparing it with the foregoing procedures, the series solution appears to be superior in the opinion of the writer. No matter how complicated the given loading may be, nor how many points are selected where soil pressure is desired, the series solution gives the answer easily. All necessary calculations can be performed quickly with the aid of a slide rule. If the series solution is used, one would never be obliged to solve as many as eleven simultaneous equations, as required in Table 4; the solution of that many simultaneous equations is complex no matter how simply they may be set up.

This discussion is not to be construed as a severe criticism of Mr. Levinton's paper; it is commendable that such an important subject, well presented, can be offered for the comments of the profession. Whether one uses Mr. Levinton's method or the series solution will remain a matter of personal preference in many cases. However, it is hoped that some idea of the scope of available literature has been helpful in giving the novice, and others interested, some direction for additional study in this interesting subject.

YI-MAI YAO,[14] ESQ.—The fundamental differential equation for studying the deflection curve of a beam of infinite length embedded in a material capable of exerting equal tensive and compressive foundation modulus is

$$E I \frac{d^4y}{dx^4} = p = -\frac{y}{k} \ldots\ldots\ldots\ldots\ldots\ldots\ldots (24)$$

or

$$\frac{d^4y}{dx^4} = -(4\beta)^4 y \ldots\ldots\ldots\ldots\ldots\ldots\ldots (25)$$

in which p is the intensity of reaction, k is the foundation modulus, and the constant

$$\beta = \sqrt[4]{\frac{1}{4 k E I}} \ldots\ldots\ldots\ldots\ldots\ldots\ldots (26)$$

In general, a discussion of the bending of a beam of finite length falls naturally into three groups:[15] (1) Short beams, $\beta L < 0.60$; (2) long beams, $\beta L > 5.00$; and (3) beams of medium length, $0.60 < \beta L < 5.00$.

In discussing beams of the first group (for example, the case of a 100-kip load at the middle, as shown in Fig. 7, assuming $L = 6.95$ ft and $\beta L = 0.50$) by the rigorous method developed by M. Hetényi[16]—in which the bending of a beam of finite length on an elastic foundation can be investigated by using the equations for an infinitely long beam, together with the method of superposition—the pressure intensities at the middle and at the end are 14.41 and 14.39, respectively. Bending can be entirely neglected and the beam considered infinitely rigid with very good accuracy; hence, $p = W/L = 14.40$.

In the case of the second group, it can be assumed in investigating one end of the beam that the other end is infinitely distant. For example (Fig. 7), assuming $L = 83.4$ ft and $\beta L = 6.00$ (by the rigorous method) the pressure intensities at the middle and at the end equal 3.66 and -0.755, respectively. Treating the beam to be of infinite length, the pressure intensities at the middle and at the end equal 3.60 and -0.152, respectively.

A beam of the third group has the characteristic that a force acting on one end of the beam produces a considerable effect at the other end. Thus, such a beam must be treated as one of finite length. This is the problem discussed in the paper.

Because of the uncertainty of the physical properties of the foundation materials, either the rigorous solution or the approximation solution is merely "mathematical play." Major advantages of the author's proposed method are the avoidance of complex mathematics and the ease with which it can be learned. The minor advantage is that it can solve the following problems:

1. Bending of a beam of finite length on an elastic foundation with variable foundation modulus;

[14] Junior Engr., TangKu New Harbor Construction Bureau, TangKu, Tientsin, China.

[15] "Strength of Materials," by S. Timoshenko, D. Van Nostrand Co., Inc., New York, N. Y., 1946, Pt. II, p. 20.

[16] "Final Report of the Second Congress of the International Association of Bridge and Structural Engineering," Berlin, 1938.

2. Bending of a beam of finite length on an elastic foundation with variable $E\,I$-values; and
3. Bending of a beam of finite length on an elastic foundation with zero tensive foundation modulus.

The disadvantage of the proposed method is the tedious work of solving the simultaneous equations, especially for nonsymmetrical loading. Having determined the symmetrical and the antisymmetrical loading, the solution for any kind of loading can be obtained readily by using the principle of superposition. Hence, routine solution of the simultaneous equations is much simplified. For instance, in Example 1, the nonsymmetrical case (Fig. 10(*a*)) is solved by superposing the solutions of the symmetrical and the antisymmetrical cases shown in Figs. 10(*b*) and (10(*c*).

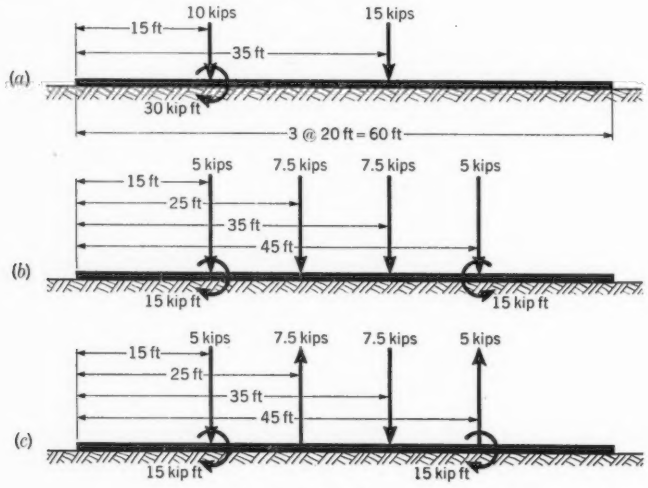

FIG. 10

For the symmetrical case, the three-panel solution (Eqs. 7*a*, 7*b*, and 8) is used. In the antisymmetrical case, since $p_1 = -p_4$, $p_2 = -p_3$, and $y_{b2} = -y_{b3}$, Eqs. 6 reduce to

$$(17 - N)\,p_1 + (39 + N)\,p_2 = \frac{1{,}080\,E\,I\,y_{b2}}{a^4} \quad \ldots\ldots\ldots (27a)$$

and

$$7\,p_1 + 6\,p_2 = -\frac{6\,M_R}{a^2} \quad \ldots\ldots\ldots\ldots\ldots\ldots (27b)$$

In Fig. 10(*b*), by Eq. 8, $N_s = \dfrac{120 \times 432{,}000 \times 5.33 \times 0.01}{20^4} = 17.28$; $E\,I\,y_{b2}$ $= 14{,}790 + 26{,}825 + 2{,}218 + 12{,}397 + 28{,}804 + 2{,}104 = 87{,}138$; and $\Sigma W = 25$. Substituting these values in Eq. 7,

$$\left.\begin{aligned} 1.72\,p'_1 + 108.28\,p'_2 &= 65.4 \\ p'_1 + \quad 2\,p'_2 &= 1.25 \end{aligned}\right\} \quad \ldots\ldots\ldots\ldots\ldots\ldots (28)$$

from which $p'_1 = +0.042$ and $p'_2 = +0.604$.

In Fig. 10(*c*), $N = 155.4$; $E\,I\,y_{b2} = 14{,}790 + 26{,}825 + 2{,}218 - 12{,}397 - 28{,}804 - 2{,}104 = 528$; and $M_R = +15 + 15 + (7.5 \times 10^{-5} \times 30) = -45$. Substituting these values in Eqs. 27,

$$\left.\begin{aligned} -34.8\,p''_1 + 194.4\,p''_2 &= 0.366 \\ 7\,p''_1 + 6\,p''_2 &= 0.675 \end{aligned}\right\} \quad \ldots\ldots\ldots\ldots\ldots\ldots (29)$$

from which $p''_1 = +0.077$ and $p''_2 = +0.023$.

TABLE 7.—PRESSURE INTENSITIES (THREE-PANEL SOLUTION) BY SUPERPOSITION

Loading	Pressure Intensities			
	p_1	p_2	p_3	p_4
Dead	+0.600	+0.600	+0.600	+0.600
Symmetrical	+0.042	+0.604	+0.604	+0.042
Antisymmetrical	+0.077	+0.023	−0.023	−0.077
Total	+0.719	+1.227	+1.181	+0.565

The total pressure intensities p are obtained by simply adding p', p'', and the pressure intensities due to the weight of the reinforced concrete slab, as shown in Table 7. In conclusion, this approximate method is very workable and accessible to the practical engineer. In the ordinary condition, the three-panel solution is simple and gives good accuracy.

JACOB FELD,[17] M. ASCE.—The results obtained from a mathematical analysis are no more accurate than the assumptions used as the basis of the formulas. The author clearly outlines his assumptions. The reader must not expect the result to agree with the actual stresses within and below a foundation unless all the assumed conditions exist in the problem being investigated. For the rigid structures floating in water or in soils of liquid consistency, the method is consistent with the physical conditions.

To extend the method to the problems of soil bearing foundations, piles, and sheet piles is not to be recommended, because of the inconsistency of assumptions and of the physical action of soils. Proportionality between settlement and pressure reaction may exist in nonplastic soils within the lower range of values, but in such soils no tension resistance can be expected. On the other hand, where some tension from adhesion or tackiness is possible, the proportionality of settlement and pressure does not exist.

In the massive foundation slabs used in the author's examples, from 3 ft to 5 ft thick, the K-values of the soil will not be much less near the ends than near the center of the beam. Actually, the edge shear resistance in some soils may result in a greater value near the edge than in the interior areas of a footing.

The results shown in Fig. 8 for piles and sheet piling are contrary to the requirements of statics. The reaction at the bottom of an embedded pile must be in the same direction as the resultant lateral load to satisfy the necessary

[17] Cons. Engr., New York, N. Y.

equality of lateral forces. The assumptions of reactions, as directly proportional to the magnitude of the soil displacement, give the impossible result of a large reaction at the surface of the soil. The more reasonable soil reaction distribution, almost always accepted, is zero at the surface. This example illustrates the necessary precaution against the use of the author's method in actual soil problems.

VICTOR R. BERGMAN,[18] ASSOC. M. ASCE.—An approximate treatment of a problem which has long attracted the more mathematically-minded engineer is presented in this paper, the noteworthy feature of which is that the author has striven, with considerable success, to reduce the mathematical refinement of analysis to a degree consistent with the effect of errors inevitably introduced by the simplifying assumptions. The latter, as stated by Mr. Levinton, are as follows:

> "(1) The foundation (or soil) is elastic, that is, its settlement at any point is proportional to the pressure at the point.
> "(2) The foundation modulus in tension is equal to that in compression. The modulus of the foundation is the elastic settlement resulting from unit pressure, or the elastic uplift that results from a unit tension."

There is ample evidence in the paper to show that the author comprehends the implications of the assumptions as he has employed them. However, it seems to the writer that the phrasing of the first assumption (and to some extent, the second) is erroneous and misleading in that it implies that the settlement at any point will be proportional to the pressure at the point if the foundation (or soil) is elastic.

The two assumptions might better read simply:

(*a*) The settlement of the foundation (or soil) at any point is proportional to the pressure at the point.

(*b*) The foundation modulus in tension is equal to that in compression. The assumed constant ratio of pressure to settlement is called the foundation modulus—

$$k = \frac{p}{y} \qquad (30)$$

As a matter of fact, even perfect elasticity of the soil would not, in general, produce proportionality between pressure and settlement. The following comments may serve to clarify this matter.

It may be instructive to start with an engineering problem in which the assumption of a constant value of k is clearly justified. Fig. 11 depicts the two rails of a single-track railway resting on a steel floor system whose principal supporting elements are the transverse beams. These transverse beams are uniform in size, length, and spacing, and are supported at their ends by main (longitudinal) girders of such large relative rigidity that the deflections of the girders may be ignored with negligible error in analyzing the distribution of the track load among the transverse beams.

[18] Vice-Pres., Godwin Constr. Co., New York, N. Y.

Here, then, is an instance in which the behavior of the foundation (the transverse beams) beneath a continuous footing (the rails) is such that the foundation reaction at any point (at any beam) is directly proportional to the deflection y at that point—that is,

$$p = k\,y \ldots\ldots\ldots\ldots\ldots\ldots\ldots\ldots\ldots\ldots (31)$$

Furthermore, with the rails clamped to the beams, "negative pressures" are possible, with foundation reactions still directly proportional to deflections. It is understood, of course, that the steel stresses remain comfortably below the yield point and, hence, below the proportional and elastic limits.

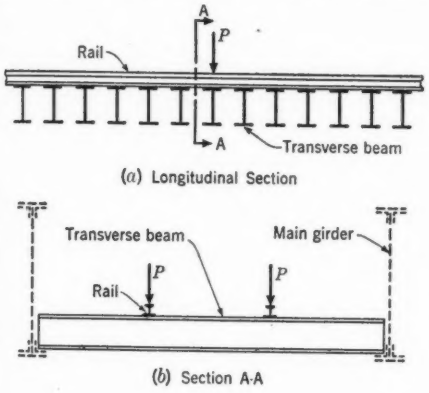

FIG. 11

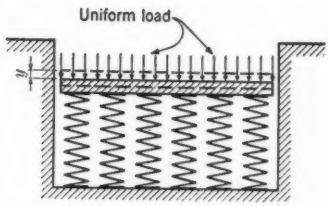

FIG. 12

To obtain such a perfect example of strict proportionality between foundation reactions and deflections, it was necessary to borrow from the bridge engineering field. It is difficult to conceive of a similarly perfect example in foundation engineering design. In fact, regarding this very matter, K. Terzaghi,[19] Hon. M. ASCE, states that

> " * * * in order to establish agreement between assumption and reality, it it would be necessary to replace the soil support of the footing by a bed of equally spaced and equally compressible springs each one of which is independent of the others."

Fig. 12 shows such an imaginary footing subjected to a uniform loading which, of course, produces a uniform settlement y, whether the footing is rigid or flexible.

It should be observed, in both Figs. 11 and 12, that the "foundations" are composed of discrete elements quite separate from, and independent of, each other, with no shearing interaction between elements. This state of zero shearing interaction does not occur in either an actual or an ideal soil subjected even to a uniform loading, if the latter is of finite extent. It does, however, exist in a liquid at rest, since shearing stresses are nonexistent in a motionless fluid. The pressure acting at any point on a body floating in a liquid is, of course, directly proportional to the depth of the point below the free surface of

[19] "Theoretical Soil Mechanics," by K. Terzaghi, John Wiley & Sons, Inc., New York, N. Y., 1943, p. 345.

the liquid—that is, to the "settlement" of the point considered. Thus, if footings were supported, not on soil, but by flotation in a very dense liquid, there would be strict compliance with Mr. Levinton's assumption of proportionality between pressure and settlement. An interesting exposition[20] of this idea has been presented elsewhere by Stanley U. Benscoter, Assoc. M. ASCE.

Consider next (Fig. 13), a perfectly flexible, continuous footing of finite length, supported on a perfectly elastic soil and subjected to a uniform loading of w pounds per square foot. As a necessary concomitant of the complete flexibility of the footing, the contact pressure between footing and soil will also be uniform and equal to w pounds per square foot. However, as the load spreads

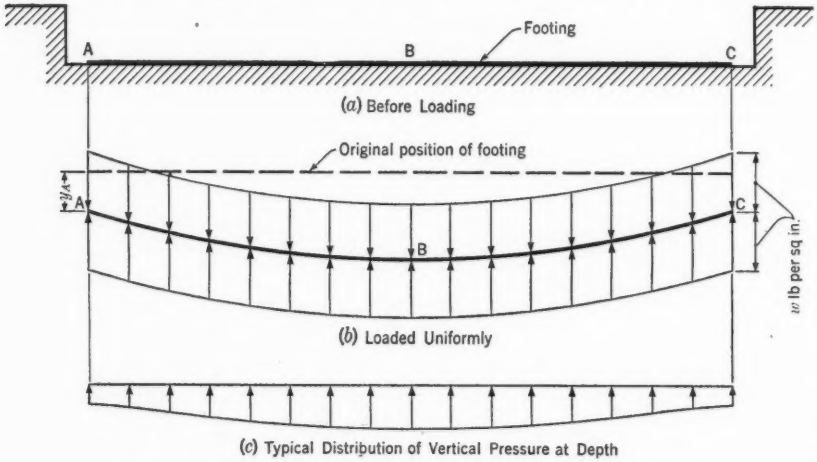

FIG. 13.—PERFECTLY FLEXIBLE STRIP FOOTING, UNIFORMLY LOADED

downward and outward through the soil, the vertical soil pressure along a horizontal line lying parallel to, but at some distance below, the longitudinal axis of the footing, will no longer be uniform, but will instead have the distribution shown in Fig. 13(*c*). It is evident that a "soil column" under the footing at, for instance, point A, will be subjected to a smaller average vertical stress than one under the center B, and will therefore undergo a smaller compression. The final position and shape (Fig. 13(*b*)) of the completely flexible footing will be determined by the unequal compressions (settlements) of the various "soil columns" beneath the footing.

Here, a uniform loading is accompanied by nonuniform deflections, and it is clear that no direct proportionality holds between footing contact pressures and corresponding settlements. Furthermore, this disproportionality would hold true even if actual foundation material (soil as found in nature) were perfectly homogeneous and elastically isotropic.

Another limiting condition worthy of consideration is illustrated in Fig. 14, which depicts an extremely rigid footing (such as a bridge pier), resting on com-

[20] "Floating Block Theory in Structural Analysis," by Stanley U. Benscoter, *Journal*, A.C.I., January, 1946 ,p. 205.

pressible soil and subjected to a centric load. Depending on the type of soil, cohesive or cohesionless, and on the depth of footing bottom below the adjacent ground surface, the base pressures will exhibit variations of the general character indicated. In Fig. 14, curve (*a*) is for a real, elastic soil ($\phi = 0$); curve

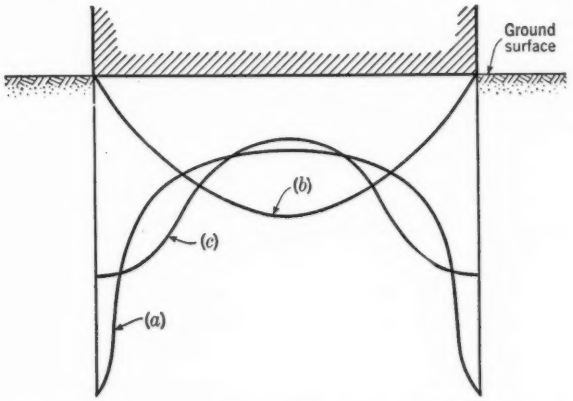

FIG. 14.—DISTRIBUTION OF CONTACT PRESSURES ON SMOOTH BOTTOM OF A RIGID FOOTING, FOR THREE DIFFERENT TYPES OF SOIL

(*b*), for a cohesionless soil ($c = 0$); and curve (*c*), for a soil intermediate between curves (*a*) and (*b*) ($\phi > 0$ and $c > 0$). (The footing is shown resting on the surface of the foundation merely in order to show the pressure variation in accentuated manner. Good practice, it hardly need be stated, dictates sinking the pier into the ground, under which condition the variations in contact pressure would be reduced to a considerable extent.) There may be some disagreement over the precise form of pressure variation, but there is little doubt that some such variations do occur. In contrast to the preceding example, which showed how uniform base pressures are accompanied by nonuniform settlements, here is an instance of uniform settlement (enforced by the rigidity of the footing), coupled with variable base pressure.

The foregoing discussion has been presented to show that the assumption of an elastic foundation does not lead to proportionality of base pressures to settlements. The examples presented show, furthermore, that in general the concept of such proportionality is theoretically unjustifiable. Nevertheless, such an assumption does provide a practical basis for mathematical treatment and consequently is frequently made. The errors thus introduced are minor enough to be acceptable, at least in some lines of investigation. S. Timoshenko states:[21]

> "* * * the simple assumption that the continuous reaction of the foundation is proportional to the deflection is a satisfactory approximation in many practical cases. For instance, in the case of railway tracks, the solution obtained is in good agreement with actual measurements."

[21] "Strength of Materials," by S. Timoshenko, D. Van Nostrand Co., Inc., New York, N. Y., Pt. II, 1941, p. 401.

Some writers on soil mechanics look with disfavor on the use of so artificial and so theoretically irrational a concept as the "coefficient of subgrade reaction." Nevertheless, what is the harassed structural engineer to do when confronted with a problem of the type treated by the author? He cannot "draw up a chair on a cloud" and discourse with Plato on ideal solutions. He must instead be pragmatist enough to accept and utilize the admittedly imperfect concept—judging its value by the practical consequences.

Professor Terzaghi and R. B. Peck,[22] Assoc. M. ASCE, state that:

> "* * * even a rough evaluation of the distribution of the real contact pressure is very cumbersome. Yet without some knowledge of the contact pressure footings or mats cannot be designed. Therefore, it is customary and necessary to estimate the contact pressure on the basis of simplifying assumptions and to compensate for the error due to these assumptions by an adequate factor of safety."

Mr. Levinton's method, although based on an assumption shown hereinbefore to be only a rough approximation to actual conditions, does provide a useful, and therefore welcome, contribution to footing analysis. For a difficult problem, he has provided a workable, practical method of analysis which takes into account the relative rigidities of footing and foundation bed. Results obtained by following the method should approximate reality more closely than do results from the two commonly adopted lines of attack—one of which treats the footing as merely an inverted, continuous, floor beam, whereas the other adopts the fictions that the footing is entirely rigid and that it produces a trapezoidal distribution of soil pressure. Of these two common methods, the first ignores the possible existence of important distributive bending moments, whereas the second may lead to calculated moments of excessive amount, resulting from failure to take into consideration the relief provided by footing flexibility.

---

[22] "Soil Mechanics in Engineering Practice," by K. Terzaghi and R. B. Peck, John Wiley & Sons, Inc., New York, N. Y., 1948, p. 214.

AMERICAN SOCIETY OF CIVIL ENGINEERS

Founded November 5, 1852

DISCUSSIONS

THE SIGNIFICANCE OF PORE PRESSURE IN HYDRAULIC STRUCTURES

Discussion

BY JOHN S. COTTON, SERGE LELIAVSKY BEY, A. H. DAVISON, R. E. BALLESTER, JOHN S. MCNOWN, AND V. T. BOUGHTON

JOHN S. COTTON, M.[26] ASCE.—This lucid demonstration of the mechanics and nature of pore pressure phenomena narrows down the uplift problem in dams to the determination of the magnitude and distribution of pore pressures for each specific condition of construction and loading. This is a great step forward in the very important and highly controversial uplift problem. It was not many years ago that some designers ignored uplift entirely.

Mr. Harza states (under the heading, "Application to a Concrete Dam"):

> "Vertical joints (such as shrinkage cracks, construction joints, and monolith joints) often, if not usually, serve as drains to reduce internal pressure as shown in Fig. 10, whereas full uplift requires that all seepage must reach the downstream face before relief of pressure."

The writer noticed such action during the recent rehabilitation work on the huge Tsao-feng-men Dam on the Sungari River in Manchuria.

This concrete gravity dam, 3,400 ft long and 300 ft high, is in a hazardous condition for a number of reasons which will not be discussed here. The dam is not complete in that large craneway benches exist on most of the downstream face. The transverse contraction joints are ungrouted; most of the concrete is of poor quality, and there are many large rock pocket lenses and poor construction joints—hence leakage is general and severe. The main objection to the leakage in this case is the freezing of the leakage water in winter and the leaching of the cement. Some of the large concrete blocks were heaved in an upward, or downstream, direction by the freezing of the leakage.

Careful examination of the leakage in the contraction joints, galleries, and shafts—as well as in the trenches, keys, and shafts excavated in the concrete

NOTE.—This paper by L. F. Harza was published in the December, 1947, *Proceedings*. Discussion on this paper has appeared in *Proceedings*, as follows: June, 1948, by William P. Creager, J. S. Kendrick, Adolf A. Meyer, E. Montford Fucik, A. C. R. Albery, and W. H. R. Nimmo.

[26] Cons. Engr., San Anselmo, Calif.

for repair work—indicates that the leakage into the transverse contraction joints decreases rapidly toward the downstream face. Although it is likely that the upstream water seals contribute to the leakage, the writer is of the opinion that most of the leakage passes into the contraction joints through the concrete and the interconnected rock pocket lenses. The plan of repair is to grout the upstream face by vertical diamond drill holes spaced 4.5 ft center to center. It is estimated that at least 1 cu ft of grout per foot of hole will be required, the grouting pressure being 100 lb per sq in.

TABLE 2.—SUMMARY OF FLOW NET STUDY OF UPLIFT PRESSURES FOR VARIOUS WATER SEAL ARRANGEMENTS
(59.2 Ft Between Transverse Joints)

Case	Location water seal No. 2[a,b]	Joints grouted[b]	Drainage[b]	Uplift on Complete Block		
				Force, in kips	Lever arm,[c] in feet	Moment,[c] in foot-kips
(1)	(2)	(3)	(4)	(5)	(6)	(7)
(a) Head Is 200 Ft and Base Length Is 166 Ft						
1	D	C	D	61,400	27.7	1,700,000
2	N	N	T, D	14,200	55.5	790,000
(b) Head Is 100 Ft and Base Length Is 83 Ft						
3	D	C	D	15,300	13.9	213,000
4	N	N	T, D	6,800	19.9	135,000
5	29.6D	N	S, D	10,000	20.6	206,000
6	29.6D	B	S, D	9,800	21.7	213,000
7	D	N	D[d]	13,400	8.4	113,000

[a] Water seal No. 1 is located on the upstream face in each case. [b] KEY: B = grouted between seals; C = grouted completely; D = downstream face; N = none; S = drainage of the joints below the second seals; and T = drainage of transverse joints. [c] About the neutral axis. [d] Drainage facilitated by ungrouted transverse joint between seals.

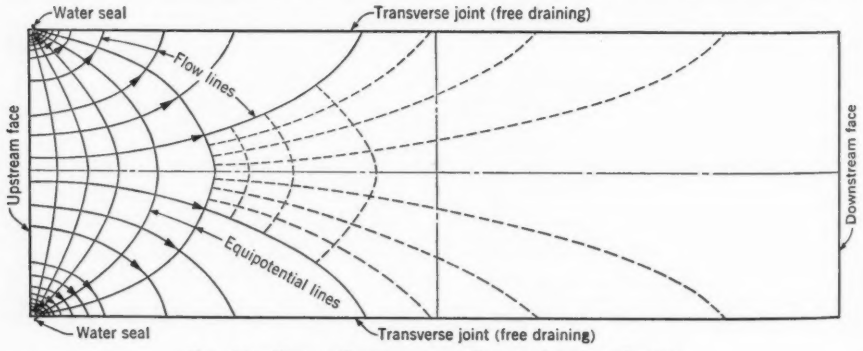

FIG. 14.—UPLIFT PRESSURES ON CENTER LINE OF BLOCKS.

The writer favors open ungrouted transverse joints in gravity dams as a method of preventing accumulation of twist moments and longitudinal thermal forces. In addition, such open joints would help reduce uplift forces. By the use of flow nets, a study was made of the uplift pressures for various water

seal arrangements. The flow nets were constructed by cut and try methods, as no electric analogy table was available. It was assumed that the concrete was uniform in porosity and that the pressure acted on 100% of the area;

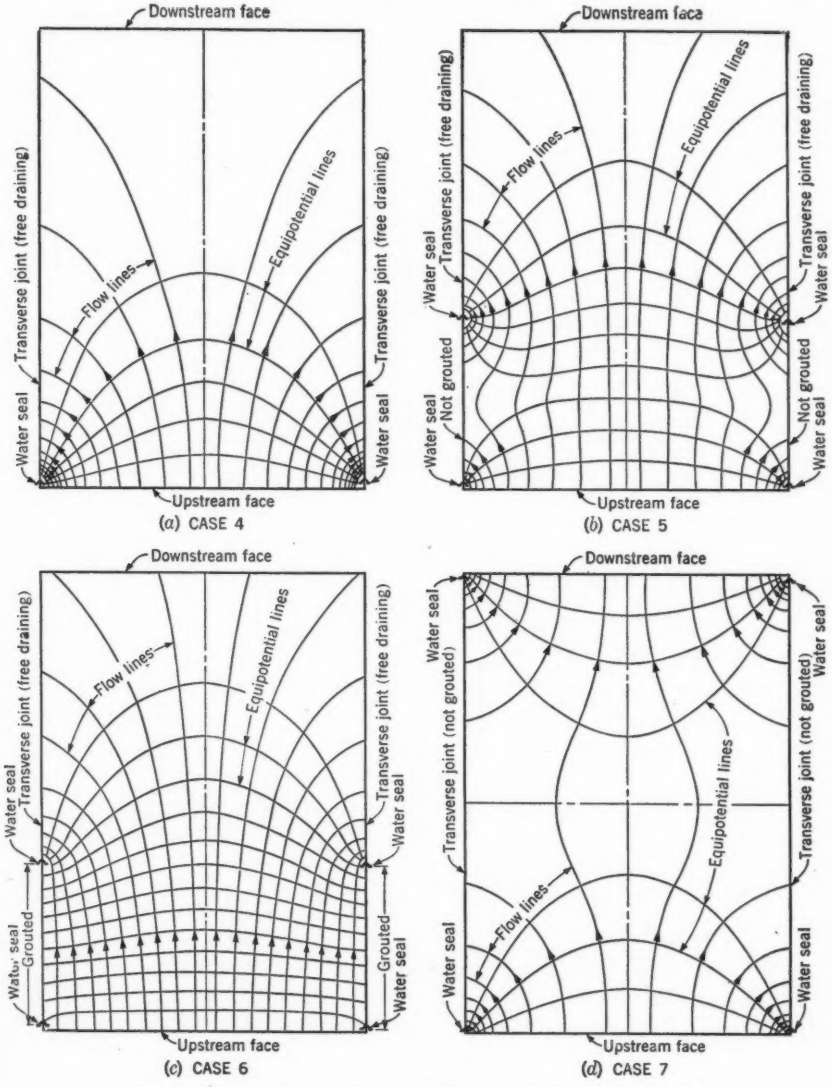

FIG. 15.—UPLIFT FORCES UNDER 200-FT HEAD (CASE 2, TABLE 2)

also, that pressure at the downstream face and in free-draining joints was 0. The results are shown in Table 2. The variation of pressure along the center lines of the blocks is shown in Fig. 14.

The uplift forces acting on 100% of the area of a completed horizontal section of dam subjected to a head of 200 ft of water are shown in Fig. 15.

This is based on the installation of water seals at only the upstream face and the absence of grout in the joints. The uplift force and the moment are only 23.2% and 46.5%, respectively, of the force and moment of a similar section where the transverse joints are grouted. The possibility of leakage at the seals because of crowding of the flow and pressure lines is obvious.

Fig. 16 shows the uplift forces acting on 100% of the area of a completed horizontal section under 100 ft of head and various conditions of transverse joint sealing and grouting. In the case of upstream seals and open joints (Fig. 16(*a*)) the uplift force and the moment are only 44.3% and 63.5%, respectively, of the force and moment of a similar section where the transverse

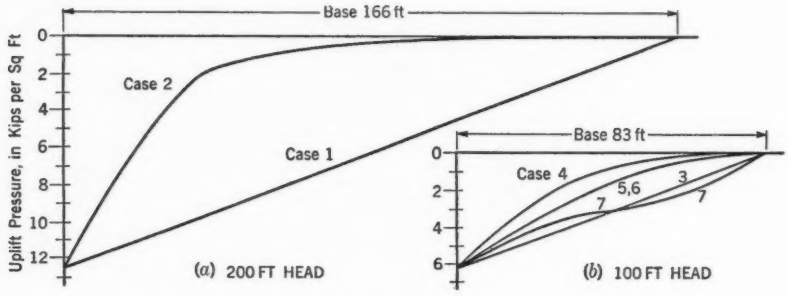

FIG. 16.—UPLIFT FORCES UNDER 100-FT HEAD FOR VARIOUS CONDITIONS IN TABLE 2
(*a*) Case 4
(*b*) Case 5
(*c*) Case 6
(*d*) Case 7

joints are grouted. As before, the likelihood of leakage at the seals is apparent. Figs. 16(*b*) and 16(*c*) show the effect of installing a second seal part way between the faces of the dam. In Fig. 16(*b*) the joints are ungrouted, and in Fig. 16(*c*) the joint is grouted between the seals. In these cases there is little reduction in uplift moment, but the uplift force is reduced to about 65%. An advantage of using two water seals in tandem in an ungrouted joint is that the twist in the block, caused by variable upstream water load, could be balanced by the unbalanced water pressure between the joints. Fig. 16(*d*) shows the effect of installing seals in the ungrouted joints at both faces of the dam, the uplift force and moment being 87% and 53%, respectively, of the uplift force and moment on a section having fully grouted joints. It will be noted that in this arrangement the variation in pressure is a reverse curve. Where there are leaky upstream seals and tight downstream seals the uplift pressure would be severe—that is, almost rectangular in shape. The flow nets for cases 1 and 3 are not shown because of their simplicity (straight lines).

The arrangements shown in Fig. 15 and Fig. 16(*a*) are the best, as far as reducing uplift and preventing the accumulation of twist moments and longitudinal thermal force, but they are conducive to leakage unless very high quality concrete is used in the vicinity of the seals. If the joints are to be grouted,

it would be best to grout the transverse joints after the dam has aged and at a time when it is under appreciable water load.

The writer has long contemplated employing a continuous vertical zone of very porous concrete located behind a very dense and highly impervious concrete upstream dam face for eliminating uplift. This porous zone would extend into the foundation, and would be connected to galleries and tunnels to provide drainage. The principal objection appears to be the possible cracking of the impervious slab.

SERGE LELIAVSKY BEY,[27] M. ASCE.—The postulate of the modern theory of resistance is that, in order to compute internal stresses, the designer must consider an element as entirely separated from the remainder of the structure by an imaginary plane, or potential surface of rupture, and he must determine the resultant of all the external forces (inclusive of such external forces as the weight and the interstitial uplift pressure) applied to this element. This resultant is then equivalent to the sum of the internal stresses acting on the assumed plane or surface of separation, from which the designer is able to determine these stresses quantitatively.

For instance, in order to compute the stresses in beam AB (Fig. 17(*a*)) the right side is separated from the left by the section *xy*, and then the inner stresses in this section are computed in such a way that their resultant and

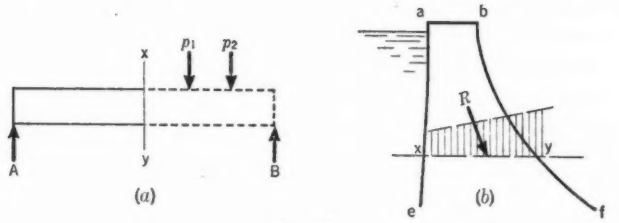

FIG. 17

moment are equivalent to the geometrical sum of all the forces on the right side (inclusive of the "active" forces $p_1, p_2, \cdots, p_n$ and of the reaction at end B). The stresses in the dam ab (Fig. 17(*b*)) are determined in the same manner, by drawing a horizontal plane, xy, separating the part, abyx, from the remainder of the structure. The resultant, R, of all the forces above xy is computed, and the stresses follow. Neither the weight of the part exyf, nor any other force which that part resists below plane xy, can affect the stresses in this plane.

This is a well-known and well-established principle which governs the entire field of modern engineering design, with the possible exception of a few instances where pure elastic theory is applied in practice. In fact, in so far as the writer knows, the method was first used by Galileo as early as the seventeenth century,[28] and, in spite of the resistance afforded by the metaphysicists of the eighteenth century, has been accepted as a teaching principle in technical schools since Navier's time (the third decade of the nineteenth century).

[27] Director, Designing Service, Reservoirs and Nile Barrages Dept., Ministry of Public Works, Cairo, Egypt.

[28] "Discorsi e Dimonstrazioni Mathematiche," Leiden, 1638.

Failure to use this principle leads the author to a basically erroneous conclusion regarding the mechanics of uplift action, particularly when he declares that the effective uplift area may be shown theoretically to be always 100%.

The literature on the uplift problem provides evidence that this is not the first unsuccessful attempt to obtain a solution from general considerations (deductive reasoning) and reveals, also, the various flaws in the conclusions thus derived. For instance, in 1934, Karl Terzaghi, Hon. M. ASCE, proved that, for the particular case of seepage in dams, the shape of the surface of separation to be adopted for the computation of stresses must depend on the microstructure of pores, and must coincide with a surface of rupture which is physically possible; in Fig. 18(*a*) Professor Terzaghi's idea[29] is applied to a pier, and in Fig. 18(*b*) the principle is applied to an elementary volume of porous structural material. In the first case the surface is represented by line ab and in the second, by line abcd.

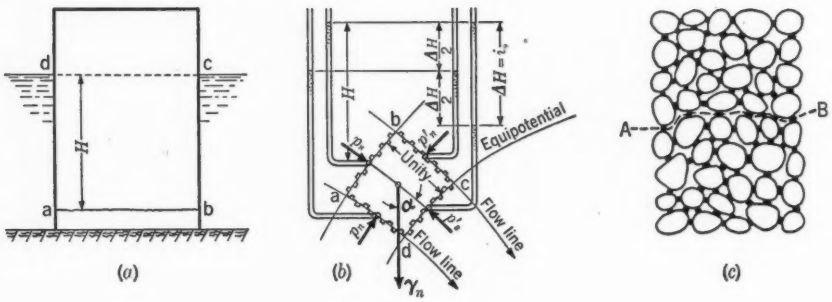

FIG. 18

The point is of considerable importance because it is thus proved that the "effective porosity," n_w, is greater than the volumetric porosity, n, and, therefore, n_w is an independent physical parameter, which cannot be arrived at by deductive reasoning. It must be found experimentally—"Der Wert n_w stellt eine unabhangige, empirsch zu bestimmende Material Konstante dar." An illustration of Professor Terzaghi's separation surface[30] is shown by section AB in Fig. 18(*c*).

Whether the Terzaghi surface of separation, or any other type of surface of separation, is assumed, it must always intersect not only "microvoids" but "microsolids," as well. Therefore, part of the area of the surface of separation, or surface of rupture, will be inaccessible to the filtering water, for the simple reason that, in materials capable of resisting tension, solid contact between elementary particles is obvious. This is substantiated by experiments, which show that the percentage of the area which is thus inaccessible to uplift action, is a measurable, empirical quantity.

Since Mr. Harza does not use the clearly defined, standard rational method of stress analysis, based on the assumed surface of separation, which engineers

[29] "Die Wirksame Flächenporosität des Betons," by Karl Terzaghi, *Zeitschrift des Oesterreichischen Ingenieur-und-Architekten Vereins*, Vol. 86, 1934.

[30] "Experiments on Effective Uplift Area in Gravity Dams," by S. Leliavsky Bey, in "Uplift Pressure in and Beneath Dams: A Symposium," *Transactions*, ASCE, Vol. 112, 1947, p. 485, Fig. 27.

employ in almost all cases during their daily design work, he is forced to resort, instead, to various comparisons and stratagems, which, by reason of their unorthodox nature and their somewhat imaginative character, cannot fail to create a certain amount of confusion, in regard to their scope, argument, and objective. In this discussion an attempt is made to systematize these various approaches, distinguishable in the paper, and to consider them seriatim.

For instance, in the text near Eq. 1 the pores are assumed flattened to form "laminations" with alternating layers of solid material and empty spaces. The object of this device is not obvious:

(*a*) The imaginary structure thus created does not resemble the true microstructure of porous solids (whatever the latter may be); and

(*b*) Such a stratified system could not resist tension at right angles to the strata, which is the main characteristic of porous solids as compared to granulated materials.

It follows then that this artificial assumption cannot serve as a starting point for deductive reasoning.

Another mental picture presented consists of projecting all the pores, contained in a volume of material, in one plane. That concept, of course, would yield an uplift on 100% of the area; but, if the stresses or pressures that occur in one plane can be projected at will into another plane, the process will never finish, and the stress intensities thus calculated will increase to infinity.

For instance, if the stresses in one section of a bridge were projected into and added to the stresses in another plane, then reprojected into a third section, and so on, the sum so obtained would be infinitely large without in any way representing the true state of stress in the material. In order to obtain a significant result, it must be based on one section only—namely, the surface of separation to which mention has been made previously (for instance, sections xy in Fig. 17(*a*) and 17(*b*)), and such surface must of necessity intersect both voids and solids which means that part of its area will be unaccessible to the interstitial water pressure.

Another point of the author's argument in defense of his thesis (theoretical 100% uplift in dams) is derived from comparison with submerged "gravel, sand, and earth." Comparisons may or may not be significant, but in this case the argument goes rather against, than for, the thesis. As Mr. Harza states (under the heading, "Buoyancy"), granulated materials when submerged in still water "* * * are reduced in weight to the full extent of the displacement of individual particles thereof * * *." If the porosity is n, the displacement of the particles per unit volume is $1 - n$, which means that, should the same principle be applied by analogy to a masonry or a concrete structure, the uplift would be $(1 - n)\ \gamma\ H$, and not $\gamma\ H$, as assumed when calculating 100% uplift for gravity dams.

A fourth concept presented in the paper is illustrated in Figs. 4 and 19. The horizontal sectional area of a pore, say, $a_1, a_2, a_3, \cdots, a_n$ is projected upward until it meets another pore, say, $b_1, b_2, b_3, \cdots, b_n$. The vertical lines joining each pair of pores represent a set of imaginary cylinders, terminated at the top and bottom by pores. Each cylinder is assumed to be subject to the

effect of two opposite hydraulic forces, F_n and f_n, the net resultant, for every cylinder, being equal to the difference $f_n - F_n$. This is offered as a theoretical demonstration of the 100% uplift action in dams.

In considering the significance of the latter demonstration, assume the cylinder used by the author as the basis of discussion, but, instead of attempting a conclusion from an isolated cylinder, extend the reasoning to its logical end, taking into account all the cylinders contained in the block above the

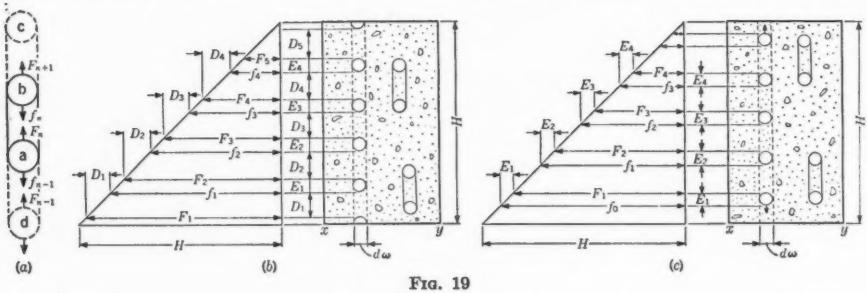

FIG. 19

surface of separation xy (Fig. (19(*b*)). In doing so, the investigator will follow a path somewhat similar to that which the author has used in Fig. 5; but, instead of assuming the base of the block to coincide with the foundation line, this base will be taken as the separation surface (Figs. 19(*b*) and 19(*c*)). The analysis will then yield both internal uplift and foundation uplift because they are indeed of the same physical nature (except, possibly, for the numerical values of the relevant constants, which may be affected by the difference in the materials above and below the separation surface).

By inspecting Fig. 19(*a*) it is obvious that, in addition to the two vertical forces, F_n and f_n, acting in every pair of pores that form an elementary cylinder, there are also two other vertical forces, f_{n+1} and F_{n-1}—that is, the upward force in the upper pore and the downward force in the lower pore. In order to take all these forces into account and to systematize the solution, it must be remembered that above pore *a* and below pore *b*, there are also many other pores. If the reasoning is to be continued to its logical end, these forces must all be taken into account. In other words, the elementary cylinder must be extended up, to the top of the concrete block, and down, to the surface of separation, xy. A column (Fig. 19(*b*)) is thus obtained having the area $d\omega$ as a base, and consisting of superposed voids and solids, in the average proportion n to $(1 - n)$, in which n is the physical porosity. Each of the solids represents the elementary cylinder visualized by the author. The resultant for all the cylinders in the column is the sum of the upward vectors, F, minus the sum of the downward vectors, f—that is,

$$\begin{aligned}\Sigma F - \Sigma f &= (F_1 + F_2 + F_3 + \cdots + F_n) - (f_1 + f_2 + f_3 + \cdots + f_n) \\ &= (F_1 - f_1) + (F_2 - f_2) + \cdots + (F_n - f_n) \\ &= D_1 + D_2 + D_3 + \cdots + D_n = \Sigma D \quad . . (15)\end{aligned}$$

It is evident from Fig. 19(*b*) that the sum of the *D*-vectors can never attain the total hydrostatic uplift H. In fact, it is clear that ΣD bears the same rela-

tion to H as $1.0 - n$ bears to 1.0, which means that

$$\Sigma D = H\,\gamma\,(1 - n)\,d\omega \ldots\ldots\ldots\ldots\ldots\ldots\ldots\ldots (16)$$

in which γ is the specific weight of water.

Attention will next be called to the fact that the argument in Fig. 19(*b*) applies to that part of the area only, in which the plane xy intersects voids. According to Delesse's law this part is $n\,\omega$, and, therefore, the total upward force thus calculated is

$$\int_0^{n\omega} H\,\gamma\,(1 - n)\,d\omega = H\,\gamma\,(1 - n)\,n\,\omega \ldots\ldots\ldots\ldots\ldots (17)$$

In addition to this force, one must also consider the part of the area (namely, $(1 - n)\,\omega$) in which the section xy intersects solid matter. The case is represented in Fig. 19(*c*). Following the same method shown in Fig. 19(*a*),

$$\Sigma F - \Sigma f = (F_1 + F_2 + F_3 + \ldots + F_n) + - (f_0 + f_1 + f_2 + \cdots + f_n)$$
$$= - (f_0 - F_1) + (f_1 - F_2) + (f_2 - F_3) + \cdots + (f_{n-1} - F_n) = - \Sigma E \ldots (18)$$

The minus sign $(-)$ shows that this is a downward vector. It bears the same relation to H as n bears to 1.00. Since the area to which this particular analysis applies is $(1 - n)\,\omega$, the total force is

$$\int_0^{(1-n)\omega} - H\,\gamma\,n\,d\omega = - H\,\gamma\,(1 - n)\,n\,\omega \ldots\ldots\ldots\ldots (19)$$

Thus, the downward force is equal to the upward force, indicating that the resultant of all the interstitial actions above plane xy (which resultant is the uplift force for this plane) is equal to zero in this case.

This result was developed from other considerations about 1913. Various attempts have since been made to explain its apparent paradox. The surface suggested by Professor Terzaghi is the true explanation, because it gives, automatically, a superficial porosity, n_w, which is greater than the volumetric porosity, n. It follows that n_w is a basic factor in the study of the uplift, and since it can only be found by tests, the value $n_w - n$ is obviously an empirical parameter.

Thus far, the writer has used the cylinder proposed by the author as the starting point of the analysis, and has shown that this leads to results that differ basically from those derived in the paper. It must now be pointed out, furthermore, that conventional assumptions such as the author's cylinder should preferably be avoided entirely, because they may easily lead to misunderstandings.

To avoid the abstract reasoning that results from such assumptions, the uplift effect must be visualized as a physical problem, and dealt with, quantitatively, as such. For instance, the following solution is often adhered to. In a porous solid capable of resisting tension and subjected to the effect of a filtering liquid, the intensity of the interstitial pressure (*Stromungsdruck*) drops gradually (hydraulic gradient) from the entrance to, to the exit from, a seepage path. In addition, a heavy liquid, such as water, is subjected to the

effect of its own weight (force of gravity) which produces an additional component of the variable pressure, depending on the relative levels of points in the microchannels (*hydrostatischer Druck*). As a result of the combined effect of these two causes, the hydraulic pressures acting on the opposite faces of an elementary pore (which constitutes an elementary length of a microchannel) are not the same.

If these infinitesimal differences are integrated for all the pores contained in a block of material, separated from the remainder by an imaginary surface of rupture, the total "force of uplift" is obtained, for that surface of rupture.

In specific applications the value of this integral can be computed as follows:[31] Consider the conditions of stability of the water contained in the pores of a solid block of material. This volume of water is subject to the effect of the following forces—(*a*) its weight and (*b*) the hydraulic pressures acting in the pores on the periphery of the block (including the external physical surfaces of the block and the imaginary surfaces of separation).

When these forces are not in equilibrium, their resultant is transmitted to the porous solid material through the interstitial pore action mentioned previously. Therefore, this resultant is the force of uplift, being equivalent to the integral of pore pressure differences. Since this reasoning is axiomatic and does not require to be substantiated by conventional assumptions about an hypothetical pore structure, informed opinion assumes as obvious, that the two methods (inductive and deductive) are equivalent.

For instance, Professor Terzaghi considers[29] that the water contained in the pores of block abcd in Fig. 18(*a*) is subject to the following forces:

(*a*) Its weight, $\gamma H A n$, in which A is the base area of the pier; H is the depth, below surface level, of the separation surface; and n denotes volumetric porosity;

(*b*) The pressures on the lateral vertical surfaces of the pier which balance each other and have no vertical component; and

(*c*) The pressure in the pores intersected by the plane of separation ab in Fig. 18(*a*). According to Delesse's law the area of these pores is $n A$, and, as the pressure is γH, it follows that the upward force acting on the water contents of the block is $\gamma H A n$.

Since the weight, defined in item (*a*), and the upward pressure, defined in item (*c*), are equal, the uplift will be zero in this case. This is a well-known result, demonstrated previously in this discussion, and quoted by other authors.

It must be realized, nevertheless, that a measurable uplift force would be found to exist in the section ab, should the separation plane be replaced by the Terzaghi surface, because, in this case, the superficial "effective" porosity, n_w, for item (*c*), would be greater than the volumetric porosity, n, for item (*a*). Therefore, the uplift would be equal to $\gamma H A (n_w - n)$.

Professor Terzaghi also analyzes the dynamic equilibrium conditions for the water contained in the pores of the elementary volume of Fig. 18(*b*). On its front and back faces (ab and cd in Fig. 18(*b*)) the pressure intensities in

[31] "Die Wirksame Flächenporosität des Betons," by Karl Terzaghi, *Zeitschrift des Oesterreichischen Ingenieur-und-Architeken Vereins*, Vol. 86, 1934, pp. 1–4.

the pores are $H\,\gamma$ and $(H - i + \cos\alpha)\,\gamma$. Multiplying these quantities by their respective areas,

$$p_s = H\,\gamma\,n_w \ldots\ldots\ldots\ldots\ldots\ldots\ldots\ldots (20a)$$

and

$$p'_s = (H - i + \cos\alpha)\,\gamma\,n_w \ldots\ldots\ldots\ldots\ldots\ldots (20b)$$

and the net difference is therefore $(i - \cos\alpha)\,\gamma\,n_w$. In the same manner, the net difference between the lateral forces p_n and p'_n is equal to $-\gamma\,n_w \sin\alpha$. In addition to these two surface forces, the water content of the element is also subject to its own weight $\gamma\,n$. Resolving these three forces, one finds an upward vertical force,

$$\gamma_a = n_w\,\gamma - n\,\gamma = \gamma\,(n_w - n) \ldots\ldots\ldots\ldots\ldots\ldots (21a)$$

and another force, acting in the direction of the flow, which is equal to

$$\gamma_s = i\,\gamma\,n_w \ldots\ldots\ldots\ldots\ldots\ldots\ldots\ldots (21b)$$

The first of these two forces is similar to the uplift acting on the pier considered in the first example, and the second is characteristic of a liquid in steady motion.

Since the resultant of all the forces acting on a volume of water in such motion must of necessity be zero, the integral of all the pressure differences transmitted from the solid to the water must be equal and opposite to the forces

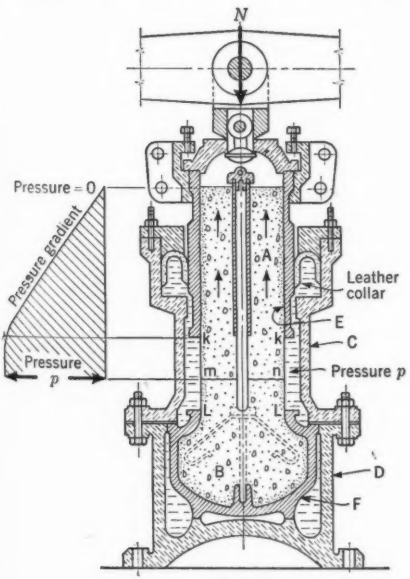

FIG. 20

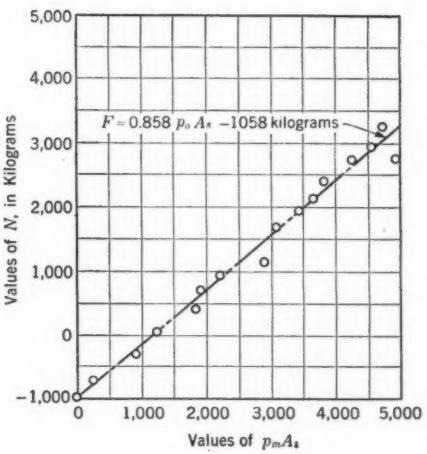

FIG. 21

γ_a and γ_s. This result indicates that the "uplift" or the total effect of the percolating water on the porous solid is equivalent to the forces γ_a and γ_s (*hydrostatischer Druck* and *Stromungsdruck*).

As a third instance, the same system of reasoning will be applied to the concrete cylinder AB, Fig. 20, which is placed in the container CD, and subjected,

at the same time, to the effect of both (*a*) the water pressure, p; and (*b*) the mechanically applied vertical load, N. For mechanical reasons (to obtain the required watertightness of connections), the test cylinder AB is provided with the top and the bottom castings, E and F, which, however, do not affect the basic process in the critical section, mn.

The pressure in the container is raised gradually so that the water penetrates through the surfaces kL into the pores of the specimen, percolates upward (as shown by the arrows in Fig. 20) and is evacuated from the top of the specimen.

At the moment when the specimen fails, the water content in its upper part (above the surface of rupture mn) is subject to two forces—(*a*) its own weight, and (*b*) the superficial pressure acting in the plane mn. The latter force is equal to $n_w A_s p_m$, in which A_s is the surface area of the section and p_m is the average water pressure in the pores intersected by the section. Since the pressure on the top of the concrete is zero, it follows that $n_w A_s p_m$ is also the uplift force transmitted by the percolating water, through pore action, to the porous material in the top of the specimen (integral of pore pressure differences). In order that this force may be capable of causing failure, it must counterbalance (1) the resistance z of the concrete, and (2) the net value, F, of all the mechanically applied downward forces (inclusive of the weight) and the force N transmitted by the rocker. One thus obtains the simple formula:

$$n_w A_s p_m = F + z \quad \ldots\ldots (22)$$

The same result can also be obtained from an elementary volume, such as abcd in Fig. 18(*b*).

For an elementary volume, in the upper part of the cylinder in Fig. 20, the force, $\gamma_s = i \gamma n_w$, is a vertical force directed upward, in which $i = dp/dh$. For the entire volume,

$$\int\int \frac{dp}{dh} n_w \, dh \, dA_s = n_w p_m A_s \quad \ldots\ldots (23)$$

in which

$$p_m = \int \frac{p \, dA_s}{A_s} \quad \ldots\ldots (24)$$

is the average pressure in section mn. Eq. 23 is the same formula as that derived by the deductive method. In this case the integral of the second force, $w \gamma (n_w - n)$, which is taken into account in calculating F, is a relatively very small value.

The author criticizes a set of experimental results obtained by the writer,[8] with the apparatus shown in Fig. 20, which disagree with his (the author's) initial conception and final conclusions.

The tests in question were conducted in such a manner that the value of the effective porosity, n_w, could be found experimentally.

The basic principle of these experiments is as follows: From Eq. 22

$$n_w = \frac{d(F + z)}{d(A_s p_m)} \quad \ldots\ldots (25)$$

[8] "Experiments on Effective Uplift Area in Gravity Dams," by S. Leliavsky Bey, in "Uplift Pressure in and Beneath Dams: A Symposium," *Transactions*, ASCE, Vol. 112, 1947, p. 444.

If, therefore, a series of identical specimens (for which the average resistance, z, is constant) is tested under various values of F, and if these values are plotted against the corresponding, experimentally determined, values of $p_m A_s$, a diagram such as Fig. 21 is obtained.

The slope of the average line in this diagram is equal to n_w. From ninety-two experiments, n_w was found to be 0.915, rather than 1.00, as claimed by the author.

In the light of these findings, the author's challenge of this result does not seem to be justified.

For instance, Mr. Harza's reference to a wedging action in connection with these tests is not relevant, because such an action does not enter into the mechanical explanation of the experiment at all. In fact, there is no more wedging action in the writer's tests than there would be in sections xy of the beam and dam in Fig. 17. It was neither stated nor implied by the writer, and may indicate that the description of the elementary aspects of the tests should have been more detailed, to avoid misunderstanding.

Mr. Harza states, also, that the failure in section mn, Fig. 20, is due to tension and not to uplift—which begs the question. The fissure is indeed caused by tension, but the tension itself is the result and consequence of the uplift force transmitted through pore action to the concrete, in the block above the separation surface.

On the other hand, although the author states explicitly that unprotected concrete subjected to hydraulic pressure is noncompressible (under the heading, "Experimental Evidence"), he nevertheless attributes the measurable results obtained by the writer (clearly defined by the slope of the average line in Fig. 21) to Poisson's ratio. This does not seem consistent, since Poisson's effect is the result of elastic deformation, and, if such deformation is impossible, its effect cannot possibly exist.

In this connection attention is called to the fact that the writer himself has stated[8] that Poisson's effect (or more precisely, the three-dimensional elastic phenomena) may have caused a secondary effect in some of his tests, in the cases when an important difference of pressure existed between the periphery and the center of the cylinder. This contingency was thoroughly considered and investigated, and was proved to be nonexistent by a statistical examination of the records.

In addition to the author's views on the effective uplift area, his paper also contains (in the "Synopsis" and the "Conclusions") the philosophy embodied in the statement (under the heading, "Application to a Concrete Dam"):

> "Hydrostatic pressure is conventionally assumed to be exerted against the upstream or back of a dam. The reasoning presented herein has proved that it is exerted progressively throughout the route of seepage. If the hydraulic gradient is uniform, as in Fig. 9(*b*), then the application of the thrust is uniformly distributed along the route of seepage from back to face."

In the writer's opinion this is the only acceptable conclusion of the paper. It was discovered in 1913, and has since been the subject of heated controversies

in German and French publications. In English, it was first stated by the writer.[8]

Although the author does not say so, the investigator is faced here with the same conditions as those in which water percolates through a granular foundation beneath a weir, which means that the methods of stress analysis applicable in one case, are also valid for the other.

It follows that Fig. 9, which is intended to represent, in the paper, the trajectories of seepage water in dams, could be much improved by the application of the theory of potential—that is, in practice, by the method of flow-net diagrams. In fact flow-net diagrams for this particular case, embodying the theory in question, have been published by Professor Terzaghi and others.

There is also much interesting material in the paper concerning such characteristics as the size of the pores, water-cement percentages, and modern concrete procedures which, however, does not seem to be relevant to its main issues.

A. H. DAVISON,[32] M. ASCE.—For its emphasis on basic engineering principles in the discussion of hydrostatic uplift on concrete gravity dams, this paper constitutes a valuable addition to the literature on the subject. The determination of hydrostatic uplift at any critical plane of the structure under investigation involves two factors: (1) The distribution of uplift force, and (2) the magnitude of uplift force. The hydraulic gradient through the structure shows that hydrostatic uplift acts over the entire horizontal area of any plane at or below the tailwater surface (TWS). In the case of any plane above the tailwater surface elevation, hydrostatic uplift acts over part of the horizontal area of that plane. The magnitude of the uplift force applied to any plane can be computed by reference to the hydraulic gradient through the structure.

Fig. 22(*a*) shows a typical section of a concrete gravity dam on rock foundation with the hydraulic gradient through the structure indicated from headwater surface (HWS) to tailwater surface. The difference in elevation between HWS and the hydraulic gradient at any point is the friction head lost by water percolating through or under the dam to that point. The uplift pressure at any point on any plane through the dam is represented by the pressure head at that point, which is equal to the vertical distance from that point to the HWS elevation less the friction head. The computed uplift on the base of the dam is represented in Fig. 22(*c*).

Fig. 22(*a*) is considered more representative of practical construction than is Fig. 9. The hydraulic gradient through the structure is theoretically limited by the straight line from points E to D. Obviously, any horizontal plane above the TWS elevation is only partly exposed to hydrostatic uplift.

M. A. Selim, Assoc. M. ASCE, has expressed the Darcy law as

$$Q = K \frac{h A}{L} \quad \ldots\ldots\ldots\ldots\ldots\ldots\ldots\ldots (26)$$

From continuity,

$$Q = A V \quad \ldots\ldots\ldots\ldots\ldots\ldots\ldots\ldots (27)$$

[32] Civ. Engr., Glens Falls, N. Y.

and

$$L = K \frac{h}{V} \ldots\ldots\ldots\ldots\ldots\ldots\ldots\ldots\ldots\ldots (28)$$

in which Q is the discharge, in cubic feet per second; h is the head, in feet; A is the gross cross-sectional area, in square feet; K is a dimensional coefficient; V is the velocity, in feet per second; and L is the length of flow path, in feet.

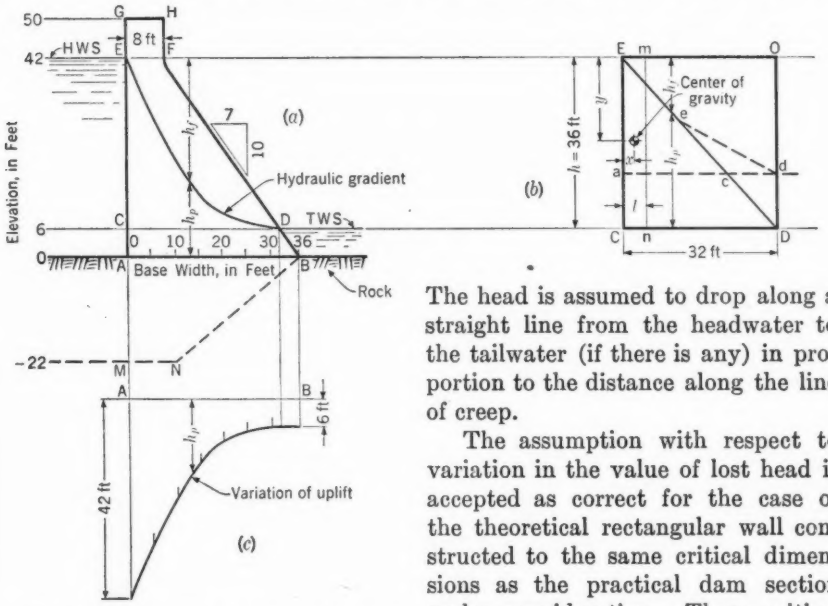

FIG. 22.—TYPICAL SECTION OF CONCRETE GRAVITY DAM ON ROCK FOUNDATION

(*a*) Hydraulic Gradient
(*b*) Theoretical Rectangular Wall
(*c*) Variation of Uplift on Base

The head is assumed to drop along a straight line from the headwater to the tailwater (if there is any) in proportion to the distance along the line of creep.

The assumption with respect to variation in the value of lost head is accepted as correct for the case of the theoretical rectangular wall constructed to the same critical dimensions as the practical dam section under consideration. These critical dimensions are (1) total head lost, and (2) total width of section as measured at the TWS elevation. For other cross-sectional shapes than the theoretical rectangular wall the variation of the lost head (or friction head) factor cannot be expected to conform to the straight line, because of the notable differences in variation of basic measurable or computable factors. These factors are (1) the distribution of the weight of the structure across the width of the section, and (2) the variation in the position of the center of gravity of accumulated sectional area across the width of the section as denoted by coordinates measured from the source of hydrostatic pressure.

Natural foundation materials, materials of construction, and pore spaces in such materials, are compressed by superimposed weight. This compressibility factor affects the friction head lost by water percolating through the mass of the structure. The mass of the structure includes that part of the foundation which is reinforced by cutoffs or otherwise made part of the above-ground structure by construction methods. The compressibility of materials and pore spaces is uniform if the superimposed weight is distributed in a uni-

form manner, as in the case of the theoretical rectangular wall. Because of the variation in weight distribution in the case of the theoretical triangular dam, and in all practical dam sections, there is a greater proportionate loss of head through or under the upstream part of the dam section. The realistic hydraulic gradient through the structure drops from HWS elevation in a curve which is concave upward.

With respect to past, satisfactory performances of existing dams, the foregoing seems to indicate a better explanation than the author's conclusion No. 6 and is confirmed by tests for uplift on existing dams.

From a structural standpoint, the base of the dam is usually the critical plane to be investigated. The modern concrete dam has such homogeneity and integrity of construction that the designer feels justified in assuming that the resultant of forces can be allowed to intersect any plane of the concrete structure above the base at or about the downstream limit of the middle third of the width of that plane. However, the foundation under the dam may be of more doubtful character, and the designer may prefer to have the resultant of forces intersect the base of the dam (which bears on the foundation) at a point near the middle of the base.

The idea that the material of a properly constructed and maintained concrete dam necessarily becomes saturated in a manner similar to the material of an earth dam does not appeal to the writer. There are many examples of relatively thin concrete bulkhead walls, decks of hollow dams, and the like, which are watertight for all practical purposes. Even the existence of occasional pinhole leaks and seepage through such structures appears to have no necessary connection with the hydraulic gradient through the structure. Even though a concrete dam has been constructed or repaired with a facing, on the upstream side, of wrought iron plate to exclude percolation through the structure, it has a hydraulic gradient as evidenced by piezometer pipes to the foundation.

With respect to present practice in assuming uplift, as stated by the author in conclusion No. 1, as a design expedient an equivalent triangle or trapezoid is often substituted for the computed uplift diagram shown in Fig. 22. This expedient may perhaps be manipulated in a manner which would justify the author's statement. Common assumptions by authorities are (1) uplift of $\frac{2}{3}\,h$ at the heel decreasing to zero at the toe, and (2) uplift of $\frac{2}{3}\,h$ at the heel decreasing to $\frac{1}{3}\,h$ at the toe—h representing the net hydrostatic head.

Since determination of hydrostatic uplift is the principal issue, it appears that the most direct approach is to compute the hydraulic gradient and attendant friction head loss through the structure from consideration of the basic factors of (1) compressibility, (2) weight distribution, (3) location of the center of gravity for progressive strips across the width of the base, and (4) the Darcy law.

Fig. 22(*b*) shows the theoretical rectangular wall corresponding to the practical section with respect to the critical dimensions of total head loss for total width of section at the TWS elevation. The straight line ED is the hydraulic grade line for the theoretical section, and area ECD is the total uplift on plane CD. Should the TWS be considered to rise from elevation CD

to elevation ad, area ecd is made equal to area cdD, and the hydraulic grade line becomes the broken line Eed. For a 1-ft length of homogeneous concrete gravity dam, l is the width and A is the area of progressive strips of the section, with x and y the corresponding coordinates of the center of gravity.

Friction head loss through the structure may be expressed by

$$h_f = K\,[w\,A\,(y + x)]^n \ldots\ldots\ldots\ldots\ldots\ldots (29)$$

in which h_f is the friction head, in feet; w is the weight of structure, in pounds per cubic foot; n is an exponent which varies with circumstances; and K is a dimensional coefficient which varies with circumstances. For a homogeneous structure or an equivalent one, like the concrete dam under discussion, the formula may become

$$h_f = K_1\,[A\,(y + x)]^n \ldots\ldots\ldots\ldots\ldots\ldots (30)$$

Modification of Eq. 30 may be required to apply it to a specific problem.

The writer's procedure includes tabulating the different elements for various values of l. The first step involves tabulation of the elements for Fig. 22(b), and satisfying the criterion that h_f must vary in a straight line from HWS to TWS. This means that computed values of the compound factor $[A\,(y + x)]^n$, or some modification thereof across the section must plot in a straight line. To do so, it is determined that the factor should be $\left[\frac{A\,(y + x)}{1{,}000} - 1\right]^{0.7}$ for the sections shown in Fig. 22.

The second step is to determine the value of coefficient K_1 in the formula. This value of K_1 for the specific problem is established by considering that part of Fig. 22(a) which is bounded by the limiting elevations HWS and TWS that determine the total lost head with which the specific problem is concerned. The formula is solved for K_1 by substituting the known value of 36 for h_f when $l = 32$. The value of K_1 is determined as 4.14, and the formula applicable to Fig. 22(a) becomes

$$h_f = 4.14\left[\frac{A\,(y + x)}{1{,}000} - 1\right]^{0.7} \ldots\ldots\ldots\ldots\ldots\ldots (31)$$

The remaining steps consist of applying Eq. 31 to the computation of the hydraulic gradient applicable to the total section area of Fig. 22(a), or any modification thereof, as long as the original ratio of total lost head to section width is maintained. For example, the total section area may include a grouted foundation area AMNB, which is an equivalent concrete area representing the effectiveness of grouted rock foundation through holes 20 ft deep under the heel. The equivalent concrete area is made 22 ft deep at the heel as shown in Fig. 22(a) because the specific gravity of rock foundation has been assumed 10% greater than concrete; for this total section the computed hydraulic gradient would drop from the HWS elevation somewhat more sharply than the hydraulic gradient curve drawn in Fig. 22(a) for the section above plane AB, before curving around to point D at the downstream face.

According to the writer's experience, computed hydraulic gradient curves are in practical agreement with results of current sound design practice and

with reports by authorities of investigations of hydrostatic pressure occurring after construction in various dams of similar type in the United States and Europe. For gravity dams of earth, concrete, or masonry, 1 lin ft of dam is the unit length considered. For hollow concrete dams or cellular type retaining wall construction, the unit length is the average spacing of buttresses or counterforts. (An earth dam is not considered of homogeneous construction. The material in the middle of the dam is more compact and has a greater unit weight than the material which forms the outer shells, and the factor of saturated weights needs consideration.)

Apparently there is little need to fear for the safety of existing structures that have been soundly designed, constructed, and maintained.

R. E. BALLESTER,[33] ESQ.—With a precision not previously found in the technical literature the author undertakes to evaluate the uplift that may occur in the cross section of a dam—particularly in a gravity section. Many uncertainties confront the designer in his effort to analyze the theoretically ideal dimensions of a gravity dam—so many, in fact, that a prominent Spanish mathematician and engineer, Alfredo Peña Boeuf, has declared (the writer's translation from the Spanish): "Gravity dams are not subject to computation."[34]

The major uncertainty is the effective value of uplift—its magnitude and the area over which it acts. General practice in Europe is to assume that an uplift force acts over the entire horizontal area. The official 1925 regulations of the Italian Government[35] applying to the design of dams reflect this general practice clearly (the writer's free translation from the Italian adapting Mr. Harza's notation):

> "In the design computations, uplift shall be assumed to vary linearly from
>
> $$P_u = h\,\omega\,c \qquad (32)$$
>
> at the upstream face of a given horizontal section, to zero at the downstream face of that section."

In Eq. 32 P_u is the total uplift; h is the hydrostatic head acting on the given section; ω is the unit weight of water; and c is a reduction coefficient which is constant for the entire height of the dam but which varies, between different dam sections, from $\frac{1}{3}$ to 1. Inasmuch as uplift area does not enter the definition of c, it is implicit that 100% area is assumed except in so far as the intensity of uplift may differ between 100% and 33% for different conditions.

The author discusses the characteristics of a hypothetical uplift force acting on a selected part of a horizontal cross section and, in progressive steps, undertakes to show that the entire area is affected since it is impossible to have a condition in which the concrete and the material in the foundation bed and in the bedrock are each entirely impermeable.

Referring to Fig 5(*b*), consider a cube with a specific weight less than water, or an empty crystal glass with a perfectly flat, smooth bottom. This cube or

[33] Prof. of Applied Hydraulics, Univ. of Buenos Aires, Buenos Aires, Argentina.

[34] "Grandes Estructuras y Presas," by Alfredo Peña Boeuf, Revista de Obras Publicas, Editor, Madrid, 1934, p. 65.

[35] "Annali delle Utilizzazioni delle Acque," Vol. III, No. 3–4, Rome, 1926, Article 21, p. 94.

crystal glass will remain on the bottom as water is poured into the receptacle, if the fit between bottom surfaces of contact is so perfect as to exclude water seepage. This ideal condition is unattainable with mortar, concrete, and rock faces. Furthermore, the cube or crystal glass in Fig. 5(*b*) may be porous, in which case the water will seep through the pores and thus create a pressure on the bottom plane of contact. In practice, a dam section will have a bouyant force at the plane of the foundation and at every other plane or seepage path through the dam. This is a statement of the author's thesis, supported by text demonstrations.

According to Eq. 32, the magnitude of uplift is the product of hydrostatic pressure and the cross-sectional area, modified (for different dams) by a predetermined reduction coefficient. To which of the two quantities—pressure or area, or to the product of the two—should the reduction coefficient be applied? The writer believes that the logical factor to be modified is the pressure, which can actually be reduced by increasing friction values or by changing paths of percolation. Nothing ever changes the cross section of a dam as long as it is in service.

The conclusions in this paper establish extremely conservative rules for the design of large dams. Conclusion No. 6 offers five explanations to account for the satisfactory performance of dams built under less conservative assumptions. One of these (conclusion No. 6(*c*)) is: "The time required to saturate a large dam, even with constantly full reservoir." In support of this conclusion the writer can cite an inspection, in 1942, of the San Roque Dam in Córdoba, Argentina, which was built in 1888. The structure is no longer in service.

A tunnel was bored through the dam at an elevation about 46 ft below the spillway crest, which was the normal level of the reservoir. The center-line length of the tunnel (41 ft) represented the width of the dam section at that elevation. The downstream face of the dam was perfectly dry, showing no signs of percolation; but at distances of from 2 ft to 3 ft in from the downstream face the mortar was humid and, when first revealed, began to sweat small drops of water. The general appearance of the exterior gave the impression that the dam was entirely free from seepage and consequent uplift, completely belying the true condition of the interior.

It will behoove designers to give attentive consideration to the author's comment, beginning with Fig. 11, concerning the round-head buttress type of dam. It is an extraordinary fact that, although this design concept originated in the United States, it has never been built there. There will be stresses in the thin sections of concrete as the result of pore pressure, as well as danger from disintegration of concrete resulting from seepage flow. In the light of the author's comment concerning this rare type of dam, engineers who have had practical experience with it should consider it a duty to record their findings.

JOHN S. MCNOWN,[36] Assoc. M. ASCE.—Although the method for evaluating the magnitude of uplift forces acting on masonry dams is not yet completely developed, the author has determined one of the factors by demonstrating

[36] Associate Prof., Dept. of Mechanics and Hydraulics, and Research Engr., Iowa Inst. of Hydr. Research, State Univ. of Iowa, Iowa City, Iowa.

convincingly that the total base area is affected by uplift. Now attention should be focused on determining the pressure magnitude and on re-examining present design criteria in the light of these findings.

The concept of a concrete dam as a porous structure introduces two factors which heretofore have not received consideration: (1) Uplift, as determined by the internal pressures, may act on the full area of any horizontal section, and (2) the hydrostatic force is distributed along the paths of seepage. Although both of the factors have been considered by the author, several points must be clarified. The impression is given (under the heading, "Application to Concrete Dam") that some uncertainty exists in determining the pattern of

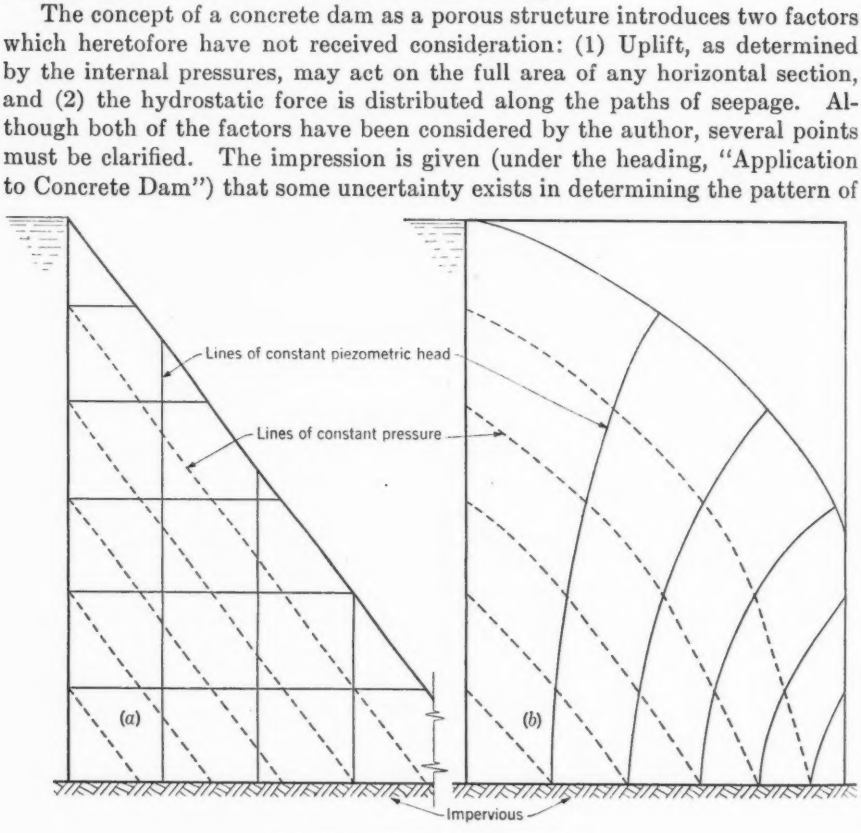

FIG. 23.—PATTERN OF SEEPAGE FOR:
(*a*) Triangular Dam
(*b*) Rectangular Dam

seepage through porous media. On the contrary, for any geometrical configuration a unique solution exists. Although exact analyses are often impossible, approximate solutions can be obtained graphically or by electrical analogy. In addition, direct methods of mathematical approximation have been developed in the past few years[37,38] which permit the solving of any problem of two-dimensional seepage, including determination of the free streamline.

For the triangular dam shown in Figs. 9 and 23(*a*), the result is very simple, the streamlines and lines of constant piezometric head being, respectively, the horizontal and vertical lines shown in Fig. 23(*a*). Lines of constant pressure are shown as dotted lines, and the uplift pressure distribution has the

[37] "Relaxation Methods in Engineering Science," by R. V. Southwell, Clarendon Press, Oxford, 1946, p. 191.

[38] "Photoelasticity," by M. M. Frocht, John Wiley & Sons, Inc., New York, N. Y., 1948, Chapter 8.

simple triangular form indicated by the author. However, this solution is unique, and Fig. 9(*c*) and the related discussion are, therefore, irrelevant.

Usually the flow pattern is far more complex than that shown in Fig. 23(*a*) and the author's generalization to the rectangular cross section is somewhat oversimplified. The solution obtained by mathematical approximation, shown in Fig. 23(*b*), differs considerably from that indicated in Fig. 9(*d*). The distributions and centers of pressure are compared in Fig. 24; the moment of the uplift pressure about the toe is 10% greater for the correct distribution than for the triangular approximation. Fortunately, much of the increase in overturning moment is characteristic of the rectangular shape; for orthodox sections the increase would be relatively small.

The simplifying assumption of an impervious foundation material is at one extreme. Since the foundation porosity may equal or even greatly exceed that of the dam, the other extreme is also of interest. A direct solution is available for an impervious dam,[39] the result, of course, being independent of the shape of the dam. The pressure variation is defined by

$$\frac{p}{p_0} = \frac{1}{\pi} \cos^{-1} \left(\frac{2x}{B} - 1 \right) \ldots\ldots\ldots\ldots\ldots\ldots\ldots\ldots (33)$$

in which p is the unit uplift pressure at any point along the base; p_0 is the unit uplift pressure at the upstream face of the dam; and x is the distance from the upstream face. The average pressure is $\frac{p_0}{2}$ and the center of pressure

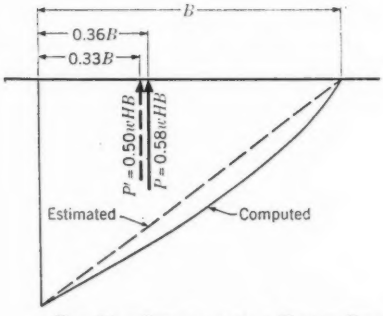

FIG. 24.—COMPARISON OF UPLIFT FORCES

is three eighths of the distance from the heel of the dam to the toe as shown in Fig. 25; the moment about the toe is 0.312 $w\,B\,H$. The relative porosities will fix the result for given conditions somewhere between the two extremes.

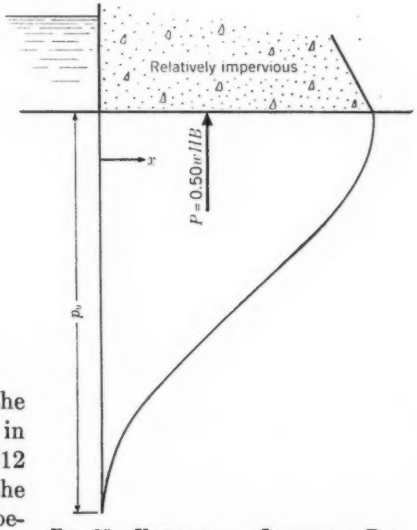

FIG. 25.—UPLIFT ON AN IMPERVIOUS DAM

The second effect of porosity—the distribution of the hydrostatic force along lines of seepage—is unimportant in the determination of external forces acting on a structure. However, the effect on internal forces may become

[39] "Higher Mathematics for Engineers and Physicists," by I. S. Sokolnikoff and E. S. Sokolnikoff, McGraw-Hill Book Co., Inc., New York, N. Y., 1934, pp. 452–454.

important, particularly where the seepage lines are curved horizontally, as shown in Figs. 10 and 11. It is an easy matter to prove that incremental forces act everywhere in the direction of flow by considering the forces on the differential element shown in Fig. 26. If horizontal flow is assumed,

$$dF_s = \left[\left(p - \frac{\partial p}{\partial s}\frac{\Delta s}{2}\right) - \left(p + \frac{\partial p}{\partial s}\frac{\Delta s}{2}\right)\right]\Delta n \cos\frac{\Delta\theta}{2} \ldots\ldots (34a)$$

and

$$dF_n = \left[\left(r - \frac{\Delta n}{2}\right) - \left(r + \frac{\Delta n}{2}\right)\right] p\,\Delta\theta + \left[\left(p - \frac{\partial p}{\partial s}\frac{\Delta s}{2}\right) + \left(p + \frac{\partial p}{\partial s}\frac{\Delta s}{2}\right)\right]\Delta n \sin\frac{\Delta\theta}{2} \ldots (34b)$$

in which F_s and F_n are the forces along and at right angles to the streamline, respectively.

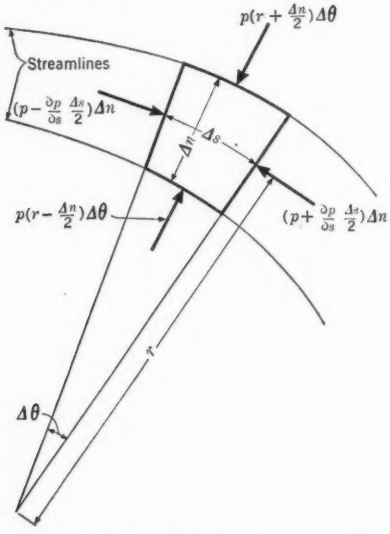

FIG. 26.—FORCES ON A DIFFERENTIAL ELEMENT

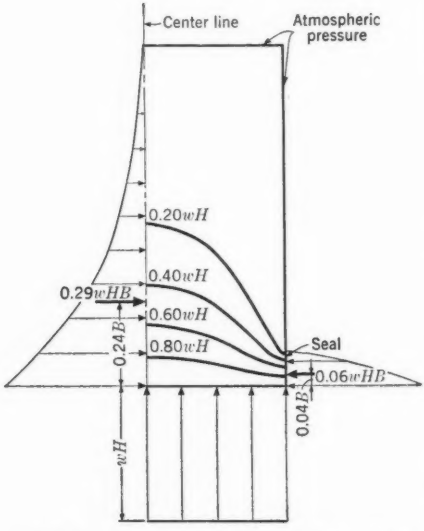

FIG. 27.—PATTERN OF HORIZONTAL SEEPAGE IN A MONOLITH

Inasmuch as the element under consideration is small, the approximations—

$$\cos\frac{\Delta\theta}{2} \approx 1 \ldots\ldots (35a)$$

$$\sin\frac{\Delta\theta}{2} = \frac{\Delta\theta}{2} \ldots\ldots (35b)$$

and

$$\Delta\theta = \frac{\Delta s}{r} \ldots\ldots (35c)$$

—are permissible. After substitution and simplification,

$$dF_s = -\frac{\partial p}{\partial s}\Delta s\,\Delta n \ldots\ldots (36a)$$

and

$$dF_n = 0 \ldots\ldots\ldots\ldots\ldots\ldots\ldots\ldots\ldots\ldots (36b)$$

The resultant force at any point is, indeed, along the streamline. In a monolith of a gravity dam, drainage from the joints along the sides (see Fig. 10) could produce appreciable tensions in longitudinal sections. For an idealized case of two-dimensional flow in a horizontal section through such a structure (that is, neglecting the downward component of flow), the pattern of flow is as shown in Fig. 27. The total tension at the axis of symmetry is the difference in the total pressures for the conditions assumed. In this case, which is somewhat extreme, a force of 0.23 w B H urges the two halves of the structure apart.

In clarifying one phase of uplift computation, the author has made a major technical contribution which may lead to modification of design criteria for masonry dams. However, uncertainties still exist, and no immediate changes are indicated. Evaluation of the porosity of concrete should permit determination of the time required for establishment of a steady seepage pattern. Field measurements may be required, because the effect of surface tension cannot be ignored; the dislodgment of air bubbles in small passageways can necessitate large forces. The solution of these and related problems should come much sooner as a result of the reorientation given to further investigation.

V. T. BOUGHTON,[40] M. ASCE.—The skilful way in which Mr. Harza leads his reader to his basic assumption serves to conceal its fundamental weakness. Neither observed conditions in well-built dams nor reasoning based on those observations gives support to that basic assumption or the conclusions drawn therefrom.

Mr. Harza's basic assumption (under the heading, "Application to a Concrete Dam") is:

> "* * * that concrete [in a dam with a full reservoir] is internally buoyant as truly as loose granular material, and that it obeys all the hydraulic and hydrostatic laws of loose granular material."

Stripped of all nonessential details and mathematics, what Mr. Harza wants the reader to believe, in order to give substance to his conclusion, is that the cement paste in concrete is so porous that water from the reservoir behind the dam moves through its pores just as it would through loose granular material, and that the pores are so numerous and interconnected as to place every particle of cement and sand and each piece of aggregate in the concrete in a state of buoyancy similar to that produced by free submergence in open water. This buoyancy, Mr. Harza states (also under the heading, "Application to a Concrete Dam"), is fully effective "* * * from back to face of dam, since each elementary vertical cylinder between pores would be buoyant."

If this statement were true, then water would exude freely from the walls of inspection galleries in large dams and would run down the face of such dams when atmospheric humidity was at or close to 100%.

Mr. Harza would have the reader believe further that the pore pressure, which he considers as acting throughout the entire mass of the dam:

[40] Associate Editor, *Engineering News-Record*, New York, N. Y.

> "* * * is as applicable at any one horizontal section as another, instead of being confined to pour joints, base contact with rock, or other horizontal planes of greater permeability or weakness."

Also, because his basic assumption places every elemental unit of the dam below water level in the reservoir in a state of bouyancy, he holds that the mass of the dam that is effective in resisting overturning is reduced by the amount of the buoyancy of almost the entire section of the dam below water level.

To show that the condition of buoyancy envisioned by Mr. Harza cannot be "fully effective * * * from back to face of dam," even though it might be true of concrete in the upstream face of the dam, it is only necessary to point to the fact that it cannot possibly be true of the concrete exposed in the downstream face of the dam. There "each elementary vertical cylinder" of concrete cannot be in a state of submergence because one side is in open air. Any moisture that is in that concrete adds to its weight instead of detracting from it by buoyancy action. Therefore, even though Mr. Harza may be correct as to his assumption with respect to the elementary units of concrete in the upstream face of the dam, somewhere between the two faces there must be a reversal in the condition of the elementary units of concrete from a condition of submergence and buoyancy to one of nonsubmergence and no buoyancy.

As to where this reversal takes place, Mr. Harza's own basic assumption that the cement paste is so porous as to permit relatively free movement of water into the concrete would seem to require the further assumption that water can also move out of the concrete toward the downstream face with equal freedom. Hence, the more logical place to locate this reversal point under his theory of porosity would be somewhere near the middle of the dam, not at the downstream face as Mr. Harza does when he used his internal buoyancy theory to demonstrate that uplift must be considered as acting over 100% of the horizontal area of the dam.

However, conditions in the inspection galleries of large dams, and the results of tests on the permeability of relatively thin sections of concrete of a density similar to that used in the face of modern dams, indicate quite clearly that the condition of buoyancy envisioned by Mr. Harza does not actually exist in the area between the midpoint and the upstream face.

In this connection, Mr. Harza's own statement in his discussion of uplift, under the heading, "Application to a Concrete Dam," seems to deny the logic of his reasoning that leads him to conclude that pore pressure is effective throughout the mass of the dam. He states:

> "Vertical joints (such as shrinkage cracks, construction joints, and monolith joints) often, if not usually, serve as drains to reduce internal pressure * * * whereas full uplift requires that all seepage must reach the downstream face before relief of pressure. Therefore, theoretical pressure probably seldom exists, except near the upstream surface as measurements verify and the theoretical is merely a mathematical limit of possibility. Such drainage reduces the magnitude of uplift pressures, but nothing can reduce the effective uplift area below 100% wherever pores are filled with water. Herein lies the fallacy of the usual assumption of one-half or two-thirds area for uplift, which it is the principal purpose of this paper to correct."

Mr. Harza states that measurements verify the fact that pressure seldom exists "except near the upstream face"; and further that his conclusion that it is effective, even though reduced in magnitude, over 100% of the horizontal cross-sectional area at any point in the dam provided that "the pores are filled with water." Nevertheless, a logical application of his basic assumption that all the hydraulic laws which apply to granular material must be applied to concrete makes it impossible for all the pores over 100% of a horizontal cross section of the dam to be filled with water.

If the concrete is so porous that it "obeys all the hydraulic and hydrostatic laws of loose granular material," then the water that comes in through the upstream face ultimately would drain out through the downstream face; and, since concrete dams have a narrow section in relation to their height (as compared to the earth dam shown in section in Fig. 8(*a*)), the line of saturation would be quite steep, not flat, as in an earth dam of uniform composition such as is shown in Fig. 8(*a*). Obviously, to maintain such a line of saturation would require that the concrete in the dam be much more porous than any concrete ever put in a well-built dam.

As it appears certain that the pores in any horizontal section through a dam of concrete, assumed to be so porous that the hydraulic laws governing loose granular material apply to it, cannot be filled with water under hydrostatic pressure from the reservoir behind the dam, the conclusion is inescapable that uplft could not act over 100% of any cross-sectional area.

Consequently, it would appear that Mr. Harza has not demonstrated that the normal assumption of uplift acting over only one half, or two thirds of the area of the base of a dam built of good quality concrete is unsafe, or illogical.

AMERICAN SOCIETY OF CIVIL ENGINEERS

Founded November 5, 1852

DISCUSSIONS

SHEARING STRESS DISTRIBUTION IN BOX GIRDERS WITH MULTIPLE WEBS

Discussion

BY J. G. CLARK AND W. E. HANSON

J. G. CLARK,[11] ASSOC. M. ASCE, AND W. E. HANSON,[12] ASSOC. M. ASCE.—Designers of civil engineering structures can benefit greatly from knowledge of various methods of analysis developed primarily for use in airplane design. It is unfortunate that literature pertaining to civil engineering structures does not present more of these methods in detail; therefore, the author should be commended for presenting to civil engineers the concept of shear flow in multiple-cell structures with thin webs. There are many other references supplemental to the one given by the author, among which the work of Alfred S. Niles, Assoc. M. ASCE, and Joseph S. Newell,[13] and Elmer F. Bruhn[14] should be mentioned.

The author's omission of the development of Eq. 3 might imply that it is exact. It can be allowed only if the walls are thin so that the shear stress can be assumed uniformly distributed across the thickness. The equation also neglects the shear components normal to the center line of the walls, which are small in comparison with those tangent to the center line of the walls in any structure such as the example used by the author. One of the relationships used in the derivation of Eq. 3 is

$$q = \frac{T}{2A} \quad \ldots\ldots\ldots\ldots\ldots\ldots\ldots\ldots\ldots\ldots (19)$$

which assumes that the member is free to warp (since there are no longitudinal stresses in the direction that tends to resist warping) and that the general shape of the section remains the same as the member warps. To make the common

NOTE.—This paper by A. S. Nieman was published in February, 1948, *Proceedings*. Discussion on this paper has appeared in *Proceedings*, as follows: June, 1948, by John E. Goldberg.

[11] Associate Prof. of Civ. Eng., Univ. of Illinois, Urbana, Ill.

[12] Asst. Prof. of Civ. Eng., Univ. of Illinois, Urbana, Ill.

[13] "Airplane Structures," by Alfred S. Niles and Joseph S. Newell, John Wiley & Sons, Inc., New York, N. Y., 3d Ed., 1943.

[14] "Analysis and Design of Airplane Structures," by Elmer F. Bruhn, John S. Swift & Co., Cincinnati, Ohio, 1943.

terminology of Eq. 19 agree with the notation of the paper, $T = M_t = 2 A q$ as used subsequently in Eq. 21.

If Eq. 3 is used to compute the angle of twist of a cell (or cells) when torsion exists at the section, it is important that θ be defined as the angle of twist per unit of longitudinal length. With the author's definition of θ, the left side of Eq. 3 should be divided by the longitudinal span of the structure.

Design loads for many structures may not pass through the shear center and the resulting torsion may be of considerable magnitude. It is clear from the symmetry about a vertical axis in Fig. 2 that the vertical shear must be applied along the vertical center line for zero torsion; but, if a transverse load is to be applied to the structure without torsion at the section, the line of action of the load is not immediately evident. An extension of the paper to include the calculations necessary to locate the vertical position of the shear center as part of an example of case II would add greatly to the value of the paper.

For any multicelled structure subjected to torsion in addition to flexure, such as shown in Fig. 2, the writers suggest the following procedure.

(*a*) Assume a distribution of shear flow, q_1, as outlined by the author in step 1.

(*b*) Correctional shear flows (constant within a given cell) must be applied to the assumed shear flows of step (*a*) in order to have the angle of twist equal for all cells. By the application of Eq. 3, write an equation similar to Eqs. 4*a* and 4*b* for each cell, keeping θ as an unknown along with the unknown correctional shear flows for each cell. Thus, the number of equations will equal the number of cells.

(*c*) One more equation is required since θ, the angle of twist per unit of span length, is also unknown in this case. This additional equation is obtained as the author states. The torque of the internal shearing forces (assumed and correctional) can be found from statics using any convenient moment center. Equating this internal torque to the torque of the external shear force about the same moment center will give the additional equation required.

(*d*) Solving for the correctional shear flows in the equations of steps (*b*) and (*c*) (preceding), and adding these corrections to the assumed shear flows of step (*a*), giving proper consideration to signs (direction of flow), the final shear flow, in each wall of all the cells, is obtained.

If the multicelled section is to be analyzed for various conditions of loading, the writers recommend the tabulation of the shear flows for the following:

(1) A convenient load (say, 1,000 kips) acting vertically through the shear center;

(2) A convenient load acting horizontally through the shear center; and

(3) A convenient torque at the section.

Then it is possible, by use of the proper ratios and by superposition, to obtain quickly the shear flows resulting from any torque producing load. If this method is used the location of the shear center must be known in order to determine the torque resulting from a load with both vertical and horizontal components. Consequently, the writers have shown the additional calcula-

tions necessary to locate the vertical position of the shear center in one of the following examples which considers a horizontal load on the structure.

The following examples consider, first, the author's vertical load of 12,000 kips applied along B′E′G′, Fig. 9, and, secondly, a horizontal load of 1,000 kips

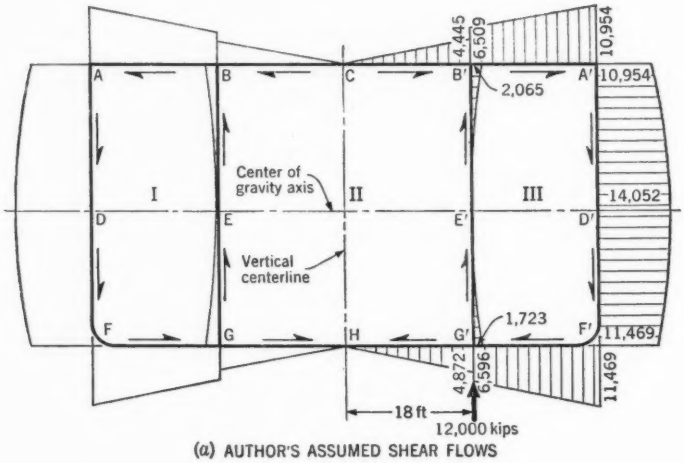

(*a*) AUTHOR'S ASSUMED SHEAR FLOWS

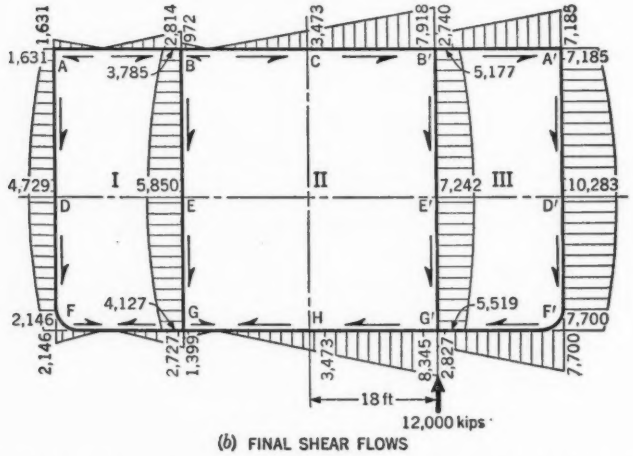

(*b*) FINAL SHEAR FLOWS

FIG. 9.—DIAGRAMS OF SHEAR FLOWS, IN POUNDS PER INCH OF PERIMETER, FOR A 12,000,000-LB LOAD ACTING VERTICALLY, 216 IN. TO THE RIGHT OF THE CENTER LINE

applied along ABC, Fig. 10. Then, for both cases, it is evident by inspection that there is torque at the section.

In their work the writers have used definitions of terms that differ from the paper, as follows:

r = perpendicular distance, in inches from a wall to the center of moments;

q_1 = assumed shear flow at any point, in pounds per inch of perimeter, due to the applied load; and q_I = a constant correctional shear flow at any point, in pounds per inch of perimeter, in cell I, necessary for conditions of continuity and static equilibrium (when the q-values are clockwise, the sign is positive);

θ_I = angle of twist in cell I, in radians per inch of length along the span of the member; and

A_I = area of cell I, in square inches.

Similarly, q_{II}, θ_{II}, and A_{II} apply to cell II, and q_{III}, θ_{III}, and A_{III} apply to cell III. For continuity, $\theta_I = \theta_{II} = \theta_{III}$, in which

$$\theta_I = \frac{\sum q_1 \frac{\Delta L}{t}\begin{bmatrix}\text{for}\\ \text{cell}\\ \text{I}\end{bmatrix} + q_I \sum \frac{\Delta L}{t}\begin{bmatrix}\text{for}\\ \text{cell}\\ \text{I}\end{bmatrix} + q_{II} \sum \frac{\Delta L}{t}\begin{bmatrix}\text{for}\\ \text{wall}\\ \text{BG}\end{bmatrix}}{2 A_I G} \quad \ldots (20a)$$

$$\theta_{II} = \frac{\sum q_1 \frac{\Delta L}{t}\begin{bmatrix}\text{for}\\ \text{cell}\\ \text{II}\end{bmatrix} + q_I \sum \frac{\Delta L}{t}\begin{bmatrix}\text{for}\\ \text{wall}\\ \text{BG}\end{bmatrix}}{2 A_{II} G} + \frac{q_{II} \sum \frac{\Delta L}{t}\begin{bmatrix}\text{for}\\ \text{cell}\\ \text{II}\end{bmatrix} + q_{III} \sum \frac{\Delta L}{t}\begin{bmatrix}\text{wall}\\ \text{B'G'}\end{bmatrix}}{2 A_{II} G} \quad \ldots (20b)$$

and

$$\theta_{III} = \frac{\sum q_1 \frac{\Delta L}{t}\begin{bmatrix}\text{for}\\ \text{cell}\\ \text{III}\end{bmatrix} + q_{II} \sum \frac{\Delta L}{t}\begin{bmatrix}\text{for}\\ \text{wall}\\ \text{B'G'}\end{bmatrix} + q_{III} \sum \frac{\Delta L}{t}\begin{bmatrix}\text{for}\\ \text{cell}\\ \text{III}\end{bmatrix}}{2 A_{III} G} \quad \ldots (20c)$$

Computing moments about any convenient point, the fourth equation becomes

$$M_t = 2 A_I q_I + 2 A_{II} q_{II} + 2 A_{III} q_{III} + \sum q_1 r \Delta L \begin{bmatrix}\text{for all walls}\\ \text{in cells}\\ \text{I, II, and III}\end{bmatrix} \quad \ldots (21)$$

Other definitions not listed are the same as those given by the author, but it should be pointed out that the writers have used all dimensions, in inches, all areas, in square inches, and the moment of inertia, in inches to the fourth power. This was done to avoid confusing multiplication factors in the writing of Eqs. 20 and 21.

Except for special cases, it is necessary to include calculations for all three cells. Consequently, in the following examples, the structure used by the author is shown in Fig. 9(*a*) with the cells numbered I, II, and III, from left to right. Also, the letter symbols on the right half have a prime for the purpose of identification.

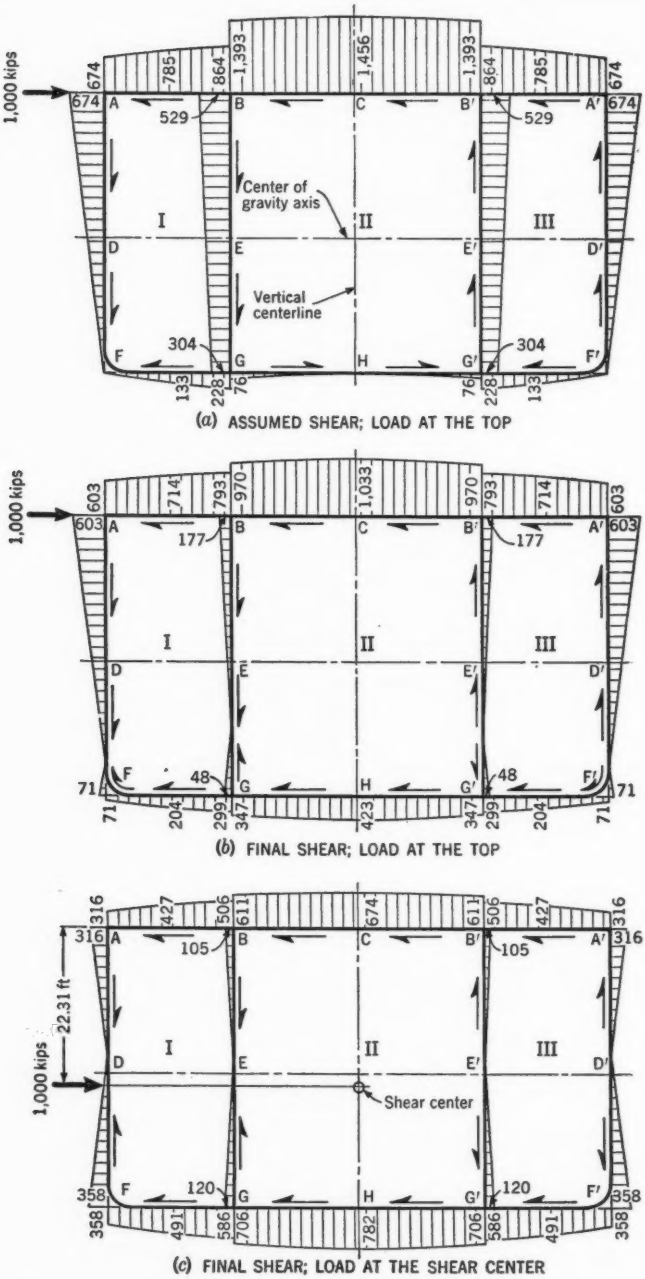

FIG. 10.—DIAGRAMS OF SHEAR FLOWS, IN POUNDS PER INCH OF PERIMETER, FOR A 1,000,000-LB LOAD ACTING HORIZONTALLY

Vertical Load With Torque.—For Mr. Neiman's 12,000-kip load applied vertically, but at a distance of 18 ft to the right of the center line, the assumed shear flow is reproduced in Fig. 9(*a*). The assumed shear flow is in equilibrium with the external force both horizontally and vertically; however, the twisting moments are not in equilibrium. Also, the conditions of continuity are not satisfied—that is, the three cells do not have equal rotations. Therefore, it is necessary to compute correctional shear flows for each cell. Substituting in Eqs. 20 and 21, point H being the center of moments for M_t, the following four equations are obtained and can be solved simultaneously:

$$\theta_{I} = \frac{-14{,}620{,}824 + 2{,}233.6\, q_{I} - 960\, q_{II}}{207{,}360\, G} \quad \ldots\ldots\ldots\ldots (22a)$$

$$\theta_{II} = \frac{0 - 960\, q_{I} + 3{,}187.20\, q_{II} - 960\, q_{III}}{414{,}720\, G} \quad \ldots\ldots\ldots\ldots (22b)$$

$$\theta_{III} = \frac{+14{,}620{,}824 - 960\, q_{II} + 2{,}233.6\, q_{III}}{207{,}360\, G} \quad \ldots\ldots\ldots\ldots (22c)$$

and

$$M_t = 12{,}000{,}000 \times 216 = 207{,}360\, q_{I} + 414{,}720\, q_{II} + 207{,}360\, q_{III} + 0 \ldots (23)$$

In Eqs. 22*a* and 22*c* the value of 1,218,402 from Table 1 has been multiplied by 12 to give 14,620,824 since the writers wish to have ΔL in inches. From the solution of these simultaneous equations, the following correctional shear flows, in pounds per inch, are obtained: $q_I = +9{,}323$; $q_{II} = +3{,}473$; and $q_{III} = -3{,}769$. For a length of span of 100 ft, the value of $\theta_I = \theta_{II} = \theta_{III} = 0.0865°$. When correctional shear flows are added algebraically to the assumed shear flows the final shear flows are as shown in Fig. 9(*b*).

TABLE 3.—ASSUMED SHEAR FLOWS FOR 1,000,000 LB ACTING HORIZONTALLY

Member	ΔA (in.²)	z (in.)	$z\,\Delta A$ (in.³)	q_1[a] (Lb per In.)	q'_1 (Lb per In.)	$\frac{\Delta L}{t}$	$q'_1 \frac{\Delta L}{t}$ (cell I)	$q'_1 \frac{\Delta L}{t}$ (cell II)
(1)	(2)	(3)	(4)	(5)	(6)	(7)	(8)	(9)
F	..	..	..	0	..	..	..	..
A(F)	360	432	155,520	− 674	− 337	640	−215,680	..
B(A)	135	324	43,740	− 864	− 779.7[b]	345.6	−269,460	..
G(F)	162	324	52,488	+ 228	+ 126.7[b]	288	+ 36,490	..
G(H)	162	108	17,496	− 76	− 25.3	288	..	− 7,290
B(G)	240	216	51,840	± 529	± 416.5	960	+399,840	−399,840
C(B)	135	108	14,580	−1,456	−1,435	345.6	..	−495,940
Σ							− 48,810	−903,070[c]

[a] q_1 is obtained by multiplying $\frac{V}{I}$ by $\Sigma z\,\Delta A$; the summation is from a point of assumed zero shear flow.
[b] To obtain this value it was necessary to compute the shear flow at midpoint of this wall (Fig. 10(*a*)).
[c] −903,070 × 2 = − 1,806,140.

Horizontal Load With Torque.—For the second example using a horizontal load of 1,000 kips acting to the right along ABC, Fig. 10, the assumed shear flows are determined as based upon the assumption that the shear flows at

F, F′, H are zero. Table 3 indicates the computations for the determination of the values of q_1, the assumed shear flows. The moment of inertia of the entire cross section about the vertical center line is 230,667,000 in.⁴ The values of q_1 are plotted in Fig. 10(*a*).

The values of the average assumed shear flows, q'_1, are given in Table 3, Col. 6. By multiplying these shear flows by their respective wall lengths the horizontal and vertical forces can be obtained. The sum of the vertical forces is equal to zero and the sum of the horizontal forces is equal to the applied load of 1,000,000 lb. However, the sum of the twisting moments of these vertical and horizontal forces is not equal to the twisting moment of the applied load about a center of moments. Also, the rotations of the three cells are not equal. By substituting in Eqs. 20 and 21, the following four equations involving the angle of twist and the three correctional shear flows, necessary to satisfy statics and continuity completely, can be obtained:

$$\theta_{\mathrm{I}} = \frac{-48{,}810 + 2{,}233.6\, q_{\mathrm{I}} - 960\, q_{\mathrm{II}}}{207{,}360\, G} \quad \ldots\ldots\ldots\ldots (24a)$$

$$\theta_{\mathrm{II}} = \frac{-1{,}806{,}140 - 960\, q_{\mathrm{I}} + 3{,}187.2\, q_{\mathrm{II}} - 960\, q_{\mathrm{III}}}{414{,}720\, G} \quad \ldots\ldots\ldots (24b)$$

$$\theta_{\mathrm{III}} = \frac{-48{,}810 - 960\, q_{\mathrm{II}} + 2{,}233.6\, q_{\mathrm{III}}}{207{,}360\, G} \quad \ldots\ldots\ldots\ldots (24c)$$

and

$$M_t = M_B = 0 = -205{,}105{,}000 + 207{,}360\, q_{\mathrm{I}} + 414{,}720\, q_{\mathrm{II}} + 207{,}360\, q_{\mathrm{III}} \ldots (25)$$

Point B is taken as the center of moments for M_t (Table 4). The moment of the applied load about point B is zero.

TABLE 4.—MOMENTS ABOUT POINT B OF q'_1 FOR HORIZONTAL LOAD

Member (1)	q'_1 (lb per in.) (2)	ΔL (in.) (3)	r (in.) (4)	M_B (in.-lb) (5)
AB	779.7	216	0	0
BB′	1,435	432	0	0
B′A′	779.7	216	0	0
FA	337	480	216	− 34,940,000
GB	416.5	480	0	0
G′B′	416.5	480	432	− 86,365,000
F′A′	337	480	648	−104,820,000
FG	126.7	216	480	+ 13,133,000
GG′	25.3	432	480	− 5,246,000
G′F′	126.7	216	480	+ 13,133,000
Σ				−205,105,000

Solving Eqs. 24 and 25 simultaneously: $q_{\mathrm{I}} = +71$; $q_{\mathrm{II}} = +423$; and $q_{\mathrm{III}} = +71$—all in pounds per inch.

These correctional shear flows, added algebraically to the assumed shear flows, give the final shear flows for the horizontal load of 1,000 kips applied along ABC (see Fig. 10(*b*)).

Horizontal Load Through Shear Center.—To locate the shear center of this cross section vertically, the assumed shear flows shown in Table 3, Col. 5,

could be used for a horizontal load of 1,000 kips. Then, in order to have zero twist in all three cells, correctional shear flows must be added to these assumed shear flows. The correctional shear flows can be determined by substituting in Eqs. 20 and equating θ_I, θ_{II}, and θ_{III} to zero. These equations are the same as those for horizontal load with torque, except that the angle of twist is equal to zero. Solving these three simultaneous equations, the following correctional shear flows, in pounds per inch, are obtained: $q_I = +358$; $q_{II} = +782$; and $q_{III} = +358$. The final shear flows for 1,000 kips acting horizontally through the shear center are obtained by adding these correctional shear flows algebraically to the assumed shear flows (see Fig. 10(*c*)).

To determine the vertical location of the shear center, the moments about some point can be computed and the moment divided by the applied load will give the vertical distance from the center of moments to the shear center. In this case, point B has been taken as the center of moments because the moments about point B for the assumed shear flows were computed in Table 4. To these are added the moments about point B of the correctional shear flows listed in the preceding paragraph; thus: The vertical distance from point B to the shear center is

$$\frac{-205{,}105{,}000 + 207{,}360\ (358) + 414{,}720\ (782) + 207{,}360\ (358)}{1{,}000{,}000};$$

that is, 267.68 in. or 22.31 ft. As thus computed and shown in Fig. 10(*c*), the shear center lies on the vertical center line 22.31 ft below the top of the cross section.

The shear flows (in pounds per inch) for a twisting moment of 1,000,000 lb times 267.68 in., or 267,680,000 in.-lb can be determined by taking the algebraic sums of the correctional shear flows for the horizontal load with torque and for the horizontal load through shear center as follows:

$$\begin{aligned} q_I &= 71 - 358 = -287 \\ q_{II} &= 423 - 782 = -359 \\ q_{III} &= 71 - 358 = -287 \end{aligned}$$

This may be done because the assumed shear flows in both cases are equal. The shear flows for other twisting moments can be obtained by applying the proper ratio to these values. As part of the check on the solution of a vertical load of 12,000,000 lb applied 18 ft to the right of the center line, the foregoing shear flows should be multiplied by $-12{,}000{,}000 \times 216 = -2{,}592{,}000{,}000$ and divided by 267,680,000 which will give the following values (in pounds per inch):

$$q_I = -287\left(\frac{-2{,}592{,}000{,}000}{+267{,}680{,}000}\right) = +2{,}778$$

$$q_{II} = -359\left(\frac{-2{,}592{,}000{,}000}{+267{,}680{,}000}\right) = +3{,}475$$

$$q_{III} = -287\left(\frac{-2{,}592{,}000{,}000}{+267{,}680{,}000}\right) = +2{,}778$$

When these values are added algebraically to the author's final shear flows for a vertical load through the shear center, the results should be the same as shown in Fig. 9(*b*), or if these values are added to the author's correctional shear flows, the results should agree with the writers' correctional shear flows for vertical load with torque. This comparison is as follows:

$$q_{I} = +6{,}544 + 2{,}778 = +9{,}322\ (+9{,}323)$$
$$q_{II} = 0 + 3{,}475 = +3{,}475\ (+3{,}473)$$
$$q_{III} = -6{,}544 + 2{,}778 = -3{,}766\ (-3{,}769)$$

AMERICAN SOCIETY OF CIVIL ENGINEERS

Founded November 5, 1852

DISCUSSIONS

EXPERIMENTAL DETERMINATION OF VIBRATION CHARACTERISTICS OF STRUCTURES

Discussion

BY F. B. FARQUHARSON, AND J. J. SLADE, JR.

F. B. FARQUHARSON,[22] M. ASCE.—The problem of the dynamic behavior of structures is one which should arouse more interest in the civil engineering profession than has hitherto been the case; and, by and large, it seems to be mainly those who have become associated with the aircraft industry who have shown the principal interest. The author is to be congratulated on the simplicity of his instrument and the ease with which it can be operated.

A troublesome matter involving the attention of a few engineers relates to the damping inherent in the modern suspension bridge. Laboratory study and mathematical analysis have both indicated that the oscillation of a suspension bridge under the action of wind may be greatly affected by the over-all damping (both structural and aerodynamic) existing on the structure.

The aerodynamic portion of the total damping can be obtained from model tests in a wind tunnel, but that portion arising from the interaction of the various parts of the structure and from the internal damping (solid friction) in the material of which the structure is built cannot be obtained from a model, nor can it be calculated. It appears that the solution for the latter part of this problem lies in the artificial vibration of the prototype itself in still air. This procedure is not new on bridges[23] but in the past it has been applied principally to railway structures of high stiffness and, consequently, of relatively high natural vibration frequencies. The instrument described by the author covers a frequency range from 150 cycles per min to 3,000 cycles per min, whereas it is estimated that a complete compilation of field data from existing suspension bridges could be confined within a range of from 5 cycles per min to 20 cycles per min.

NOTE.—This paper by Samuel J. Loring was published in December, 1947, *Proceedings*. Discussion on this paper has appeared in *Proceedings*, as follows: March, 1948, by Alexander Klemin; and June, 1948, by R. K. Bernhard, Carl A. Ludeke, and M. J. Turner.

[22] Director, Eng. Experiment Station, and Prof., Civ. Eng., Univ. of Washington, Seattle, Wash.

[23] "Dynamic Tests by Means of Induced Vibrations," by Rudolf K. Bernhard, *Proceedings*, A.S.T.M., Vol. 37, 1937, Pt. II, p. 634.

Not the least attractive feature offered by the author's proposal is the fact that extreme excitation of the structure is not required. All the alternative methods discussed for use on the suspension bridge have involved significantly large amplitudes of oscillation. Furthermore, the devices under consideration involve serious interruption of the traffic which, together with a required amplitude of from 12 in. to 15 in. of vertical motion, might make it difficult to obtain permission for a clinical study on some of the most important bridges.

The application of the author's system to a suspension bridge involves complications, arising out of low frequency and great weight, which would require a radical departure from the simple design of the existing vibration mode analyzer. An example of the difficulty involved arose through correspondence with the author some months ago, when it was pointed out that a simple extension of the existing instrument would require the spring suspension of a mass capable of executing linear vertical vibrations at a natural frequency of 6 cycles per min. This condition implies a static deflection of the spring of 81 ft.

The special problem surrounding the suspension bridge involves the need of measuring both vertical and torsional vibration characteristics. In the course of the continued study of the application of the theory contained in the paper, it seems that it might be possible to provide an instrument not exceeding 2 tons in weight which might be mounted on a truck and used in the investigation of a series of representative structures.

J. J. SLADE, JR.,[24] ESQ.—This is an interesting method of detecting the normal modes of vibrations of full-scale structures that, because of the lightness of the equipment required, should prove useful in field tests. The interpretation of the results obtained by this method, however, raises a question which, in the writer's opinion, deserves investigation.

The classical theory of small oscillations, on which the author's theoretical work is based, assumes that coupling of the various members of a structure, to the motion of which the theory applies, may be considered perfect for sufficiently small displacements and velocities. If this assumption is made, then, if a point in a structure suffers a displacement x, the force $F(x)$ that opposes this displacement may be taken to be an analytic function of x near the zero value of the displacement and therefore may be written

$$F(x) = a_0 + a_1 x + a_2 x^2 + \cdots \quad (66)$$

If x is measured from the unstrained position, $a_0 = 0$ since $F(0) = 0$, and if x is restricted to sufficiently small values, the powers higher than the first may be neglected. Under these conditions the expression for the restoring force becomes

$$F(x) = a_1 x \quad (67)$$

in which a_1 is the generalized Hooke's constant. Thus, the essential nonlinearity of the force (Eq. 66) is eliminated.

Let the "upper nonlinearity" be the nonlinearity suppressed by the theory of small oscillations. The writer wishes to call attention to a "lower non-

[24] Director, Eng. Experiment Station, Rutgers Univ., New Brunswick, N. J.

linearity" that exists whenever coupling is imperfect and which may show its effects when the amplitude of the displacement is too small. When such a condition exists, Eqs. 66 and 67 are invalid for extremely small values of x, although they may still be used for ordinarily small values of the displacement when these are greater than those required to insure complete coupling. The smallness of a displacement for dynamical purposes must be estimated with respect to the intrinsic geometry of a structure, of course, and not with respect to the observational limit imposed by a measuring technique.

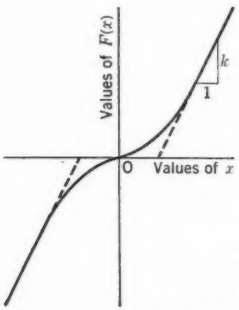

FIG. 5.—RESTORING FORCE IN GRADUALLY COUPLING MASS-SPRING SYSTEM

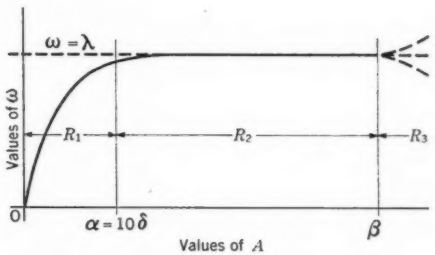

FIG. 6.—DEPENDENCE OF FREQUENCY ON AMPLITUDE

Consider, for example, a simple mass-spring system in which the spring coupling occurs gradually through small displacements about the unstrained position. A possible form of the restoring force in such a system is shown in Fig. 5. This type of restoring force may be represented by an expression such as

$$F(x) = k\,(\sqrt{\delta^2 + x^2} - \delta)\,\operatorname{sgn} x \quad \ldots\ldots (68)$$

in which sgn denotes signum, so that sgn x is $+1$ when x is positive and -1 when x is negative; k is the spring constant after complete coupling has resulted; and δ is a linear quantity of the order of magnitude of the displacement required to insure substantial coupling. If m is the mass of the system, and

$$\lambda^2 = k/m \quad \ldots\ldots (69)$$

the equation for the free oscillations is

$$\ddot{x} + \lambda^2\,(\sqrt{\delta^2 + x^2} - \delta)\,\operatorname{sgn} x = 0 \quad \ldots\ldots (70a)$$

When δ is negligibly small or, what amounts to the same thing, when x is not too small, Eq. 70*a* reduces to

$$\ddot{x} + \lambda^2 x = 0 \quad \ldots\ldots (70b)$$

and λ is the natural frequency of the system. Eq. 70*b* is valid for $\alpha < x < \beta$, in which α is a sufficiently large multiple of δ and β is a displacement at which upper nonlinearity becomes evident.

If $x < \alpha$, an approximate solution may be assumed of the form,

$$x = A \cos \omega t \quad \ldots\ldots (71)$$

in which ω is the frequency to be determined as a function of the amplitude. The result of substituting this assumed value of x in the left-hand member of Eq. 70*a* is

$$-\omega^2 A \cos \omega t + \lambda^2 (\sqrt{\delta^2 + A^2 \cos^2 \omega t} - \delta) \operatorname{sgn} \cos \omega t = \psi (A, t) \ldots (72)$$

in which $\psi (A, t)$ is merely an abbreviation of the expression to the left. Eq. 70*a* is satisfied as nearly as possible by this assumed form of x when A is determined for a given ω so that ψ is as nearly zero as possible throughout a cycle. Therefore, let

$$I = \int_0^{2\pi/\omega} \psi^2 \, dt \ldots (73)$$

be a minimum, which requires that

$$\frac{dI}{dA} = 0 \ldots (74)$$

The resulting integrals are readily evaluated and a compact approximate expression for the frequency is found to be

$$\omega^2 = \frac{2}{\pi} \lambda^2 \tan^{-1} (A/\delta) \ldots (75)$$

This relation is illustrated in Fig. 6, in which are shown three ranges of the amplitude: R_1, in which A varies from 0 to about 10 δ, the range of lower nonlinearity; R_2, the linear range; and R_3, the range in which upper nonlinearity occurs.

As an illustration of the practical occurrence of conditions such as those discussed herein, consider a beam built into massive walls. If an imperfection in the connections allows the ends of the beam to rotate through a small angle before the built-in feature is established, the beam can oscillate with any frequency from that corresponding to pin connections to that corresponding to rigid connections, depending on the amplitude of the oscillations. The opposite condition would be encountered in a pin-supported beam, since friction could prevent the small rotations corresponding to very small amplitudes.

Inasmuch as the amplitudes of the oscillations excited by the author's method will generally be intrinsically small, it seems likely that inhomogeneities in the connections of the various parts of a structure will affect the observed results. The possibility of detecting modes of vibration by the use of a small test mass is not questioned; it is merely suggested that the use of micro-amplitudes to determine the dynamic characteristics of a structure introduces problems that transcend the theory of small oscillations.

AMERICAN SOCIETY OF CIVIL ENGINEERS

Founded November 5, 1852

DISCUSSIONS

ANALYSIS OF FRAMES WITH ELASTIC JOINTS

Discussion

BY GEORGE W. LAMB, A. A. EREMIN, AND J. CHARLES RATHBUN

GEORGE W. LAMB,[18] M. ASCE.—Use of the traverse method of analysis is well adapted to frames with elastic joints. However, there are several points in the paper that need clarification. Some of the reasons for certain parts of the analysis are not clear, due possibly to the fact that the writer is not as familiar with the procedure and the analysis as is the author.

Fig. 1 would be clearer if all the angles were expressed in terms of the △-angle instead of using three symbols. For the conditions assumed in the paper (joint yield being equal to one half of the angular change in direction of the elastic curve of the member, caused by the moment that produces the joint yield), the angular displacements in Fig. 1 could be more advantageously shown as in Fig. 10.

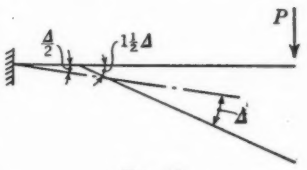

FIG. 10

Some additional information would help in explaining Figs. 2(*a*) and 2(*b*). The total rotation at joint B is $2\frac{1}{2}$, as shown in Fig. 11, which shows all the rotations instead of groups of them. One reason for having the same rotation at joint E and joint B is to take advantage of Maxwell's theorem of reciprocal deflections (angular), and thus obtain a check on the final results. In addition, this is necessary, of course, to obtain final moments. Fig. 11 shows a unit rotation at the top of column AB. A moment of 4 is required to rotate the top of the column one unit. The stiffness used in Fig. 11 is the $\frac{I}{L}$-value and is not an assembly stiffness. This is done becuuse the rotation angles are separated, not grouped into composite angles. Fig. 11 should be compared with Fig. 2(*a*).

A comparison of the moments obtained in the structure having semi-rigid joints with the moments in the structure having rigid joints indicates that some economy could be obtained by considering semi-rigid joints in the design.

NOTE.—This paper by Ralph W. Stewart was published in December, 1947, *Proceedings*. Discussion on this paper has appeared in *Proceedings*, as follows: May, 1948, by L. E. Grinter; and June, 1948, by Arthur B. McGee, and C. W. Jenkins.

[18] Dist. Engr., Am. Inst. of Steel Constr., Inc., Topeka, Kans.

This economy is obtained only if the joints are of such simplicity that little extra fabrication cost is involved.

The author has selected for his analysis a type of joint in which the rotation occurring in the joint is a constant ratio to the total angular change in direction of the elastic curve of the member. A joint having these properties can be

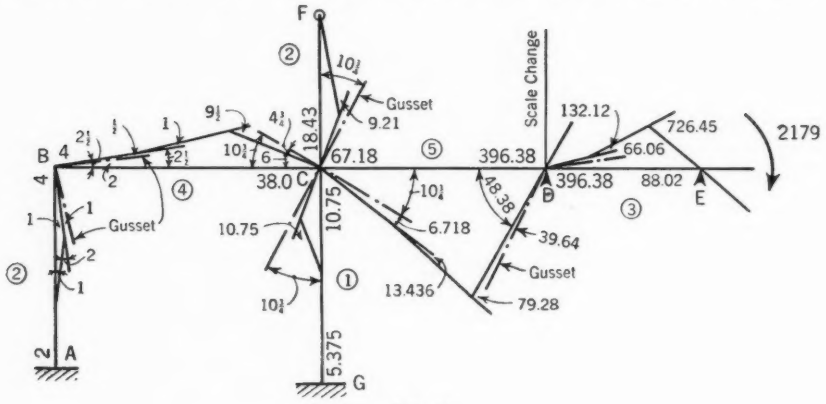

FIG. 11

selected from a family of moment-rotation curves. Joints also could be selected from this same family of curves that would result in almost any joint yield for a given moment. With the properties of joints expressed as a family of moment-rotation curves from which many different joint yield (angles) can be obtained from one moment, a joint can be selected that would yield the proper amount to accommodate the moment and the slope of the joining members for many different ratio values.

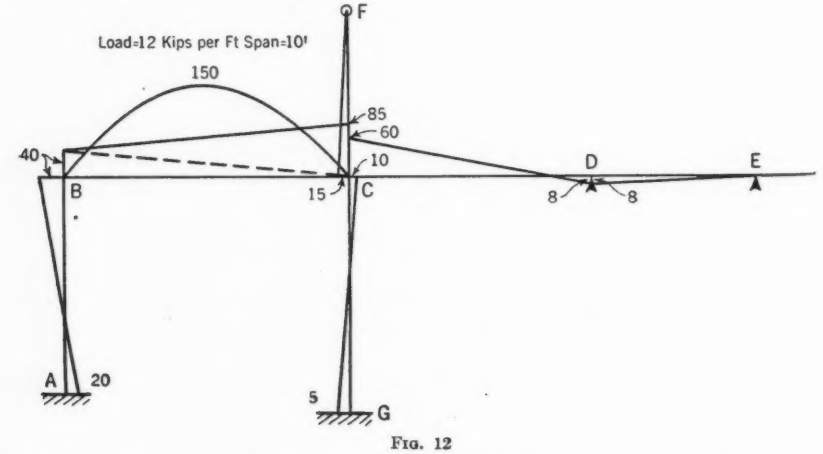

FIG. 12

If a joint works within the elastic limit the moments and rotations can be added for different loading conditions. If, however, the moment-rotation curve of the joint is a curved line, the maximum load conditions would be used.

When the ratio values between joint yield and curvature in the member can be selected by judgment from test data, the problem can be solved in the following manner. Using the frame given in the author's example (Fig. 2) and applying a load of 12 kips per ft on span BC, the moments in the ends of all members can be determined by inspection, and the slope between members determined by the traverse method. In this case the ratio between curvature and joint yield will not be constant. The moments selected are as shown in Fig. 12, and the slopes between members are obtained by the traverse method as shown in Fig. 13 and Table 5.

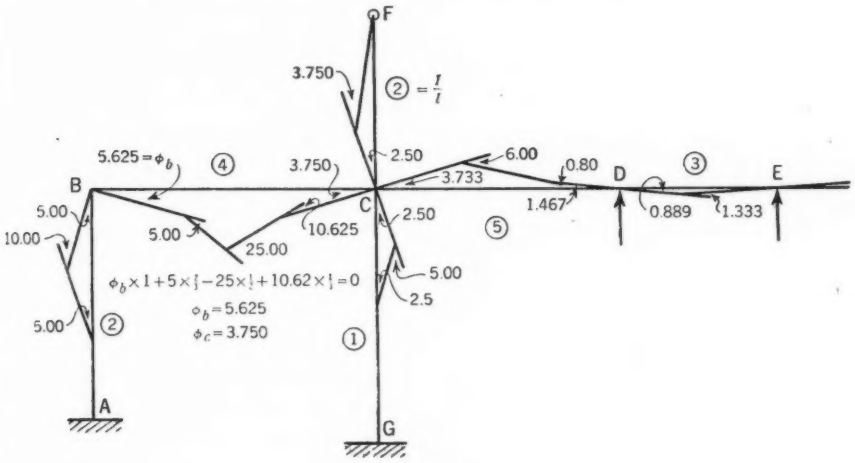

FIG. 13

TABLE 5.—SUMMARY OF JOINTS

Members	Slope between members	Moment between members	Coordinates on Moment-Rotation Curve	
			M (kip-ft)	φ (radians)[a]
AB and BC.....	5.000 − 5.625 = 0.625	40.0	40.0	0.0002500
BC and CF.....	3.75 − 2.50 = 1.250	15.0	15.0	0.0005000
BC and CG.....	3.75 − 2.50 = 1.250	10.0	10.0	0.0005000
BC and CD.....	3.75 − 3.733 = 0 017	60.0	60.0	0.0000068
DC and DE.....	1.467 − 0.889 = 0.578	8.0	8.0	0.0002312
FC and CG.....	2.50 − 2.50 = 0	0	0	0

[a] φ is the slope between members divided by 2,500.

From Table 5, joint B will have a connection delivering 40 kip-ft of moment with a joint yield of 0.00025 radian. Columns FC and CG have equal slopes at joint C and would be fully rigid, spliced columns, with member BC fastened to it by a connection that would yield 0.00050 radian under a moment of (10 + 15) or 25 kip-ft. In addition to the connection to column FC and CG member BC connects to member CD by a joint carrying 60 kip-ft and having a joint yield of 0.0000068 radian. The remaining joints are treated in the same

manner. The joint yield is a property of the actual connection and its moment. When considering the construction of such a frame, the small rotations should be thought of as deformations caused by the additional stresses from the applied load.

The traverse method of analysis is relatively simple in application and is easily adapted to frames with any degree of flexibility at the joints. When the ratio of curvature of the member is fixed in relation to joint yield, its application is better visualized when all the rotations are shown, as in Fig. 11.

A. A. EREMIN,[19] Assoc. M. ASCE.—By varying the distances between the deflection angles in continuous frames Mr. Stewart expresses the effect of elastic deformations at the joints. The method is simple and convenient for checking, by visual inspection. A further simplification of the method is possible by the graphical construction of moments. For example, let Fig. 14 represent span BCD of Fig. 2. Assume that each joint is rigid and that moments are obtained by "crosslines."[20] The elastic deformations at the joints were determined (see Fig. 14(*b*)) by considering that the distance from a support to its nearest point of inflection is one half the distance shown in Fig. 14(*a*). The

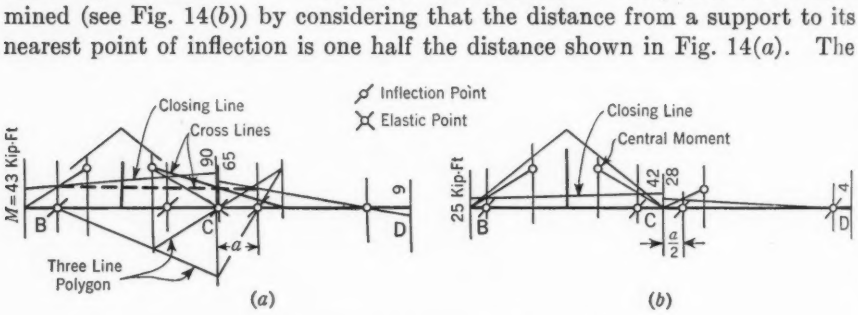

FIG. 14.—DISTRIBUTION OF MOMENTS

moments corresponding to the elastic deformations at the joints were determined by interpolating the values shown in Fig. 14(*a*). When Fig. 14(*b*) is superposed on Fig. 14(*a*) the resulting values afford a convenient method for selecting a design moment visually.

By clarifying the effect of elastic deformations at the joints, Mr. Stewart has enlarged the range of application of rigid frames, and thereby has made an important contribution to the literature on the subject.

J. CHARLES RATHBUN,[21] M. ASCE.—Once again Mr. Stewart has brought before the engineering profession the importance of the effect of the elasticity of the connections and, at the same time, has presented a practical and useful method of allowing for these properties. This has been done before by other methods but these do not have the advantage of giving the analyst the visual concept obtained by the author's diagrammatic method.

---

[19] Associate Bridge Engr., Bridge Dept. of California State Highways, Sacramento, Calif.
[20] *Transactions*, ASCE, Vol. 111, 1946, p. 887.
[21] Prof., Civ. Eng., College of the City of New York, New York, N. Y.

In the routine analysis of frames it is quite customary to assume the joints as either hinged or rigid and to design them on the assumption that the stresses lie between these limits. The saving in material may not warrant a more careful analysis and in this case it would be academic. In a conference called in 1934 to consider the use of the elastic properties of the connections in analysis and design, the late Otis Hovey, M. ASCE, emphasized the necessity of reform and development of the theory. He prophesied that commercial design would adjust itself to the theory when perfected. The same situation prevailed a few decades before regarding statically indeterminate analysis. Mr. Stewart's paper is a step toward this goal.

That the proper design and the incorporation of the properties of a joint may result in a material saving can be shown by a simple problem of frequent occurrence: ABC is a simple two-span beam under a uniform load of w pounds per foot. The length of each span is l. If designed and built as two beams, the bending moment will be $+\frac{w\,l^2}{8}$ at the center of each span. If it is a continuous beam, the bending moment at point B, the central support, is $-\frac{w\,l^2}{8}$. An elastic connection can be placed at support B which will relieve the negative moment there and increase the positive moment until they are equal and of the value of $0.0859\,w\,l^2$—a material saving of 32%. In this particular problem the same effect may be obtained by lowering the support at point B an amount equal to $0.013\,\frac{w\,l^4}{E\,I}$ thus pre-stressing the beam.

Mr. Stewart's paper is of value in again calling attention to the traverse method and its adaptibility in incorporating the properties of connections in rigid-frame analysis.

AMERICAN SOCIETY OF CIVIL ENGINEERS

Founded November 5, 1852

DISCUSSIONS

PANAMA CANAL—THE SEA-LEVEL PROJECT
A SYMPOSIUM

Discussion

BY GEORGE B. PILLSBURY, KENNETH S. M. DAVIDSON, JOEL D. JUSTIN, W. H. MCALPINE, W. E. R. COVELL, WILLIAM HERBERT HOBBS, HIBBERT HILL, KENNETH C. REYNOLDS, GREGORY P. TSCHEBOTARIOFF, CHARLES W. DOHN, AND DONALD F. HORTON

GEORGE B. PILLSBURY,[62] M. ASCE.—The basic differential equations for hydraulic flow in open channels have long been established. For the varying flow in tidal channels the term dependent on the acceleration of the velocity with respect to time must be included. On the other hand, the turbulence set up by the slowly changing tidal currents cannot differ appreciably at any moment from that produced by a steady current of the same velocity. The friction term may then be taken as that applicable to steady flow under the same conditions, although it must change its sign with the direction of the current. Since the slope of the water surface, in a given direction, is alternately upward and downward, it is more convenient to consider surface slopes and heads, as well as elevations of the water surface, as positive in an upward direction. The basic equations for the currents in a tidal channel may then be written

$$\frac{\partial y}{\partial x} + \frac{v}{g}\frac{\partial v}{\partial x} + \frac{1}{g}\frac{\partial v}{\partial t} + \frac{v\,[v]}{C^2 R} = 0 \quad \ldots\ldots\ldots\ldots\ldots\ldots (3a)$$

and

$$\frac{\partial Q}{\partial x} + b_W \frac{\partial y}{\partial t} = 0 \quad \ldots\ldots\ldots\ldots\ldots\ldots\ldots\ldots (3b)$$

In Eqs. 3*a* and 3*b*—at any given cross section distant x from an assumed origin, and at the time t—y is the elevation of the water surface above any assumed datum; v is the algebraic value of the mean velocity in the cross section and $[v]$ its arithmetical value; R is the hydraulic radius; C is the Chézy coeffi-

NOTE.—This Symposium was published in April, 1948, *Proceedings*. Discussion on this Symposium has appeared in *Proceedings*, as follows: June, 1948, by Hans Kramer, and Philip G. Nichols.

[62] Brig.-Gen., Corps of Engrs., U. S. Army (*Retired*), Ross, Calif.

cient applicable to the hydraulic radius under any of the formulas derived for steady flow; b_W is the width of the water surface; and Q is the discharge.

In a navigable channel, the velocities cannot be so great that the second term in Eq. 3*a* (which may be called the "velocity-head" term) becomes of major importance.

The form of these equations is such that the currents at any station along a tidal channel must depart somewhat from simple harmonic fluctuations, even when the tides at the entrances are assumed to have such fluctuations. These departures may be eliminated by omitting the velocity-head term, disregarding the changes in the area of the cross sections with the variations in y, and adopting an harmonically varying friction term most nearly conforming to its true fluctuation. Under these assumptions, a mathematical solution of the equations for tidal flow in a long canal of uniform cross section was derived many years ago.[63] The resulting exponential equations are unwieldy, and do not afford a satisfactory method for computing even an approximation to the currents in a canal of varying cross section, such as is proposed at Panama.

Under the same assumptions, Eq. 3*a* affords an algebraic relation between the amplitude and phase of a simple harmonic fluctuation of the surface slope in an elementary reach of a tidal canal and those of the resulting harmonically varying current; and Eq. 3*b*, the means for determining the changes in the current from reach to reach because of the storage and release of water with the rise and fall of the tide, as well as the variation due to changes in the cross section. Through a procedure developed by the writer,[8] which does not warrant repetition here, the harmonically varying, or "primary" currents produced by "primary" tides (with a simple harmonic fluctuation) at the entrances to a canal may be computed from these relations by successive approximations. For these computations, the canal is divided into sufficiently short reaches, such as those used in backwater and similar hydraulic computations. In a canal of the length and dimensions proposed at Panama, three successive computations afford a satisfactory determination of the amplitudes and phases of the "primary" currents in the several reaches and of the tidal fluctuations which establish the surface profiles through the canal.

By a somewhat laborious set of computations, the primary currents and surface profiles may be adjusted at sufficiently short intervals of time (such as the half lunar hour) to develop their distortions because of the factors disregarded in their derivation—including any departures of the selected entrance tides from the simple primary tides, from which the primary currents were determined. For a first adjustment—in order to develop the major distortions—the currents and discharges in the middle reach of the canal may be corrected (at the adopted time intervals) to conform to the correct values of the friction term as it varies with the changing values of R and C with the rising and falling tides, and also to the consequent variations in the acceleration term. The currents in the other reaches are then derived by dividing the resulting discharges in these reaches by the varying area of their cross sections. If the

[63] "The Cape Cod Canal," by William Barclay Parsons, *Transactions*, ASCE, Vol. LXXXII, December, 1918, p. 1.

[8] "Tidal Hydraulics," by George B. Pillsbury, *Professional Paper No. 34*, Corps of Engrs., U. S. Govt. Printing Office, Washington, D. C., 1940.

entrance tides selected for the computation depart from a simple harmonic variation, these departures are distributed between the several reaches.

A more involved second adjustment includes the effect of the velocity-head term, the entrance and recovery heads, and the minor changes in the water-surface profiles resulting from the current distortions developed in the first adjustment. The diagrams in Fig. 35 indicate the smallness of the distortions developed by this second adjustment, even when the current velocities are as large as those that would occasionally occur in an uncontrolled sea-level canal at Panama. It may be noted that the model tests afford a highly satisfactory confirmation of the adjusted currents as computed; but without such adjustment the primary currents afford an approximation sufficient for all practical purposes.

Needless to say, the currents derived by these calculations are the mean values at a given cross section at a given time. The midstream currents encountered by vessels navigating the canal would be somewhat larger. Current measurements in the Cape Cod Canal in Massachusetts before it was enlarged to its present dimensions showed midstream currents 25% in excess of the mean; but the model tests are understood to show that, in a canal of the dimensions proposed at Panama, the midstream currents are not much in excess of the mean velocities.

It should be emphasized, perhaps, that the tides at the Pacific entrance, which would largely determine the currents in an uncontrolled sea-level canal at Panama, run through a marked variation from springs to neaps in a period of about a week, and back to springs the following week. The semidaily fluctuations of the spring tides vary from fortnight to fortnight, but occasionally attain a range of about 20 ft, or 10 ft above and below mean sea level at the time. The average spring range is given as 16.4 ft. The neap tides may have a semidaily fluctuation of as little as 3 ft above and below their mean elevation, although sometimes they are as much as 6 ft above and below that level. The vagaries of the small tides at the Atlantic entrance are described by Messrs. Meyers and Schultz, and as stated by them the long-term mean sea level at the Pacific entrance is nearly a foot above that at the Atlantic entrance. In addition, the monthly mean sea level at the Pacific entrance varies by about a foot during the year, coincidently with the changing temperature of the water in the Gulf of Panama. Long-term records do not show marked disturbances of the water levels at either entrance such as those sometimes produced in other regions by violent storms.

Because of the tidal variations, the strength of the currents in an uncontrolled sea-level canal would vary widely each week, and from week to week. The currents would not reach their strength simultaneously throughout the canal, and the currents at the one end of the canal would be increasing quite rapidly at the time of slack water at the other end. It does not seem possible to time the transits of the large traffic through the canal in such manner so as to avoid the maximum currents for the day. Furthermore, shipping will be concerned with the currents that might be encountered at any date of arrival, rather than with those which would be met were their arrivals so timed as to afford a passage at the time of neap tides, or even when the currents would have

their average strength. For this reason, the principal emphasis is given to the currents produced by the highest spring tides to be expected ordinarily at the Pacific entrance. These should not be interpreted as a prediction of the currents usually encountered during a transit of an uncontrolled canal.

As shown in the Meyers-Schultz paper, the current strengths would increase toward the Atlantic entrance where the tides are the least. The main reason for this seeming anomaly is the reduction in the cross section of the canal in this direction at the higher tidal stages, as is clearly shown in Fig. 33. Fig. 33 also shows that the maximum inflow and outflow is somewhat the larger at the Atlantic entrance, as the flow through this entrance has a larger part in the filling and emptying of the tidal prism of the canal than the flow through the Pacific entrance. The maximum currents in a tidal canal are generally, but not always, found at whichever entrance the tidal range is the least.

The extended investigations, computations, and tests described by the authors of the fourth Symposium paper have removed any doubt as to the strengths and the timing of the currents to be expected in an uncontrolled canal at Panama of the dimensions now proposed. Although all evidence indicates that such a canal could be navigated by the largest vessels in the strongest currents that might at times be encountered in a transit, its navigation would be safer and easier if the currents were reduced to an insignificant value by the construction of tide locks. A grounding of a vessel against the bank of the canal, because of failure of its steering gear or propelling machinery, might result in the complete loss of the vessel and the temporary blocking of the canal if it occurred at a time when the currents were as strong as they often would be were they uncontrolled. Tide locks, moreover, would eliminate the possibility of a more or less serious maintenance problem because of the deposit in the approaches and at the teminal wharves of material eroded from the bed and banks of the canal. Without entering into a discussion of the relative advantages of a high-level lock canal and a sea-level canal, the writer believes that (if the latter is decided upon) the inclusion of tide locks is advisable, but that the canal would remain usable even if these were destroyed by hostile air attack.

KENNETH S. M. DAVIDSON,[64] ESQ.—An extensive series of model experiments relating to the handling of ships in restricted channels is presented in the fifth Symposium paper by Messrs. Lee and Bowers. This is a subject on which there has been all too little reliable information in the past.

The writer is particularly impressed by the bold choice of method, which makes a "direct frontal attack" on the problem of selecting channel dimensions. The phenomenon of "bank suction" and the practical difficulties to which it may lead have been recognized for many years. There has been, too, a certain amount of scattered information on the force and moment magnitudes introduced by bank suction, and on other technical factors involved. Ultimately, however, the proper selection of channel dimensions depends only partly on these basic aspects of the matter, and rests primarily on the answers to the specific questions: "What is feasible, and what is practicable, in the actual business of steering ships in channels?" Hence, the method of employing free,

[64] Director, Experimental Towing Tank, Stevens Inst. of Technology, Hoboken, N. J.

self-propelled models, with provisions for steering them in the same fashion as full-scale ships, strikes at the heart of the problem.

The adoption of this method, however, does not in itself dispose of all questions. There are two separate aspects of steering: (1) "What pattern of rudder angle changes is required under given circumstances, and is it physically possible for the rudder to control the ship?" and (2) "What responses will the helmsman make—that is, how successful will he be in getting the rudder to the proper angles at the proper times?" Of course, if the circumstances impose requirements beyond the capacity of the rudder for control, steering is obviously impossible and the helmsman's responses are of no consequence. On the other hand, it does not follow that steering is necessarily possible if the requirements are not beyond the capacity of the rudder. Even with an ideal helmsman, it might be impossible to maneuver the ship into the kind of nearly steady motion needed for practical operation, and, further, it might be impossible to do this with a "human" helmsman although possible with an ideal one. Thus, the helmsman's responses may become an exceedingly important, if not a controlling, consideration.

The employment of professional Panama Canal pilots to steer the models during the experiments, therefore, is at least as significant a feature of the method adopted in this instance as the use of free, self-propelled models. There is, however, one last, but by no means least, question. A pilot may have little trouble in handling a full-scale vessel, and plenty of trouble in handling its model, under exactly corresponding circumstances. A 1:45 scale model has only about 1/90,000 of the ship's mass and, perhaps more important, goes through the same (geometric) cycle of events in about one seventh the time. One would expect a professional ship's pilot to be bothered by both these ratios, and particularly by the time ratio. A reduction to one seventh of the allowable reaction time could, in principle, make quite impossible a chain of human responses that would otherwise be simple enough. Hence, there must have been, at the start of the present experiments, some misgivings regarding the chances of success, and it is no small tribute to the experimenters that they had the courage to go ahead nevertheless.

They seem to have been well rewarded. The writer talked with one or two of the professional pilots while the experiments were in progress, and can vouch for their feeling of confidence in the method. One can rationalize, of course, that nothing happens very fast in a ship and that, especially at the low speeds imposed by canal operation, rudder movements are seldom needed more frequently than, say, once in 10 sec, which corresponds to about once in 1.5 sec in a 1:45 scale model, so that no great strain is imposed on the pilot. Fighter airplane pilots are generally believed to respond to control needs in approximately 0.2 sec and the ordinary person driving an automobile, in from 0.4 sec to 0.5 sec; but it is easier to accept this kind of reasoning after the event than before. Flying-boat models of only 1:12 scale are being handled in laboratory tests—mostly, however, with specially trained pilots.

Without belaboring the point unduly, the writer nevertheless considers that the attempt to integrate ship pilots' reactions with the more purely technical factors constitutes perhaps the most significant feature of the present

experiments, and one that deserves emphasis. These experiments are among the very few instances in which "the feel in the seat of the pilot's pants," a factor that has been taken seriously by airplane designers for years, has been taken directly into account in a ship handling problem. The Panama Canal pilots have expressed satisfaction that their experience and advice were sought and they have evinced interest in having similar model facilities permanently available for pilot training and practice.

The scope of an experimental project of this type can all too easily expand to impossible proportions, as anyone can testify who has tried to lay down a program for one of them. Strict economy, sometimes amounting to almost "brutal" curtailment, is usually unavoidable. This accounts, of course, for the limited number of ship types worked with in the present instance. The writer does not believe, however, that a serious limitation has been imposed thereby on the generality of the experimental indications; the ship types were well selected.

The experiments go far toward providing a "workable" answer to the problem at hand. Even a casual examination of the force and moment data in Figs. 47 and 48 shows, for instance, that "perfect" equilibrium may be difficult to attain, but that an approximation to equilibrium is good enough in practice; that moment balance is probably more important than lateral force balance; and that the effectiveness of the rudder varies with the lateral position of the ship in the channel. Similar conclusions could probably be drawn regarding the effect of speed, and of other factors, and these would form a substantial framework upon which to hang further work directed toward a more "complete solution"—a phrase used by Messrs. Lee and Bowers.

Going a little more into detail, consider the 720-ft tanker traveling at 4.5 knots in the 770-ft channel of 45-ft depth, on a path 60 ft to the right of the center line. Then (Fig. 48) the force toward the bank is 1.0 ton and the counterclockwise moment, 400 ton-ft. The displacement of the ship, for comparison, is approximately 50,000 tons. A rudder angle of 3.3° is sufficient to offset the moment, the water force on the rudder acting away from the bank. Since the rudder is about 350 ft aft of the center of gravity, the rudder force must then be about 400/350, or 1.14 tons. Fig. 47 shows, however, that in free running a rudder angle of 5° is in fact needed, corresponding presumably to a rudder force of 5/3.3 times 1.14, or 1.7 tons. The forces and moments then are not balanced, and so the ship must assume a small yaw angle. The required force is $1.7 - 1.0 = 0.7$ ton, toward the bank; the required moment is $(1.7 \times 350) - 400 = 200$ ton-ft, counterclockwise. This combination would require the ship to be yawed toward the near bank and the force resulting from yaw to be concentrated at a point on the hull aft of the center of gravity and very near the stern. A yaw toward the near bank, however, does not agree with the experimentally determined "equilibrium" conditions and a yaw force concentrated aft of the center of gravity is out of line with independent open water tests of models of similar vessels. One is almost forced to the conclusion that it must be very difficult, if possible at all, to work a ship into a position of complete equilibrium. Apparently, however, small unbalances are not serious.

For instance, if, the ship is assumed to be yawed away from the near bank in a manner to produce a balance of moments, the resulting force unbalance can be shown to have very minor consequences. Moment equilibrium would insure a constant ship heading and could be attained with a slight counterclockwise yaw. This attitude would result in a force of perhaps 0.7 ton away from the bank. The force unbalance would then be 1.7 tons of rudder force plus 0.7 ton of yaw force minus 1 ton of bank suction force, or a net of 1.4 tons of force away from the bank. With a ship weight of about 50,000 long tons, the accelerating force proves to be a very small fraction of g—that is, $\frac{1.4}{50{,}000 \times 2{,}240/2{,}000} = 0.25 \times 10^{-4}\, g$. Neglecting the resistance of the ship to lateral motion, this accelerating force, α, in 100 sec, or about the time required for the ship to travel one length, would move the ship laterally a distance of $x = \frac{1}{2}\alpha t^2 = 0.125 \times 10^{-4} \times 100^2 = 0.125$ ft. In ten ship lengths (which is more than a mile and would require some 16 min of travel time) the lateral travel would be only 12.5 ft, an almost insignificant amount.

It appears, then, that unbalance of forces is acceptable as long as it is not excessive; unbalance of moments is more serious, however, since a small change of heading soon results in a change of lateral position. The pilot's ability to apply forces and moments is limited to use of the rudder (with perhaps some help from the propellers in ships having more than one); the saving grace is that the rudder can apply a substantial moment without imposing a dangerously large lateral force.

The data amply bear out the danger of having canal dimensions that are too small. If the limit of 5° of rudder, as set by Messrs. Lee and Bowers, is accepted (and it seems entirely reasonable to do so), Fig. 47 shows that the pilot must keep his ship very close to the center line. If the ship wanders appreciably, the forces and required rudder angles mount rapidly. The bank suction force on a 720-ft tanker 200 ft off the center line of a 770-ft channel (Fig. 48) is 9 tons (about half of the propeller thrust required to drive the ship), and a rudder angle of 24½° is required to provide a "workable" equilibrium (Fig. 47). In the narrower 500-ft channel, the conditions are almost identical when the ship is only 100 ft off the center line. Thus, if a ship is allowed to move very far from the center line, complications mount rapidly—and more rapidly in a narrow channel than in a wide one. Here lies the real danger, it seems.

Taken as a whole, the fifth Symposium paper does not seem to do full justice to the experiments—or at least to the experimental method. The method appeals to the writer as a sound one for the practical purpose of selecting channel dimensions in relation to operating conditions. Beyond that, it seems a logical choice for the deeper purpose of clarifying the issues preparatory to undertaking "a complete solution to the general problem." It could scarcely have been expected to yield a complete solution. Messrs. Lee and Bowers might well have made more of the method in its own right, by emphasizing practical conclusions more strongly, and by indicating the gaps that will need to be filled before a complete solution is obtained.

It may be pertinent to state herein that the general problem of ship control —steering and turning—is currently under study, both analytically and ex-

perimentally, by several agencies and organizations interested primarily in ships. The work described by the authors of the fifth Symposium paper deals with a special problem of ship control, and demonstrates the need for continued study of ship handling problems, and of the fundamental factors that affect control.

JOEL D. JUSTIN,[65] M. ASCE.—At the time of construction of the Panama Canal the late Donald F. MacDonald was a relatively young geologist in the employ of the canal. He realized during the construction that the philosophy, still held by some engineers, of "Let her slide and dig it out afterwards until she stops sliding" was unnecessarily expensive. As the result of full-scale laboratory experiments in the great outdoors, he decided that it was much better to determine the slope that would be safe in advance and cut to that slope, thus avoiding considerable unnecessary excavation. The essential correctness of his conclusions has been demonstrated throughout the years.

Mr. MacDonald had the advantage of observing slides which had already taken place in the canal. He did determine in advance one slope in Cucaracha and the engineers cut to that slope. The slope stands today substantially as he left it as a testimonial to his judgment.

As Messrs. Binger and Thompson have shown, the history of the Panama Canal has been deeply concerned with the Cucaracha formation. It is difficult to find a piece of this formation large enough to test, and when a piece is found it shows a strength much greater than the 10° internal friction and the 2,300-lb cohesion per sq ft stated by the authors of the seventh Symposium paper.

However, some of the "weakest materials could not be tested." Much of the Cucaracha formation breaks down to little slickensided, more or less cubical, pieces of perhaps ½ cu in. Each piece feels slippery to the touch.

Confronted with conditions like these, Messrs. Binger and Thompson have done well in adopting the method of determining Cucaracha slopes which they did. Friction was determined by test on small slickensided samples, and cohesion was determined from an actual slope just south of Zion Hill which has stood for many years. In other words, the friction as determined by laboratory test was used, and the necessary cohesion required to keep the slope in place with a factor of safety of 1 was determined. It should be noted herein that the error, if there be one in the adopted method, would be on the safe side for great heights.

In setting slopes for a sea-level canal, the factor of safety decided on from the extensive Binger-Thompson studies was 1.3 for sudden drawdown.

With the accumulated mass of data now available, the establishment of safe slopes for static conditions has become relatively simple compared with the problem of establishing safe slopes when the Cucaracha formation is overlain with the harder denser rocks.

As Mr. MacDonald explained to the writer, many of the hills prevalent in the Canal Zone were like mushrooms. They had been formed by molten volcanic rock forcing its way up through the soft greasy Cucaracha formation roughly forming the stem of a mushroom-like structure. When it had passed

[65] Cons. Engr., Justin & Courtney, Philadelphia, Pa.

through the Cucaracha it blossomed out, forming the top of the mushroom. On cooling these buttons of igneous material became agglomerates or basalt, or other igneous rock (Fig. 103).

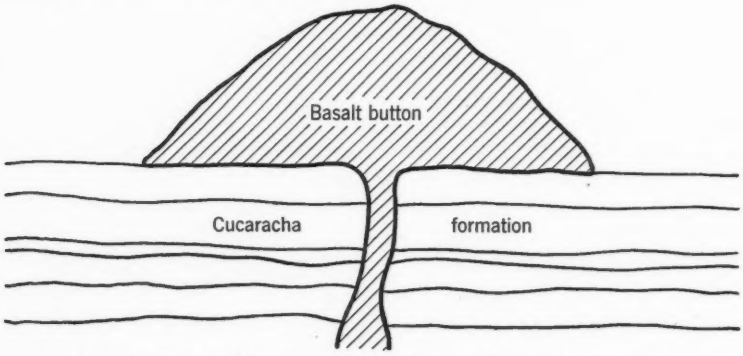

FIG. 103.—IGNEOUS MATERIAL BREAKS THROUGH STRATA OF CUCARACHA FORMING MUSHROOM-LIKE STRUCTURE (IDEALIZED)

The resulting pressure on the Cucaracha, tending to crush it because of the overlying igneous rock, was often excessive. The surrounding softer Cucaracha was often worn away by erosion, leaving the igneous rock buttons sticking up on the landscape as the caps of the steep hills. In many cases the erosion of the Cucaracha left slopes unstable because of the heavy overburden of denser rock which was overhanging and which tended to crush the weak Cucaracha. In particular, the basalt often gave way and broke up in sliding down the steep hill. Hence, slides are nothing new in the Canal Zone, but started long before the white man discovered America (Fig. 104).

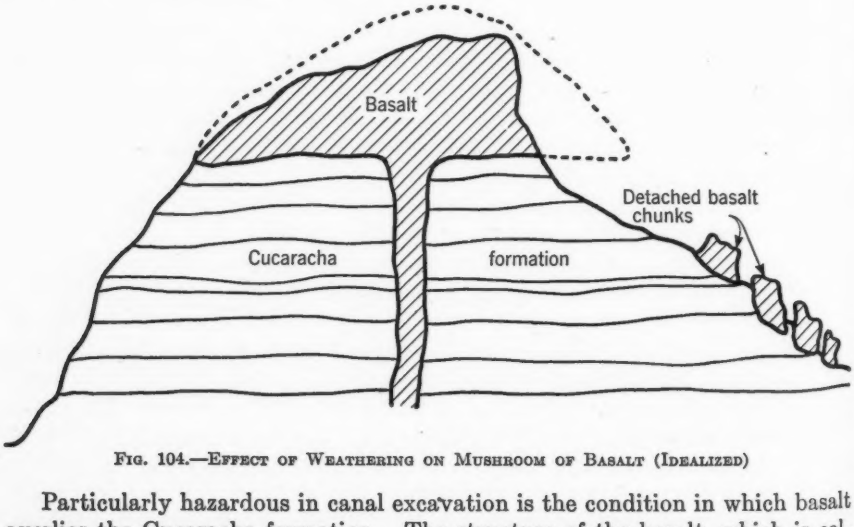

FIG. 104.—EFFECT OF WEATHERING ON MUSHROOM OF BASALT (IDEALIZED)

Particularly hazardous in canal excavation is the condition in which basalt overlies the Cucaracha formation. The structure of the basalt, which is columnar, is geologic evidence that this igneous rock is unable to span material

distances by cantilever action, which means that most of the pressure from the weight of the basalt will be directly downward. Zion Hill is one of the cases in which an overburden of basalt on the Cucaracha formation has led to considerable slides.

To make canal slopes stable under such conditions requires considerable investigation and study of each particular case. In some cases it requires flattening the slopes to a Cucaracha slope as 1 on 6.3 for a 300-ft cut.

W. H. MCALPINE,[66] HON. M. ASCE.—An excellent general description of the construction features of the proposed sea-level canal is presented in the last Symposium paper. It is mainly devoted to a description of the methods considered for (*a*) conversion to a sea-level canal by multiple-stage and single-stage dredging, (*b*) dry excavation, and (*c*) wet excavation. Such features involving conventional methods of construction as tidal-regulating structures, flood-control structures, and housing facilities are only mentioned.

(*a*) *Conversion to a Sea-Level Canal by Multiple-Stage and Single-Stage Dredging.*—It was found that conversion by the multiple-stage method is best accomplished in three steps. In this plan, the construction of two temporary single-lift locks is proposed in order to provide two lanes of traffic, because without them dependence for uninterrupted traffic would be placed on a single lane. The single-stage conversion, or deep-dredging plan, permits traffic and pool levels to be maintained until the tidal structures have been completed and the canal made ready for draining to sea level in a single operation, requiring only a few days.

The advantages of the single-stage conversion plan are quite apparent, as shown by the authors of the last Symposium paper, with the exception that it involves excavating in Gatun Lake from a pool elevation of +85 to −60, or a total depth of about 145 ft. Dredging to such depths has very little precedent. However, designs for hydraulic and ladder dredges to excavate to such a depth have been prepared by expert manufacturers. Furthermore, it is understood that one of each type will be constructed for trial prior to their actual needs. This should serve to correct any defects that may develop and also to furnish valuable data to bidders. It is the writer's belief that the deep-dredging plan is feasible and should be adopted.

(*b*) *Dry Excavation.*—It is noted that of the total excavation of 1,000,000,000 cu yd or more, three fourths, or 750,000,000 cu yd, is dry excavation, which (except for about 50,000,000 yd) is to be handled with large shovels and draglines of 25-cu-yd capacity or more. The 50,000,000 cu yd lying above El. 270 is to be excavated by 5-cu-yd equipment and hauled by truck or other land carriers to spoil areas. The remaining 700,000,000 cu yd of dry material which is to be excavated by large shovels and draglines will be deposited in dump scows of 2,500-cu-yd capacity and towed to Gatun Lake or to the Pacific Ocean for disposal. The average towing distance is stated as 15 miles.

The plan of excavating a system of auxiliary or feeder canals within the excavation areas to permit loading the scows directly from the draglines and

[66] Special Asst., Office, Chf. of Engrs., Dept. of the Army, Washington, D. C.

shovels is an ingenious one and has considerable appeal. The writer is quite aware of the economy of water transportation over land methods when the loading facilities and the waterways are adequate, but questions whether conditions would exist under the proposed plan sufficiently favorable to justify disposal of such a large proportion of the excavation in scows, particularly that in the upper levels. Conditions for loading the material from the draglines into scows lying alongside the sloping banks are particularly bad and quite different from loading a scow lying alongside a dredge. These scows must be either constantly held in position by a tug, or mooring facilities would have to be provided. Dropping the material directly into the scow from the higher elevation is dangerous if not unfeasible. Lowering the bucket directly over the scow from such a height is time consuming. Then, there is the time lost waiting for scows delayed by fog and other causes tending to disrupt a highly organized schedule of towing operations. Towing approximately 70,000,000 cu yd of material, or 100,000,000 tons per yr, an average distance of 15 miles—coupled with the commercial traffic—would slow up scow movements to some extent.

The writer questions the statement by Messrs. Rose, Dye, Watson, and Crook that the average cost of disposal by truck haul would be approximately twice as much as by scow haul. In this connection, it is understood that most of the excavation for the Third Locks Project on the Atlantic side was removed by truck haul at low cost. The plan of dry excavation should be re-examined with a view to a much greater disposal by land operations than now contemplated by limiting it to that lying above the 270 contour. An examination of the contours indicates that a considerable proportion of the excavation lying below the 270 contour could be disposed of economically by truck, belt conveyor, or other means of land transportation. This should tend to result in a better balanced and more flexible system of disposal.

(*c*) *Wet Excavation.*—The plan outlined for wet excavation, including the deep-dredging scheme, has been studied carefully and appears quite feasible.

In general, the construction, planning, and methods for conversion of the existing Panama lock canal to a sea-level canal, as outlined by the authors of the last Symposium paper, appear basically sound. Further and more intensive studies and conferences with contractors and equipment suppliers will modify or confirm the estimate and methods for disposal of excavated material by scows.

W. E. R. Covell,[67] M. ASCE.—After 40 short years engineers are again discussing the same problem so bitterly fought over in 1905—the problem of the sea-level canal versus the lock canal at Panama. Once more a basic, and now a controlling, item is safety.

In February, 1904, the Hay-Bunau-Varilla Treaty was ratified and the Isthmian Canal Commission was appointed, consisting of two retired officers of the United States Army and the United States Navy (Maj.-Gen. George W. Davis and Rear-Admiral John G. Walker), William Barclay Parsons, Hon. M. ASCE, and four other civilian engineers. In June, 1904, John F. Wallace, Past-President, ASCE, was appointed Chief Engineer of The Panama Canal,

[67] Parsons, Brinckerhoff, Hogan and Macdonald, Engrs., New York, N. Y.

being notified of his selection by a letter from General Parsons.[68] President Theodore Roosevelt appointed a new commission in March, 1905, with Theodore P. Shonts as chairman. In June of the same year, Mr. Wallace resigned and John F. Stevens, Past-President and Hon. M. ASCE, was appointed in his place. The latter stated[69] that the question of the lock or sea-level canal was still undecided, and that the advocates of both were pressing their claims on Congress. About this time, Congress authorized the appointment of a consulting board made up of eminent foreign and American engineers to advise President Roosevelt on this question. Their reports[70] were made public in 1906.

The "majority report," signed by General Davis, General Parsons, William H. Burr, William Henry Hunter, M. ASCE, Ad. Guérard, Eugen Tincauzer, J. W. Welcker, and E. Quellennec, advocated the sea-level route, whereas the "minority report," signed by Alfred Noble, Past-President, ASCE, Henry L. Abbot, Frederick P. Stearns, Past-President, ASCE, and Joseph Ripley and Isham Randolph, Members, ASCE, recommended a lock canal. The latter were all Americans, whereas five of the eight signers of the majority report were Europeans.

The main argument submitted by the majority was one of safety as is acknowledged in the minority report,[71] as follows:

> "The most plausible arguments advanced by advocates of a sea-level canal to justify its greater cost and the greater time required to build it are the alleged danger of carrying away the lock gates at either end of the summit level if a ship moving at speed should strike them, and the possible danger to structures through malice or in time of war."

The very first paragraph in the majority report[72] covers "safety and protection," part of which states as follows:

> "The modern lock for ocean going vessels is a work which an enemy through stratagem could with no great difficulty put out of use in an hour or even a few minutes. If a small detachment from the enemy's fleet, armed with high explosives landing secretly by night at some nearby shore or inlet, hiding in the neighboring jungle, should surprise the canal guards, or if a few malicious individuals in disguise should succeed in exploding against the lock gate under high water pressure as much explosive as they could carry, they could disable the lock and could probably cause damage of such colossal magnitude as would put the canal out of use for months. This danger is one that very strict watch and guard might prevent in great measure, but it is well nigh impossible to provide effectually and always against such peril."

The last sentence quoted is especially true today, even though the writers of the report in 1905 did not and could not have been expected to foresee either the modern airplane or the atomic bomb!

---

[68] "History of the Panama Canal," by Ira E. Bennett, Historical Publishing Co., Washington, D. C., 1915, p. 187.

[69] "Early Days at Panama," by John F. Stevens, *Engineering News-Record*, Vol. 115, 1935, p. 216.

[70] "The Report of the Board of Consulting Engineers for the Panama Canal," *Engineering News*, Vol. 55, 1906, p. 202 and p. 234.

[71] *Ibid.*, p. 238.

[72] *Ibid.*, p. 205.

Another interesting section of the 1906 majority report[72] quotes part of the instruction of President Roosevelt to the Consulting Board dated September 11, 1905, as follows:

> "I desire also to know whether if you recommend a high level multi-lock canal it will be possible after it is completed to turn it into or to substitute for it in time a sea level canal without interrupting the traffic upon it."

The Board answered that query[72] in the following language:

> "1. That it is possible to turn any lock canal which it [the Board] has considered into a sea level canal without interrupting the traffic upon it. 2. That it is practicable from an engineering standpoint to transform any lock canal which it [the Board] has considered, into a sea level canal but that the cost and difficulty of such transformation would be so great as to render such a change impracticable from a financial standpoint until the traffic should have so increased as to tax the capacity of the lock canal, or until other good and sufficient reasons existed for such a change. 3. That if a sea level canal is to be constructed in the future, it should be built directly without first building a lock canal."

The majority report recommended the sea-level canal[73] because of its "indispensible features of a convenient and safe ship canal" and estimated the cost of its construction to be $247,000,000, with a total cost including houses, floating equipment for operation, etc., at $333,000,000.[74] It estimated the time of construction at from 12 to 13 years.

Increased economy and speed won over increased safety, however, and the lock canal was approved and built. Today Colonel Stratton is recommending (and most properly) the expenditure of more that $2,000,000,000 for safety alone! It might be of a little interest, therefore, to make a rough approximation of the financial saving, or loss, which would have resulted if safety had been the original, controlling factor, and if the sea-level canal had been built in 1905.

The following calculation is admittedly neither accurate nor thorough, but it is a good and probably a sufficient indication of the correct answer. Any savings that would accrue from a reduced military garrison are omitted as are any savings resulting from shorter passage and waiting time. Similarly, the increased safety is ignored. After all, either by good luck or by good defense, the canal has passed successfully through two major wars, unharmed to date.

The construction of the present canal was begun in 1906 and finished in 1914 at a cost of approximately $350,000,000. Additions made up until June 30, 1947, have increased this amount to $372,000,000. To this sum should be added interest during construction which amounted to $129,000,000, resulting in a total of $501,000,000. Annual interest charges at 3% computed but not charged on the total amount comparable to that given previously, as it varied from year to year, equal $409,000,000. The actual operating cost of the canal as represented by appropriations was $316,000,000. Thus, the original cost of the canal, plus interest and operating expenses—all as of June

[73] *Engineering News*, Vol. 55, 1906, p. 210.
[74] *Ibid.*, p. 209.

30, 1947—equals $1,226,000,000. The income from the canal deposited with the United States Treasury amounted to $587,000,000 for the same period. This has been omitted from the totals on the theory that the sea-level canal proposed in 1905 would have returned at least an equal income. This latter canal would not have been finished as early as the present canal, but the difference probably would have been made up by the attractiveness of quicker transit and less waiting.

To advance the total cost figure of $1,226,000,000 from 1947 to 1960, the assumed date of completion of the new canal, one must add interest amounting to 39% of $372,000,000 and also assumed operating expenses at $10,000,000 a year, or $145,000,000 and $130,000,000, respectively—a grand total of $1,501,000,000 as the cost of the present canal to 1960.

To arrive at a comparable cost of the originally proposed sea-level canal requires several assumptions, all wide open to just criticism. The first, of course, is the question of whether the canal could or would have been built. Considering the well-known impatience of the American public and Congress, it is entirely possible that, with the inevitable huge slides and the cost (which at that time would have been considered astronomical), the construction of the canal might very well have been abandoned in disgust. The lock canal originally estimated at $140,000,000[75] actually cost $350,000,000, or 2.5 times the estimated cost, due to improved cross sections, increased excavation, and other causes. Taking the original estimate of the sea-level canal and increasing it in the same proportion gives $833,000,000. The Special Engineering Division of The Panama Canal estimates the ratio of the 1946 construction costs to the 1906–1914 costs as 2.5 to 1, or 3 to 1. Applying this ratio to the estimated cost ($2,483,000,000) of the proposed canal results in $830,000,000 to $1,000,000,000—a reasonable check. To be conservative, assume the cost to be $1,000,000,000. Add to this sum the interest during construction at $347,000,000 (the same ratio as for the present canal) and the annual interest (also in the same proportion) at $1,489,000,000. The result is a total of $2,952,000,000, to which must be added the cost of operation (assumed at 75% of this cost for the present canal), $334,000,000, which yields a grand total of $3,286,000,000.

The 1960 cost of the present canal plus the new canal (including $372,000,000 for interest during construction) amounts to $4,356,000,000, indicating an apparent saving of more than $1,000,000,000 if the sea-level canal had been adopted in 1905. It is evident that had the canal originally been built at sea level, there would have been a very substantial financial saving, in addition to an increase in safety and ease of operation. Time, and the atom bomb, have proved the soundness of the recommendations of General Parsons and his associates.

It would be neither fair nor just, however, to cast aspersions on the minority report of 1905. The recommendations of that group were correct as based on their assumptions. Thus far, the Panama Canal has accomplished its mission superbly in peace and war. As one of the commanders of a theater service of supply in the Far East, the writer can testify to the great service

[75] *Engineering News*, Vol. 55, 1906, p. 239.

it rendered in World War II—the value of which cannot be stated in dollars alone; but the nation has been "riding its luck." The fact that the canal has come safely through two wars is no guarantee of future security. As the advertisements point out, a new element has been added. The present canal is nearly defenseless against modern weapons of attack and the quicker the proposed canal is completed the better.

WILLIAM HERBERT HOBBS,[76] ESQ.—A possible sea-level, ship canal across the Tehuantepec Isthmus in Mexico does not appear to have been very seriously considered in these studies, inasmuch as attention was given to that along the circuitous route proposed for a canal by R. W. Schufeldt, a Captain in the United States Navy, in 1870. This was for a lock canal which would

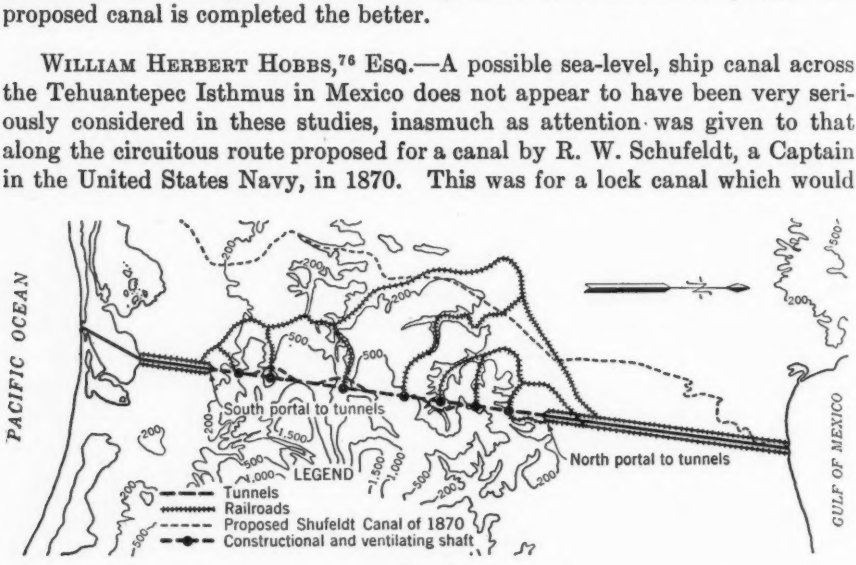

FIG. 105

have been 165 miles long (see route in Fig. 105). The Isthmus of Tehuantepec offers the best possible location for an interocean, combined open ditch and tunnel ship canal at sea level, which could be made largely secure from successful attack.

In contrast to a canal which would follow the Schufeldt route, the Tehuantepec canal herein proposed would be on a direct line from Puerto Mexico, the Atlantic terminus, almost due south to the Lower Lagoon on the Pacific front (see Fig. 105). Its length is thus reduced from 165 statute miles to 126 miles, and of this distance one half, or 63 miles, is across a featureless plain generally less than 50 ft above the sea. The subsurface rocks of this plain are soft Tertiary sediments which could be easily excavated by power shovel or bulldozer.

It is proposed to pierce the central hardrock mountain, which is the backbone of this isthmus, by a tunnel 63 miles in length. By reason of seven constructional and ventilating shafts, it is, in reality, a continuous succession of eight tunnels between its two portals. The longest of these tunnels would be 14 miles, with five tunnels each less than 8 miles. The tunnel cross section would have a maximum width of 175 ft and the same maximum height, which gives a cross section of 2,222 sq yd (see Fig. 106). This should accommodate the largest proposed battleships and "flattops," and the present trend is toward

[76] Prof. Emeritus of Geology, Univ. of Michigan, Ann Arbor, Mich.

increased length, rather than beam, in the interest of greater speed of both types and of longer runways on aircraft carriers. The very largest ships may find it necessary to provide a knee joint in their lofty radar masts for partial lowering when making the passage through the canal.

From the proposed constructional shafts of the tunnel, each only a few hundred feet in depth, conveniently located canyons will permit the building of railways, all with downgrades to the open ditch sections of the canal, so that the excavated rock can be dumped to form high riprap walls on both sides of the open ditch, and to build harbor moles in addition. This should protect the ditch from all but direct bomb hits. For the tunnel itself protection is complete, provided that the portals are of thick heavily reinforced concrete. Behavior of the German submarine pens so constructed proved them to be almost indestructible, both during World War II and after it as well.

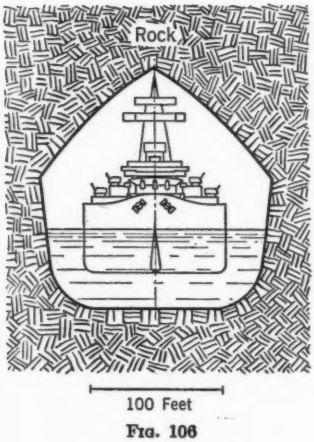

FIG. 106

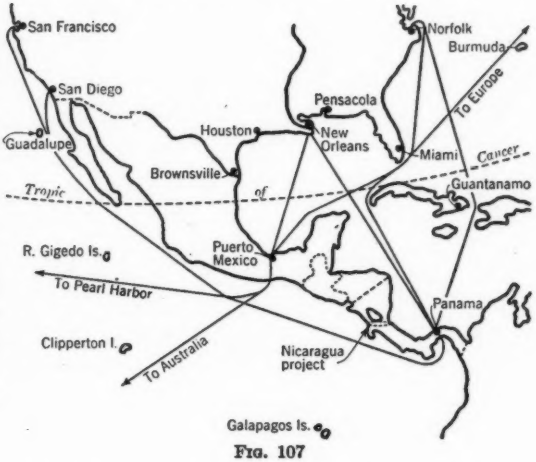

FIG. 107

To the east of three of the shafts (the third, fifth, and sixth counting from the north in Fig. 105) the dams erected in the canyons would provide large reservoirs which, if combined with hydroelectric plants, would furnish power for the operation of the hoists and railway, as well as for electrification of the tunnel. These reservoirs would also provide water supply for the workmen's villages high above the unhealthy lowlands.

Three or more tunnel sidings, each 2 miles in length would permit uninterrupted two-way traffic through the tunnel, and would also afford protection for the fleet if the canal were to be under attack from the air in wartime. The seven shafts of the tunnel would permit its construction, simultaneously, in two directions from each shaft, and in one direction from each portal. This should reduce, considerably, the time required to complete it, which is especially important in the event of an early national emergency.

The open sections of the canal should be separated into two waterways, each for one-way traffic. Excavation should thus be greatly reduced and danger of collisions within a single narrow channel be obviated. Two ditches, each 175 ft wide, would serve as much traffic as a single ditch very much wider

than the combined breadth of the two. Intercommunicating passages would maintain the normal surface level of the water when disturbed by the bow waves of the moving vessels.

The advantages of this proposed Tehuantepec canal, over that recommended for conversion of the Panama Canal to sea level, are many and convincing. They are as follows:

1. The Panama project would provide only a single interocean canal, as it does at present. The Tehuantepec project provides two, which are more than 1,000 miles apart.

2. During the period of construction (possibly as much as 10 years) the Panama Canal, in the case of the Tehuantepec project, would continue to be in unobstructed use.

3. Throughout its length the Tehuantepec canal would be almost invulnerable to attack, the tunnel section completely so. The converted Panama Canal would be insecure under attack and the studies have indicated that, if blocked, it would require weeks to reopen it. The portals of the proposed tunnel at Tehuantepec, if constructed of heavily reinforced concrete (as were the German submarine pens during World War II), would be almost completely indestructible.

4. In time of war with menace from both ocean fronts, the fleet, when at the canal, could have a fully protected two-ocean base from which to move to either front as might be required. Such protection for a fleet would be quite unique anywhere in the world.

5. The proposed Tehuantepec canal would cut 3,000 miles of sea lanes from the Panama route between the naval base at Norfolk, Va., and the San Diego (Calif.) or Pearl Harbor (Hawaii) bases; and equal reductions would be secured for commercial sea travel between ports on the East Coast and the Gulf of Mexico and those on the West Coast (see Fig. 107).

6. In time of war, the sea approaches to the Tehuantepec canal could be guarded on the Atlantic front by air patrols and by radar operated from airfields at Brownsville, Tex., Houston, Tex., New Orleans, La., Pensacola, Fla., Miami, Fla., Guantánamo, Cuba, and Yucatan, whereas the Panama Canal cannot be thus guarded. The recent enforced withdrawal of air outposts from Panamanian territory, and the 1948 uprisings at Bogotá, Colombia, only 500 miles from the Panama Canal, demonstrated only too clearly the insecurity of the Canal Zone.

7. Off the Pacific front the sea approaches to the Tehuantepec canal could be guarded in part by air patrols and by radar operating from bases in the Revilla Gigedo and the Galápagos island groups and from Clipperton Island (see Fig. 107).

8. A canal on the Isthmus of Tehuantepec is much favored by its known immunity from destructive earthquakes throughout the last three centuries, although earthquakes have been disastrous for most of Mexico and Central America.[77]

[77] "New Volcanoes and a New Mountain Range," by William Herbert Hobbs, *Science*, Vol. 99, 1944, pp. 289–290, maps.

9. The northern third of the Tehuantepec Isthmus is a highly productive oil field, so that local fuel oil would be available for vessels transiting the canal. This field, which was opened as late as 1921, yielded 5,842,000 bbl of oil in 1946.

10. The Pacific terminal of the proposed Tehuantepec canal is within the Lower Lagoon (see Fig. 105), and inasmuch as this lagoon has a narrow connection with the sea, no tidal locks will be required on this front, although they are necessary for the Panama project.

11. The operational advantages of the straight course of the proposed Tehuantepec canal over the sinuous one at Panama are considerable. Electrification will be available not only for illumination, but also for the propulsion of vessels; and thus it should obviate the wear on the canal walls by the currents from churning screws.

Without unnecessary delay a precise profile of the line of this proposed canal should be surveyed, and drill borings should be put down within the tunnel section. Until this has been done, no reliable estimate of costs is possible. Purely tentative ones based on an assumed average depth of 120 ft for the open ditch sections (probably a liberal estimate) are as follows: For the 63 miles of tunnel, plus 6 miles for three tunnel sidings, 271,000,000 cu yd; and, for the two open ditch sections, 340,000,000 cu yd—a total of 611,000,000 cu yd. This is roughly two thirds that estimated as necessary to convert the existing canal at Panama to a sea-level canal.

In conclusion, the writer would emphasize as the greatest of all advantages of the Tehuantepec project over the Panama one, its very much greater measure of security. Colonel Stratton, for the committee, has admitted for the latter its vulnerability under bombing attack, but he believes the blocked canal could probably be reopened in a matter of weeks. In a modern war, this period of weeks, during which the canal was blocked to the U. S. Navy, might well spell the difference between ultimate victory and crushing defeat.

HIBBERT HILL,[78] M. ASCE.—The slides that occurred during construction of the Panama Canal made a deep impression on the popular consciousness. The undertaking to construct the Panama Canal was of world-wide interest. The construction forces were in some degree the representatives of all men in a struggle against gigantic and imperfectly understood natural obstacles—a struggle whose outcome was far from certain. Nature, in the slides, brought up her shock troops. To the construction forces and to the world, the entire contest became epitomized in the struggle with the slides.

Now that a new and deeper excavation is under consideration, the fact will be recalled that the slides were overcome by only a narrow margin and at great added expense, and the question will be asked why can this greater work be undertaken with assurance now. The answer to this question, in brief, is that, in the four decades since the United States undertook to construct the canal, great progress has been made in understanding the cause and prevention of slides.

A Board of Consulting Engineers, drawn from the world's most eminent engineers, aided in the design of the present canal. As stated by Messrs.

[78] Hydr. Engr., Northern States Power Co., Minneapolis, Minn.

Binger and Thompson this Board established slopes of 3 vertical on 2 horizontal for all slopes in rock through the region of the Continental Divide. The slide history of the French construction and some few borings in the area of the Continental Divide were available to the Board. The Board and all those concerned with the construction seem to have been satisfied with the information available and with the slopes established. The record indicates that with these slopes some slides were anticipated, but that the volume of slide material to be removed was expected to be less than the additional excavation which initially flatter slopes would have caused. This was substantially proved by the event, except in the case of the great slides in the Cucaracha formation.

The East and West Culebra slides in this formation began to move in October, 1907, and continued to move at an increasing rate. The method of combating them was principally that of digging to remove the slide material from the cut. It was not until 1910 that C. W. Hayes, Chief Geologist of the United States Geological Survey, was sent to study the slides. He made a brief study in which he diagnosed the causes correctly. In January, 1911, D. F. MacDonald was appointed resident geologist, and at that time began a continuous study of the slides and of the soils and geology of the Canal Zone.

This history is not recited in criticism but rather in support of the view that, although the engineers responsible took all measures which they thought justified to prevent and combat the slides, the state of knowledge at the time did not provide a basis for anticipating the slides, nor for corrective measures once the slides were encountered. It is much to the credit of those in charge that, before construction was completed, a fundamental understanding of causes was developed, and a beginning made in the application of that understanding.

The designers of the canal did not appreciate that the 3-on-2 slopes which they adopted were certain to result in slides of great magnitude in the weak rocks of the cut. Furthermore, they were unaware that they were compounding trouble by inducing slides in the Cucaracha formation. With respect to the latter point, Messrs. Binger and Thompson remark briefly that if slides occur the total amount of material to be removed would be greater than the excavation required had the canal banks been excavated initially to stable slopes. This statement is based on the fact that the Cucaracha loses strength upon disturbance; hence, the stable slope of the material disturbed by a slide is considerably flatter than the stable slope of the undisturbed material.

This characteristic is now well recognized as common to many clay soils, but the possibility of such an occurrence was totally unknown to the builders of the canal. Study of the slides of the present canal has shown that the residual strength of the Cucaracha formation, after sliding, is about 20% of its undisturbed strength. Therefore, the existing slopes in the slide area are now as flat as 1 on 12, whereas the same slopes would have been stable if initially excavated about 1 on 5. This characteristic of the Cucaracha formation provides an impelling reason for stable initial slopes in the cuts of the proposed sea-level canal.

Since completion of the canal the science of soil mechanics has become a well-established branch of engineering. Also, study and exploration have immensely expanded knowledge of the geology of the Canal Zone—of the proper-

ties of the soils and rocks, and of the behavior of those rocks in cut slopes. As a result engineers now not only understand the mechanics of slides but are able to compute with reasonable certainty the slopes required to avoid the slides. The gulf between the knowledge of 1905 and the present understanding is dramatized by the difference between the 3-on-2 slopes adapted for the original cut, and the slopes ranging from 1 on 4.6 to 1 on 9.4 shown in Fig. 71.

The stable slopes determined by Messrs. Binger and Thompson depend in part on observations, by Mr. MacDonald and others, of actual slopes in the rocks of the region; in particular, for deep cuts, they depend on analyses by the Swedish circular slide method, a tool of modern soil mechanics. The responsibility which soil mechanics is thus assuming may be measured in the light of the description of past slides, given by Messrs. Binger and Thompson, and in the light of the tremendous volumes of excavation required to obtain the stable slopes shown in Fig. 71. Very important reliance is thus being placed upon the method, and it is proper to inquire whether it is justified.

The writer believes that such reliance is justified. The method has been in wide use since before 1928 and has met with general acceptance. It has been used to design many slopes that have proved stable, and, perhaps more important, it has explained many observed slope failures very well. The writer recently had occasion to apply the method to a past failure, and not only did it explain the failure accurately, but it also located the failure surface in the position actually occupied. The authors of the seventh Symposium paper mention that the value of cohesion for the Cucaracha formation was checked by analytical studies of the East and West Culebra slides. These studies were made by the Swedish circular slide method, and were particularly convincing to the writer in that the computations not only predicted the occurrence of a slide, but also predicted (by the location of the critical arc) the position of the break and the upheaval of the canal bottom as observed.

The eighth Symposium paper, by Messrs. Casagrande and Shannon, describes the beginning of a research which may provide important new conceptions and, in any case, will explore a field—the effect of transient loading—which, in a world subjected to high speed traffic and higher speed explosions, needs exploration. The immediate objective—determination of the effect of explosive impulses on the stability of the Panama Canal slopes—is an important one, and the indications of the published results are reassuring in that respect.

As Messrs. Casagrande and Shannon state, the effect of transient loads on soils is important in many applications. It seems to occur to every questioner to ask, for example, why airfield pavements do not fail at the point of impact of landing planes. Measurement of stresses in the landing gear has demonstrated that such impact loads are often several times the static load, yet failures of pavements at the point of landing are not observed. In accelerated traffic tests by the Corps of Engineers, Department of the Army, pressure cells recorded subgrade pressures approximately 30% less in the case of a wheel moving at from 5 miles per hr to 7 miles per hr than when the same wheel was static. These tests indicated that, for unexplained reasons, the load when moving was spread over an area 20% greater than when static. It is reasonable to suppose that at higher speeds these effects would be intensified. The investigation

reported in the eighth Symposium paper should aid considerably in explaining these observations and similar phenomena.

The writer realizes fully that this research is in its initial stages. It is his hope, however, that Messrs. Casagrande and Shannon will be able to clarify the indicated parts of their presentation in their closure.

KENNETH C. REYNOLDS,[79] M. ASCE.—The interesting and valuable paper by Messrs. Meyers and Schultz presents two methods used to predict the velocities to be expected in the proposed 40-mile Panama sea-level canal. The first method utilized computations based on analytical methods developed by George B. Pillsbury,[8] M. ASCE; the second method involved observations made on an undistorted model of the entire canal.

Velocities in the new channel could have been computed had the flow in the canal been steady. Such will not be the case because the water surfaces of the two oceans pass through tidal cycles of different heights and phases (Fig.26), with successive days having different tidal ranges.

General Pillsbury has developed a basic equation for examining the velocity of current in a tidal canal. The rate of flow is increasing or decreasing continuously, and the direction of the flow is reversed periodically. The usual equations for steady flow were expanded to account for the work done in the acceleration and deceleration of the current. The basic equation included the following four terms: The surface head, to describe the slope of the water surface; the velocity head; the acceleration head; and the friction head.

The term for the friction head depended on the Chezy coefficient, C, which at once involved some roughness coefficient such as Manning's n. Both the computations and the model investigations required an evaluation of the roughness coefficient for nature or for the prototype, whereas the model studies also necessitated knowledge of the roughness coefficient of the miniature canal.

The investigators obtained information as to the probable roughness coefficient of the prototype from two sources—from data on large channels in the United States and from field observations of flow in Gaillard Cut for two trial runs. These will be examined in detail subsequently.

The roughness data on large channels were obtained for several waterways in the United States and led to two conclusions. The first was:

> "* * * that the Manning coefficient for a river channel is least when the stage is at or somewhat above normal bankfull stage, and tends to increase for both higher and lower stages."

The velocity of flow in an open channel depends in part on the shear at the boundaries. This must be reflected in the methods used to evaluate Manning's n. The latter varies with the boundary roughness and probably with the viscosity of the water, particularly for small values of the Reynolds number. The foregoing conclusion that, for a natural channel, n has a minimum value at a certain stage or hydraulic radius (Fig. 27) raises the question as to what other factors enter the picture. Does the relative roughness of the channel vary

[79] Head, Dept. of Gen. Eng., College of Eng., Univ. of Southern California, Los Angeles, Calif.

because of changes in the vegetation of the presence of silt? A clarification of this conclusion is desirable. Data from other large natural channels should be studied.

The second conclusion was:

> "* * * that the bankfull roughness coefficients do not vary greatly for rivers and canals in different kinds of materials and in widely separated locations."

In view of the foregoing discussion, this conclusion needs further study. The important point has not been the geographical location of a channel, but the type of boundary roughness; and yet this conclusion is for different kinds of bank material.

The second source of data on the roughness coefficient was the field observations of flow in Gaillard Cut. The outermost stations were 37,100 ft apart, and this distance was divided into reaches of 8,100 ft, 4,300 ft, 7,600 ft, 8,400 ft, and 8,700 ft, respectively. The mean areas varied from 14,900 sq ft to 21,500 sq ft and the hydraulic radii, from 36.0 ft to 38.0 ft during the two tests. The gages at the end stations were recording gages; the six intermediate ones were hook gages. It was essential to "zero" the gages carefully since the observed differences in water levels were to be small for the anticipated flow.

Supposedly, no flow was established through the cut. It appears to the writer that it would be difficult, if not impossible, to quiet the 7-mile-long body of water so that there would be no motion. To eliminate surges, wind action, or any velocity of flow is indeed difficult. Of course, errors in "zeroing" the gages would affect data based on subsequent gage readings.

The test runs were made during two succeeding nights. Current meters were used at each end of the test reach to evaluate the mean velocity and the average discharge of 22,000 cu ft per sec. For the several reaches, the mean velocity was from 1.02 ft per sec to 1.48 ft per sec. It would require about 8 hours for a particle of water to traverse the entire 37,100 ft, and, hence, presumably it would take more than this time for equilibrium conditions to become established.

The mean difference in water-surface elevations lay between 0.021 ft ($\frac{1}{4}$ in.) and 0.041 ft ($\frac{1}{2}$ in.). Small differences in these values would have affected the computed slope of the average energy gradient, which ranged from between 0.0000023 and 0.0000060.

From the foregoing data it was possible to evaluate the roughness coefficients of Manning, Kutter, and others. The average Manning n was about 0.026, which in the writer's opinion is only an approximate value. The field difficulties of stilling the large body of water, of setting hook gages at night, and of obtaining uniform flow made it difficult to obtain reliable data.

The second method for predicting velocities was by making observations on a model of the entire 40-mile canal. This model intrigues the writer, as he directed the research program at the Massachusetts Institute of Technology in Cambridge, on the 110-ft-long model of the Cape Cod Canal in Massachusetts for the Boston (Mass.) Office, Corps of Engineers, Department of the Army. Space limitations necessitated a 10:1 distorted scale model, with its attendant

uncertainties. Messrs. Meyers and Schultz are to be commended on using an undistorted model, even though it required a model nearly ½-mile long.

The procedure involved creating, artificially, a rise and fall of the water surfaces at the ends of the model to simulate the tides of the two oceans. The resulting motion of the water within the canal section was presumed to be indicative of that to be expected in the prototype. Such a procedure is accepted model practice, provided the requirements for a true model are met fully.

The model scale was 1:100. Based on the authors' experience, an ordinary concrete surface in a model of this scale was used as simulating best the roughness of the prototype. When the model was completed, steady flow was established, and the resistance coefficient for the model "was found to correspond to the selected Manning coefficient of 0.024." The significance of the word "correspond" is not clear. Does it mean that n for the model and for the prototype was the same; or were these n's unequal?

Subsequently, it was pointed out that, since gravity was the predominant force, the Froude law was used to interrelate times, velocities, and discharges. This does not preclude the existance of any friction along the model canal. To the writer it would imply that, with the times for the model one tenth those for the prototype, the roughness of the model should be so adjusted that, under gravity flow conditions, the loss of head in the model should be geometrically similar to that in the prototype. Since no prototype data were available, it is assumed that data from other studies of comparable prototype and model roughnesses by Messrs. Meyers and Schultz led to the use of the Froude law.

Using the adopted model scale, the minimum depth of water was 0.60 ft and the minimum bottom width of channel was 0.50 ft. The velocities in such a model would have produced some side-wall effects, although these might not have been serious.

Water levels along the model canal channel were measured by automatic records and manually-operated hook gages. It is difficult to visualize how the recorders gave reliable data. Usually they consist of a float on the water surface whose vertical motion is recorded on a paper mounted on a slowly rotating drum. If the float were in the canal, the flowing water would create uncertain errors introduced by surface tension and by dynamic effects. Should the water surface in the canal be connected to a stilling well and the float be on the water surface in the well, other errors would arise. If the stage in the canal were rising, the water in the well would lag behind that outside. As the rate of rise decreased, the lag would grow less, and at high tide, or soon thereafter, there would be no lag. The correction for a falling stage would be different from that for a rising stage. Were corrections applied to the data from the automatic recorders? Since prototype errors would be one hundred times the model values, great care was needed in collecting model data.

At other stations manually-operated hook gages were used. The writer has always cautioned students not to use hook gages in flowing water, since the conventional hook dips below the water surface so that in flowing past it, water creates a surface disturbance which is likely to affect the gage setting. The magnitude of the disturbance would change with the varying velocity and the reversal of flow. The writer would have recommended the use of point gages.

To set such gages accurately and to read them at 30-sec intervals in the model required considerable skill by the observers. The writer believes that the electric water level indicator developed by H. L. Hazen[80] for the Cape Cod Canal model, or some other similar device, would have given more accurate readings and would have given average values of the elevation of the wavy water surface at an observation station.

GREGORY P. TSCHEBOTARIOFF,[81] M. ASCE.—The present discussion is concerned mainly with the paper by Messrs. Casagrande and Shannon. Other papers of the Symposium will be mentioned only in so far as the recommendations contained in them are based on the reported findings of these two authors.

The writer is in general agreement with these findings, but only in a qualitative sense. The manner in which the tests were performed does not permit any quantitative evaluation of the results for the purpose of their direct application to slope-design problems. The writer's qualitative agreement is based on the results of an earlier extensive program (from 1934 to 1946) of dynamic tests performed under his direction at Princeton University (Princeton, N. J.) for the Technical Development Service of the Civil Aeronautics Administration.[82,83,84] This program was intended to provide some insight into the relative importance of the various factors affecting the bearing properties of soils in airport subgrades and base courses when subjected to vibratory and to slow repetitional loading by warming up and by taxying aircraft. Inspite of the different objectives and corresponding differences in the test equipment employed by the two test programs, the data obtained at Princeton University may nevertheless serve for an analysis of, and comparison with, the results reported from Harvard University (Cambridge, Mass.).

The Princeton tests[82,83,84] have shown that sands could be very strongly affected both by vibratory and by slow repetitional loading. For uniform types of sand the deformation produced by the vibratory force could be as much as one hundred and forty times greater than the deformation produced by a single application of an equivalent static load.[85,86] However, in the case of clay soils, other factors remaining equal, the continuous application of a vibratory load produced approximately the same deformation as a single application of an equivalent static load.[87,88,89]

---

[80] "Electrical Water-Level Control and Recording Equipment for Model of Cape Cod Canal," by H. L. Hazen, *Electrical Engineering*, February, 1937.

[81] Associate Prof. of Civ. Eng., Princeton Univ., Princeton, N. J.

[82] "Effect of Vibrations on the Bearing Properties of Soils," by Gregory P. Tschebotarioff, *Proceedings*, Highway Research Board, National Research Council, Vol. 24, 1944, pp. 404–425.

[83] "Vibratory and Slow Repetitional Loading of Soils," by Gregory P. Tschebotarioff and George W. McAlpin, *ibid.*, Vol. 26, 1946, pp. 551–562.

[84] "The Effect of Vibratory and Slow Repetitional Forces on the Bearing Properties of Soils," by Gregory P. Tschebotarioff and George W. McAlpin, *Technical Development Report No. 57*, Civil Aeronautics Administration, October, 1947.

[85] "Vibratory and Slow Repititional Loading of Soils," by Gregory P. Tschebotarioff and George W. McAlpin, *Proceedings*, Highway Research Board, National Research Council, Vol. 26, 1946, p. 556, Fig. 14.

[86] "The Effect of Vibratory and Slow Repetitional Forces on the Bearing Properties of Soils," by Gregory P. Tschebotarioff and George W. McAlpin, *Technical Development Report No. 57*, Civil Aeronautics Administration, October, 1947, p. 561, Fig. 31.

[87] "Effect of Vibrations on the Bearing Properties of Soils," by Gregory P. Tschebotarioff, *Proceedings*, Highway Research Board, National Research Council, Vol. 24, 1944, p. 421, Fig. 28.

[88] "Vibratory and Slow Repetitional Loading of Soils," by Gregory P. Tschebotarioff and George W. McAlpin, *ibid.*, Vol. 26, 1946, p. 554, Figs. 5 and 6.

[89] "The Effect of Vibratory and Slow Repetitional Forces on the Bearing Properties of Soils," by Gregory P. Tschebotarioff and George W. McAlpin, *Technical Development Report No. 57*, Civil Aeronautics Administration, October, 1947, pp. 53 and 54, Figs. 38 and 41.

"Continuous load application" means the application of a vibratory force for a period of from 10 to 20 min—that is, more than 10,000 load repetitions. The rate of deformation produced by the continuous application of dynamic load decreases with time;[90,91] the time-deformation curve has a parabolic shape, as illustrated in Fig. 108. Since after a large number of dynamic load repetitions the final deformation Δ is approximately equal to the static deformation produced by a single application of an equivalent static load, it would follow that a single application of a dynamic load should produce only a fraction of that deformation. Therefore, conversely, to produce a deformation leading to failure, by a single loading, a dynamic load greater than a static load would be needed. This is exactly what was found during the Harvard tests, and such results are therefore in agreement with the deductions that can be drawn from the earlier tests at Princeton.

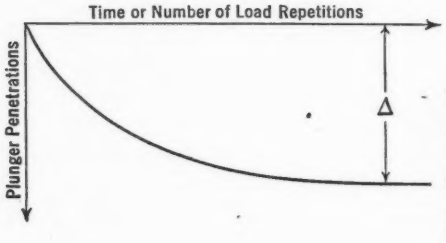

FIG. 108.—RELATIONSHIP BETWEEN TIME AND THE INCREMENT OF SOIL DEFORMATION PRODUCED BY THE CONTINUOUS APPLICATION OF A VIBRATORY LOAD SUPERIMPOSED ON A STATIC LOAD OF CONSTANT INTENSITY (1944 TESTS, PRINCETON UNIVERSITY, PRINCETON, N. J.)

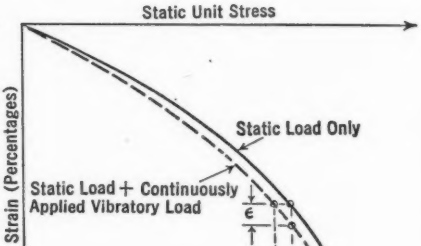

FIG. 109.—EFFECT OF CONTINUOUSLY SUPERIMPOSED VIBRATORY LOAD ON THE STRESS-STRAIN RELATIONSHIP OF CLAY SAMPLES SUBJECTED TO STATIC UNCONFINED COMPRESSIVE STRENGTH TESTS (1946 TESTS, PRINCETON UNIVERSITY, PRINCETON, N. J.)

The writer, however, has one criticism concerning the manner in which the Harvard tests were performed with the aim of providing design data for the Panama Canal slopes. It would appear from the paper under discussion that, during both the unconfined compressive strength tests and the triaxial shear tests, the dynamic load was not superimposed on a static load which had already induced shearing stresses in the test specimen; instead, all the shearing stresses during the tests were produced entirely by dynamic loads in one series of tests and entirely by static loads in another series of tests. This procedure has undoubtedly given results of considerable theoretical interest which have been reported in the paper. However, no comparable condition can ever exist in nature in connection with the problem of the stability of slopes in cohesive soil. Certain static shearing stresses are always present in an embankment and, depending on how closely these static stresses approach the limit of resistance of the material, an increase of these stresses as the result of dynamic

[90] "Effect of Vibrations on the Bearing Properties of Soils," by Gregory P. Tschebotarioff, *Proceedings*, Highway Research Board, National Research Council, Vol. 24, 1944, p. 413, Figs. 8 and 9.

[91] "The Effect of Vibratory and Slow Repetitional Forces on the Bearing Properties of Soils," by Gregory P. Tschebotarioff and George W. McAlpin, *Technical Development Report No. 57*, Civil Aeronautics Administration, October, 1947, pp. 36 and 37, Figs. 12 and 13.

loading may or may not produce failure. The writer is familiar with a case of a clay bank, a 500-ft section of which slid out into a river during the driving of a cluster of piles for a dolphin close to its edge. The relatively small shocks caused by this pile driving obviously produced stress intensities that exceeded the resistance of the bank. In this particular case the bank was composed of varved glacial clay. The rock flour characteristics of the material may have rendered it particularly susceptible to impact stresses superimposed on a near-critical static stress condition. The Harvard installation can provide valuable data by extending its studies to include different combinations of dynamic and static loading applied to various soil types.

However, the Harvard tests, as reported thus far, cannot yield any numerical data on the effect on the shearing strength of soils of dynamic forces superimposed on static forces—that is, under conditions generally existing in nature and as are certain to exist in the slopes of the Panama Canal.

Nevertheless, where clays are concerned the writer does not believe (on the strength of his earlier, 1946, tests) that this condition of superposition of dynamic forces on static forces would cause an appreciably detrimental increase of the effect of dynamic loads. In 1946 several unconfined compressive strength tests were performed on clay cylinders of 3.4-in. diameter and 7-in. height.[92,93] The results of these tests are illustrated diagrammatically by Fig. 109. In one test series the unconfined compressive strength test was performed as a controlled stress test by the gradual increase of only the static load. In the other test series the same type of unconfined compressive strength test was performed while a small vibratory force, equal to approximately 7% of the ultimate load, was applied from the very start of the experiment. It may be seen from Fig. 109 that for the same value of the static unit stress, the strain increment ϵ of the vibrated specimen can be related to an increment of stress p_d which was found to have the same order of dimension as the dynamic unit stress produced by the centrifugal force of the vibrator.

Therefore, the writer believes that the factor of safety of 1.3 which has been used for the design of the slopes, as reported by Messrs. Binger and Thompson, may be sufficient to take care of the increment of shearing stresses in the banks such as will be produced by dynamic loading. However, the paper by Messrs. Casagrande and Shannon leaves the impression that dynamic forces may well be neglected entirely in most slope stability problems. Such an impression would seriously hamper further research in this field and might lead to unsafe design proposals. This actually happened at the January, 1948, Annual Meeting of the Society when an oral discusser suggested decreasing the static factor of safety of the proposed Panama Canal slopes to 1.0.

The purpose of this discussion is to warn against any such over-simplifications. It is to be hoped that the Harvard tests will be amplified to determine the effect of impact forces on the strength of soils when such impact forces are superimposed on existing static stresses. A comprehensive further program

[92] "Vibratory and Slow Repetitional Loading of Soils," by Gregory P. Tschebotarioff and George W. McAlpin, *Proceedings*, Highway Research Board, National Research Council, Vol. 26, 1946, p. 555, Fig. 10.

[93] "The Effect of Vibratory and Slow Repetional Forces on the Bearing Properties of Soils," by Gregory P. Tschebotarioff and George W. McAlpin, *Technical Development Report No. 57*, Civil Aeronautics Administration, October, 1947, p. 60, Fig. 51.

of research along these lines in coordination with other related studies should permit, in time, the numerical evaluation of dynamic loading effects under natural field conditions and the consideration of these effects in computations of the factor of safety, which otherwise should be considered as still requiring the inclusion of a "factor of ignorance" component.

CHARLES W. DOHN,[94] JUN. ASCE.—It is significant that this Symposium does not mention the income-producing capabilities of the Panama Canal. The need for a sea-level canal by commercial traffic definitely exists. The decrease in ship operating costs alone nearly equals the differential in cost between a sea-level canal and a lock canal designed to meet the needs of commerce for the remainder of the twentieth century. Significance of the canal as an aid to commerce is often missed and it would be well if studies were made and kept accessible and up to date, as well as publicized, of the amount and value of commerce carried and the cost of alternate routes.

Hence, the Panama sea-level canal can be justified as an economic enterprise. It would be well for domestic economy, however, if construction were postponed for some years. In the intervening years experimental research and actual exploratory, advanced, and perhaps unique methods of construction could be developed and tested. Two steps which should be used to improve financing of the canal are: (1) Increase the tolls, and (2) decrease the canal construction costs. The consulting services of private design and construction engineers should be utilized to a large extent to report on and supervise both of these steps. Canal tolls can be increased on a yearly increment basis extended over a long period with provisions for flexibility. The project can be financed from tolls and the over-all cost reduced by the development of special construction methods. For example, the cubic yards of excavation times the average length of haul can be multiplied by an efficiency factor and reduced to power units and compared with available and potential local sources of hydraulic power. From Table 34, in the last Symposium paper, the total excavation is approximately 1×10^9 cu yd and, assuming an average haul of 10,000 ft, an average unit weight of 120 lb per cu ft, and a factor of 4 to allow for removal, friction and dredge losses, and reserve—this yields: $\frac{1 \times 10^9 \times 10{,}000 \times 4 \times 120}{33{,}000 \times 60}$ $= 2{,}500 \times 10^6$ hp-hr required.

There are indications that it might be possible to obtain one half this amount of power over approximately a 10-year period with modifications and additions to existing reservoirs, utilizing almost all the runoff. Runoff from these reservoirs would still be available for lockage use. Additional power sources could be sought within, say, a 200-mile radius of the canal. Development of these sources could be partly of a temporary nature and partly of a permanent form to be sold under agreement to local governments in return for from 10-year to 20-year power rights. Thus, the canal would be excavated by the same methods that nature uses to form valleys.

To operate hydraulic giants and to service hydraulic pool excavation methods use would be made of high-level sources of water, in addition to pos-

[94] Engr., Chf. Engrs. Office, Headquarters Dept., New York City Board of Water Supply, New York, N. Y.

sible booster pumps run by hydroelectric power and supplementary steam electric power. In hydraulic earth dam construction, small boulders and rock are sluiced out. This need not be done for canal excavation. Hydraulic dredge pipe and sluiceways with renewable linings would be advantageous. The dredge pipe can be siphoned over ridges into low areas and also used to construct dams and dikes as needed. A cutter head and pump such as illustrated in Fig. 100, supplemented by hydraulic giants, might be adapted to hydraulic pool methods and even to excavation on dry land. Much of the rock excavation is indicated to be of a soft nature (see Table 34). It may be possible to break the soft rock by hydraulic methods, inserting high pressure lines into seams, fissures, and drill holes sealed at stategic points, etc. Blasting is not always economical in soft rock because of the dissipation of concussion energy. This is particularly true of rock that has been exposed to weathering at some time in its life cycle. It might be economical also to break large rock fragments somewhat by mechanical crushers and dispose of this product with other hydraulic excavation. It would not be necessary to convey all material to Gatun Lake, which is at a high elevation and somewhat distant from much of the excavation. Such haulage also would impede operation of the lock canal.

Furthermore, using hydraulic methods, a higher continuous rate of removal can be maintained with less load on construction personnel working under tropical climatic conditions. The application of atomic energy to construction projects at present can only be surmised, but, it might be available for later stages of sea-level canal construction.

DONALD F. HORTON,[95] Assoc. M. ASCE.—All the papers presented in the Panama Canal Symposium are of interest and value not only to civil engineers but to the public generally. The paper by Messrs. Meyers and Schultz was of particular interest to the writer. The major results of the analyses which are used as the bases for determination of tidal currents agree with those derived from similar studies of the Cape Cod Canal in Massachusetts, with which the writer was associated some years ago. This fact is of importance to engineers who in the future may be faced with the problem of determining probable tidal currents in a canal differing in size from the Panama Canal. In tackling this problem, reference can be made profitably not only to this paper but also to the results of analysis of tidal currents in the Cape Cod Canal which have been presented previously.[96]

Reference is made in the paper by Messrs. Meyers and Schultz to an estimate of 2.6 knots for a Panama sea-level canal based on the Eytelwein formula with the comment that this formula was stated to agree reasonably well with observed velocities in the Cape Cod Canal. Since this velocity differs radically from the 4.4 knots to 4.6 knots reported by Messrs. Meyers and Schultz as having been determined from the methods described, some readers may infer that these methods would not be applicable to the Cape Cod Canal. However, the writer believes that methods of computation applicable

[95] Hydr. Engr., Beach Erosion Board, Corps of Engrs., Dept. of the Army, Washington, D. C.

[96] "The Proposed Improvement of the Cape Cod Canal," by E. C. Harwood, *Transactions*, ASCE, Vol. 101, 1936, p. 1440.

to the proposed Panama sea-level canal are equally applicable to the sea-level Cape Cod Canal and vice versa.

Since the range of applicability of the methods described by Messrs. Meyers and Schultz is a matter of importance to future investigators, some amplification is warranted. The crux of the matter is the conclusion by Messrs. Meyers and Schultz that, at the time of maximum current, the situation is nearly that of ordinary steady flow between the extreme tide levels. Exactly the same conclusion was reached during model studies of the Cape Cod Canal.[97]

The proposed Panama sea-level canal will have a 60-ft by 600-ft cross section and a length of about 35 miles. Maximum heads between the ends of the Panama Canal approximate 10 ft. The Cape Cod Canal has a 32-ft by 540-ft (project) cross section and a length of about 9 miles (not including approach channels). Maximum heads between the ends of the Cape Cod Canal approximate 7 ft. For canals ranging between these characteristics, maximum velocities may be computed on the assumption of steady flow with sufficient accuracy for all practical purposes.

Review of the various methods which have been proposed and used for determination of tidal flow in the Cape Cod Canal indicates the comparative simplicity of computations based on the assumption of steady flow. For example, a rather complicated method of solution by harmonic analysis was developed by William Barclay Parsons, Hon. M. ASCE, and applied by him to the Cape Cod Canal.[63] This method was based on the theory of tides in canals derived by Sir George Biddell Airy, as interpreted by Maurice Lévy.

Complicated tidal-flow formulas may have to be used for canals with characteristics which differ markedly from the range between the Panama and Cape Cod canals. For example, the steady-flow method of computation will not give accurate results for a very long canal of very small cross section. However, whenever applicable, much time and effort can be saved through use of the steady-flow method in the manner outlined in the paper by Messrs. Meyers and Schultz.

[97] "Model Study of Cape Cod Canal and Approaches," by K. C. Reynolds, Rpt. to Dist. Engr., Corps of Engrs., U. S. Army, Boston, Mass., December 21, 1936.

AMERICAN SOCIETY OF CIVIL ENGINEERS

Founded November 5, 1852

DISCUSSIONS

LATERAL EARTH PRESSURES ON FLEXIBLE RETAINING WALLS A SYMPOSIUM

Discussion

BY E. DE BEER

E. DE BEER,[59] ESQ.—The very extensive tests reported by Professor Tschebotarioff have engaged the writer's interest since his visit to the Soil Physics Laboratory at Princeton University (Princeton, N. J.) in 1947. In the intervening time, substantial results have been obtained, one of the most conclusive being the influence of a sand dike on the reduction of the pressure exerted by a backfill of liquid clay.

Some interesting phenomena were observed: (1) The reduction of the pressures on a bulkhead when a more rigid subsoil is near by; and (2) a decrease of the pressure on a bulkhead during the consolidation of the backfill while the relative movement of the wall is inward toward the fill. This second phenomenon has been verified in a report by E. C. W. A. Geuze mentioned by Professor Tschebotarioff and also in observations made during the performance of cell tests by the writer.

The subject of the report is limited essentially to a description of the results, and the author does not offer a mathematical interpretation. Nevertheless, the results are found to be sufficiently conclusive to serve as a basis for rules for the computation of pressures on anchored bulkheads. Since the results have not been given a physical and mathematical interpretation, and since they have not been confirmed by a larger number of tests, it seems advisable to be cautious in applying them in practice. It is in this spirit that the writer places great importance, on the one hand, to the need for continuing and extending the testing program and, on the other hand, to the need for a more refined analysis of the quantitative results.

In Section 5, paragraph *b*, of his paper, Professor Tschebotarioff makes the statement that there was no agreement between the measured pressure and the values calculated by the Rankine-Résal theories, although they are based on

NOTE.—This Symposium was published in January, 1948, *Proceedings*. Discussion on this Symposium has appeared in *Proceedings*, as follows: June, 1948, by Ralph B. Peck, Howard C. Roberts, Armand Mayer, S. Packshaw and J. Owen Lake, and Jacob Feld.

[59] Director of the Institut Géotechnique de l'État, Ghent, Belgium.

shearing resistances obtained from laboratory tests. On the other hand, he states that the measured pressures can be expressed by Eq. 7. That formula can also be written as follows:

$$p_h = \gamma_w h + \gamma_e h (1 - \tan \phi_q) \ldots\ldots\ldots\ldots\ldots\ldots (54)$$

Assigning numerical values to ϕ_q at intervals of 5° an interesting comparison between computed values of $1 - \tan \phi_q$ and $\tan^2 (45° - 0.5 \phi_q)$ is afforded by Table 4. In this table the values of $1 - \tan \phi_q$ for values of ϕ_q higher than 40° have been placed in parentheses, because they become smaller than the values of $\tan^2 (45° - 0.5 \phi_q)$ and thus no longer have any real physical significance. Measured as the slope of Curves II and III in Fig. 11, ϕ_q is about 24°, which by interpolation in Table 4 yields

$$1 - \tan \phi_q = 0.56 \ldots\ldots\ldots\ldots\ldots\ldots\ldots\ldots (55)$$

The pressure on the bulkhead as measured certainly approaches most nearly the case of the pressure at rest. The function $1 - \tan \phi_q$ should thus vary more or less in relation to the coefficient of the pressure at rest. Table 4 shows that the smaller the value of the angle ϕ becomes, the smaller the difference between the functions $1 - \tan \phi$ and $\tan^2 (45° - 0.5 \phi)$ will be. Consequently, the tests seem to indicate that the consolidation pressure on a moving wall, behind which the soil has the opportunity to consolidate, approaches the active or minimum pressure, as the angle of friction of the soil becomes smaller. This is the general tendency as the soil becomes more clayey. On the other hand, for pronounced sandy soils, the consolidation pressure against a wall that is moving in response to consolidation can be noticeably larger than the minimum or active pressure.

This different behavior of clayey and sandy soils has been known for a long time from the results of the numerous cell tests performed in Holland and in Belgium. The findings of these tests are now confirmed by the large-scale tests described by Professor Tschebotarioff, and they help one to understand partly the problems concerning the difference between the measured pressures and the values calculated from Eq. 5*b*.

TABLE 4.—COMPARISON OF $1 - \tan \phi$ WITH $\tan^2 (45° - 0.5 \phi)$

Quantity	VALUES OF ϕ									
	0°	5°	10°	15°	20°	25°	30°	35°	40°	45°
$1 - \tan \phi$	1	0.913	0.824	0.732	0.636	0.534	0.423	0.300	(0.16)	(0)
$\tan^2 (45° - 0.5 \phi)$	1	0.840	0.704	0.589	0.490	0.406	0.333	0.271	0.217	0.172

For that matter, Fig. 19 indicates clearly that, when the supports A and B are released after consolidation, the decrease in pressure is larger in the case of the sand-clay mixture than in the case of the pure clay.

In Fig. 19 it would be helpful to know how Professor Tschebotarioff explains values of K_{s+w} less than 0.5. The lateral pressure is given by

$$p_h = \gamma K_{s+w} h \ldots\ldots\ldots\ldots\ldots\ldots\ldots\ldots (56)$$

With $\gamma = 2\frac{t}{m^3}$, at depths where $K_{s+w} < 0.5$, the total pressure should be even less than the hydrostatic pressure of the water. In the case of complete consolidation, this seems to indicate some leakage at the considered depth.

The results of the second series of tests (see Part III) are also in agreement with the preceding statements in this discussion. After consolidation of the fluid red clay, $K_s = 0.50$ The value of ϕ derived from $K_s = \tan^2 (45° - 0.5\,\phi)$ is a little smaller than 20°, that derived from $K_s = 1 - \tan \phi$, a little larger than 25°. Both values occur in the range in which the value of the angle of internal friction of a clay may be expected. In that range the values of $1 - \tan \phi$ and $\tan^2 (45° - 0.5\,\phi)$ do not differ greatly, and thus the measured pressure cannot be very different from the minimum or active pressure.

This explains why (see Part III, end of Section B) a release of the ring supports equal to 0.3 in., or to 2.5% of the sample diameter, did not continue to decrease the lateral pressure exerted against the upper rings.

A last question concerns the results of the third series of tests (Part III, Section C) in which a K_s-value of 0.22 is reported. From this value Professor Tschebotarioff claims a substantiation of the earlier statement that the tentative recommendations shown in Fig. 25(*a*) are of a conservative nature. It is not the writer's intention to discuss the recommendations revealed in Fig. 25(*a*), but he cannot agree that the results in Fig. 28 substantiate their conservative nature. Indeed, the third series of tests were performed on a sand backfill with a height of only 39 in. (1 m). Therefore, the maximum effective pressure σ_e does not exceed 1 ton per sq m; yet even sands have some interlocking cohesion c (generally about 0.2 ton per sq m). With $\sigma_e = 1$ ton per sq m the corresponding shearing resistance τ is

$$\tau = c + \sigma_e \tan \phi = 0.2 + 1 \tan 30° = 0.778 \text{ ton per sq m} \quad \ldots\ldots (57)$$

The dry density of the sand (Part III, Section C) being 93 lb per cu ft (1,540 kg per cu m), the angle ϕ was adopted as 30°. Consequently,

$$\frac{\tau}{\sigma_e} = 0.778 = \tan 37°50' \quad \ldots\ldots (58)$$

and

$$K_s \leq \tan^2 \left(45° - \frac{37°50'}{2} \right) = 0.24 \quad \ldots\ldots (59)$$

The value given by Eq. 59 agrees very well with the measured value of 0.22; but the low value of K_s is only obtained because of the low value of σ_e, and thus because of the large relative influence of c. For instance, in a sand backfill with a height of 10 m, one should get

$$\sigma_e = 10 \text{ tons per sq m} \quad \ldots\ldots (60)$$

$$\tau = c + \sigma_e \tan \phi = 0.2 + 5.78 = 5.98 \text{ tons per sq m} \quad \ldots\ldots (61)$$

$$\frac{\tau}{\sigma_e} = \frac{5.98}{10} = 0.598 = \tan 30°50' \quad \ldots\ldots (62)$$

and

$$K_a < \tan^2\left(45° - \frac{30°50'}{2}\right) = 0.321 \quad \ldots\ldots\ldots\ldots\ldots\ldots (63)$$

The value given by Eq. 63 is much greater than that given by Eq. 59 and by the tests, indicating that the numerical values found in the third series of tests on small sand backfills may not be extrapolated to the higher backfills encountered in practice.

The results obtained with the tests performed at Princeton are exceedingly valuable. It is to be hoped that the unique equipment available there will also be used in the future to continue the program of testing, and that the profession will receive regular reports of the test results. If an extension of the testing program were possible, it would be worthwhile to include measurements of the pressure changes on the anchored bulkhead when the surface of the consolidated backfill is alternately loaded and unloaded.

AMERICAN SOCIETY OF CIVIL ENGINEERS

Founded November 5, 1852

DISCUSSIONS

THE RELATIONSHIP BETWEEN PILE FORMULAS AND LOAD TESTS

Discussion

BY DONOVAN H. LEE

DONOVAN H. LEE,[20] M. ASCE.—In a clear manner, the author has compared the results obtained by the variety of impact formulas selected, and by loading tests.

It is not difficult to demonstrate that the Hiley formula and the two adaptations of it are the only formulas that have any claim to reasonably accurate forecasts of the ultimate supporting value of piles. This position has been taken for granted, in the United Kingdom, at least, for the last ten years, although it must be admitted that there are still a few engineers in England who are reluctant to give up the Dutch (or Eytelwein) formula. Similarly, in the United States the Engineering-News formula "dies hard."

The author states that he purposely avoids the comparison of results by the impact formula and the test loads in the case of cohesive soils. In the writer's opinion this is particularly to be commended as there is little or no direct relationship between the resistance to penetration of piles in cohesive soils and their ultimate supporting value.

Actually, the author does include among his comparisons a number of tests in which clay strata are involved, but presumably has set aside tests in which the tip of the pile is bearing in clay. Nevertheless (as the author would probably agree), the methods of comparison used in Figs. 1 and 2 leave much to be desired; too much attention has been directed to showing the inaccuracy of formulas which are noted to be entirely unsuitable for the purposes to which they have been applied and too little to ascertaining in what respects and for what reasons the Hiley formula is not in close accordance with the test results.

The Hiley formula is intended to give the ultimate resistance to penetration and, although it is generally hoped that this is closely related to the ultimate supporting value of noncohesive soils, those cases for which the Hiley formula seems to give seriously incorrect results might be explained by the manner in which the loading tests were made, or the cohesive properties of some

NOTE.—This paper by Robert D. Chellis was published in May, 1948, *Proceedings*.

[20] Cons. Engr., London, England.

of the soils penetrated—rather than by some fundamental deficiency in the formula itself to allow properly for the subsoil conditions encountered.

The paper seems essentially to reinforce the already well-established belief that the Hiley formula is at present the best available. Notwithstanding this fact, the writer does not believe that the Hiley formula is theoretically correct; he is of the opinion that in a few years certain anomalies will be explained.

A study of the research by W. H. Glanville, Geoffrey Grime, and W. W. Davies[21] and of the paper by A. E. Cummings,[22] M. ASCE, published in 1940 supports this view.

---

[21] "The Behaviour of Reinforced-Concrete Piles During Driving," by W. H. Glanville, Geoffrey Grime, and W. W. Davies, *Journal*, Inst. C. E., Vol. 1, 1935–1936, p. 150.

[22] "Dynamic Pile Driving Formulas," by A. E. Cummings, *Journal*, Boston Soc. of Civ. Engrs., Vol. 27, 1940, No. 1, p. 6.

AMERICAN SOCIETY OF CIVIL ENGINEERS

Founded November 5, 1852

DISCUSSIONS

HIGHWAY BRIDGE FLOORS
A SYMPOSIUM

Discussion

BY SEARCY B. SLACK

SEARCY B. SLACK,[26] M. ASCE.—Publication of this group of papers has made available an excellent summary of results of tests and analyses of steel beam bridge spans with concrete floors. With the introduction of the deep beam and girder sections and wider roadways, the design of highway bridges with spans ranging from 40 ft to 100 ft or more changed very quickly to this simple type and the problem of load distribution and interaction of beam and floor slab became more acute. The Bridge Committee of the American Association of State Highway Officials spent endless hours in discussions but E. F. Kelley, then chairman of that committee, did the basic work of formulating the design specifications for loads and distribution which, with modifications due to later developments, are now in general use.[18] With the meager information then available, Mr. Kelley did an excellent piece of work.

In 1930, 1931, and 1932, quite a number of measurements and tests were made in Georgia under the direction of the writer on steel beam spans with concrete slab floors. These measurements showed quite clearly that the spans were stiffer than expected. The measured deflections were only from 50% to 75% of the computed deflections. This result indicated some interaction of the beams and slab and a wider distribution of the live, or added, load than expected. As no shear connectors between the concrete slab floor and the top of the beams had been provided, the interaction must have been due to friction or to partial bond.

To compare the stiffness of beams with shear connectors between the beam and floor slab with beams with no shear connectors, a test was carried out in 1931 on a simple 62-ft-span beam bridge. The roadway of this bridge was a 22-ft-wide concrete floor slab supported by five beams, 36 in. deep, spaced 5 ft apart. The slab was $7\frac{1}{2}$ in. thick. The location, spacing, and detail of the $\frac{3}{4}$-in.-round-steel shear ties are shown in Fig. 36. The deflections were measured

NOTE.—This Symposium was published in March, 1948, *Proceedings*.

[26] Cons. Engr., Decatur, Ga.

[18] "Standard Specifications for Highway Bridges," A. A. S. H. O., Washington, D. C., 1944.

from constant tension wires and the strain measurements were made with a set of ten electric strain gages. The strain measurements in the beam flanges were checked with a mechanical strain gage.

Temporary intermediate pile bent supports were driven at the quarter points and the beams were wedged until the loads on these bents were about equal. The floor slab formwork was built and the floor poured of concrete with 1.58

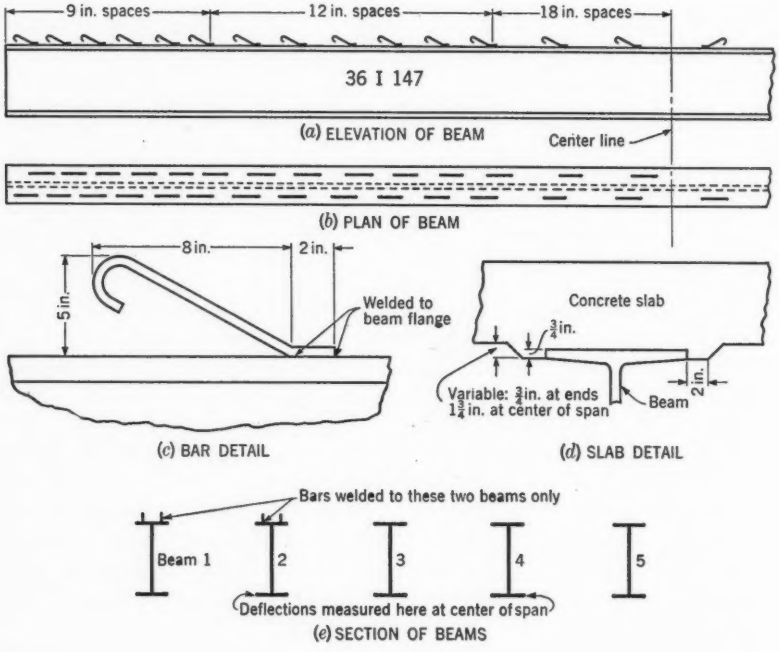

FIG. 36

bbl of cement per cubic yard of concrete, with a slump of 3½ in. Test cylinders of the concrete indicated a strength of 3,620 lb per sq in. at 28 days. When the slab was 28 days old, the forms were removed, the strain gages were set, and the initial readings were taken. The wedges were then driven out from the intermediate supports and the readings were taken for dead-load strains and deflections. A load of 15,000 lb was then placed on the span concentrated at the center of beams 2 and 4. This added load is referred to as the live load in Tables 4 and 5, which present the test results. Stresses were computed on the basis of $E = 4{,}000{,}000$ for concrete and $E = 30{,}000{,}000$ for steel.

When the tests were planned, it was not realized how stiff the slab and cross walls would be. It is evident from the measurements that beams 1 and 2, which were tied to the slab with shear ties, were much stiffer than the other three beams and carried much more than their share of the dead and live load.

At the time the measurements were made on this bridge span, it was not known how much changes in temperature would affect beam and slab bridges. Measurements of deflection of a concrete deck girder bridge showed that sudden

changes in air temperature would cause more deflection of the span than would be caused by a live load of two 12-ton trucks. Because of the exposed steel under the concrete floor slab, it might be expected that changes in the temperature would greatly affect deflection in a composite or semicomposite beam and slab span.

TABLE 4.—MEASURED AND COMPUTED STRESSES IN TEST SPAN SHOWN IN FIG. 36

Location	Measured Stress[a] (Lb per Sq In.)		Computed Stress[a,b] (Lb per Sq In.)	
	Dead load only	Dead plus live load	Dead load only	Dead plus live load
Slab over beam 2	− 468	− 567	0	0
Slab over beam 4	− 394	− 458	0	0
Top flange, beam 2	−1,080	−1,680	−7,930	−9,930
Top flange, beam 4	−2,550	−4,080	−7,930	−9,930
Bottom flange, beam 2	+6,720	+8,340	+7,930	+9,930
Bottom flange, beam 4	+5,490	+6,970	+7,930	+9,930

[a] − denotes compression, + denotes tension. [b] Assuming no interaction between slab and beams.

TABLE 5.—TOTAL MEASURED AND COMPUTED DEFLECTION AT CENTER OF TEST SPAN SHOWN IN FIG. 36

Location	Measured Deflection (In.)		Computed Deflection (In.)	
	Dead load only	Dead plus live load	Dead load only	Dead plus live load
Beam 1	0.425	0.475	0.85	1.02
Beam 2	0.500	0.575	0.85	1.02
Beam 4	0.550	0.675	0.85	1.02
Beam 5	0.575	0.725	0.85	1.02

In 1932, measurements were made of deflections of two spans, each 60 ft long, for a period of about 2 weeks after the spans were completed. Measurements were made early in the morning when the temperature was near the daily minimum, and at 2 p.m. when the temperature was near the maximum. The greatest change in temperature in a single day during the time of measurement was from a low of 57° F at 6 a.m. to 80° F at 2 p.m. The deflection for span 21 at 57° F was 0.706 in.; for span 22 it was 0.673 in. At 80° F the deflections were 0.739 in. for span 21 and 0.712 in. for span 22. This was a change of about 5% in the deflection for a 23° F change in temperature. Incidentally, the computed deflection for these two spans was 0.94 in. for dead load only. Under two 12-ton trucks the total measured deflection for dead load and live load was 0.86 in. as compared with a computed deflection for this combined load of 1.28 in. With no shear connectors these spans had been greatly stiffened by composite action of the beam and slab. Friction and partial bond must serve to transfer some of the shear between the top of the beam and the bottom of the slab.

These measurements and observations on full-size bridge spans give interesting support to the laboratory scale tests reported in the Symposium. The authors are to be congratulated on suggesting rather simple design methods. With the large number of variables and uncertain factors in the information available, refinement in design is scarcely warranted. The methods they suggest do not take into account the stiffening brought about by friction or partial bond between slab and beam. In the laboratory scale model tests it was evidently possible to eliminate this factor, but field measurements on full-size bridges show that computations of stress or deflections are from 20% to 40% in error.

A series of tests and measurements was made late in 1932 on both full-size bridges in the field and laboratory models. Unfortunately, it was found that the electric strain gages used would not hold calibration and the information gathered was of value only qualitatively. The measurements of deflection, however, were direct and consistent. As the sets of measurements reported in this discussion are typical and in line with the later work, little would be accomplished by repetition in detail.

Neglect of the factor of interaction due to friction or partial bond is a conservative reaction and possibly is proper until further information is available on both the curling and the longitudinal effect of a sudden change in temperature. The effect of plastic flow over a long period on a composite beam and slab span built with temporary intermediate supports is another question worthy of consideration. As this type of bridge floor will probably continue to be widely used, it is to be hoped that these tests will be continued and extended.